CONTROL OF THE ADSORPTION OF DYES ON COTTON

Martin Ferus-Comelo

Submitted in accordance with the requirements for the degree of Doctor of Philosophy

The University of Leeds

The Department of Colour Chemistry

September 2002

Acknowledgements

I would like to thank my supervisors Dr. J. H. Nobbs and Prof. J. Carbonell for their help and advice throughout the course of this study. I am grateful to the Worshipful Company of Dyers of the City of London and the Worshipful Company of Clothworkers of the City of London. Their financial contributions, and the support for this project by Prof. D. M. Lewis, enabled the department to purchase the pilot-scale jet dyeing machine that was essential for this work.

My thanks also go to the circle of textile dyeing enthusiasts and practitioners, both inside and outside the department, who shared their thoughts and comments with me on various occasions. Thanks finally to many of the staff and students of the Department of Colour Chemistry whose co-operation and help were much appreciated.

Abstract

The present work examines and models physico-chemical aspects of dyeing processes of cotton fibre with a direct dye (C.I. Direct Yellow 162). The models and methods in this thesis were developed with the aim of providing analytical tools that could help to cut back dyeing process times compared to current standard industrial practice, to reduce the need for dye additions and re-works, and to diminish or eliminate the use of some types of auxiliary, such as levelling agents.

Theoretical considerations revealed that three parameters appear to be central to the scaling of jet dyeing equipment: the liquor ratio, the number of fabric as well as of dyeliquor revolutions per minute and the dimensionless parameter L, which describes the influence of the flow regime in the dyeing machine on the exhaustion kinetics. Experiments on the pilot-scale jet dyeing machine showed that, under scaled-down industrial process conditions, the dye uptake rate was not affected by boundary layer effects.

Several thermodynamic models were examined for their accuracy to predict the dye amount sorbed by the fibre under equilibrium conditions. Two versions of the Gouy-Chapman model and three models derived from the Donnan membrane equilibrium were evaluated. Best overall results were obtained with a Gouy-Chapman model using a variable fibre saturation molality for the dye. The average back-prediction error of this model for the dye on fibre amount was below two per cent.

A newly developed model of the exhaustion kinetics of the dyeing process interprets the dye uptake rate as a combination of rapid dye adsorption at the fibre surface with slow diffusional dye transfer from the surface into the fibre interior. The model predicted the exhaustion values of isothermal experiments with an average accuracy of +/- 2.3%. It also accounted well for the effect of changes in the liquor ratio on the dye uptake rate and predicted the exhaustion speed satisfactorily in dyeings with changing salt dosing gradients.

A series of experiments was carried out on the pilot-scale jet machine in order to identify the process parameters that significantly influence dyeing unlevelness. They showed that neither the dye amount nor selected non-ionic surfactants nor the holding time at maximum temperature had a notable effect. They also suggested that the critical dye uptake rate per contact was 1.0% when the exhaustion profile was linear. The significant influence of the shape of the exhaustion curve on unlevelness was expressed in the newly introduced variable of the significant fibre surface molality change per contact. A statistical analysis indicated that the dye addition time, compensated for the dye-amount dependent effect of the First Strike, had a significant influence on unlevelness, too.

Table of Contents

List of Figures

List of Tables

1 Introduction

Cotton is the most popular textile fibre world-wide with a market share of slightly over 42% in 1998 (Aizenshtein 1998). Its production process, however, involves the consumption of large quantities of water, energy and chemicals. Much of the pollution emitted during the production and life cycle of the cotton fabric occurs at the coloration stage. The coloration of 1kg of cotton by the universal exhaust process consumes 50 to 150dm^3 of water, 10 to 15kWh of energy and around 100g of different textile auxiliaries (European Commission 2001). Additionally, between 5 and 100$g.dm^{-3}$ of electrolyte is required to exhaust the colorant onto the fibre. Environmental problems arise because of the high resource consumption and because some of the dyes and chemicals are difficult to eliminate from the wastewater stream (Schulze-Rettmer 1998).

The situation of the cotton textile industry is characterised by not only mounting environmental pressure but also by fierce international competition. Production lot sizes are becoming smaller and smaller, especially in the Western World due to competition from Far Eastern countries, colour changes are becoming more frequent and the number of colours continues to increase. It is therefore important that laboratory formulae reproduce in bulk production without problems so that the fabric fulfils the market requirements and is delivered on time despite short lead times. At the same time the dyeing cost as well as the ecological impact have to be minimised without negatively influencing the physical properties of the dyed goods. Despite progress in dyeing machine controls, the shades produced by dye mixture formulations from the laboratory often do not repeat in bulk production. The issue is complicated by the fact that machines of different types and from different manufacturers are used on the production floor. Therefore the laboratory has to be able to adjust the coloration process in a way that the characteristics of each machine can be taken into account.

The pressure to continuously reduce cost partly explains why the expensive traditional end-of-pipe types of technology to clean up dyehouse effluents, such as biological and physico-chemical treatments, have not been widely accepted in industry. Efforts to increase the efficiency of use of resources in industry therefore have to focus on process modifications that combine a reduction in environmental pollution with cost savings for the company. Advancements in the scientific understanding of dyeing processes, the availability of sophisticated sensors as well as the cost reductions of electronic equipment provide new possibilities to comply with these requirements. They make it technically possible today to create largely automated dyeing processes which are much faster and much more efficient

in terms of water, chemical and energy consumption than ever before, minimising human errors and ensuring good reproducibility. However, process control in industry is mostly limited to generic time-temperature profiles, which consider the dyeing machine as a "black box" and leave much room for improvement. In this sense, it is still true today that the coloration industry in general has not yet achieved the "stage of industrial maturity" (Carbonell, Mack 1981).

This work shall examine the possibilities of using physico-chemical modelling of the dyeing process and the principles of controlled sorption (Carbonell 1973) in order to suggest changes to the dye selection and dyeing process that should provide economical and environmental benefits. It is hoped that this goal can be achieved by, for example, the selection of suitable dyes and process conditions that exhaust the dyes to nearly one hundred percent on the cotton substrate, thereby almost completely eliminating any dye in the effluent. A better understanding of the dyeing process should also improve its reproducibility and therefore reduce resource consumption associated with dye additions and re-works. It is also conceivable that the consumption of certain auxiliaries, such as levelling agents, can be significantly reduced or even entirely eliminated if the process is controlled appropriately.

Jet dyeing equipment has been chosen for the investigation because it is the most important and popular method of dyeing textiles fibres in the western, possibly even in the entire, world.

1.1 The Dyeing of Cotton: An Overview

Cotton is a member of the family of cellulosic fibres which also comprises bast fibres like jute or linen and regenerated fibres such as viscose (Nevell 1995). The cellulosic fibres derive their name from the fact that their major constituent is cellulose. Cotton, the purest form of cellulose found in nature, is the seed hair of the Gossypium plant (Segal, Wakelyn 1985).

1.1.1 The Substrate

Cellulose, of which a cotton fibre contains over 90%, can be described chemically as 1,4-β-D-glucan and is the condensation product of individual β-D-glucopyranose units, its chemical structure is shown in figure 1.1.

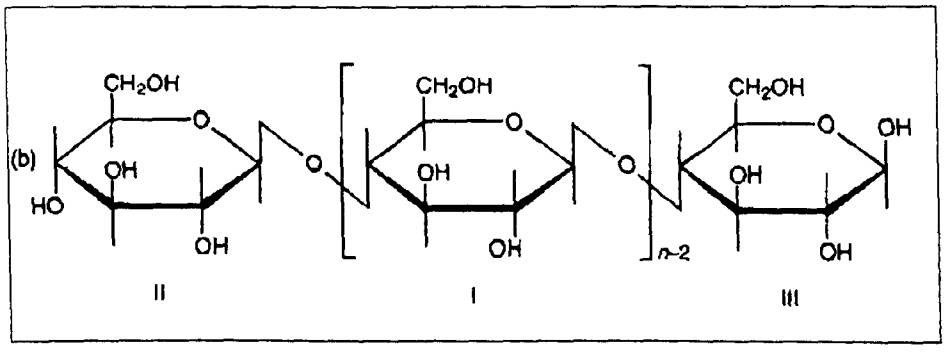

Figure 1.1: Haworth Projection of Cellulose (n = Degree of Polymerisation) (Shore 1995)

1.1.1.1 Morphology

The fibrillar structure of cotton comprises the primary and secondary wall as well as the so-called lumen (figure 1.2, Nevell 1995). In the primary wall cellulose fibrils are covered by a layer of pectin, protein, mineral matter and wax. The latter renders the fibre impermeable to water, which would make a successful dyeing difficult so that this outer layer has to be removed during the preparation of the cotton.

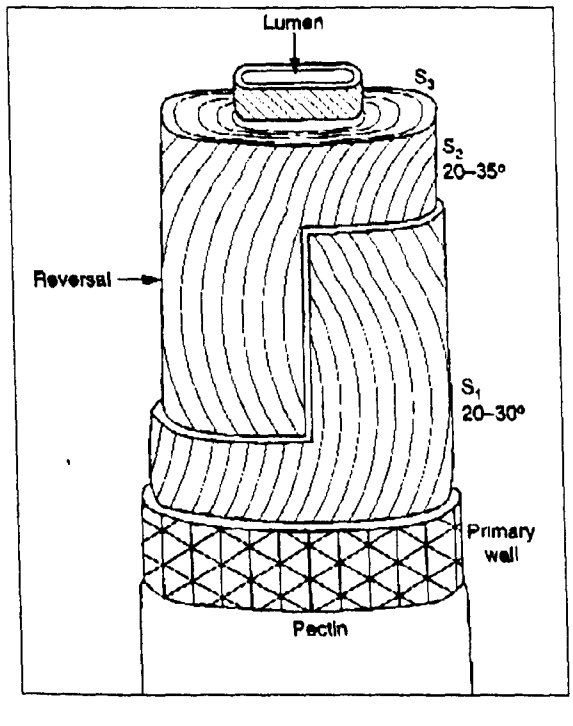

Figure 1.2: Cotton Morphology (Nevell, 1995)

The secondary wall (subscript S) consists of mature fibre, i.e. cellulose fibrils that are twisted around the fibre axis. The fibrils are made of bundles of microfibrils which in turn are composed of elementary fibrils. Even though it is difficult to quantify a diameter of a cotton fibre due to its irregular shape, the elementary fibrils are approximately three orders of magnitude smaller than the entire fibre. The lumen, as the third main feature, is the

leftover of the canal from which the layers of cellulose were laid down in the secondary wall while the fibre was growing.

As the degree of fibril orientation varies in the fibre, so does its accessibility to dye and other molecules. Areas of high orientation and crystallinity, which are held together by hydrogen bonding, cannot be accessed even by water molecules without simultaneously disrupting the structure (Peters, Ingamells 1973). The changing degrees of crystallinity imply that the accessible surface area is a function of the molecule size. As a result, dye molecules of different sizes, which can exist due to differences in the chemical formula (chromophore) or because of dye aggregation, will have different accessibility to areas of the same cotton fibre. This phenomenon is of great importance for dye application.

1.1.1.2 Properties

Some important physical properties of cotton, here for a 1.7dtex fibre, are summarised in table 1.1. It shows that fibre tenacity and elongation are higher in its wet state than when it is dry. A water imbibition of 50% has the practical consequence that any water removal beyond this level cannot be achieved by mechanical means such as centrifuging or mangling. Its moisture content is a function of the air's relative humidity (r.h.) and temperature.

Tenacity/[cN.tex^{-1}]	22
Elongation [%]	8
Wet Tenacity/[cN.tex^{-1}]	28
Wet Elongation [%]	13
Water Imbibition [%]	50
Moisture Content @ 65% r.h. and 20°C [%]	7

Table 1.1: Some physical properties of cotton (Nevell 1995)

Although cellulose is fairly stable under normal conditions, damage can result from exposure to acids (Fan 1987) and hot alkalis (Davidson 1934). Cellulose, as would be expected for a natural material, can also be degraded by enzymes, a fact which is increasingly exploited for industrial applications (Holme 2001). It can additionally be damaged by oxidation, which can for example occur at excessive exposure to hydrogen peroxide under alkaline conditions (Lewin 1969). Finally, cellulose can de-polymerise considerably in dry air at temperatures of more than 120°C within a couple of hours or, at

higher temperatures, even sooner (Peters, Still 1979). Temperatures beyond around 200°C, as they are for example employed in the continuous thermofixation process of polyester-cotton fabrics, may lead to yellowing of the fibre that could be enough to alter pale shades (Lewin 1965).

1.1.2 Dye Classes

Cellulosic fibres can be, and are, dyed with a variety of dye classes.

1.1.2.1 Direct Dyes

Direct dyes have been defined as anionic dyes with substantivity for cellulosic fibres which are normally applied from an aqueous dyebath containing an electrolyte (Shore 1995:152[1]). They are relatively easy to apply and represented about a quarter of all dyes applied to cellulosics in the early 1990s (Shore 1991) but their market share has probably slightly diminished in recent years, as dyehouses have switched to reactive dyes with sometimes higher wet fastness. Novel after-treatment agents for direct dyes, however, make it possible to achieve acceptable wash fastness for selected dyes up to 60°C (Hook 1988). Another reason why direct dyes might regain popularity in the future is their normally higher exhaustion rate and lower electrolyte requirement compared to reactive dyes. Both contribute to a better environmental performance.

Around three quarters of all direct dyes are unmetallised azo-molecules (Shore 1990). The majority of them are diazo structures. Metal-complex direct dyes are used for duller navy blues and blacks. Other chromophores are of the stilbene and thiazole-type or can be based on phthalocyanine or dioxazine (Zollinger 1992:84).

Compared to other dye classes, direct dyes have a high molecular weight which, as a general rule, promotes dye aggregation and substantivity to the fibre (Shore 1995:152). Water solubility is usually conferred by sulphonation. Interestingly, the high substantivity of many direct dyes not only leads to higher exhaustion values, and consequently to good colour reproducibility, but also to higher adsorption ratios on the activated sludge of wastewater treatment plants (Churchley et al. 2000). High substantivity may therefore result in a double environmental benefit.

Direct dyes and their application to cotton will be examined in more detail in chapter two.

---

[1] When books are cited, the page number of the section to which it is referred is provided also.

1.1.2.2 Reactive Dyes

Reactive dyes were commercially introduced in 1956 by ICI (Shore 1995:189). Their most interesting feature was the possibility to produce brilliant and pure colours, which could sometimes not be obtained with other types of dyes for cellulosic fibres. In 1990, it was estimated that reactive dyes accounted world-wide for around 10% of the total dye amount consumed for cotton coloration, although their market share in certain segments was far higher (Renfrew 1990). Since then, reactive dyes have gained market share at the expense of other dye classes (Taylor 2000), a trend that was partially due to the substantial marketing efforts of the dye manufacturers.

This dye class derives its name from the fact that its members form covalent bonds with the cellulose, giving dyeings with excellent wash fastness. Dye molecules consequently have a reactive group that enables them to react with the hydroxy group of the cellulose. The reactive group is normally attached to the chromophore via a bridging group. As for direct dyes, solubility is usually guaranteed by attaching sulphonic acid groups to the molecule.

There are a number of reactive groups commercially available (Rys, Zollinger 1975) and recently efforts have been made to use several of them, either of the same kind or different ones, in one dye molecule in order to increase dye fixation (Taylor 2000). The chromogen is often of a monoazo-type (green, yellow, orange, and scarlet) (Shore 1995:189). Blue colours have often used anthraquinone chromogens but recently triphenodioxazine-types have gained market share.

As far as their application is concerned, reactive dyes can be classified into three categories (Shore 1995:189):

1) Alkali-controllable dyes
2) Salt-controllable dyes
3) Temperature-controllable dyes

The alkali-controllable dyes exhaust only moderately in neutral salt solutions and their temperature range for optimum fixation is only 40 to 60°C. They are highly reactive and are therefore very sensitive to alkali addition. Reactive groups falling into this category include dichlorotriazines and vinylsulphones. The hydrolysed dye molecules sorbed by the fibre of this type of dye can be relatively easily removed during the washing off and/or soaping step.

The salt-controllable dyes exhaust higher than the alkali-controllable types in neutral salt solution and are normally applied at temperatures between 80 and 100°C. The high exhaustion before the addition of alkali requires care in the addition of electrolyte. Their reactive groups, such as aminochlorotriazine or trichloropyrimidine, have lower reactivity. The hydrolysed dye molecules sorbed by the fibre are more difficult to remove during the washing off and/or soaping step.

The temperature-controllable dyes do not need alkali for the reaction with cellulose but have to be fixed at temperatures above the boil. They can be applied like salt-controllable dyes. There are fewer dyes falling into this category. An example for a reactive group is bis(aminonicotinotriazine).

There are several reasons why reactive dyes have not come to dominate the market for cotton dyes despite their very good washfastness. Their application requires the addition not only of salt but also of alkali and part of the dye hydrolyses during the process and therefore cannot react with the cellulose any more. As the hydrolysed dye must be removed in order to ensure the expected washfastness, lengthy wash off cycles can be the result. These considerations, however, tend to diminish in importance as reliable dosing control for alkali is available and machine manufacturers and dye suppliers have found new techniques to shorten and to intensify the washing cycle (Bradbury 2001).

1.1.2.3 Vat Dyes

One of the oldest dyes known to the human race belongs to this dye class, Indigo. Indigo, like other vat dyes, is water insoluble in the presence of air (i.e. it is actually a pigment rather than a dye) and has to be converted into the water-soluble form by alkaline reduction (Aspland 1997:55). Once the reduced dye has diffused into the fibre, it is oxidised and becomes water insoluble again. The water insolubility of the vat pigment in the fibre leads to outstanding wash fastness. Their, generally speaking, very good fastness against other environmental impacts such as light or chlorine bleach make them the dye class of choice for demanding applications despite their high cost. The high cost is largely a result of the difficult synthesis (Aspland 1997:62). Nevertheless, total processing cost is often lower than in the case of reactive dyes. The decline of their usage may be due in part to their fairly complex application process and a corresponding lack of know-how in many textile dyehouses. The high exhaustion values of many vat dyes leads to very good colour reproducibility from laboratory to plant and from lot to lot.

Most vat dyes are anthraquinoid and usually have between five and ten aromatic rings (Latham 1995). Their main feature is the oxygen atom that is double-bonded to a carbon atom. Under strong alkaline conditions, the oxygen is reduced and the water-soluble leuco-

vat ion is formed. Otherwise, vat dyes normally contain very few substituents (Aspland 1997:75).

The reduction under industrial conditions is normally achieved by the addition of sodium dithionite as a reducing agent and sodium hydroxide for pH adjustment. Once the dye is diffused into the fibre, hydrogen peroxide is conventionally used to oxidise the leuco form. After the oxidation, and once the excess alkali and reducing agent are washed off, the dyeings have to be treated in boiling water with a surfactant (Latham 1995). This step, known as "soaping", is specific to vat dyes and is necessary in order to achieve the expected fastnesses. The difference between "soaping" of vat dyes and "soaping" of reactive dyes lies in the elimination of un-diffused pigment in the first case and the elimination of diffused hydrolysed dye in the second case.

Vat dyes can be classified into four sub-groups: IK, IW, IN and IN special (Aspland 1997:64). Dyes belonging to the IK category are to be applied at room temperature at fairly high salt concentration but lower sodium hydroxide amounts. IW dyes are more substantive and can be applied at 40 to 50°C with less salt but more alkali. IN dyes are even more substantive so that no salt is required but increased amounts of alkali. The application temperature is typically 60°C. The IN special dyes, finally, require even more alkali than the IN dyes.

Difficulties arise because dithionite is not only oxidised by the vat dye but also by the oxygen in the air and because some vat dyes can be over-reduced, i.e. they cannot be re-oxidised. The application is further complicated by the fact that some dyes are also sensitive to over-oxidation and that the colour changes during the soaping stage. Efforts are currently under way to replace reducing agents by electrochemical means (Blatt 1999). This would greatly reduce the environmental impact of vat dyeing and could also lead to a renaissance of this type of dye.

1.1.2.4 Other Dye Classes

Sulphur and azoic dyes can also be applied to cellulosics. Sulphur dyes are widely used in industry in certain segments, although their application often raises environmental concerns (Aspland 1997:83, Aspland 1997:91). The main attraction of sulphur dyes is their low cost and their application is mainly restricted to dark, dull shades like navy blue and black. In sulphur dyes, the chromophores are linked by a disulfide bond. Chemically, they are similar to vat dyes in that they possess no solubilising groups and, therefore, also require reduction under alkaline conditions for application to textiles. They also give textiles with good washfastness but their lightfastness is often inferior to that of vat dyes. Many commercially available sulphur dyes are mixtures and their exact chemical formula is unknown.

Azoic dyes are based on the finding that aromatic amines can be converted to diazonium compounds (Shore 1995:321). The particularity of azoic dyes is that the diazonium compounds are formed in situ on the fibre during the dye application (Colour Index 1992). The reaction takes place between the coupling component, normally naphthols, and the diazo component, usually an aromatic amine. After the coupling is completed, the water-insoluble compound is trapped inside the fibre. The process may take place at room temperature. The importance of azoic dyes has been declining over time, partly due to the complexity of their application and a limitation in hue selection (Shore 1995:321). They remain very important, however, for dark and brilliant red shades, which cannot be obtained with other classes of dyes.

1.1.3 Mechanisms of Dye Sorption

During the dyeing process, dye is transferred from the dyebath to the fibre. The dyeing process includes typically three stages, any of which can control the dyeing speed and also the dyeing result (Jones 1989:373):

1. Transport of the dye through the dyebath to the fibre surface
2. Adsorption of the dye molecule at the fibre surface
3. Diffusion of the dye from the surface to the interior of the fibre.

In some cases, such as azoic, metallisable, vat, sulphur or reactive dyes, the dye molecule additionally reacts with or in the fibre after diffusion, which can be considered a fourth stage. In the case of disperse dyes, dissolution of the disperse dye particle precedes the first step.

In this thesis, the word adsorption refers to a surface phenomenon. When it is intended to refer either to no specific step of the dyeing process or to all steps simultaneously, the term sorption is used.

To provide an explanation of the dyeing process based on physico-chemical laws, models have been developed which are described in more detail in chapters three and four. Typically, these models require simplifications in their assumptions in order to allow for mathematical solutions. As a consequence they might not quantitatively predict the behaviour of a dyeing system. When no physico-chemical models are available, empirical relationships are often used.

In the following paragraphs, some of the various mechanisms of the dyeing process are introduced.

1.1.3.1 Transport from Bath to Fibre

The flow of the dyeliquor in a dyeing machine, which is normally generated by a pump, results in a macroscopic speed of the dye molecule on its way to the fibre that is called convective diffusion (Breuer, Rattee 1974:105). Immediately at the fabric surface, however, there is no macroscopic flow. Consequently, the liquid speed increases from zero at the fibre surface until it reaches the value of the bulk phase. The area where the speed has not reached that of the bulk phase can be interpreted as a liquid layer, extending from the fabric surface some distance into the dye bath. This hydrodynamic boundary layer, defined as the area in which the liquid speed is less than 99% of the bulk flow speed, causes in turn a dye concentration gradient. The area of the concentration gradient is sometimes called the diffusional boundary layer and has about one tenth of the thickness of the hydrodynamic boundary layer (McGregor 1965).

The last section of the dye molecule's path from the liquid to the fibre surface is therefore confined to diffusion through this liquid layer. If the dye uptake rate is liquid diffusion controlled, it increases linearly with time (equation 1.1, Peters 1975:775):

$$[D]_f = \frac{DA[D]_s}{\delta} t \qquad (1.1)$$

$[D]_f$ = Amount of dye on the fibre [$kg.kg^{-1}$]
D = Diffusion coefficient of dye in solution [$m^2.s^{-1}$]
A = Surface area of fibre [$m^2.kg^{-1}$]
$[D]_s$ = Dye bath concentration [$kg.m^{-3}$]
δ = Thickness of the boundary layer [m]
t = Time [s]

Liquid diffusion becomes more important at low dyeliquor flow rates when the boundary layer at the fibre surface is very thick and the diffusion in the fibre is comparatively fast (Peters 1975:775). The convective speed of the dye is normally fast compared to the rate of adsorption at the fibre surface and does not determine the rate of dye uptake (Breuer, Rattee 1974:110). Nevertheless, at low flow rates, an increase in liquor flow may result in a higher exhaustion rate as the boundary layer thickness diminishes (Vickerstaff 1954:124). It is also possible that liquid diffusion controls the process at certain stages of the dyeing process only.

1.1.3.2 Adsorption

There are two types of adsorption, physical adsorption and chemical adsorption. In the case of physical adsorption, physical forces of attraction cause the dye to interact with the fibre. Chemical adsorption is a result of the formation of chemical bonds between the dye and the fibre.

The adsorption of the dye to the fibre surface can be regarded as instantaneous and much faster than the following process of diffusion into the fibre centre (Breuer, Rattee 1974:87). As a consequence, if the dye bath liquid turbulence is high enough, the dye will arrive at the fibre surface more rapidly than it can diffuse into the fibre and will accumulate at the surface. Due to the high speed of the adsorption, this quasi-equilibrium is almost immediately established and differs from the true thermodynamic equilibrium only because the dye continues to diffuse from the surface to the inside of the fibre. The difference between true and quasi equilibrium can be regarded as very small (Vickerstaff 1954:124). Thus it is not the speed of the adsorption that is of primary interest but the amount of dye adsorption and how it is influenced by various parameters. The homogeneity of the adsorption can affect the so-called final levelness of a dyed substrate, especially if the bath turbulence varies in a machine near the surface of the material to be dyed.

1.1.3.3 Diffusion

For cellulosics and direct dyes the generally accepted diffusion mechanism is dye transfer from aqueous solution by adsorption on and migration over capillary surfaces (Jones 1989), which are also called pores. The dye adsorbs on these pores in a dynamic reversible equilibrium that exists between the dyes in the water of the pores and the adsorbed dye molecules (Breuer, Rattee 1974:87).

The diffusion from the fibre surface into the interior, which may be termed film diffusion as opposed to liquid diffusion in the boundary layer, is usually the slowest of the three stages. It therefore determines in some dye systems, such as basic dyes on acrylic or disperse dyes on polyester, the overall speed of the process which can be controlled by temperature regulation. For direct dyes on cotton the situation is often different, as explained in the next section. The diffusion in the fibre is several orders of magnitude slower than in water because of the greater mechanical obstruction to movement caused by the fibre and because of the greater physico-chemical attractions between fibre and dye (Vickerstaff 1954:123).

The mathematics of diffusion will be described in more detail in chapter four.

1.1.3.4 The Rate-determining Step of Exhaustion under Finite-Bath Conditions

Dyeings of cotton with direct dyes under industrial conditions aim to achieve a high final exhaustion, i.e. high substantivity conditions are created by using considerable amounts of electrolyte. When high final substantivity is desired, the uptake rate is usually far more sensitive to substantivity changes than to temperature changes. This can be explained as follows: As the electrolyte concentration is increased during the process, leading to higher substantivity (and more dye association), the dye adsorbs rapidly at the fibre surface. Even

when the exhaustion speed is controlled, it is likely that most of the dye at the end of the exhaustion phase is concentrated in a small ring at the fibre surface because application is from a finite bath and dye amounts are fairly small compared to the saturation concentration of cotton (Vickerstaff 1954:274). During the remaining process time, the dye is then merely re-distributed between the fibre surface and the fibre interior with no change in the dyebath concentration. Consequently, as a first approximation, the uptake rate is controlled by the rate of electrolyte addition (Carbonell 1984). Exceptions to this rule may be found at low dye concentrations when the dye exhausts to a considerable degree without salt additions, thanks mainly to electrolyte present in the commercial product. Then, even for direct dyes, diffusion may become the rate-determining step.

1.1.4 Key Quality Criteria

If one aims at improving a process, as this work does, it is important to identify and, if possible, also to quantify the quality criteria that the finished product has to meet. The two criteria most important for the present discussion are, first, the accuracy of the colour match and, second, the levelness of the dyed product. There are other important aspects for the evaluation of coloured textiles, namely the fastness properties of the dyeing and the physical appearance of the substrate, but they will not be considered here as the intended process alterations should not adversely affect them.

1.1.4.1 Colour Match

The colour of a textile can be evaluated instrumentally by reflectance measurements with the help of a spectrophotometer (Patterson 1987). For quality control purposes, this usually involves the comparison of the coloured sample with a previously defined standard. The colour difference between sample and standard in the textile industry is usually expressed in terms of ΔE units (McLaren 1987). Among the several formulae developed for the calculation of ΔE, the one developed by the Colour Measurement Committee (CMC) of the Society of Dyers and Colourists is currently the most popular in the textile industry (Aspland 1997:387). A colour difference of $1.0\Delta E_{(CMC2:1)}$ between standard and sample is often deemed to be the maximum that is commercially acceptable.

Even though today's spectrophotometers, provided that they are well maintained, have attained a degree of accuracy and precision that is beyond the perception sensitivity of the human observer, colour evaluations can still be erroneous or incompatible. One source of variation is introduced by the type of light source of the spectrophotometer as colour appearance changes depending on the illumination (Rigg 1987). Errors may also result from improper preparation or mounting of the samples on the spectrophotometer (Connelly

1997). Finally, the dye may not be distributed equally over the entire sample so that measurements at different locations result in different readings. This phenomenon, termed unlevelness and more closely examined the following sub-section, is particularly important for many textile applications.

1.1.4.2 Levelness

Levelness can be defined as the homogeneous distribution of the dyestuff on the fabric (Carbonell et al. 1974). Another definition suggests that a dyeing can be termed level when the dyed good has everywhere the same colour (Rouette 1995:468). The homogeneity can be evaluated, for example, by first converting the reflectance data into colour strength and then by determining the maximum difference of colour strength for any two points on the fabric (Hoffmann 1989, Brooks 1974). Alternatively, multiple colour strength measurements can be interpreted by statistical means such as the variation coefficient (Carbonell et al. 1974, Brossmann et al. 1999). Semi-quantitive evaluation methods, such as the "Fransentest" have also been developed (Rouette 1995:468). The "Fransentest" does not evaluate the surface distribution of the dye but evaluates the penetration of the dye in the yarn intersections of a fabric.

Due to an unavoidable experimental error a dyeing is never completely level. Various authors have come to the conclusion that this level lies somewhere between one and three percent if expressed in terms of the variation coefficient of numerous reflectance measurements (Brossman et al. 1999, Carbonell et al. 1974). How big the concentration difference may be and still be visually acceptable, depends on the sensitivity of the human eye to a particular colour difference. If the ratio of colour difference (ΔE) to fractional difference in dye deposition is used as parameter, it was found for acid dyes on wool that the tolerance for unlevelness increases with dye amount on the fibre and is therefore not a constant. If a colour difference of $\Delta E = 1$ was assumed to be acceptable the tolerable dye deposition relative error for yellow, blue and red single dyes was approximately 10 to 15%. The acceptable error for a green shade obtained by a dye mixture was slightly less than 5%. In general, binary dye mixtures were found to be less tolerant for deposition errors than single dye applications if the error was asymmetric and more tolerant if the error was symmetric (Medley, Holdstock 1980, Gilchrist 1995:134). Other authors have found that a dye deposition relative error of 10% can lead to a colour difference for single dyes of between 0.2 and $0.7\Delta E_{(CMC2:1)}$. For combination dyeings this colour difference can be 2 to 2.5 times as high, whereby the higher colour difference is obtained for brilliant shades (Brossmann 1989). Overall, it would therefore appear that samples with colour strength differences of up to 5% would pass a visual examination in almost all cases and that in

some cases the difference could amount to up to 15% before the sample would have to be rejected.

Unlevelness can have several causes which can be categorised in the following manner (Hoffmann 1977):

1. Unequal distribution of the dyes in the dyebath or at the fibre surface because of
   a) too rapid dye exhaustion
   b) fast adsorption at the fibre surface or filtration through the goods
2. Varying dyeing conditions in the dyeing vessel, e.g. temperature differences
3. Differences in the substrate

The causes will be examined in more detail in chapter five.

1.2 Jet Dyeing Machines

Jet dyeing machines are, compared to other equipment types, a fairly recent invention. They derive their name from the principle of using a jet of dyeliquor to transport an endless rope of fabric in the dyeing machine (Wyles 1983). The first machine was introduced by Victor Fahringer, chief engineer of the Pacific Division of Burlington Industries, USA. Burlington licensed the technology to the US-American Gaston County Dyeing Machine Company which presented the machine for the first time to the public in Atlantic City in 1961 (Wyles 1983).

The commercial breakthrough for this machine type had to wait for another couple of years when it turned out to be very suitable for the dyeing of textured polyester jersey fabrics which were fashionable in the late 1960s. These fabrics were difficult to dye satisfactorily, especially in dark shades, with the machines then available. Winches at the time were not able to dye at temperatures above the boil and although pressure beams allowed dyeing temperatures of up to 130°C, fabric appearance was poor. Even though attempts were made to up-grade winches to pressure vessels, the jet machine proved to be far superior.

Jet dyeing has greatly developed since then and it is now the most popular form of fabric batch dyeing in the western world (White 1998). It is estimated that there are now more than 100 different machine models on the market the design of which falls, when classified in the most simple way, into two categories: long style (or "banana-type") machines and compact (or "apple-type") machines (Bone 1999). The design differences arise mainly from the need to strike a balance between widely different fabric properties and demands for the

commercial viability of their processing. Some substrates, like cotton, can be packed together quite densely without damaging the fabric while others, such as some synthetics or elastane-containing blends, are sensitive to high packing densities. The former are preferably processed on compact machines, the latter on long-style machines.

Since cotton was employed in the experiments described here, the machine description below focuses more on compact machines than on long-style ones. Nevertheless, as most of the features are shared, the majority of the descriptions adequately covers both types. Moreover, it would be expected that the different machine designs do not affect the physical chemistry of dye application with which this work is mainly concerned as modern machines tend to ensure adequate fabric-liquor interchange independent of their design (Hoffmann 1989:381).

1.2.1 Principle of Operation

In a jet dyeing machine, both the fabric and the dyeliquor are in motion, which distinguishes it from all other major batch machine types which either only move the fabric (jigger, winch) or only move the liquor (package, beam). This is an important design feature as it ensures very good fabric-liquor interchange and as it enables corresponding faster processing times.

During one revolution, the fabric is lifted up from the storage chamber by the combined action of the winch reel and the jet nozzle (figure 1.3). The high fabric speed of up to 600 $m.min^{-1}$ means that for physical reasons most of the force is exerted by the jet nozzle and little by the winch reel (Boehnke 1998). Some manufacturers even have designed machines that rely entirely on the jet action but most seem to have concluded that the reel is stabilising the fabric movement (Kaup 2001).

On many machines of the compact type the fabric has to pass after the jet nozzle through a fairly narrow tube which aids fabric-liquor interchange and distributes the jet forces on the fabric rope more evenly (Vernazza 1974). The fabric is then either plaited into the storage chamber or drops into it without any plaiting action. In the storage chamber, there is some fabric-liquor interchange as the liquor travels over and through the packed fabric to the suction side of the main circulation pump. On modern low liquor ratio machines, with which the processing of cotton at liquor-to-good ratios of around 5:1 is possible, the dyebath level is so low that only a fraction of the fabric in the storage chamber is submerged. Additional dye transfer occurs between the surfaces of the wet, compressed fabric layers.

On its way from the storage chamber to the reel the fabric is accelerated quickly from a fabric speed of almost zero to its maximum speed. This acceleration and the gentle squeezing effect of the reel reduce the liquor amount of the fabric rope, which in the case of cotton for example is around three times the fabric weight (Fox 1968). Both actions contribute to a better overall fabric-liquor interchange as mechanical agitation assists dye penetration and because a higher liquor amount is subsequently replenished in the nozzle. From there, a new cycle commences.

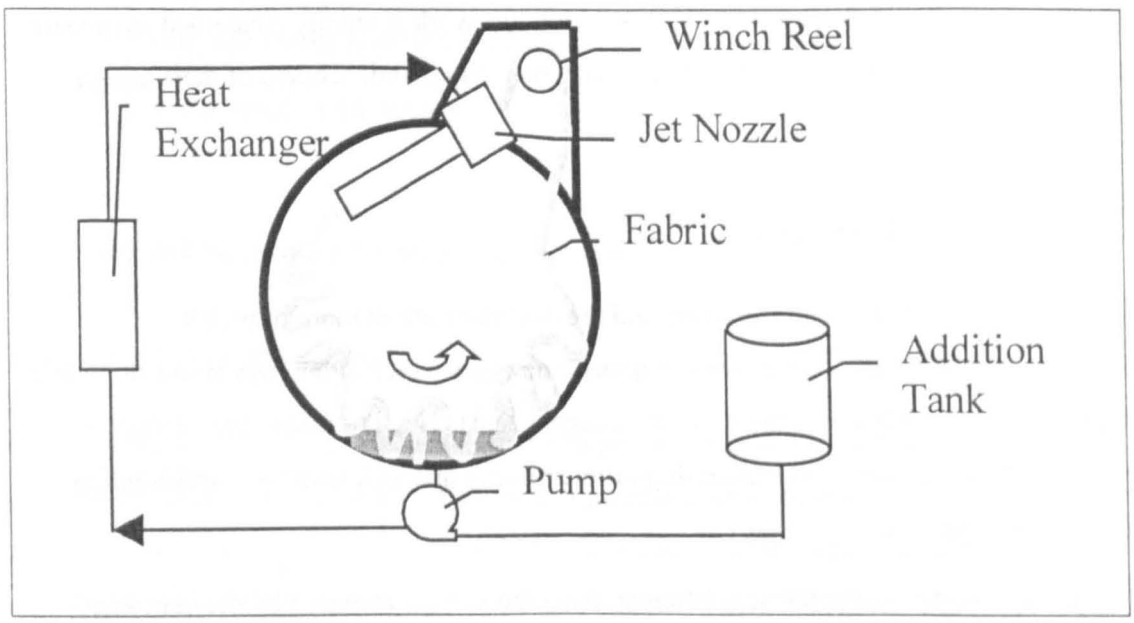

Figure 1.3: Principle of Operation of a Jet Dyeing Machine

One revolution of the dyebath can be described as follows: The liquor is sucked from the bottom of the storage chamber, passes through a lint filter and enters the main circulation pump. The pump pushes it over an external heat exchanger, which is used for heating and cooling purposes, and through the jet nozzle. The liquid is then collected by the vessel walls and accumulates again at the bottom of the storage chamber.

Additions of dyes and chemicals are usually made via a separate tank which is normally connected to the suction side of the main pump. If more accurate dosing is required, the addition tank has its own pump and valves.

Within one dyeing machine there can be between one and twelve ropes of fabric running in parallel. The fabric is loaded in and out of the machine through openings at one side. When the desired amount of fabric for one rope has entered the machine, the two ends of the rope are sewn together so that one endless rope is formed. The fabric mass per rope that can be accommodated depends on the machine design, fabric substrate and the fabric's

construction. In typical production-scale machines it lies between 100 and 300kg (White 1998).

The machines can be designed as pressure vessels allowing dyebath temperatures of up to 140°C but in many cases, e.g. for the processing of pure cotton, this is not required so vessels are specified to operate at atmospheric pressure only in order to reduce cost.

1.2.2 Features of a Modern Jet Machine

Many design development efforts have been aimed at improving processing productivity and efficiency. In pursuit of these goals, much attention has focused on reducing the liquor-to-goods ratio which is required to run the machines. A lower liquor ratio reduces water, energy and also chemical consumption, as some auxiliaries relate to the amount of water rather than the amount of fabric. It also improves productivity as draining and filling times are reduced and heating and cooling gradients may be increased. While early, fully-flooded jets had a liquor ratio of between 12:1 and 15:1 (Wyles 1983), modern low liquor ratio machines operate at a liquor ratio of 5:1 (White 1998). At these low liquor ratios there is very little liquid in the storage chamber so that the fabric is far from being covered.

Other design changes have improved the jet nozzle, the process control, the addition of dyes and chemicals and the rinsing technology.

1.2.2.1 Jet Nozzle

The jet nozzle is the centre piece of this machine type because it ensures that the fabric rope is transported by impulse transfer from a high speed liquor stream (figure 1.4). In the nozzle, fabric, liquor and air flows meet to create a situation of high fabric-liquor interchange. The nozzle's design and the fluid velocity determine how much of the kinetic energy of the dyeliquor is transferred to the fabric. The liquor is accelerated, by reducing the exit area of the water jet at the nozzle slits, to roughly twice the fabric speed (Schomakers 2001). If 200m.min^{-1} were assumed as the average fabric speed, then the dyeliquor velocity would be around 400m.min^{-1}. The air, which is sucked in through the gap between nozzle and fabric rope, helps to realign the fabric in the nozzle so that permanent creases are avoided.

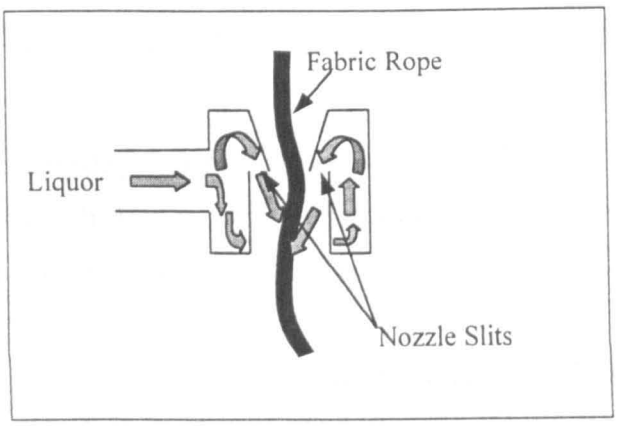

Figure 1.4: Jet Nozzle Schematic

On older machines, a flap valve in the circulation line controlled the liquor speed in the jet nozzle. Modern machines allow variable speeds of the main circulation pump. The speed is indirectly monitored by a pressure sensor in the main circulation line which is usually located close to the nozzle.

A recent innovation allows the adjustment of the jet nozzle diameter by the machine controller (White 1998). This eliminates the need to change the nozzle for fabrics of different widths and bulkiness.

1.2.2.2 Process Control

Initially temperature was the only process parameter that was automatically controlled. This proved to be adequate for some dye system types such as disperse dyes on polyester or basic dyes on acrylic but left much to be desired, especially for cellulosics dyeing (Carbonell, Heetjans 1984). The next steps, which are described in more detail below, saw the integration of liquid and solid dosing sequences and of combined cooling and rinsing steps into automatic process control. If it is also considered that there now exist self-cleaning lint filters, auto-untangling devices for the fabric ropes and spray systems for more efficient machine cleaning, the manual labour requirements of this type of machine are reduced to loading and unloading of the machine.

In addition to the above-mentioned features, modern controllers also monitor as standard the fabric circulation frequency, the reel speed and the jet pressure. Often the level in the addition tank can be monitored also. The measurement of the rope turnaround time requires that a small magnet be sewn into the fabric during the loading. A detector, usually located next to the jet nozzle housing, then sends a signal to the controller each time the magnet passes.

Recently, pH measurement systems have been offered commercially as an integrated part of the jet dyeing control system that can be used to ensure that the intended pH-value for

polyamide or reactive dyeing is actually attained (Hoffmann 2000, Adaptive 2001). In a similar way, continuous redox measurements should help to adjust the quantities of reducing agent and/or alkali for vat dyeing processes.

1.2.2.3 Dye and Chemical Addition

On the early machines, all additions of dyes and chemicals had to be made manually by using the side tank from where they were transferred to the main circulation line. Accurate dosing was therefore not possible. During the 1980s the major dyestuff suppliers, often in co-operation with machine manufacturers, introduced various systems to facilitate dosing of liquids, especially alkali for reactive dyes (Hildebrand 1984, Ungermann 1984, Sandoz 1986, Carbonell, Heetjans 1984). Liquid dosing also proved useful for dosing of acids for the dyeing of polyamides and wool (Annen et al. 1980, Hoffmann 2000) and the dosing of liquid dyes (Hoffmann 1987). Liquid dosing is today an established practice in many companies.

The extension of dosing techniques to include solid chemicals, such as sodium chloride or sodium dithionite, was more difficult. One main attraction of solid dosing is that it does not increase the liquor ratio which is particularly important when large amounts are used. In the case of many reactive dyes, for example, large quantities of salt are required and if the salt were introduced as a solution then the liquor ratio would increase substantially and equilibrium uptake would be reduced. Although it was shown early on in the development of dosing control that metering salt is beneficial (Hasler 1985, Carbonell, Heetjans 1984, Luebbers 1990), it is only recently that several manufacturers have offered the appropriate technology (White 1998). This delay seems to have been partly caused by handling difficulties of the solids which tend to form cakes when exposed to humidity. Accurate dosing of solids also seems to require gravimetric measurements which are not needed for liquid dosing where the pump transports, in sufficient approximation, the same volume per unit movement (Hickman 2001).

1.2.2.4 Rinsing

The traditional method of rinsing is to fill the vessel with rinse-water up to a certain level, to circulate for several minutes at the desired temperature and then to drop the bath. This fill-and-drop technique makes efficient use of rinse-water but is time consuming as each time the vessel has to be filled, heated to the required temperature and then drained (Bradbury 2000). Carried out in this way, the rinsing stage can take more than 50% of the total processing time of a cotton reactive dyeing. It also may lead to fabric contamination because the fabric acts like a filter for the dyebath liquid as it flows to the drain.

A way of overcoming the last mentioned shortcoming that has been employed for a long time is to rinse in overflow mode. In this technique the machine has a second drain valve located some height above the normal drain valve. During the rinsing, the normal drain valve is closed and the second drain valve is kept open so that the draining liquid does not have to pass through the fabric. For an efficient overflow rinsing it is advisable to pre-establish the quantity of water to be used.

This method is taken one step further in Combined Cooling and Rinsing (CCR) (Bradbury 2000). The main difference to the overflow technique is that in CCR the thermal energy of the water sent to the drain is transferred by a heat-exchanger to the in-flowing rinsing water which is then fed directly into the main circulation line. Both processes, filling and draining, occur simultaneously and the quantity of rinsing-water is controlled depending on the desired rate of cooling. The idle time during the cooling period is thus effectively eliminated. This method is also very efficient for the elimination of oligomers after the dyeing of polyester fibres.

A variation on the same theme is Controlled Rinsing (CR) which also uses simultaneous filling and draining (White 1998). In this case, however, there is no intention to cool the fabric so that the incoming water must be heated by a separate source, either locally at the machine or centrally in the dyehouse. This type of isothermal rinsing should be used at the end of a dyeing process when there is a considerable amount of residual dyes in the bath.

1.2.2.5 Novel Designs

In the early 1980s, tests on a pilot-scale machine were successfully completed that used a stream of air rather than a water jet to propel the fabric rope (von der Eltz 1985). This ingenious concept separates the two functions of the traditional jet, fabric transport and fabric immersion, into two distinct circulation systems. While the air circuit, powered by a blower, transports the fabric, the liquid circuit ensures that the fabric is adequately supplied with dye solution. This approach has two main advantages: Firstly, the liquor ratio can be further reduced to the volume that is minimally required to wet out the goods and to fill the pipe work. On a hydraulic jet a major additional concern is that cavitation of the circulation pump must be avoided. Secondly, as the air speed is so much greater than the fabric speed, changes in the fabric speed hardly affect the frictional forces exerted on the fabric (Boehnke 1998). This reduces fabric tension and allows considerably higher fabric speeds (up to 1000m.min^{-1}) compared to a hydraulic jet.

Another novel design, albeit less revolutionary, replaces two to six individual ropes in one vessel with one single rope (White 1998). The machine has still the same number of jets and reels as a conventional machine so that the entire rope passes through all the jets.

According to the manufacturer, this ensures that the differences from the first to the last rope metre are kept to a minimum.

1.3 Aims and Objectives of this Research

The aim of the work was to contribute to the improvement of the dyeing process of cotton materials by making it more reproducible and more efficient. In particular, it was hoped that process methods and process models would be developed that help to cut back process times compared to current standard industrial practice, to reduce the need for dye additions and re-works and to diminish or eliminate the use of some types of auxiliary, such as levelling agents. This would help to make the coloration of cotton simultaneously cheaper and more environmentally friendly. To achieve this end, the following plan for the research was made.

Models of physical chemistry shall be developed, resulting in a better understanding and prediction of the dyeing process, both regarding its kinetics and its equilibrium state. An attempt will be made to use, where available, mostly fundamental physico-chemical laws in the model such as those of diffusion, instead of purely empirical equations. It is believed that this will increase the prediction accuracy under varying dyeing conditions and will widen the scope of possible application of the models to other dyestuff classes and fibre systems.

Cotton will be chosen as a substrate because it is the most popular textile fibre in the world and its coloration is particularly polluting. Direct dyes will be used because they have inherent environmental advantages over reactive or vat dyes thanks to their generally high exhaustion and their moderate electrolyte requirements. If the material is suitably after-treated, an acceptable wash-fastness at up to 60°C wash temperature can be achieved with selected dyes, which is sufficient for many end-uses. They also offer the additional advantage that, compared to reactive dyes, the dyeing process is simpler to model as there is no reaction with the fibre nor is there any dye hydrolysis. It is thought that many of the anticipated findings of this work would be transferable to reactive or vat dyes.

Jet dyeing equipment has been favoured because it is the most important and popular method of dyeing textiles fibres in the western world.

The individual objectives of this thesis can be detailed as follows:

1) Comparison of the process conditions on a pilot-scale jet dyeing machine with those on a bulk-scale machine. Particularly the establishment of a parameter set that most closely simulates bulk-scale process conditions on a pilot-scale jet dyeing machine.

2) Development of a mathematical model that predicts the equilibrium sorption of a direct dye on cotton for various temperatures, dye amounts, liquor ratios and electrolyte concentrations.

3) Development of a mathematical model that simulates the exhaustion kinetics of a direct dye on cotton for various temperatures, dye amounts, liquor ratios and electrolyte concentrations.

4) Establishment of a correlation between the process parameters and the dye levelness with the aim of defining the most efficient process. Of special interest is the correlation with the rate of dye uptake.

1.4 References

1. Adaptive Control, Technical Information, Bradford (2001)
2. Aizenshtein E M, Fibre Chem. 30 (1998) 281
3. Annen O, Carbonell J, Engeler E, Textilver. 15 (1980) 296
4. Aspland J R, Textile Dyeing and Coloration (Research Triangle Park: AATCC 1997)
5. Blatt W, Schneider L, Mell. Textilber. 80 (1999) 624
6. Boehnke B, Mell. Textilber. 79 (1998) 346
7. Bone J A, M J Bradbury, BASF ITMA 1999 Review (1999)
8. Bradbury M J; Collishaw P S; Moorhouse S, AATCC Review 1 (11) (2001) 45
9. Bradbury M, Collishaw P, Moorhouse S, J.S.D.C. 116 (2000) 144
10. Breuer M M, Rattee I D, The Physical Chemistry of Dye Adsorption, (London: Academic Press 1974)
11. Brooks J H, J.S.D.C. 90 (1974) 158
12. Brossmann R, Mell. Textilber. 70 (1989) 852
13. Brossmann R, Van Chambers T, Krayer M, Kunze M, Lange A, Leaver A T, Oesch H P, Dyes & Pigments 41 (1999) 111
14. Carbonell J, Hasler R, Walliser R, Mell. Textilber. 55 (1974) 149
15. Carbonell J, Heetjans J H, AATCC International Conference, Book of Papers (1984) 70
16. Carbonell J, Knobel R, Hasler R, Walliser R, Mell. Textilber. 54 (1973) 68
17. Carbonell J, Mack R, Mell. Textilber. 62 (1981) 193

18. Churchley J H, Greaves A J, Hutchings M G, Philipps D A S, Taylor J A, J.S.D.C. 116 (2000) 279

19. Colour Index International, 3rd edition, (Bradford: SDC 1992)

20. Connelly R L, in Color Technology in the Textile Industry, (Research Triangle Park: AATCC 1997) 78

21. Davidson G F, J. Text. Inst. 25 (1934) T87

22. European Commission, European IPPC Bureau, Integrated Pollution Prevention and Control, Best Available Techniques for the Textile Industry, Seville (2001)

23. Fan L T, Gharpuray M M, Lee Y H, Cellulose Hydrolysis (Berlin: Springer-Verlag, 1987)

24. Fox M R, J.S.D.C. 84 (1968) 401

25. Gilchrist A, PhD Thesis, Department of Colour Chemistry, University of Leeds (1995)

26. Hasler R, AATCC International Conference, Book of Papers (1985) 89

27. Hickman W S, Rev. Prog. Col. 31 (2001) 65

28. Hildebrand D, Bayer Farben Revue (1984) 26

29. Hoffmann F, Mell. Textilber. 58 (1977) 588

30. Hoffmann F, Mell. Textilber. 68 (1987) 740

31. Hoffmann F, Textilver. 24 (1989) 381

32. Hoffmann F, Woydt M, Heetjans J H, Hennemann J, Mell. Textilber. (2000) E73

33. Holme I, Int. Dyer, 186 (2) (2001) 8

34. Hook J A, Welham A C, J.S.D.C. 104 (1988) 329

35. Jones F in Johnson A (Ed.): The Theory of Coloration of Textiles, 2nd edition, (Bradford: SDC 1989) 373

36. Kaup S, personnel communication, July 2001

37. Latham F R, in Shore J (Ed.): Cellulosics Dyeing, (Bradford: SDC 1995) 246

38. Lewin M, Ettinger A, Cell. Chem. Techn. 3 (1969) 9

39. Lewin M, Text. Res. J. 35 (1965) 836, 935, 979

40. Luebbers A, Souren I, Rouette H K, Mell. Textilber. 71 (1990) 371

41. McGregor R, Peters R H, J.S.D.C. 81 (1965) 393

42. McLaren K, in McDonald R (Ed.): Colour Physics for Industry, (Bradford: SDC 1987) 97

43. Medley J A, Holdstock C R, J.S.D.C. 96 (1980) 286

44. Nevell T P, in Shore J (Ed.): Cellulosics Dyeing (Bradford: SDC 1995) 1

45. Patterson D, in McDonald R (Ed.): Colour Physics for Industry, (Bradford: SDC 1987) 35

46. Peters R H, Ingamells W C, J.S.D.C. 89 (1973) 397

47. Peters R H, Still R H, in Happey F (Ed.): Applied Fiber Science, Vol. 2 (New York: Academic Press 1979)

48. Peters R H, Textile Chemistry, Vol. III, The Physical Chemistry of Dyeing, (Amsterdam: Elsevier 1975)

49. Renfrew A H M, Taylor J A, Rev. Prog. Col. 20 (1990) 1

50. Rigg B, in McDonald R (Ed.): Colour Physics for Industry, (Bradford: SDC 1987) 63

51. Rouette H P, Lexikon der Textilveredlung, (Duelmen: Laumann Verlag 1995)

52. Rys P, Zollinger H, in Bird C L, Boston W S (Eds.): The Theory of Coloration of Textiles (Bradford: SDC 1975) 326

53. Sandoz, US 4 629 465 (1986)

54. Schomakers P, personnel communication, July 2001

55. Schulze-Rettmer R, Text. Chem. Col. 30 (5) (1998) 19

56. Segal L, Wakelyn P J, in Lewin M, Pearce E M (Eds.): Fiber Chemistry (New York: Marcel Dekker 1985)

57. Shore J (Ed.), Colorants and Auxiliaries, Vol. 1 (Bradford: SDC 1990)

58. Shore J, in J Shore (Ed.): Cellulosics Dyeing (Bradford: SDC 1995) 152

59. Shore J, in Shore J (Ed.), Cellulosics Dyeing (Bradford: SDC 1995) 189

60. Shore J, in Shore J (Ed.): Cellulosics Dyeing (Bradford: SDC1995) 321

61. Shore J, Rev. Prog. Col. 21 (1991) 23

62. Taylor J A, Rev. Prog. Col. 30 (2000) 93

63. Ungermann E, Textil Praxis 39 (1984) 493

64. Vernazza J, Textilver. 9 (1974) 151

65. Vickerstaff T, The Physical Chemistry of Dyeing, 2nd Edition (London: Oliver & Boyd 1954)

66. von der Eltz H U, Christ W, Int. Text. Bul. 31 (3) (1985) 27

67. White M, Rev. Prog. Col. 28 (1998) 80

68. Wyles D H, in Duckworth C (Ed.) Engineering in Textile Coloration (Bradford: SDC 1983) 1

69. Zollinger H, Colour Chemistry, 2nd edition (Weinheim: VCH 1991)

2 The Dyeing of Cellulosics with Direct Dyes

The properties of direct dyes and their method of application on cellulosic materials have been the subject of numerous investigations, especially during the first half of the 20th century. Many of these studies made important contributions to the development of physico-chemical models of textile dyeing in general. For example, isothermal dyeings of C.I. Direct Blue 1 on cotton showed that the Donnan membrane theory is a useful tool to quantify equilibrium dye sorption for ionic dye-fibre systems (Hanson et al. 1935). C.I. Direct Blue 1 was also used in kinetics of dyeing experiments on cellulose sheets proving that Fick's laws of diffusion could be successfully employed to describe the dye uptake rate (Garvie, Neale 1938). During this time, the mathematics of diffusion and the theoretical understanding of the exhaustion kinetics were developed in close partnership. It is therefore not surprising that the subject of direct dyeings on cellulosics constituted a considerable part of Vickerstaff's classical work on the physical chemistry of dyeing (Vickerstaff 1954). In fact, many of the models that have been employed in this work are based on the work of these pioneers.

It is also noteworthy that many of the parameters that are of secondary importance in the influence on the kinetics and thermodynamics of direct dye application were already recognised at that time. They include the substrate properties and its pre-treatment (Neale 1940) as well as the rate of fabric-liquor interchange (Hanson 1935, Lemin 1946).

The amount of research effort relating to direct dyes and their application to cellulosics is now somewhat diminished. However, there are several areas in which research activity can still be identified. Some workers continue to develop new mathematical models to simulate dye sorption and dye uptake. These types of investigation will be reviewed in more detail in chapter three. Many projects are driven by the desire to improve the environmental performance and to propose methods for increased productivity. In the first category, work is undertaken to illuminate the relationship between chemical structure of the dye and its substantivity to cellulose (Shore 1991) as well as to the biomass in wastewater treatment plants (Churchley 2000, Baughman 2000). In both cases, higher substantivity is desirable in order to reduce effluent load. Another option is to pretreat the cotton so that higher exhaustion values are obtained and electrolyte can be omitted from the dyebath (Jang 2001, Rajendran 1999, Kamel 1999).

In the second category, the aim is often to combine previously separate process steps into one single step. The suggestions are, for example, to combine preparation and dyeing in one bath, i.e. to desize, scour and dye in one bath (Min 1998) or bleach and dye in one step

(Walker 1988, Min 1999). Alternatively, the dyeing and finishing steps can be combined (Ritz 1990, Raheel 1998).

The aim of the following sections is to provide detailed information about the application methods and characteristics of direct dyes and to introduce the direct dye chosen for this investigation. They also include a brief analysis of the significant influence that the substrate and its pretreatment as well as dye aggregation can have on the physical chemistry of dyeing.

2.1 Dye Application

Very early on, it was realised that during the dyeing process, the various direct dyes reacted very differently to the amount of electrolyte in the dyeliquor and that the control of electrolyte addition during dyeing was necessary to obtain satisfactory results (Whittaker 1942). Efforts were therefore made to classify direct dyes in groups in order to assist the dyer in choosing the appropriate application conditions and in selecting those dyes that are compatible with each other.

2.1.1 Classification Schemes

Early attempts to classify direct dyes were based upon the required amount of sodium carbonate in the dyebath (Cegarra 1992:265). The three categories were:

1. Dyes applied from a neutral bath
2. Dyes applied from a slightly alkaline bath
3. Dyes applied from a strongly alkaline bath

As it was found, however, that the dye sensitivity to the concentration of electrolyte played a much more important role than the sensitivity to pH, a new scheme was proposed that is still widely used today. This classification owes much to the work at Courtaulds (Boulton 1944) and at ICI (Lemin 1946) in the 1940s. The results were summarised by a committee of the Society of Dyers and Colourists (SDC) (SDC 1946, SDC 1948) and it was concluded that four parameters need to be considered: the levelling power of the dyes, their salt controllability and the influence of temperature as well as liquor ratio on the exhaustion. This led to the following classification scheme (Shore 1995:152):

1. Class A: Dyes with good levelling properties.
2. Class B: Dyes with worse levelling properties, but which can be controlled by the addition of salt. They are therefore referred to as salt-controllable dyes.
3. Class C: Dyes with equally bad levelling properties, but which are so sensitive to salt that they require the additional control of temperature. They are described as temperature-controllable dyes.

One possibility to graphically express the differences in dyeing properties is shown in figure 2.1 (Aspland 1997:30). It shows the dyeing behaviour of the different classes when equal amounts of dyed and undyed cotton fabrics are immersed into a dyebath containing electrolyte. As the time increases, dye is transferred from the dyed to the undyed fabric and eventually both would hold the same amount of dye. The dye transfer is due to migration and levelling out and it is clear that more time is needed to equalise the dye concentrations for a class B dye than for a class A dye and still more time is required for a class C dye. The recommendation is thus to ideally combine only dyes of the same class in one recipe or at least to avoid using dyes of class A and C in one bath.

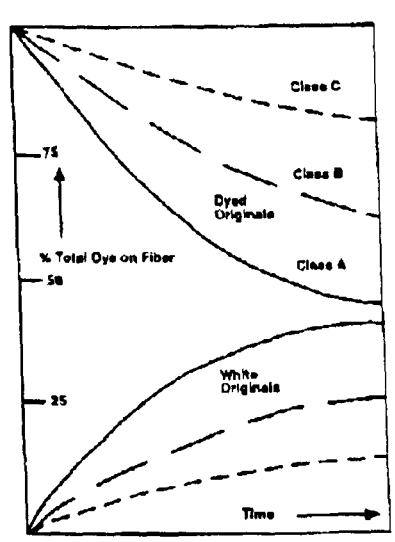

Figure 2.1: Migration and Levelling Behaviour of Direct Dyes (Aspland 1997)

Besides the SDC scheme, other classification parameters are possible. They include the chemical nature of the chromophore, the fastness properties, the suitability for a certain type of process such as continuous dyeing, the temperature stability, the ability to cover dead cotton and others (Aspland 1997:28, Cegarra 1992:267). As fastness requirements

play an increasingly important role in dye selection, the following section will briefly review some of their major aspects.

2.1.2 Fastness and Aftertreatment

The fastness of the dyed material to washing and to light are usually the most important performance requirements to be met. There are enormous differences in performance between direct dyes and even for the same direct dye the fastness of the dyed material can be a function of the dye amount. Thus, the wash fastness normally decreases with increasing dye amount and the light fastness increases (Aspland 1997:31).

There exist several different scales to characterise the fastnesses. The standard for washfastness is a scale from one to five, five being the best rating. For light fastness the scale usually includes ratings from one to eight, eight being the optimum. Many direct dyes show moderate to good fastness to light but exhibit poor washfastness (Shore 1995:152).

For more than a century aftertreatments have therefore been developed to increase the washfastness (Cook 1982). One early method consisted of diazotising direct dyes containing primary amino groups on the fibre with naphthols and other developers (Shore 1995:152). This method has largely disappeared because the application process was complicated, the colour of the substrate often changed as a consequence of the treatment and the lightfastness was sometimes reduced.

Another aftertreatment that has greatly diminished in importance is using metal salts, usually copper sulphate (Aspland 1997:40). The washfastness is improved because the copper either forms an insoluble salt with the dye anion on the fibre or because metal-dye complexes are formed within the material. Some of the copper invariably ends up in the effluent stream which partly explains the decline of this practice.

Very popular however, is the usage of cationic fixing agents. The agents usually consist of long hydrocarbon chains with a positive charge that is contributed, for example, by quaternary ammonium or cyanamide derivatives (Aspland 1997:40). Thanks to their positive charge, they form compounds with the sulphonate groups of the dye molecule which remain stable until washing temperatures of around 60°C (Shore 1995:152). A possible disadvantage is that the lightfastness of the material could be impaired by the treatment.

The latter-mentioned disadvantage could also be true for another widely used means to improve the washfastness, the treatment with cross-linking agents (Shore 1991). Their main purpose is normally to confer durable press or crease resistance properties to the cotton material but they also tend to improve the washfastness. This effect is not durable and

disappears when the cross-linking agents is washed off, for example by frequent laundering.

A combination of two of the above-mentioned mechanisms, the formation of copper complexes and the cross-linking with cellulose, is used to advantage in reactant-fixable dyes. They are a range of copper-complex dyes which were introduced together with a patented cross-linking and dye fixation agent in 1981 (Egger 1981). Their dye application method is analogous to direct dyes but when in a second step the cross-linking and fixation agent is applied by a padding process, satisfactory washfastness up to 60°C and higher can be achieved (Robinson 1983). The agent is a blend of different components, one of which forms covalent bonds both with the fibre and with the dyestuff. A second component acts like a cross-linker and improves the crease recovery of the cotton. Since the first introduction, the range of after-treatment agents has been extended (Hook 1988). They now additionally include two agents applicable by the exhaust process. Neither of these agents show any cross-linking effects and they are therefore mainly targeted at knit-goods. Both agents form complexes with the copper of the dye molecule.

2.1.3 Conventional Process Profile

A typical manufacturer's recommendation for the exhaust application of a direct dye would be to start the process at 40°C, when the dyes and possible auxiliaries such as levelling and anti-creasing agents are to be added to the dyebath (figure 2.2, DyStar). The temperature would then be raised by 1.5°C.min^{-1} up to 100°C in order to take advantage of the good levelling properties of the dyes (often Class A). When the maximum temperature is reached the salt (common salt or Glauber's salt) would be added in increasing portions, e.g. one fifth, two fifth and three fifths of the total amout. After the temperature has been kept for 60 minutes at 100°C, it would be reduced to 80°C in order to increase the dye yield. Then, the dyebath would be dropped and the fabric would be rinsed with warm water and then with cold water. Finally, if desired, the fabric may be aftertreated, for example with cationic fixing agents.

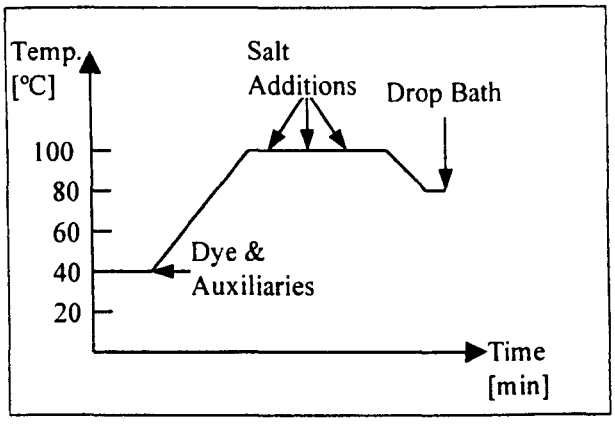

Figure 2.2: Conventional Process Profile (DyStar)

Instead of adding the salt at the boil, some manufacturers suggest to add the entire amount of salt together with the dye and auxiliaries at the start of the process ("All-in"). The recommended salt amount depends on the substrate, the type and amount of dye applied and, to a lesser degree, also on the liquor ratio. Usually, the dye manufacturers group their dyes according to their salt requirements in classes which are not necessarily identical to the SDC classification (section 2.1.1). The concentrations of common salt in the example given in table 2.1 are recommended for a liquor ratio of 10:1 and should be doubled up to a limit of 40 $g.dm^{-3}$ for a liquor ratio of 20:1 (DyStar).

% (omf) Dyestuff	Bleached Cotton	Mercerised Cotton
	Salt Group 1	
0-0.5	2.5	1.5
0.5-1.0	5.0	2.5
1.0-2.0	7.5	4.0
2.0-4.5	12.5	6.0
More than 4.5	30-40	15-20
	Salt Group 2	
0-0.25	2.5	1.5
0.25-0.5	5.0	2.5
0.5-1.0	10.0	5.0
1.0-2.0	15.0	7.5
2.0-4.5	25.0	12.5

Table 2.1: Example Salt Recommendations in $g.dm^{-3}$ for a Liquor Ratio of 10:1 (DyStar)

Direct dyes may also be applied in continuous applications but their fairly high affinity for the cellulose means that preferential adsorption occurs in the dye padder, leading to colour

differences between the first and the last metres of dyed fabric ("tailing"). Tailing can be reduced by using the "re-enforcing"-method, which consists of continuous addition of dye to the application trough in order to compensate for the loss of dye due to substantivity. The preferred application method is nonetheless batch dyeing.

2.1.4 The Dye selected for this Work

Before a decision on the dye selection was made, a specification list was drawn up. It included the following requirements:

1) At the maximum permissible salt concentration in the dyeliquor for the particular dye, the exhaustion should be nearly 100% at dyebath temperatures between 80 to 100°C.

2) The dye should have low migration and poor levelling properties and thus provide a "worst case"-scenario that arises from the dye application process for the resulting unlevelness.

3) The dye should not be a metal-complex dye, for environmental reasons.

4) The dye should be a standard, commercially available product.

Several direct dyes were considered and experimentally evaluated. It was finally decided to conduct all dyeings with C.I. Direct Yellow 162 in its commercially available form (Clariant Optisal Yellow 2RL). It is a metal-free azo-dye with low migration properties (SDC class B/C). Although its chemical structure is not published in the colour index, it is known that the dye molecule has a molecular weight of 1237g.mol^{-1}, possesses four sulphonic acid groups and two azo-bonds (Clariant). The impurities, mostly sodium sulphate, constitute 56% of the commercial dye according to the dye manufacturer.

Clariant recommends a process profile similar to the one described in section 2.1.3 (Clariant). From the starting temperature of 40°C it should be raised at 2°C.min^{-1} until 100°C and then kept constant at that level for 45 minutes. After the end of the holding period, the temperature should be lowered to 80°C when the bath can be dropped. Rinsing and the optional aftertreatment follow. Dyes and, if required, auxiliaries are to be added at the start. The instructions foresee the addition of between 0 and 5g.dm^{-3} common salt or sodium sulphate during the heating phase. Separate information sheets provided by the manufacturer showed that if these process recommendations were followed, the exhaustion at the end of the process of a 1.35% (omf) dyeing would be 70% at 5g.dm^{-3} salt. The value increases to 90% at 10g.dm^{-3} and to 95% at 15g.dm^{-3} salt.

2.1.5 Influence of the Fibre and its Preparation

For cellulosic fibres, substrate differences typically affect the dyeing speed - due to different diffusion and adsorption properties - and may also result in different quantities of sorbed dyestuff at the end of the process (Hoffmann 1990). The substrate differences can be caused by morphological differences within the fibre, by different fabric constructions or by fabric pretreatment differences.

2.1.5.1 Equilibrium Sorption

Influence of Fibre Type

Different types of cellulosic materials, such as cotton, viscose, modal and lyocell, sorb different quantities of dye at equilibrium conditions. These differences are normally explained not by a different dyeing mechanism but by the different accessibilities of the fibre to the dye due to their differences in morphology (Peters 1975:389), i.e. their surface area, their accessible volume and their electrical charge (Vickerstaff 1954:216).

The sub-microscopic fibre pores where the dye sorption takes place seem to be the most important morphological feature in this respect. The total fibre surface area, which is accessible to the dye depends upon the pore size distribution. While the accessible surface area mainly impacts equilibrium sorption, the pore size distribution additionally influences the exhaustion kinetics, as described in the next sub-section.

The pore size distribution plays a role in determining the equilibrium sorption because the pores have to be of a certain size to allow the sorption of the comparatively large dye molecules (Bredereck 1989). The distribution of the pore sizes has been determined for different cellulosics (Giles 1983). Column chromatography has been used to determine the accessible volume for water for several cellulosics, their internal surface area and their average pore diameter (Bredereck 1996). The findings are summarised in the Table 2.2.

Fibre	Accessible Volume/[$cm^3.g^{-1}$]	Internal Surface/[$m^2.g^{-1}$]	Pore Diameter/[A]
Cotton (scoured)	0.295	204	29
Modal (1.7 dtex)	0.490	403	24
Viscose (filament)	0.600	438	31
Viscose (staple 1.7 dtex)	0.680	438	31
Tencel (1.7 dtex)	0.440	372	24
Lyocell Lenzing (1.3 dtex)	0.530	411	26

Table 2.2: Data for water-swollen Cellulosics (Bredereck 1996)

The accessible surface area correlates in first approximation with the fibres' crystallinity, i.e. the higher the crystallinity the smaller the surface area, but other morphological features seem to play a role, too (Bredereck 1996)[2]. Furthermore, the accessible volume and surface area do not seem to be influenced by temperature in any practically significant way (Kulkarni 1969:131, Bredereck 1989).

One would assume that equilibrium dye uptake would closely correlate with the fibres' accessible surface area. In many instances this is indeed the case but there are notable exceptions. Pretreatment of the fibres with strongly alkaline solutions, for example, lead to increases in the equilibrium sorption that could not be explained by the increase in the surface area alone (Bredereck 1996). Additionally, if dye aggregation occurred, the correlation between the accessible surface area for water and the sorbed dye amount weakened as many areas became inaccessible for the bigger dye-aggregates. Overall, the relationship between pore size, molecule size and distribution coefficient appears to be very complex (Bredereck 1992, Bredereck 1996).

The answer to the question as to the causes of the differences in the equilibrium dye sorption for different substrates of the same principal type, such as cellulosics, has implications for the theoretical, thermodynamic treatment. For if it is assumed that the sorption differences are solely caused by morphological and electrical differences that affect dye accessibility, rather than by different attractive forces, then the affinity of a dye

---

[2] In that context it may be noted that experimental results indicate that the crystalline parts of the cotton also take up dyes (Ladchumananandasivam et al. 1994).

would correctly be treated as a constant for all cellulosic fibres (Sumner 1989). There is not complete agreement in the literature about the validity of this assumption, as it was found, for example, that phthalocyanine dyes showed such a substantially higher affinity for cotton than for viscose and modal that morphological differences alone might not be enough to explain the difference (Annen 1992).

Influence of Preparation

Fibre preparation processes, such as scouring, bleaching, mercerising and drying, change the pore size distribution of a material and therefore may also affect the equilibrium uptake of a dye.

It was shown, for example, that never-dried fibre has a higher accessible volume than fibre that has been dried at least once. Multiple dryings seem to have little further influence on the volume (Ladchumananandasivam 1994). This effect can lead to a loss of colour strength in padding applications of up to 30% (Schaub 1990).

Swelling of the fibre, e.g. by treatment with high caustic soda concentrations as in mercerisation, increases the accessible fibre surface area and therefore normally also the maximum dye uptake (Vickerstaff 1954:218). Recent measurements were able to quantify these changes and are summarised in table 2.3 for cotton (Bredereck 1996). Interestingly, alkaline treatment increased rather than decreased the crystallinity of other cellulosics but nevertheless their accessible volume augmented, too.

	Crystallinity [%]	Accessible Volume/[$cm^3.g^{-1}$]	Internal Surface/[$m^2.g^{-1}$]	Pore Diameter/[A]
Not causticised	0.80	0.295	204	29
Causticised	0.65	0.480	328	29

Table 2.3: Influence of Treatment with 200 $g.dm^{-3}$ NaOH on Cotton Properties (Bredereck 1996)

An additional factor that would explain the increased dye uptake, is the indication that the surface charges of cotton might be smaller after mercerisation (Vickerstaff 1954:218, Annen 1992).

2.1.5.2 Influence on Kinetics

A different dyeing rate could affect the total dye uptake under bulk production conditions because equilibrium might not be reached (Vickerstaff 1954:215). As will be discussed later, the dyeing rate has also important implications for dye levelness.

Dyes on cotton more than on other cellulosics are known to show a high initial exhaustion speed, a phenomenon which is known as "First Strike" (Boulton 1940). The First Strike appears to be independent of the cotton's provenance and pretreatment (Elgert 1989b). In experiments with several direct dyes the dye amount adsorbed during the First Strike increased linearly with the dye concentration in the dyebath and also increased with the amount of electrolyte added. It is likely that the enhanced effect in cotton can be explained by a higher proportion of larger pores in cotton compared to other cellulosics (Peters 1975:756, Bredereck 1989). As the dye initially adsorbs at the bigger pores, the uptake rate is increased, although the total accessible surface area on cotton is small compared to other cellulosic fibres (Bredereck 1996). The smaller pore size of viscose in comparison to cotton is confirmed by experiments investigating the ability to retain aggregates of acid dyes in a printing process. In these tests viscose proved to retain many dyes whereas they were easily removed from cotton (Vickerstaff 1954:170).

The diffusion speed of a given dye therefore depends on the substrate and changes with one type of cellulosic to another. The fact might be attributed to the different openness of the intercrystalline fibre regions. The irregular cross-section of cotton makes it difficult to determine the diffusion speed and there is also an indication that diffusion takes place not only from the outside of the fibre but also from the lumen (Bredereck 1989). For cotton and viscose a linear correlation between the free water content (i.e. water that is not chemically or physically bound to the fibre such as in bigger pores) and the diffusion speed was found experimentally (Bredereck 1989). This would confirm the sensitivity of the diffusion speed to the relation between pore and dye particle size. As a result, it becomes clear that dyes that show a similar diffusion coefficients on one substrate might exhibit significantly different coefficients on another substrate that has a different range of pore sizes (Vickerstaff 1954:269).

Another factor that influences the diffusion speed is the number of available dye adsorption sites. Thus, the higher rate of dye uptake of mercerised fabric was explained by more surface binding sites which reduce the blocking effect of the porous surface layer (Gooding 1998).

It is not only the fibre morphology that influences the kinetics. The fibre diameter as well as the fabric construction play a role, too. If the half-dyeing time, i.e. the time it takes to reach 50% of the equilibrium exhaustion, is used to indicate the rate of dye uptake, it can be said that the dyeing rate increases with the fineness of the fibre filaments although the final exhaustion might be unaffected. This is due to a higher surface area and the smaller diffusion distance of the finer fibre (Etters 1995). Fabric tension, which can be influenced by the construction and by the conditions in the dyeing vessel, leads to a reduction in the dye uptake speed, probably due to compression of the pores (Flath 1991).

The spinning method (e.g. ring-spun versus open-end) and knitting style (e.g. interlock versus jersey) have also been shown to exert an influence on the dye-uptake of a reactive dye on cotton (Micheal 2001). The differences were explained by differences in dye accessibility.

It was pointed out earlier that the pore volume is increased by strongly alkaline treatments such as mercerisation. In line with the interactions explained above it is thus not surprising that these treatments also increase the rate of the diffusion and therefore possibly also the dyeing rate (Peters 1975:450).

2.1.6 The Substrate selected for this Work

The fabric used in all the experiments reported in this thesis was a pure cotton jersey, i.e. circular-knit fabric, made up of 38count US cotton yarn, weighing 170g.m^{-1} in the greige state and having a width of approximately 87cm when slit. The supplier of the fabric guaranteed that the total amount of fabric requested came from the same yarn batch in order to minimise substrate differences. For the same reason, it was decided to pretreat the fabric in bulk rather than on the pilot-scale machine and to merely scour it instead of using a hydrogen peroxide bleach.

The pretreatment consisted of an alkaline scour with 1g.dm^{-3} soda ash and 1g.dm^{-3} of an anionic surfactant (CLARIANT IMEROL XN) for 30 minutes at 60°C in a winch dyeing machine at a liquor ratio of 20:1. The total fabric amount was processed in two batches. After the scour the fabric was rinsed on the winch machine, hydroextracted and dried in tubular form. The bone-dried fabric after the pretreatment had a mass of 136g.m^{-1} and a width of around 43cm in tubular form. The 20% change of mass between the scoured and the un-scoured fabric was caused in part by the removal of impurities of the cotton (primary wall) and in part by tension during the drying, leading to a stretch of the fabric tube.

2.1.7 Dye Aggregation

Direct dyes often form aggregates of two or many more dye molecules in aqueous solutions. These aggregates are fairly amorphous in composition although there is a tendency for the individual molecules to orient their ionic groups towards the water phase (Shore 1995:152). Aggregation can affect the exhaustion kinetics and the equilibrium sorption of a dye. It could also be said that the dye aggregates become more lypophilic and less hydrophilic.

It is generally recognised that the exhaustion rate of direct dyes on cotton increases with the amount of electrolyte present in the dyebath as would be expected from theoretical considerations (Breuer, Rattee 1974) and as confirmed empirically by Elgert and coworkers (Elgert 1989a, 1989b). However, early experiments showed that the dye uptake in the initial 30 minutes of the dyeing process was reduced by salt concentrations of more than approximately $1 mol.dm^{-3}$ and this has been attributed to the increasing size of dye aggregates (Bubser 1965). Furthermore, it has been found that increasing the concentration of three reactive dyes decreased both the absorptivity and the adsorption rate constant when $50 g.dm^{-3}$ electrolyte was present (Snyder 1997). This effect was also attributed to an increased particle size due to aggregation. Other researchers found, too, that there is a correlation between pore size, dye molecule size and adsorption rate (Denter 1994b). They calculated the adsorption rate for three different direct dyes on bone-dry, normally conditioned and wet cotton fabric. Their findings indicate that at a fairly low salt concentration of $2.5 g.dm^{-3}$ the adsorption rate in the first couple of seconds did not depend on the humidity of the cotton substrate and its pore size. After 20 seconds, however, the bigger direct dyes adsorbed much more slowly on the dry cotton than on the wet cotton, whereas the adsorption rate of the smaller direct dye did not depend on the humidity of the cotton. It was concluded that the smaller pores of the bone-dry cotton reduced the adsorption rate of the bigger dye molecules.

Dye aggregation in solution could also influence the equilibrium dye fibre amount as some parts of the fibre surface become inaccessible for the aggregated dye (Taylor 2000). This can be explained by the fact that, as mentioned in the previous section, the accessible area on cellulosic substrates is a function of the molecule size. Recent research has shown that the accessible volume of a cellulosic fibre for a molecule with an effective diameter of 2.5nm was about four times higher than that for a molecule with an effective diameter of 5nm (Bredereck 1996).

A review on dye aggregation showed that aggregation is a function of temperature, electrolyte concentration and various other parameters such as surfactant type and concentration (Wang 2000). It is well documented that surfactants can interact in complex ways with dye molecules in solution (Denter 1994a, Denter 1991, Denter 1994, Shore 1995). For example, the presence of non-ionic surfactants based on ethoxylated fatty alcohols or polyglycol ethers can have an anti-agglomeration effect on direct dyes in solution (Kuehni 1997). Addition of these surfactants might simultaneously reduce equilibrium dye uptake (Shore 1991).

The simplest, and crudest, way of analysing the aggregation behaviour of dyes in solution is to use spectrophotometric analysis since dye aggregates normally have a lower extinction coefficient and their maximum absorbance is at shorter wavelengths compared to the monomolecular species (Wang 2000, Coates 1969), although exceptions are known (Szadowski 1997).

2.2 References

1. Annen O, Gerber H, Seuthe B, J.S.D.C. 108 (1992) 215
2. Aspland J R, Textile Dyeing and Coloration (Research Triangle Park: AATCC 1997)
3. Baughman G L, Textile Chemist and Colorist and American Dyestuff Reporter 32 (1) (2000) 51
4. Boulton J, J.S.D.C. 60 (1944) 5
5. Boulton J, Morton T H, J.S.D.C. 56 (1940) 145
6. Bredereck K, Bader K, Schmitt U, Textilver. 24 (1989) 143
7. Bredereck K, Buehler A, Mell. Textilber. 73 (1992) 652
8. Bredereck K, Gruber M, Otterbach A, Schulz F, Textilver. 31 (1996) 194
9. Breuer M M, Rattee I D, The Physical Chemistry of Dye Adsorption (London: Academic Press 1974)
10. Bubser W, Eichmanns H, Melliand Textilchemie 1 (1965) 23
11. Cegarra J, Puente P, Valldeperas J, The Dyeing of Textile Materials (Biella: Texilia 1992)
12. Churchley J H, Greaves A J, Hutchings M G, Philipps D A S, Taylor J A, J.S.D.C. 116 (2000) 279
13. Clariant, technical information Optisal/Indosol dyes, without year

14. Coates E, J.S.D.C. 85 (1969) 355

15. Cook C C, Rev. Prog. Col. 12 (1982) 73

16. Denter U, Schollmeyer E, Textilver. 26 (1991) 113 & 29 (1994a) 288

17. Denter U, Schollmeyer E, Textilver. 29 (1994b) 238

18. DyStar, shade card for Sirius direct dyes, without year

19. Egger W B, B Kissling, T Robinson, Mell. Textilber. 62 (1981) 947

20. Elgert K F, Denter U, Heidemann G, Mell. Textilber. 70 (1989a) 377

21. Elgert K F, Denter U, Heidemann G, Mell. Textilber. 70 (1989b) 465

22. Etters J N, Amer. Dye. Rep. 84 (1995) 38

23. Flath H J, Mell. Textilber. 72 (1991) 132

24. Garvie, Neale S M, Trans. Far. Soc. 34 (1938) 335

25. Giles C H, in Parfitt G D, Rochester C H (Eds.), Adsorption from Solution at the Solid/Liquid Interface (London: Academic Press 1983) 321

26. Gooding J J, Compton R G, Brennan C M, Atherton J H, J.S.D.C. 114 (1998) 85

27. Hanson J, Neale S M, Stringfellow W A, Trans. Far. Soc. 31 (1935) 1718

28. Hoffmann F, Textilver. 25 (1990) 49

29. Hook J A, Welham A C, J.S.D.C. 69 (1988) 329

30. Jang J, Ko S W, Carr C M, Coloration Technology 117 (2001) 139

31. Kamel M M, Youssef B M, Shokry G M, Amer. Dye. Rep. 88 (6) (1999) 28

32. Kuehni R G, in Color Technology in the Textile Industry (Research Triangle Park: AATCC 1997) 46

33. Kulkarni G G, PhD Thesis, University of Leeds (1969)

34. Ladchumananandasivam R, Miles L W C, Hawkyard C J, J.S.D.C. 110 (1994) 300

35. Lemin D R, Vickers E J, Vickerstaff T, J.S.D.C. 62 (1946) 132

36. Micheal M N, Dyab W A, AATCC Mag. 1 (3) 2001 53

37. Min R R; Huang H S, American Dyestuff Reporter 87 (7) 1998 40

38. Min R R; Huang H S, J.S.D.C. 115 (1999) 69

39. Neale S M, Stringfellow W A, J.S.D.C. 56 (1940) 17

40. Peters R H, Textile Chemistry, Vol. III, The Physical Chemistry of Dyeing, (Amsterdam: Elsevier 1975)

41. Raheel M, Chen G, Text. Res. J. 68 (1998) 571

42. Rajendran S, Ramasamy S S, Mishra S P, Amer. Dye. Rep. 88 (3) (1999) 16

43. Ritz V, Kuzmek B, Soljacic I, Tekstil 39 (1) 1990 23

44. Robinson T, Egger W B, Textilver. 18 (1983) 41

45. Schaub A, Schick B, Mell. Textilber. 71 (1990) 137

46. SDC Committee on Direct Dyes, J.S.D.C. 62 (1946) 280

47. SDC Committee on Direct Dyes, J.S.D.C. 64 (1948) 145

48. Shore J, in J Shore (Ed.), Cellulosics Dyeing (Bradford: SDC 1995) 152

49. Shore J, Rev. Prog. Col. 21 (1991) 25

50. Snyder W, Berkstresser G, Smith B, Beck K, McGregor R, Jasper W, Text. Res. J. 67 (1997) 571

51. Sumner H H, in A Johnson (Ed.), The Theory of Coloration of Textiles, 2nd edition (Bradford: SDC 1989) 255

52. Szadowski J, Niewiadomski Z, Dyes and Pigments 33 (1997) 97

53. Taylor J A, Rev. Prog. Col. 30 (2000) 93

54. Vickerstaff T, The Physical Chemistry of Dyeing, 2nd edition (London: Oliver and Boyd 1954)

55. Walker B, American Dyestuff Reporter 77 (1988) (8) 48

56. Wang J C, Advances in Colour Science and Technology 3 (2000) 20

57. Whittaker C M, J.S.D.C. 58 (1942) 253

3 Mathematical Models of Equilibrium Dye Sorption

The equilibrium dye uptake is an important parameter to characterise dye-fibre systems. It is not only of theoretical interest but also of practical importance since under industrial conditions dyeing equilibrium is usually reached, in good approximation, at the end of the process. Thus, colour reproducibility under industrial conditions can be improved by ensuring that the dye exhaustion of each production lot reaches the same final value.

3.1 Affinity and Substantivity

The main objective of mathematical models of equilibrium dye sorption is to quantify the affinity of a dye for a certain substrate. The standard affinity, $\Delta\mu^0$ [J.mol^{-1}], is defined for thermodynamically reversible systems, such as cotton and direct dyes, as a measure of the tendency of the dye component to move from its standard state in the dye solution to its standard state in the fibre (Burdett 1989). It can be regarded as the driving force of the kinetics of the dyeing process.

The affinity may be calculated from the chemical potentials of dye molecules within the fibre, μ_f, and within the solution, μ_s. The chemical potential is an intensive quantity that represents an increase in the Gibbs free energy resulting from the addition at constant temperature and pressure of one mol of a component to such a large quantity of the system that its composition remains virtually unchanged (Burdett 1989). At equilibrium, μ_f is equal to μ_s:

$$\mu_f = \mu_s = \mu_f^0 + RT\ln a_f = \mu_s^0 + RT\ln a_s \qquad (3.1)$$

R = Gas constant [J.mol^{-1}.K^{-1}]

T = Temperature [K]

a_f = Activity of dye in fibre [-]

a_s = Activity of dye in solution [-]

The subscript "f" refers to the fibre and the subscript "s" refers to the solution. The standard affinity can then be defined as

$$\Delta\mu^0 = (\mu_f^0 - \mu_s^0) = -RT\ln\frac{a_f}{a_s} \qquad (3.2)$$

For physico-chemical processes, which include change of state and change of location, i.e. dyeing processes, the activities can be related to amounts of products and reactants if it is assumed that the laws governing ideal gases hold. It follows (Breuer, Rattee 1974:43) that:

$$-\Delta\mu^0 = RT \ln K \tag{3.3}$$

where K is the equilibrium sorption constant.

The affinity should be a constant for a particular dye and a particular substrate at any one temperature (Sumner 1989)[3]. In the case of a direct dye on cotton, for example, it should therefore be possible to predict the amount of sorbed dye at equilibrium for varying dye amounts and electrolyte concentrations from the value of the affinity, if known. Hence it is interesting to formulate an equation to calculate the affinity such that all the predictor variables in the equation can be determined experimentally.

Substantivity is sometimes used synonymously with affinity (Vickerstaff 1954:173). More recently, however, it has been defined as "the attraction between a substrate and a dye or other substance under the conditions of test whereby the latter is selectively extracted from the application medium by the substrate" (Sumner 1989). This definition accentuates that the substantivity varies with application conditions and would normally not be a constant at constant temperature. In this thesis, the term substantivity is utilised in the latter meaning.

There are at least two different hypotheses explaining why direct dyes have affinity for cellulose. One is based on chemical attractions (ion-dipole interaction, hydrogen π-bonds, acid-base bonds) the other is based on mechanical effects due to the pore structure of the cellulose. The molecular features responsible for affinity to cellulosics have been recently reviewed (Greaves 2000). The mechanical explanation rests on the observation that affinity typically rises with ease of dye association, so that in some cases a linear relationship between length of the conjugate chain and their affinity for cellulose can be found. According to this hypothesis, the water of solvation carried by the dye is preferentially adsorbed at the pore surfaces, increasing the tendency of the dyes to aggregate. The pore structure of the cellulose thus plays a significant role, encouraging the formation of dye multilayers (Giles 1989). Chemical attractions and mechanical effects could be the two sides of the same coin because a high tendency of the dye to form hydrogen bonds with cellulose may go hand in hand with a high tendency to associate with other dye molecules (Vickerstaff 1954:187).

---

[3] This statement is not uncontested. Several authors have found that dye-fibre interactions increase at low dye concentrations, leading to an increased affinity (Daruwalla 1963, McGregor 1972:546, Vickerstaff 1954:233)

3.2 Sorption Isotherms

A classical method to express the results of equilibrium sorption experiments, not only in textiles, is to plot the equilibrium amount of "product" against the amount of "reactant", i.e. the dye molality[4] on the fibre against the concentration in solution at constant temperature, the sorption isotherm (Vickerstaff 1954:97). For textile applications, three types of isotherms are often encountered, Nernst, Freundlich, Langmuir. Figure 3.1 illustrates the different types of sorption isotherms.

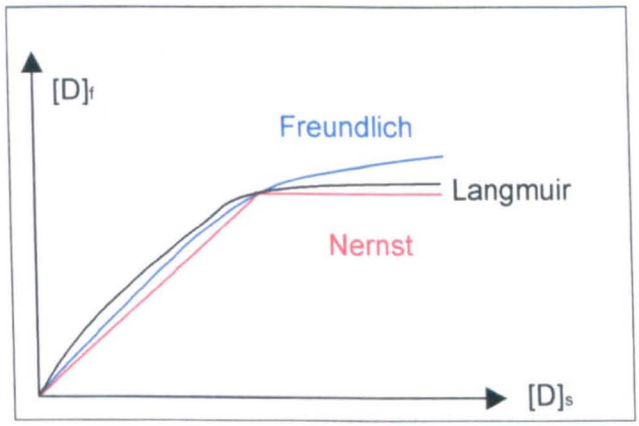

Figure 3.1: Comparison of Isotherm Types

Each of the three types can be linked to a certain sorption mechanism. Even so, it may be noted that even a good fit between experimental data and the particular isotherm-type does not necessarily imply that the underlying mechanism is identical to the one suggested by the model (Burdett 1989).

3.2.1 Nernst Isotherm

In the case of a Nernst isotherm, the equilibrium dye molality on the fibre, $[D]_{f,eq}$, is a linear function of the dye concentration in the bath, $[D]_{s,eq}$, until the fibre saturation molality is reached.

$$[D]_{f,eq} = K[D]_{s,eq} \tag{3.4}$$

---

[4] The term molality refers to the amount of substance of solute divided by the mass of solvent and is usually expressed in $mol.kg^{-1}$. The term concentration refers to the amount of substance divided by the volume of solvent and is usually expressed in $mol.dm^{-3}$ (Atkins 1998:3).

The proportionality constant, K, is called partition coefficient (Aspland 1997:176). The equation can be derived from the kinetics of the reversible adsorption of ideal gases (Breuer, Rattee 1974:33).

This type of isotherm indicates that the fibre behaves as a solvent for the dye. The sorption of disperse dyes on polyester, acetate or nylon can often be described in such a form (Aspland 1997:176).

3.2.2 Freundlich Isotherm

In most dye-fibre systems, the partition coefficient decreases at increasing dyebath concentrations. This decrease may have many reasons (Aspland 1997:19, Breuer Rattee 1974:34). For example, the dye's activity in solution could be diminished at higher concentrations due to aggregation or the fibre surface could be heterogeneous, so that dye-fibre interactions in some early filled locations are stronger than in others.

Freundlich isotherms are of the general form

$$[D]_{f,eq} = K[D]^{n}_{s,eq} \tag{3.5}$$

where the exponent, n, is an empirical constant between zero and one. Dyeing systems usually have values of "n" of around 0.5 (L Peters 1975). Although the equation was originally purely empirical in nature (Freundlich 1907), equations of this type can be derived mathematically from the assumption of certain heterogeneous surfaces (Breuer, Rattee 1974:34). One characteristic of the equation is that no saturation value is attained so that the dye amount on the fibre keeps increasing with the concentration in solution.

The experimental results of direct dyeings on cellulosics are often interpreted by assuming a Freundlich isotherm (Vickerstaff 1954:227, Willis 1945). It has also been successfully used to distinguish between effects on equilibrium sorption of pretreatment and fibre provenance on one hand and dyeing conditions on the other hand (Elgert et al. 1989). The exponent appeared to depend only on the dyeing conditions whereas the proportionality constant varied with pre-treatment and fibre origin.

There are two important drawbacks when Freundlich isotherms are employed. First, it is difficult to relate the coefficients to fundamental values such as the dye's affinity (L Peters 1975). This reduces the capability to accurately predict dye uptake at salt concentrations different to the ones employed in the original experiments. Second, saturation effects of the fibre are neglected. The second aspect is taken into account in a Langmuir isotherm.

3.2.3 Langmuir Isotherm

The Langmuir isotherm was originally derived to describe the adsorption of gases on metal surfaces (Langmuir 1916). It assumes that there is a limited number of sorption sites, $[D]_{sat}$ [mol.kg^{-1}], and that the sorption speed is proportional to the number of unoccupied sites as well as to the concentration of the molecules in contact with the solid phase. These assumptions yield the following equation:

$$[D]_{f,eq} = \frac{K[D]_{sat}[D]_{s,eq}}{1 + K[D]_{s,eq}} \tag{3.6}$$

It has been argued that competition for sorption places cannot be important for cotton dyeing as the fibre is normally far from being saturated. Experiments with direct dye mixtures have shown, however, that a Langmuir-type isotherm yielded better agreement with experimental data than a Freundlich type isotherm (Porter 1992, Gerber 1996). This supports the suggestion that there is dye competition for sites at the fibre surface.

One of the major difficulties in using the Langmuir approach to describe the application of direct dyes to cotton is to calculate the dye saturation molality on the fibre. Due to the lack of specific sorption sites on the cellulose for the dye anions, there is no clear theoretically predictable maximum dye-uptake or saturation value. Nevertheless, a semi-quantitative prediction can be developed (Peters 1975:414). It takes into account that as more negatively charged dye molecules accumulate in the surface layer, then increased electrical work against electrostatic forces has to be performed by additional dye anions. Saturation is reached when the free energy of sorption is equal to electrical free energy. The saturation value increases with the affinity, with the fibre morphology dependent volume term (e.g. viscose higher than cotton) and with a decreasing dye basicity.

It is experimentally difficult to verify the saturation molality because the direct dyes associate, especially at higher concentrations, and form multi-layers at the fibre surface. As a result direct measurement at high concentrations leads to inaccurate results (Peters 1975:400). The situation is additionally complicated by the fact that in practical dyeing systems the fibre saturation value is not a constant but changes continuously during the process, depending, for example, on temperature and salt concentration (Carbonell 1969). While the influence of temperature on the saturation value, at least in the range of 40 to 100°C that is relevant for the colouration of cotton, appears to be negligible (Kulkarni 1969), there is an increase in the saturation value with salt concentration (Peters 1975:402). The most likely explanation for this effect is multilayer formation at the fibre surface, accompanied by aggregation in solution (Ladchumananandasivam 1994).

Despite limitations, a common way to calculate the saturation value from experiments is to plot the inverse of the dye molality on the fibre against the inverse of the dye concentration in solution and determine the intersection with the y-axis by linear regression and extrapolation (Burdett 1989). Alternatively, the ratio of dye fibre molality and dye solution concentration may be plotted against dye fibre molality. The intercept on the dye fibre molality axis then yields the saturation molality.

The three types of isotherm may be combined to better reflect experimental results. A combination of a Langmuir and Nernst isotherm, for example, can be used to express the characteristics of acid dyeings on wool, on silk and on nylon (Aspland 1997:252).

None of the models discussed so far explicitly take into account ionic interactions between dye and fibre. This, and the already mentioned difficulty to relate these isotherm equations to more fundamental thermodynamic properties, make an extension of the models desirable. Two theories often used to express electrical effects are the Donnan membrane equilibrium model and the Gouy-Chapman model.

3.3 Electric Double Layer

The Donnan and the Gouy-Chapman models both quantify the effect of the ionic interaction between fibre and dye. When, in the case of cotton, the fibre is immersed in water the surface assumes a negative charge due to the adsorption of dye anions and ionic groups on the fibre itself. The negative charge attracts counterions, which accumulate in the dye solution adjacent to the fibre surface (figure 3.2). The excess of cations over anions gradually diminishes with increasing distance from the fibre surface. The resulting electrical potential has to be overcome by the negatively charged direct dye ions when they approach the fibre. The potential difference important for the dyeing process is between the electrical potential at the point of dye adsorption at the fibre surface and at the point in the dye bath far away from the fibre.

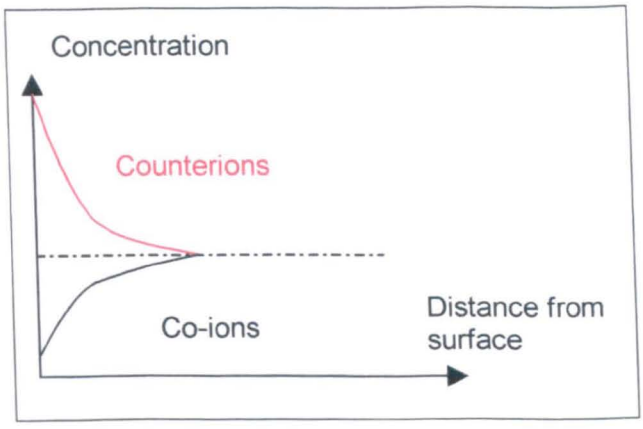

Figure 3.2: Graphical Representation of the diffuse electric double Layer

The effect of the electrical potential difference, Ψ_0 [V], has to be included in the calculation of the affinity so that equation 3.3 becomes (Burdett 1989)

$$-\Delta\mu^0 = RT \ln K + zF\Psi_0 \tag{3.7}$$

In case a Nernst-isotherm is assumed ($K = [D]_f.[D]_s^{-1}$) the result is

$$-\Delta\mu^0 = RT \ln \frac{[D]_f}{[D]_s} + zF\Psi_0 \tag{3.8}$$

z = Number of charges on the dye anion [-]

F = Faraday constant [$C.mol^{-1}$]

The Donnan and the Gouy-Chapman model represent two mathematical methods to calculate Ψ_0.

3.4 Donnan Model

The Donnan method is based upon the assumption that the distribution of ions is determined by a membrane potential that has exclusively electrostatic origins. Any chemical effects that could play a role in the ion distribution are therefore not considered. The membrane potential is created by the fact that some ions cannot freely move, while others can (Burdett 1989). When the Donnan theory is applied to cotton, the fixed charge relates to the ionised hydroxyl and carboxyl-groups of the cellulose.

In the simplest case, the system is divided into two parts, the bulk solution and the fibre surface layer, which is also called the internal solution. In the 2-phase model the sorbed molecules are considered dissolved in the surface layer which lacks specific adsorption points, hence also the term "diffuse adsorption". The Donnan model of diffuse adsorption has been widely used to describe the sorption of dyes on cellulosics (Peters 1975, Sumner 1989).

3.4.1 2-Phase Model

The Donnan model interprets Ψ_0 as the potential difference between the internal solution and the bulk solution (Gerber 1994). Ψ_0 can be related to the newly introduced Donnan coefficient of distribution, λ [-], which describes the partition of ions between the internal (subscript i) and the bulk solution (subscript s):

$$\Psi_0 = -\frac{RT}{F}\ln\lambda \tag{3.9}$$

Substituting 3.9 in equation 3.8 yields

$$-\Delta\mu_0 = RT\ln\left(\frac{[D]_i}{[D]_s}\frac{1}{\lambda^z}\right) \tag{3.10}$$

In the simplest case a dye Na_zD fully dissociates into z Na^+-ions and one D^{z-}-ion and the only other ions present are Na^+-ions and Cl^--ions from sodium chloride. Since the chemical potential in the bulk solution is equal to that in the internal solution the following Donnan relationship applies (ionic charges are omitted for simplicity reasons, Vickerstaff 1954:114):

$$[Na]_i^z[D]_i = [Na]_s^z[D]_s \tag{3.11}$$

Then λ is (Sumner 1989)

$$\lambda^z = \frac{[Na]_s^z}{[Na]_i^z} = \frac{[D]_i}{[D]_s} \tag{3.12}$$

and the affinity becomes:

$$-\Delta\mu^\theta = -RT\ln\left(\frac{[Na]_i^z[D]_i}{[Na]_s^z[D]_s}\right) \tag{3.13}$$

For the equation to be dimensionally correct, the two amounts on the fibre, $[Na]_i$ and $[D]_i$, must be expressed in amount per volume of internal solution (i.e. the volume of the surface layer) rather than amount per fibre mass. This can be achieved by division of $[Na]_f$ and $[D]_f$ with the so-called internal volume of the fibre, V, which quantifies the volume of internal solution per kg of fibre and has $dm^3.kg^{-1}$ as unit.

The internal volume can interpreted as the total micellar fibre surface accessible to the dye (Vickerstaff 1954:216) or the volume of the diffuse electric double layer adjacent to the fibre surface (Sumner 1989). The volume is a function of the accessibility of the fibre surface to the dye molecules, i.e. the better the accessibility of the fibre surface, the higher

the internal volume. The following internal volume values for cellulosics have been determined experimentally, using two different direct dyes (values in $dm^3.kg^{-1}$) (Sumner 1989):

Cotton:	0.22 – 0.30
Viscose rayon:	0.45
Cuprammonium rayon:	0.60 – 0.65.

All the variables in equation 3.13 can be derived easily from an experiment with the exception of $[Na]_i$, i.e. $[Na]_f.V^{-1}$. $[Na]_i$ can be calculated by using the condition that the internal solution and the bulk solution must both be electrically neutral (Sumner 1986). In the simplest case, the electrical neutrality condition for the internal solution can be written as:

$$[Na]_i = [Cl]_i + z[D]_i \tag{3.14}$$

Additionally, the following Donnan relationship may be applied:

$$[Na]_i[Cl]_i = [Na]_s[Cl]_s \tag{3.15}$$

Various substitutions and rearrangement of equation 3.13 then yield:

$$[Na]_i = [D]_i\left[\frac{z}{2} + \left(\frac{z^2}{4} + \frac{[Na]_s[Cl]_s}{[D]_i^2}\right)^{\frac{1}{2}}\right] \tag{3.16}$$

3.4.2 3-Phase Model

In order to take into account saturation effects on the fibre surface and dye competition for adsorption sites, the 2-phase Donnan model of diffuse adsorption can be extended to a 3-phase model (Porter 1992). It will be assumed here, as is usually presumed (Daruwalla 1963, Weedall 1981:41), that specific adsorption sites exist for the dye molecules, whereas the inorganic ions are adsorbed diffusely according to the Donnan equilibrium. The dye-fibre system is divided into three phases: fibre (subscript f, $[mol.kg^{-1}]$), bulk solution (subscript s, $[mol.dm^{-3}]$) and internal solution (subscript i, $[mol.dm^{-3}]$) next to the fibre surface (figure 3.3).

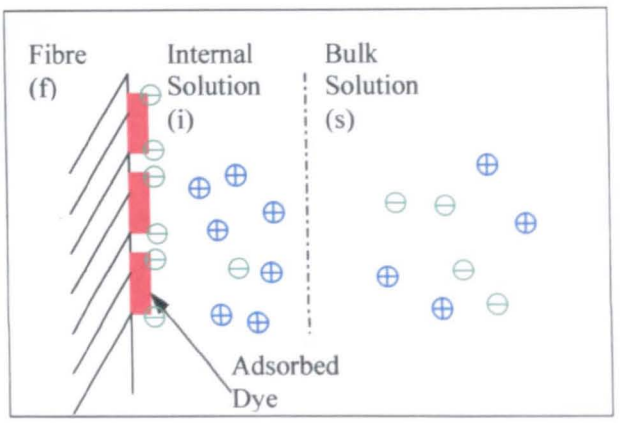

Figure 3.3: 3-Phase Donnan Model

The 3-phase model may be combined with different adsorption mechanisms. In the case of a constant partition coefficient (Nernst), essentially identical results as in the diffuse adsorption are obtained (Hanson 1935). If dye adsorption on the fibre occurs according to a Langmuir-type mechanism, then the partition coefficient (K) between the internal solution[5] and the fibre can be obtained by rearrangement of equation 3.6:

$$K = \frac{[D]_f}{[D]_i([D]_{sat} - [D]_f)} \tag{3.17}$$

Substitution in 3.7 with equations 3.9 and 3.12 yields:

$$-\Delta\mu^\theta = RT \ln\left(\frac{1}{[D]_{sat} - [D]_f}\frac{[D]_f}{[D]_i}\frac{[Na]_i^z}{[Na]_s^z}\right) \tag{3.18}$$

The dye saturation concentration on the fibre can be determined experimentally by plotting the inverse of $[D]_f$ versus the inverse of $[D]_i$ (Porter 1970).

Equation 3.18 was extended for mixtures of two direct dyes, which required the introduction of empirical correction factors in order to fit experimental results (Porter 1992).

$$-\Delta\mu^\theta = RT \ln\left[\left(\frac{1}{[D]_{sat,a} - [D]_{f,a} - y[D]_{f,b}^x}\right)\frac{[D]_{f,a}}{[D]_{i,a}}\frac{[Na]_i^z}{[Na]_s^z}\right] \tag{3.19}$$

y, x = empirical constants
subscript a = primary dye
subscript b = secondary dye

---

[5] Some researchers have used Langmuir sorption between bulk solution and fibre (Porter 1992) but it would appear that the more consistent method is to use the internal solution instead, since it is the internal solution that is in contact with the fibre (Sivarajan 1964).

3.4.3 Variable internal Volume

The theory of the electrical diffuse double layer theory requires a compression of the layer with increasing ionic strength, i.e. with higher electrolyte concentration (Atkins 1998:251). It has therefore been argued that the internal volume should become smaller as the electrolyte concentration in the dyebath increases since the electrical double layer is compressed while the surface area of the fibre remains constant (Sivarajan 1964). The internal volume, V, thus becomes a function of the thickness of the double layer which in turn depends on the dimensionless ionic strength of the solution, I.

$$V = Ar_D = A\left(\frac{\varepsilon_r \varepsilon RT}{2\rho F^2 I b^\theta}\right)^{\frac{1}{2}}$$
$$I = \frac{1}{2}\frac{\left(\sum b_+ z_+^2 + \sum b_- z_-^2\right)}{b^\theta} \qquad (3.20)$$

A = Fibre surface accessible to dye [$m^2.kg^{-1}$]

r_D = Thickness of electrical diffuse double layer ("Debye length") [m]

ε_r = Relative permittivity or dielectric constant of water [-]

ε = Vaccum permittivity [$C^2.J^{-1}.m^{-1}$]

ρ = Density of liquid [$kg.m^{-3}$]

F = Faraday constant [$C.mol^{-1}$]

b^θ = Conversion factor = 1 [$mol.kg^{-1}$]

$b_{+/-}$ = Molalities of ions in solution [$mol.kg^{-1}$]

$z_{+/-}$ = Charge number of ions in solution [-]

The variable volume approach is independent of the method to describe the ion distribution between dyebath and fibre and can therefore be used in the 2- or 3-phase Donnan model.

3.4.4 Fibre Ionisation, Dyestuff and Fabric Impurities

In real dyeing systems, there are more ions to be taken into account than the dye anion, the corresponding cation and the added electrolyte. Firstly, commercial dyes contain impurities that are often ionic in nature. Secondly, the substrate may also contain electrolyte, originating for example in the case of cotton from the cultivation and from alkaline or acidic pretreament. Furthermore, cellulose contains hydroxyl- and carboxyl-groups the ionisation of which is pH dependent.

Additional ions in the dyebath, be it from dye or from fabric impurities, can be fairly easily taken into account by modifying the electrical neutrality equation. Thus, if the additional ions were of the general form Na_2An, the electrical neutrality equation would become

$$[Na]_i = [Cl]_i + 2[An]_i + z[D]_i \qquad (3.21)$$

The integration of the cellulose's ionic groups extends the neutrality equation further to:

$$[H]_i + [Na]_i = [Cl]_i + 2[An^{2-}]_i + z[D]_i + [CellO]_i + [CellCOO]_i \qquad (3.22)$$

The quantification of ionised hydroxyl, $[CellO]_i$ [mol.dm^{-3}], and carboxyl, $[CellCOO]_i$ [mol.dm^{-3}], group contents is more complicated because their dissociation is pH dependent. From the dissociation equations the following dissociation constants, K_{OH} and K_{COOH}, can be defined (Sumner 1989):

$$K_{OH} = \frac{[CellO]_i[H]_i}{[CellOH]_i} = \frac{[CellO]_i[H]_i}{Q_{OH} - [CellO]_i} \qquad (3.23)$$

$$K_{COOH} = \frac{[CellCOO]_i[H]_i}{[CellCOOH]_i} = \frac{[CellCOO]_i[H]_i}{Q_{COOH} - [CellCOO]_i} \qquad (3.24)$$

Q_{COOH} = Total concentration of available carboxylic acid groups in the fibre phase [mol.dm^{-3}]

Q_{OH} = Total concentration of available hydroxyl groups in the fibre phase [mol.dm^{-3}]

Q_{COOH} and Q_{OH} may vary from one type of cellulosic to another and can also be influenced by pretreatment, e.g. by oxidation (Neale 1940). K_{COOH} and K_{OH} are temperature dependent but not highly so. For cotton, total carboxyl concentrations of 6 and $9.1.10^{-3}$mol.dm^{-3} fibre have been measured at an internal volume of 0.22dm^3.kg^{-1} (Bilsbury 1954). Estimates about the degree of carboxyl-ionisation differ considerably. While some assume complete ionisiation at pH 7 and above (Daruwalla 1961), others find a better correlation with experimental data if a lower dissociation constant, implying about 50% dissociation at pH 7, is assumed (Porter 1992). The latter assumption was explained by the fact that most of the carboxylic groups can be attributed to pectins and other polybasic acids that are either easy to remove or hardly hydrolysed. Measurements of the zeta potential of cotton showed that the potential stayed constant above a pH value of about 6, indicating that all carboxyl groups are ionised beyond this pH level (Pusic 1999). The potential approaches zero, i.e. no groups ionised, for a pH of around 2. The suggested K_{COOH}-values range accordingly from 1.10^{-3} (Kulkarni 1969), over $1.1.10^{-4}$ (McGregor 1972) to $1.35.10^{-6}$ (Porter 1992).

The total number of available ionisable hydroxyl-groups in cotton has been determined to be 11.2mol.dm^{-3} at an internal volume of 0.22dm^3.kg^{-1} (Sumner 1960). The dissociation constant, K_{OH}, was measured to be $1.84.10^{-14}$ at 25°C (Neale 1929).

If it is also taken into account that [H][OH] is the ionic product of water, K_W, then rearrangement of the equations 3.23 and 3.24 leads to the following results:

$$[CellO]_i = \frac{K_{OH}Q_{OH}[OH]_i}{K_W + K_{OH}[OH]_i} \qquad (3.25)$$

$$[CellCOO]_i = \frac{K_{COOH} Q_{COOH} [OH]_i}{K_W + K_{COOH}[OH]_i} \tag{3.26}$$

When these relationships and the respective Donnan equalities are used, the electric neutrality equation becomes

$$\frac{K_W}{[OH]_i} + [Na]_i = \frac{[Na]_s[OH]_s}{[Na]_i} + \frac{[Na]_s[Cl]_s}{[Na]_i} + 2\frac{[Na]_s^2[An]_s}{[Na]_i^2} + z[D]_i + \frac{K_{COOH} Q_{COOH}[OH]_i}{K_W + K_{COOH}[OH]_i} + \frac{K_{OH} Q_{OH}[OH]_i}{K_W + K_{OH}[OH]_i} \tag{3.27}$$

If $[OH]_i$ is calculated from the Donnan relationship

$$[OH]_i = \frac{[Na]_s[OH]_s}{[Na]_i} \tag{3.28}$$

then all parameters, with the exception of $[Na]_i$, are either constants or can be measured in the dyebath. The solution for $[Na]_i$ can be found by iteration.

3.5 Gouy-Chapman Model

The Gouy-Chapman model provides an alternative mathematical treatment of the diffuse electric double layer. It regards the fibre as a flat and uniformly charged surface with an electrical potential and the dye anions are considered to be point charges (Burdett 1989). The concentration of dyes in the double layer is determined by competition between the effects of the potential field and the kinetic energy of the ions. The thickness of the double layer is expressed as Debye length, r_D, i.e. the distance from the surface where the potential has fallen to e^{-1} of the potential at the surface.

3.5.1 Simple Model

In the Gouy-Chapman model, the initial charge density of the fibre surface, σ_0 [$C.m^{-2}$], is gradually increased by dye adsorption. For a one-dye solution the charge density of the fibre, σ, is (Gerber 1990)

$$\sigma = \sigma_0 + \frac{Fz[D]_i}{A} \tag{3.29}$$

A = Fibre surface area accessible to the dye [$m^2.kg^{-1}$]

The surface charge gives rise to the electrical potential, Ψ_0:

$$\psi_0 = \frac{r_D \sigma}{\varepsilon_0 \varepsilon} = \frac{r_D\left(\sigma_0 + \frac{Fz[D]_f}{A}\right)}{\varepsilon_0 \varepsilon} \tag{3.30}$$

In equation 3.30, the permittivity of water, ε [$C^2.J^{-1}.m^{-1}$], is temperature dependent (Gerber 1996):

$$\varepsilon = 91.6e^{-\frac{4.675}{1000}(T-273+7.78)} \tag{3.31}$$

By substituting equation 3.30 in equation 3.8, the affinity becomes:

$$\Delta\mu^0 = -RT\left(\ln\frac{[D]_f}{[D]_s} + A_1 r_D + A_2 r_D \sum z_i[D]_f\right)$$

$$A_1 = \frac{zF\sigma_0}{RT\varepsilon_0\varepsilon} \tag{3.32}$$

$$A_2 = \frac{zF^2}{RT\varepsilon_0\varepsilon A}$$

The two coefficients A_1 and A_2 contain information about the fibre properties. The term A_1 [m^{-1}] is related to the initial charge density of the fibre, σ_0, A_2 [$kg.mol^{-1}.m^{-1}$] is related to the specific fibre surface area accessible to the dye, A.

Rearrangement of equation 3.32 yields:

$$\ln\left(\frac{[D]_f}{[D]_s}\right) = -\left(\frac{\Delta\mu^0}{RT} + A_1 r_D + A_2 r_D \sum z_i[D]_f\right) \tag{3.33}$$

This equation is of the general form

$$y = A_0 + A_1 x_1 + A_2 x_1 x_2 \tag{3.34}$$

and A_1 and A_2 may be determined by multiple linear regression from dyeings at different dye and salt concentrations (Gerber 1994). Using this method, values for $\Delta\mu^0$, A_1 and A_2 have been published for several dyes on cotton and other cellulosics (Gerber 1990, Annen 1992).

Once $\Delta\mu^0$, A_1 and A_2 are known for a certain substrate, the dye molality on the fibre for certain dyeing conditions (i.e. dye and salt concentration) can be predicted if the following additional mass balance equation is taken into account:

$$[D]_\Sigma = [D]_f + LR[D]_s \tag{3.35}$$

$[D]_\Sigma$ = Total amount of dye [$mol.kg^{-1}$]

LR = Liquor ratio [$dm^3.kg^{-1}$]

Using equation 3.35, $[D]_s$ can be substituted in equation 3.33:

$$-\ln\left(\frac{[D]_f LR}{[D]_\Sigma - [D]_f}\right) - \frac{\mu}{RT} + A_1 r_D + A_2 r_D \sum z_i [D]_f = 0 \qquad (3.36)$$

This equation can be solved by iteration as all the parameter values are known except $[D]_f$.

The volume of the diffuse electric layer in the Gouy-Chapman model may be regarded as the equivalent to the internal volume of the Donnan model and is the product of the fibre surface area accessible to the dye and the thickness of the diffuse electric layer, r_D. Since r_D decreases with the ionic strength of the solution, this volume decreases with higher electrolyte concentrations. There are therefore strong similarities between the Gouy-Chapman treatment and the Donnan method with variable internal volume.

3.5.2 Model with Saturation Value

There is experimental evidence that at low dye concentrations, a dye monolayer forms at the fibre surface which then develops into a multilayer as dye and electrolyte concentration increase (Daruwalla 1963). This conforms to a treatment of the diffuse double layer in the form of the Stern model, which assumes that the double layer consists of two parts: a compact, immobile surface layer with a maximum ion molality, $[D]_{sat}$, and the diffuse double layer as described by the simple Gouy-Chapman model (Burdett 1989).

The simple Gouy-Chapman model assumes a Nernst-type sorption mechanism. Saturation effects may be conveniently simulated by postulating a Langmuir-type sorption behaviour instead (Gerber 1996). Equation 3.32 then develops into:

$$\Delta\mu^0 = -RT\left[\ln\left(\frac{[D]_f}{[D]_s}\right) - \ln\left([D]_{sat} - [D]_f\right) + A_1 r_D + A_2 r_D \sum z_i [D]_f\right] \qquad (3.37)$$

Substituting $[D]_s$ by incorporating the mass balance equation 3.35, the equation to be solved for $[D]_f$ then becomes:

$$\ln\left(\frac{[D]_f LR}{[D]_\Sigma - [D]_f}\right) + \frac{\Delta\mu^0}{RT} - \ln\left([D]_{sat} - [D]_f\right) + A_1 r_D + A_2 r_D \sum z_i [D]_f = 0 \qquad (3.38)$$

3.6 Effect of Temperature

Because of the exothermic nature of the dye sorption, dye affinity drops with temperature and so does the amount of sorbed dye, all other factors remaining constant. This effect on

average increases the equilibrium amount of sorbed direct dye by about 4% per degree of temperature fall (Vickerstaff 1954:230).

The thermodynamic quantity that predicts the fall in the affinity is the standard enthalpy of dyeing, ΔH^0 [kJ.mol^{-1}], also called heat of dyeing. It may be defined as the thermal energy released when dye is transferred from its standard state in solution to its standard state on the fibre (Sumner 1989). Provided that ΔH^0 is a constant, independent of the temperature, it can be related to the standard affinity

$$\Delta H^0 = \frac{d\left(\frac{\Delta\mu^0}{T}\right)}{d\left(\frac{1}{T}\right)} \tag{3.39}$$

The standard enthalpy can be obtained from experimental results by plotting $\Delta\mu/T$ against 1/T (Vickerstaff 1954:215) or by linear regression of the two parameters.

The assumption of a constant enthalpy of dyeing seems to hold for some direct dyes on cellulosics (Marshall 1949) but exceptions occur at the transition from mono- to multilayer formation (Daruwalla 1963) and if the dye aggregates change notably with temperature. The standard heat appears to be independent of the type of cellulosic (Peters 1975:415, Vickerstaff 1954:229).

3.7 References

1. Annen O, Gerber H, Seuthe B, J.S.D.C. 108 (1992) 215
2. Aspland J R, Textile Dyeing and Coloration (Research Triangle Park: AATCC 1997)
3. Atkins P W, Physical Chemistry, 6th edition (Oxford: Oxford University Press 1998)
4. Bilsbury M M, Martin J T, Standing H A, J. Text. Inst. 45 (1954) T1
5. Breuer M M, Rattee I D, The Physical Chemistry of Dye Adsorption (London: Academic Press 1974)
6. Burdett B, in Johnson A (Ed.), The Theory of Coloration of Textiles, 2nd edition (Bradford: SDC 1989)
7. Carbonell J, Lerch U, Textilver. 4 (1969) 229
8. Daruwalla E H, D'Silva A P, Text. Res. J. 33 (1963) 40
9. Daruwalla E H, Kangle P J, Nabar G M, Text. Res. J. 31 (1961) 712
10. Elgert K F, Denter U, Heidemann G, Mell. Textilber. 70 (1989) 377

11. Freundlich H, Zeitschrift fuer Physikalische Chemie 57 (1907) 388

12. Gerber H, Textilver. 25 (1990) 207

13. Gerber H, J.S.D.C. 110 (1994) 375

14. Gerber H, J.S.D.C. 112 (1996) 153

15. Giles C H, in Johnson A (Ed.), The Theory of Coloration of Textiles, 2nd edition (Bradford: SDC 1989)

16. Greaves A, Advances in Colour Science and Technology 3 (2000) 74

17. Hanson J, Neale S M, Stringfellow W A, Trans. Far. Soc. 31 (1935) 1718

18. Kulkarni G G, PhD Thesis, University of Leeds (1969)

19. Ladchumananandasivam R, Miles L W C, Hawkyard C J, J.S.D.C. 110 (1994) 300

20. Langmuir I, J Amer. Chem. Soc. 38 (1916) 2221

21. Marshall W J, Peters R H, J.S.D.C. 65 (1949) 17

22. McGregor R, Text. Res. J. 42 (1972) 536

23. Neale S M, J. Text. Inst. 20 (1929) T373

24. Neale S M, Stringfellow W A, J.S.D.C. 56 (1940) 17

25. Peters L, in Bird C L, Boston W S (Eds.): The Theory of Coloration of Textiles (Bradford: SDC 1975)

26. Peters R H, Textile Chemistry, Vol. III, The Physical Chemistry of Dyeing (Amsterdam: Elsevier 1975)

27. Porter J J, Perkins W S, Limb Y, Text. Res. J. 40 (1970) 704

28. Porter J J, Text. Res. J. 62 (1992) 236

29. Pusic T, Grancaric A M, Soljacic I, Ribitsch V, J.S.D.C. 115 (1999) 121

30. Sivarajan S R, Srinivasan G, Baddi N T, Ravikrishnan M R, Text. Res. J. 34 (1964) 807

31. Sumner H H, J.S.D.C. 76 (1960) 672

32. Sumner H H, J.S.D.C. 102 (1986) 301

33. Sumner H H, in Johnson A (Ed.), The Theory of Coloration of Textiles, 2nd edition (Bradford: SDC 1989)

34. Vickerstaff T, The Physical Chemistry of Dyeing, 2nd edition (London: Oliver and Boyd 1954)

35. Weedall P J, PhD thesis, University of Bradford (1981)

36. Willis H F, Warwicker J O, Standing H A, Urquhart A R, Trans. Faraday Soc. 41 (1945) 506

4 Mathematical Models of Dyeing Kinetics

Since dyeing is a three or, in the case of some types of dye, a four stage process and as each individual stage may limit the dye uptake rate, a mathematical model aiming at simulating all steps of the dye transfer would be a very complicated one. It is therefore usually presumed that only one or maybe two of the steps determine the overall speed and the model consequently focuses on these.

As transport of dye by diffusion within the fibre is often the slowest of all steps, it is at the centre of many models. Some of these diffusion-based models will be reviewed first. But, as was pointed out in chapter one, adsorption processes may determine the dye uptake rate in the case of high substantivity cotton dyeing. Those models will be analysed in the second part of this chapter.

4.1 Dye Diffusion Models

4.1.1 Diffusion Equations and their Solution

Modelling of diffusion through a film is usually based on Fick's Second Law of unsteady state diffusion (Jones 1989). For one-dimensional diffusion into a plane sheet the dye uptake rate becomes:

$$\frac{\partial [D]_f}{\partial t} = \frac{\partial}{\partial x}\left(D \frac{\partial [D]_f}{\partial x} \right) \tag{4.1}$$

where D is the diffusion coefficient of the dye in the fibre and has the units [$m^2.s^{-1}$]. In order to simplify the analytical solution of model equations, it is often assumed that D is a constant. The equation may then be written as:

$$\frac{\partial [D]_f}{\partial t} = D \frac{\partial^2 [D]_f}{\partial x^2} \tag{4.2}$$

Textile fibres are frequently considered to have the shape of a cylinder as a first approximation. The diffusion equation is therefore expressed in cylindrical coordinates. The radial diffusion into a one-dimensional cylinder can be written as:

$$\frac{\partial [D]_f}{\partial t} = \frac{1}{r} \frac{\partial}{\partial r}\left(rD \frac{\partial [D]_f}{\partial r} \right) \tag{4.3}$$

A solution of this second order partial differential equation requires three boundary conditions, two related to space and one related to time. Boundary conditions may take many different forms but frequently the following assumptions are made:

$$[D]_{f,(t=0)} = 0 \tag{4.4}$$

$$\frac{\partial [D]_f}{\partial r}_{(r=0)} = 0 \tag{4.5}$$

$$[D]_{f,(r=a)} = [D]_{fs} \tag{4.6}$$

The first boundary or initial condition states that the fibre is initially free of dye. The second boundary condition implies that there is no concentration gradient at the fibre centre (r = 0) and the third boundary condition says that the dye molality at the outer layer of the fibre equals the dye molality at the fibre surface, $[D]_{fs}$.

$[D]_{fs}$ can be any reasonable function of time. In the simplest case, under infinite bath conditions $[D]_{fs}$ is a constant. Under finite bath conditions $[D]_{fs}$ changes over time.

Several authors have developed analytical solutions of these equations in the form of a series of algebraic functions, usually assuming a constant diffusion coefficient. They include diffusion from infinite bath into a film (Crank 1968, McBain 1909) and into an infinitely long cylinder (Hill 1928). Solutions have also been found for finite bath and diffusion into a plane sheet (Carman 1954) and for an infinite cylinder (Barrett 1977).

In many systems, however, the diffusion coefficient of a direct dye within a cellulosic substrate is not a constant but depends in complex ways upon dye and electrolyte concentration, temperature and substrate properties.

4.1.1.1 Influence of Substrate

The influence of substrate properties on the diffusion speed has already been reviewed in chapter two and shall therefore not be repeated here. It shall be mentioned, however, that for many direct dyes the diffusion coefficient in water is about 1 000 to 10 000 times higher than the measured diffusion coefficient in the cellulosic fibre (Vickerstaff 1954:124, Inglesby 2001). Since the dye diffuses within the pores from an aqueous phase, it could be argued that the "true" diffusion coefficient of the diffusion in the fibre pore should be identical to the one observed in water (Zollinger 1991:285). Much theoretical and experimental work has been dedicated to verify this hypothesis and led to the development of the so-called pore model of the diffusion process.

The pore model was originally suggested in the 1930s and later extended and further developed by Weisz and co-workers (Weisz 1967, Weisz 1968). It was shown that the measured diffusion coefficient in the substrate can be converted into a "real" diffusion coefficient, which is close to the coefficient in water if it is assumed that diffusion takes place only in water-filled pores and that adsorption occurs from the inner surfaces of these pores. Agreement with the "true" value in water could be further improved when the reduction of effective pore radii posed by the presence of dyes was taken into account (Hori 1982). Despite the model's shortcomings (Peters 1973) it provides a better understanding of the crucial role that the substrate plays in affecting the diffusion properties of dyes in cellulosic fibres.

4.1.1.2 Influence of Electrolyte

In tests with C.I. Direct Blue 1 on viscose and cellulose sheets it was found that the apparent[6] diffusion coefficient increased with the salt concentration up to a maximum at between 5 to 10g.dm^{-3} sodium chloride and then decreased (Vickerstaff 1954:258). Other studies have found the diffusion coefficient of direct dyes to decrease with an increased amount of salt, except for very low salt concentration, i.e. considerably less than 1g.dm^{-3} (Peters 1975:452, Peters 1975:461). The latter results appear to be more accurate and generally applicable. The influence of electrolyte on the diffusion coefficient appears to vanish at extremely low dye concentrations (McGregor 1962:1050).

The increase of the diffusion coefficient at very low salt concentrations is believed to be due to the elimination of an electrostatic barrier between the anionic dye and the negatively charged cellulose at higher salt concentrations (McGregor 1962:2490). It was concluded that when the electrostatic barrier is present, i.e. at very low salt concentrations, the rate of dye uptake may not be diffusion-limited but dependent on the rate constants of the adsorption process.

In an effort to explain the electrolyte dependency theoretically, it has been postulated that D is a linear function of the dye concentration in the internal solution, $[D]_i$ as defined by the Donnan membrane equilibrium (Vickerstaff 1954:263):

---

[6] Since many parameters influence simultaneously the diffusion coefficient, its true value is difficult to determine experimentally. The experimentally obtained values are therefore considered to be average values and the term apparent diffusion coefficient is used.

$$D = D_0 \frac{[D]_i}{[D]_f} = D_0 \lambda^z \frac{[D]_s}{[D]_f} \tag{4.7}$$

D_0 = Standard diffusion coefficient [$m^2.s^{-1}$]

At low salt concentrations the Donnan coefficient λ is small so that the measured diffusion coefficient is also small. λ increases with the addition of salt, asymptotically approaching unity value. At higher salt concentrations, however, $[D]_s.[D]_f^{-1}$ decreases, thereby more than compensating the influence of lambda. As a result, the measured diffusion coefficient decreases.

Even though D decreases with increasing salt concentration, the diffusion speed actually steadily increases because at high electrolyte concentrations the reduced diffusion coefficient is more than compensated by the increased molality gradient in the fibre (Vickerstaff 1954:259).

4.1.1.3 Influence of Dye Amount

Up to a medium concentration level a linear relationship between dye amount and diffusion coefficient was found (Peters 1975:453):

$$D = D_0(1 + \beta[D]_f) \tag{4.8}$$

β = Coefficient decreasing with increasing salt concentration

The influence of the dye concentration on D may be explained theoretically by the different ion mobilities in the fibre surface layer. Since the small cation, e.g. sodium, moves more quickly than the dye anion, an electrical potential is created that increases the diffusion speed of the dye. If it is assumed that the dye in the internal solution, $[D]_i$, is adsorbed according to a Nernst-type isotherm, then the measured diffusion coefficient (D) would be expected to be a function of the partition coefficient (K) and the electrolyte concentrations in the internal solution, $[Na]_i$ and $[Cl]_i$ (Peters 1975:467):

$$D = D_D^0 K\left(1 + \frac{z^2[D]_f}{[Cl]_i + [Na]_i}\right) \tag{4.9}$$

This equation qualitatively describes well the fact that the measured diffusion coefficient increases with increased dye amount and decreases with increased salt concentration.

In dye mixtures, D may be influenced by the presence of a second or a third dye. In experiments with five binary mixtures, the diffusion coefficients were reduced by about 50% compared to a single dye application (Neale 1943).

4.1.1.4 Influence of Temperature

An increase in temperature leads to increased kinetic energy of the dye molecules and thus augments the diffusion coefficient. Its temperature dependency can be expressed in the form of the Arrhenius equation (Jones 1989):

$$D = D_0 e^{-\frac{E_A}{RT}} \tag{4.10}$$

E_A = Activation energy of diffusion [J.mol^{-1}]

Taking the natural logarithms yields

$$\ln D = \ln D_0 - \frac{E_A}{RT} \tag{4.11}$$

The activation energy of diffusion, E_A, may therefore be estimated by plotting lnD against T^{-1}. Experiments with direct dyes on viscose gave a value of around 60 KJ.mol^{-1} (Jones 1989).

4.1.1.5 Influence of Dye Selection

The diffusion coefficients of fifty different direct dyes were found to vary in magnitude over a range of 250:1 (Neale 1936). Consequently changes in the diffusion coefficient due to different salt and dye concentrations are small compared to the differences from one dye to another (Vickerstaff 1954:271).

A part of this variation can be explained by the dyes' different affinities. For example, higher affinity disulphonated direct dyes generally have a lower diffusion coefficient than the equivalent tetrasulphonated ones (Peters 1975:450). Other correlations between dyestuff constitution and their diffusion coefficient appear to be difficult to establish (Griffiths 1934). Nevertheless, it seems clear that the dye particle size is a second factor influencing the diffusion coefficient because the dye molecule size is comparable to that of the fibre pore (Vickerstaff 1954:267, Denter 1994). The particle size, and therefore the diffusion coefficient, is of course influenced by the tendency to form aggregates (Shore 1995).

Before some of the diffusion-based kinetic models of the dyeing process are presented in more detail, a cautious note about the limits of these models: There is an indication that even for systems of which the dye uptake obeys the diffusion laws, the actual situation might be more complicated. Experiments with a direct dye on cellulose sheet revealed, for example, that the fibre surface molality increased during the process, despite infinite bath conditions, several fold (McGregor 1964). This effect could be attributable to several

factors: dye aggregation, dead end pores in the cellulose acting as a sink to the dye and/or an adsorption speed that is somewhat slower than the diffusion speed (Peters 1975:455).

4.1.2 Reddy et al. Model

The model combines a one-directional diffusion into a cylinder of radius 0.1mm with dye adsorption at the fibre surface according to a modified Langmuir isotherm (Reddy 1997). The two remaining boundary conditions are: The fibre is initially free of dye and the molality gradient at the fibre core is zero. The diffusion coefficient is assumed to be independent of dye amount and salt concentration, but dependent on temperature.

The model was tested with a binary direct dye mixture and the equations employed to derive the fibre surface molalities of dye A and B, $[D]_{fs,A}$, and $[D]_{fs,B}$, have the following form:

$$[D]_{fs,A} = K_A[D]_{s,A}\left([D]_{sat,A} - [D]_{f,A} - c_{B/A}[D]_{f,B}\right) \tag{4.12}$$

$$[D]_{fs,B} = K_B[D]_{s,B}\left([D]_{sat,B} - [D]_{f,B} - c_{A/B}[D]_{f,A}\right) \tag{4.13}$$

The coefficients $c_{A/B}$ and $c_{B/A}$ are scaling factors to convert the molality of one dye into the equivalent molality of the other dye:

$$c_{B/A} = \frac{[D]_{sat,A}}{[D]_{sat,B}} = \frac{1}{c_{A/B}} \tag{4.14}$$

The partition coefficients, K_A and K_B, are a function of dyebath temperature and salt concentration and also depend on the molalities of dye A and B. The dependency on temperature is:

$$K = e^{\frac{m}{T}+c} \tag{4.15}$$

The coefficients m and c were determined by linear regression from experiments and differed, of course, between dye A and dye B.

The dependency on electrolyte is modelled according to:

$$K = a_0 + a_1[NaCl] + a_2[NaCl]^2 \tag{4.16}$$

The coefficients a_0, a_1 and a_2 were determined empirically by least square fits for dye A and B.

The partition coefficient is also affected by dye-dye interactions in the dyebath:

$$K_{A,mix} = \frac{[D]_{s,A}}{[D]_{s,B}} K_A e^{-\frac{a_{AB}[D]_{s,B}}{[D]_{s,A}}} \quad (4.17)$$

$$K_{B,mix} = \frac{[D]_{s,B}}{[D]_{s,A}} K_B e^{-\frac{a_{BA}[D]_{s,A}}{[D]_{s,B}}} \quad (4.18)$$

The coefficients of interaction, a_{AB} and a_{BA}, were chosen so as to give the best fit to experimental results.

Due to the complex functions for the dyes' surface molalities, no analytical solution is available and numerical methods have to be employed instead. To this end, the fibre was approximated by a grid of ten annual rings.

The model was verified with dyeings of C.I. Direct Red 80 and C.I. Direct Yellow 106 and predicted accurately the effect of temperature, salt gradients and of changes in the dye amount on the dye uptake rate. The range of parameter variations tested was however fairly narrow (60 to 80°C, 2 to 6g.dm^{-3} salt, less than 0.25g.dm^{-3} dye) and a considerable number of calibration dyeings had to be carried out initially in order to determine the empirical model coefficients by statistical means. As a further shortcoming the model ignored established thermodynamic concepts, such as the Donnan membrane equilibrium, in its calculation of the fibre surface molality. It is suggested here that the use of such models would have reduced the number of necessary calibration dyeings as well as the number of empirical coefficients.

4.1.3 Vosoughi and Burley Model

Vosoughi and Burley developed this model to describe the exhaustion kinetics of a yarn package in a package dyeing machine (Vosoughi 1993) based upon a previously developed model of a packed bed chemical reactor (Burley 1985, Wai 1984). The reactor can operate in axial flow mode, such as would be used for example for loose stock dyeing of fibres, or radial flow mode, which would be typical for a yarn package dyeing operation. For the purposes of this thesis, the axial flow mode is more relevant because it is considered to be closer to the situation found in a jet dyeing machine so that the following description only applies to this type of flow.

The axial flow model consists of a fibrous packed bed of density ρ_P and voidage ε through which a solution of concentration $[D]_s$ is flowing at a flow rate of Q with an interstitial velocity of u. The packed bed consists of fibres that are represented by cylinders (figure 4.1).

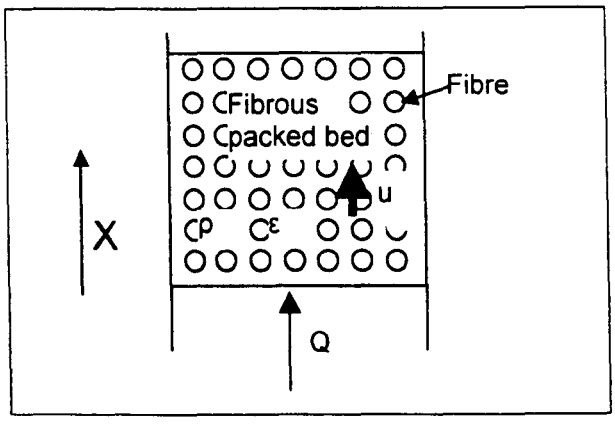

Figure 4.1: Axial Flow Model of Vosoughi et al.

The transport in the packed bed is represented by a dispersed plug flow model. Thus the supply of dye from the dyebath to the fibre surface consists of the additive effects of convective and dispersive flow. This dispersive flow, R_D, is defined similarly to the diffusional transport but represents a macroscopic transport of material. In analogy to Fick's First Law of diffusion, a dispersion coefficient, D_D, is defined so that the dispersive flow is:

$$R_D = D_D \frac{\partial [D]_s}{\partial x} \tag{4.19}$$

A mass balance of the system within an elemental volume of the packed bed yields the following second order partial differential equation:

$$D_D \frac{\partial^2 [D]_s}{\partial x^2} - \frac{\partial [D]_s}{\partial t} - u \frac{\partial [D]_s}{\partial x} = \frac{\rho_p}{\varepsilon} \frac{\partial [D]_f}{\partial t} \tag{4.20}$$

The first term in the equation constitutes the amount of dye transferred by dispersive flow and the third term the amount of dye transferred by convective flow. The right hand of the equation describes the amount of dye taken up or lost by the fibre. A solution of this equation will give the dye distribution in the interstitial spaces along the packed bed. For its solution four boundary conditions are required. They are:

1) At the entrance of the packed bed for time equal to zero:

$$D_D \frac{\partial [D]_s}{\partial x} = u\left([D]_{s(x=0)} - [D]_{s(x=0-)}\right) \tag{4.21}$$

x=0-: Location immediately before entering the packed bed

2) At the exit of the packed bed:

$$\frac{\partial [D]_s}{\partial x} = 0 \tag{4.22}$$

3) At time equal to zero, within an elemental volume of the packed bed

$$[D]_s = 0 \tag{4.23}$$

$$[D]_f = 0 \tag{4.24}$$

From the interstitial solution, the dye adsorbs on the surface of the fibres according to modified Langmuir kinetics:

$$\frac{d[D]_{fs}}{dt} = k_a [D]_s^{\alpha} \left([D]_{sat} - \beta [D]_{fs} \right) - k_d [D]_{fs} \tag{4.25}$$

The exponent α and the coefficient β are empirical constants, which assume a value of one for the normal Langmuir equation and can be adjusted to improve the fit of experimental data.

From the fibre surface, the dye enters into the fibres by radial diffusion which is simulated by Fick's Second Law, assuming a diffusion coefficient that is independent of the dye molality and salt concentration. The temperature dependency of D is modelled with the Arrhenius equation. The two remaining boundary conditions, in addition to the fibre surface molality, correspond to those employed by Reddy et al. described in the previous section.

The dye molality at any location in the packed bed, $[D]_f$, is equal to the average molality in the fibre, i.e. the integral of the dye concentration in the fibre, $[D]_{fi}$, over the radius a for the fibre, at that same location:

$$[D]_f = \frac{2}{a^2} \int_0^a [D]_{fi} \, r dr \tag{4.26}$$

The solution of this system of coupled differential equations was found by finite difference numerical methods. The accuracy of the numerical solver was generally better than 3% and therefore sufficient for practical applications.

The model's predictions have not been verified experimentally. From a theoretical point of view the inclusion of dispersive flow is noteworthy. The treatment of dye adsorption at the fibre surface is rather simplistic since all electrostatic effects are ignored. This lack would be expected to reduce the accuracy of predictions for ionic dye systems such as direct dyes on cellulosics.

4.2 Other Models

One characteristic of cotton fibres is the fast initial dye uptake speed, as has been pointed out before. The phenomenon of the "First Strike" led some researchers to develop 2-phase exhaustion models that consist of a surface layer that is rapidly accessible to the dye and an interior layer that is accessible only by diffusion (Cleve 1997, Kretschmer 1990a). The surface layer acts like a buffer in which dye is temporarily stored before it diffuses into the interior of the fibre. An important difference to diffusion-only models is that in the diffusion-only models the dye surface layer has no volume of its own. It merely enters the diffusion equation as a boundary condition at the fibre surface. In 2-phase models, however, the surface layer has a finite volume capable of "storing" dye. The model of Cleve et al. is presented in more detail below.

4.2.1 Cleve et al. Model

Instead of using a dyeing vessel, the researchers employed column chromatography for their kinetic analysis. The thermostatted column was filled with cotton yarn in lengthwise direction and dye solution of constant dye concentration was pumped into the column from a reservoir. At the column's exit, transmittance of the solution was measured spectrophotometrically to estimate dye uptake (figure 4.2).

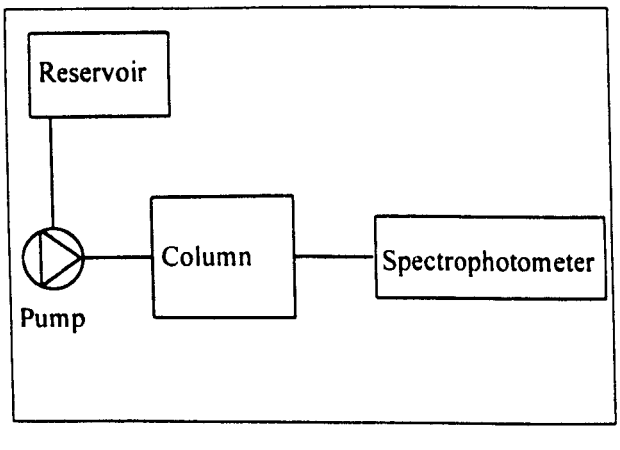

Figure 4.2: Experimental Set-up of Cleve et al.

The 2-phase model distinguishes between the outer fibre surface (subscript fs) and inner fibre surface (subscript fi) which adsorb (k_{fs}, k_{fi}) and desorb (d_{fs}, d_{fi}) the dye at different rates (figure 4.3).

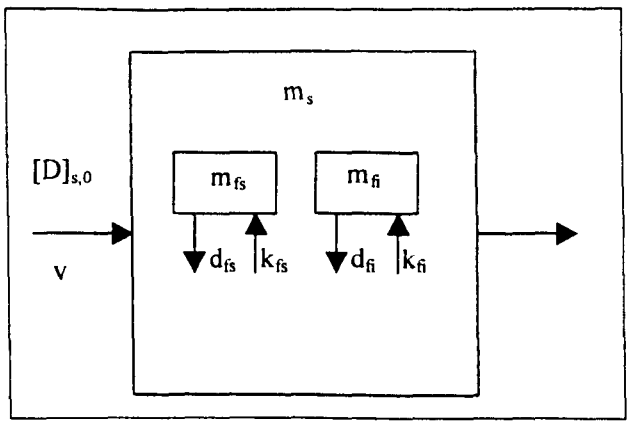

Figure 4.3: Scheme of Mass Flows Cleve et al.

The mass balance for the amount of dye in the solution of the column, m_s, is:

$$\frac{dm_s}{dt} = [D]_{s,0}v - \left(k_{fs} + k_{fi}\right)m_s - \frac{v}{V}m_s + d_{fs}m_{fs} + d_{fi}m_{fi} \qquad (4.27)$$

v = Flow rate solution [$cm^3.min^{-1}$]

V = Volume column [cm^3]

d_{fs}, d_{fi} = Dye desorption constants [min^{-1}]

k_{fs}, k_{fi} = Dye adsorption constants [min^{-1}]

m_{fs}, m_{fi} = Dye amounts in fibre [mg]

The first term in the equation describes the amount of dye entering the column. The second term shows that the model assumes first-order kinetics for the dye uptake from solution. The third term quantifies the amount of dye leaving the column and the last two terms describe the amount of dye desorbed from the inner (m_{fi}) and outer (m_{fs}) fibre layer.

The change of the dye amount in the fibre surface and the fibre interior may then be written as:

$$\frac{dm_{fi}}{dt} = k_{fi}m_s - d_{fi}m_{fi} \qquad (4.28)$$

$$\frac{dm_{fs}}{dt} = k_{fs}m_s - d_{fs}m_{fs} \qquad (4.29)$$

Substitution of these two equations in equation 4.27 yields a linear third order differential equation which has an analytical solution of the general form:

$$m_s = c_1 e^{\lambda_1 t} + c_2 e^{\lambda_2 t} + c_3 e^{\lambda_3 t} + [D]_{s,0}v \qquad (4.30)$$

The coefficients c_1 to c_3 can be calculated from six boundary conditions which essentially state that the column is initially free of dye. The coefficients λ_1 to λ_3 are derived from a separate set of algebraic equations.

Once m_s is known as a function of time, the time dependency of the dye amounts in the outer and inner layer of the fibre can be also determined. Cleve et al. used the least square method to choose the adsorption and desorption constants that gave the best fit of experimental data. From experiments with C.I. Direct Blue 225 they suggested that about 50% of the total dye on the fibre were sorbed in the fast-adsorbing surface layer at equilibrium condition. The surface layer reached equilibrium condition after about 5 minutes in their simulation. The adsorption and desorption constants of the surface layer were about 2000 times higher than those of the fibre interior. The model was later used to analyse the sorption behaviour of trichromatic direct dye mixtures (Duffner et al. 2000).

Overall, the model appears to be very well suited to simulate the dyeing characteristics of direct dyes on cotton, especially their First Strike. The model has the advantage that an analytical solution exists, eliminating the need for a numerical solver and its associated error. This could only be achieved by sacrificing any attempt to make use of more fundamental thermodynamic and kinetic laws and the assumption of a uniform dye concentration in the column is also simplistic. As a result employing the model for predictions under varying dyeing conditions would involve a large number of dyeings for the calculation of the coefficients by statistical means. Even then, extrapolations to dyeing conditions differing from those employed in the experiments would probably be of doubtful quality.

4.3 Boundary Layer Phenomena

As was pointed out in chapter one, the exhaustion can be delayed if the dyeliquor circulation rate is not sufficient to transport the dyestuff faster to the fiber surface than the rate it is sorbed by the fibre. The influence of the liquor flow rate on the exhaustion rate has been known for a long time (Armfield 1947) and was confirmed several times since then (Etters 1988, Alexander 1950, Vickerstaff 1954:144, Brooks 1972). The reduced uptake is caused by a lack of dye supply at the fibre surface, the adsorption speed, however, does not change.

The effect of the boundary layer on the exhaustion speed can be explained mathematically under certain assumptions. Provided a constant diffusion coefficient, a Langmuir-type or Freundlich-type sorption isotherm and infinite bath, it can be shown that the overall diffusion speed depends on the dimensionless variable L[7] (McGregor 1965). For a Langmuir isotherm, L becomes:

---

[7] L is introduced in one of the boundary conditions in the solution of Fick's Second Law.

$$L = \frac{D_s l}{D_f \delta K}\left(\frac{[D]_{sat}}{[D]_{sat} - [D]_{f,eq}}\right) \tag{4.31}$$

For a Freundlich isotherm (n = 0.5) L becomes

$$L = \frac{D_s l}{D_f \delta K^2}\left([D]_{f,eq} + [D]_f\right) \tag{4.32}$$

D_s = Diffusion coefficient in the boundary layer [$m^2.s^{-1}$]

D_f = Diffusion coefficient in the fibre [$m^2.s^{-1}$]

δ = Diffusional boundary layer thickness [m]

K = Equilibrium partition coefficient

l = Fibre radius or half-thickness of sheet [m]

The smaller the value of L is, the more the system is controlled by liquid diffusion, i.e. the higher the influence of the boundary layer on the dye uptake rate. The equations show that L is reduced by an increase in the boundary layer thickness, δ, e.g. due to a lower flow rate. Bulk flow velocity, v_0, and boundary layer thickness can be quantitatively correlated if the model of a plane sheet immersed in a flow parallel to its axis is employed. In this system, the average boundary layer thickness is (McGregor 1965):

$$\overline{\delta} = 1.47\left(\frac{D_s}{\nu}\right)^{\frac{1}{3}}\sqrt{\frac{\nu l}{\upsilon_0}} \tag{4.33}$$

ν = Kinematic viscosity of water [$m^2.s^{-1}$]

l = Length of plate in the direction of flow [m]

v_0 = Bulk flow velocity [$m.s^{-1}$]

The term "average" boundary layer thickness is used to indicate that δ is a function of l and that δ is averaged over l. Using equation 4.33 the correlation between L and v_0 becomes:

$$L \propto \frac{1}{\delta} \propto \sqrt{v_0} \tag{4.34}$$

Thus doubling the bulk flow velocity results in a 1.4-fold increase in L. While the boundary layer thickness therefore decreases fairly rapidly with an increase in the bulk flow rate for flow parallel to the fibre surface, δ hardly varies with the velocity of the bulk liquid for sideways flow through the fabric, i.e. if the fabric and the liquor flow are at a 90 degrees angle to each other (Kretschmer 1990b).

Equations 4.31 and 4.32 also show that L becomes smaller for a high partition coefficient, i.e. high dye substantivity and for a high diffusion coefficient in the fibre. The dyeing process would therefore be more sensitive to changes in the liquor flow rate under high substantivity conditions. However, L does not change during the dyeing process with direct dyes if a Langmuir isotherm is assumed as the increase in K with increasing salt

concentration is compensated by a decrease in the D_f (McGregor 1965). Since, additionally, many high affinity direct dyes (high K-value) have lower than average diffusion coefficients it would seem that both effects on L tend to cancel each other out. In the case of a Freundlich isotherm, L increases (i.e. less sensitivity to boundary layer) during the dyeing process because $[D]_f$ increases. For both types of isotherm it is true that L is smaller at low dye concentrations (small $[D]_{f,\infty}$).

For L-values bigger than 10, the system is for practical purposes determined by film diffusion only. Commercial dyeing machines are estimated to have an L-value of about 20 and would therefore be little influenced by boundary layer phenomena (Etters 1994).

The initial model for which the parameter L was derived applied only to an infinite dyebath. Since then, the model has been extended to cover transitional (initially constant then continuously decreasing dyebath concentration) and finite (continuously decreasing dyebath concentration) dyebaths (Etters 1991). The model has been shown to be helpful in the explanation of polyester dyeing with disperse dyes (McGregor 1979).

Experiments with C.I. Reactive Blue 109 on cotton print cloth could only partially confirm the relationship expressed in equations 4.31 and 4.32 (Etters 1988). The tests showed, as expected, that a higher agitation rate led to a shorter half-time of dyeing, i.e. the time necessary to achieve 50% of equilibrium sorption. On the other hand, however, changes in dye concentration did not influence significantly the half-time. An explanation forwarded by the authors is that the relatively low values of K obtained for the range of dye and salt concentrations used in these experiments meant high values of L, indicating that the uptake is film diffusion and not liquid diffusion limited. That would explain why dye systems with higher partition coefficients like acid dyes on wool exhibit a dye uptake rate that is sensitive to the dye concentration.

A similar model was suggested by Gooding et al. who concluded from measurements with a channel flow cell, that for certain dyes the rate of adsorption is controlled by a porous surface layer (Gooding 1998). They confirmed that higher flow rates increased the rate of adsorption. They also found that high dye concentrations in the liquid bulk phase block the passage of the dyes through the porous surface layer and reduce the rate of adsorption.

One factor which has not been considered in the equations above, but nevertheless may led to the formation of a boundary layer, is the accessibility of the fibre to the dye which is heavily influenced by the geometrical arrangement of the fibres within the fabric. Compared to individual fibres for example, the exhaustion speed of cotton fabrics can be reduced by this effect by up to half. The effect decreases with increased dye concentration (Peters 1975:771, Hoffmann 1989:381). Interestingly, if the fibre density is further

increased, e.g. in yarn packages, the liquor circulation only barely influences the exhaustion speed unless the liquor circulation pump is very weak or the fabric construction very tight. This phenomenon is explained by the fact that a slower exhaustion in the outer parts of the package is compensated by an increased exhaustion speed due to the higher concentration in the inner package parts (Hoffmann 1977:668, Hoffmann 1989:382).

4.4 References

1. Alexander P, Hudson R F, Text. Res. J. 20 (1950) 481
2. Armfield N, J.S.D.C. 63 (1947) 381
3. Barrett N A, Cook C C, J.S.D.C. 93 (1977) 335
4. Brooks J H, J.S.D.C. 88 (1972) 184
5. Burley R, Wai P C, McGuire G R, Appl. Math. Modelling 9 (1985) 33
6. Carman P C, Haul R A W, Proc. Roy. Soc. 222A (1954) 109
7. Cleve E, Bach E, Schollmeyer E, Text. Res. J. (1997) 701
8. Crank J, in Crank J, Park G S (Eds.), Diffusion in Polymers (London: Academic Press 1968) 16 & 45
9. Denter U, Schollmeyer E, Textilver. 29 (1994) 238
10. Duffner H, Bach E, Cleve E, Schollmeyer E, Text. Res. J. 70 (2000) 223
11. Etters J N, Text. Chem. Col. 26 (1) (1994) 13
12. Etters J, J.S.D.C. 107 (1991) 114
13. Etters N, English S J, Text. Chem. Col. 20 (6) 1988 21
14. Gooding J J, Compton R G, Brennan C M, Atherton J H, J.S.D.C. 114 (1998) 85
15. Griffiths L H, Neale S M, Trans. Far. Soc. 30 (1934) 395
16. Hill A V, Proc. Roy. Soc. 104B (1928) 39
17. Hoffmann F, Mell. Textilber. 52 (1977) 665
18. Hoffmann F, Textilver. 24 (1989) 381
19. Hori T, Ikeoh S, Shimizu T, Sen-i Gakkaishi (Engl. Ed.) 38 (1982) T-83
20. Inglesby M K, Zeronian S H, Dyes and Pigments 50 (2001) 3
21. Jones F, in Johnson A (Ed.), The Theory of Coloration of Textiles, 2nd edition (Bradford: SDC 1989)

22. Kretschmer A, Text. Prax. Int. 45 (1990a) 265

23. Kretschmer A, Text. Prax. Int. 45 (1990b) 36

24. McBain J W, Z. Physikal. Chemie 68 (1909) 471

25. McGregor R, Etters J N, Text. Chem. Col. 11 (9) 1979 59

26. McGregor R, Mahajan I Y, Trans. Faraday Soc. 58 (1962) 2484

27. McGregor R, Peters R H, J.S.D.C. 81 (1965) 393

28. McGregor R, Peters R H, Petropolous J H, Trans. Faraday Soc. 58 (1962) 1045

29. McGregor R, Peters R H, Petropolous J H, Trans. Faraday Soc. 60 (1964) 2062

30. Neale S M, J.S.D.C. 52 (1936) 252

31. Neale S M, Stringfellow W A, J.S.D.C. 59 (1943) 241

32. Peters R H, Ingamells W, J.S.D.C. 89 (1973) 397

33. Peters R H, Textile Chemistry, Vol. III, The Physical Chemistry of Dyeing (Amsterdam: Elsevier 1975)

34. Reddy M, Jasper W J, McGregor R, Lee G, Text. Res. J. 67 (1997) 109

35. Shore J, in Shore J (Ed.), Cellulosics Dyeing, (Bradford: SDC 1995) 152

36. Vickerstaff T, The Physical Chemistry of Dyeing, 2nd edition (London: Oliver and Boyd 1954)

37. Vosoughi M, PhD Thesis, Heriot-Watt University, Edinburgh (1993)

38. Wai P C, PhD Thesis, Heriot-Watt University, Edinburgh (1984)

39. Weisz P B, Hicks J S, Zollinger H, Trans. Far. Soc. 63 (1967) 1801, 1807, 1815

40. Weisz P B, Zollinger H, Trans. Far. Soc. 64 (1968) 1693

41. Zollinger H, Color Chemistry, 2nd edition (Weinheim: VCH 1991)

5 Models correlating Dye Unlevelness with Process Parameters

It was pointed out in chapter one that an even dye distribution on the fibre at the end of the dyeing is, next to an acceptable colour match, the most important requirement that a successful process control has to fulfil. Mathematical models can be useful to identify major process parameters that are likely to have an influence on dye levelness and some important models are therefore reviewed below. In the second part of this chapter, the controlled sorption principle is explained because it constitutes the axiom of the method of approach underlying the present work.

5.1 Mathematical Models

Many of the models that quantify unlevelness, including the ones that are described below, refer to package, beam or loose stock dyeing machines. The operation principle that these machines have in common is that a dye solution is pumped (mostly in a radial manner) through a fibre mass, resulting in depletion of dye solution as dye is sorbed by the fibre. The fibre sections which are first exposed to the dye solution initially pick up more dye, since they sorb from a solution of higher concentration, than subsequent sections. This causes different dye amounts on the fibres in different locations and thus unlevelness.

The popularity of an analysis of the unlevelness in yarn packages results partly from their susceptibility to mathematical treatment thanks to their regular, geometrical shape. In many ways the system is similar to that of a packed bed reactor, which has been extensively modelled by chemical engineers. Additionally, yarn dyeing was and is an important method of dyeing textiles.

5.1.1 Hoffmann and Mueller Model

The model of Hoffmann and Mueller (figure 5.1, Hoffmann 1979) is based upon an earlier model of Boulton and Crank (Boulton 1952). It describes the one-directional flow through a package (or packed bed) of fibres and is essentially a simplified pre-cursor of the model of Vosoughi and Burley described in chapter four. Since the aim of the model is to make qualitative and not quantitative predictions about the influence of various process parameters on levelness, its simplicity is not a disadvantage. In fact, it may even be an advantage because the simulation results can more easily be related to the relationship between the parameters as they are expressed in the underlying equations.

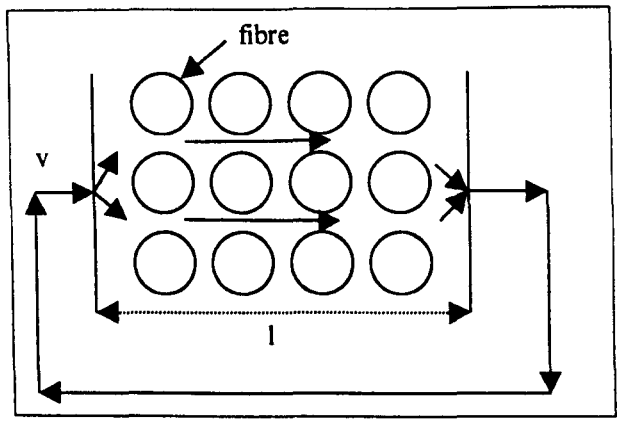

Figure 5.1: Schematic View of Hoffmann and Mueller Model

The mass balance for this system is:

$$v\frac{\partial[D]_s}{\partial x} = -\rho_p \frac{\partial[D]_f}{\partial t} - \left(1 - \frac{\rho_p}{\rho_f}\right)\frac{\partial[D]_s}{\partial t} \tag{5.1}$$

v = Flow velocity of dyebath [$m.s^{-1}$]

ρ_p = Package density [$kg.m^{-1}$]

ρ_f = Fibre density [$kg.m^{-1}$]

The dye molality $[D]_f$ and the concentration $[D]_s$ are not only a function of time but also of place. The dye is assumed to diffuse into the fibre interior according to Fick's Second Law for one-directional flow into a cylinder. The diffusion coefficient is deemed to be independent of dye and salt concentration and its temperature dependency follows the Arrhenius equation. The fibre surface molality is defined by a Nernst-isotherm and the usual boundary conditions apply. The two differential equations are linked since

$$[D]_f = \frac{2}{a^2 \rho_f}\int_0^a [D]_{fi}\, r\, dr \tag{5.2}$$

$[D]_{fi}$ = Dye molality fibre interior [$mol.kg^{-1}$]

It is further assumed that the dyebath is well mixed, so that it is of uniform concentration once it leaves the package. Dye levelness, Le, is evaluated by the (dimensionless) ratio of the maximum and minimum dye concentration in the package:

$$Le = \frac{[D]_{f,\min}}{[D]_{f,\max}} \tag{5.3}$$

The equations were solved analytically and calculations with this model have been made for isothermal conditions and varying other process parameters.

For the purposes of the current work, the model is of only limited usefulness because its assumption of a diffusion-controlled process generally does not apply to the dyeing of

cotton with direct dyes. Furthermore, the assumption of an adsorption that follows a Nernst-isotherm does not describe the situations for direct dyes correctly. Nevertheless, there are important conclusions that may be drawn from the simulations:

1) Le increases, and unlevelness therefore decreases, in approximately linear fashion with the dyebath flow rate at constant exhaustion speed.

2) There is an approximately inverse linear relationship between the fraction of the dye remaining in the dyebath at the end of the process and the time it takes to reduce dye unlevelness to an acceptable degree. Consequently, at high bath exhaustion values process time increases drastically if dye application is not level from the start onwards.

5.1.2 Medley and Holdstock Model

The model of Medley and Holdstock does not attempt to accurately simulate dyeing kinetics. The focus is rather on the derivation of a theory that would allow the determination of the process profile for a package dyeing machine that yields the specified unlevelness in the minimum amount of time (Medley 1980, Holdstock 1988). Their efforts lead to the development of the "Simple Depletion Theory" described below.

On its way through the fibre bed or package of volume V (figure 5.2), the dye solution concentration reduces from $[D]_s$ to $[D]_s - \Delta[D]_s$. The drop in $[D]_s$ per liquor circulation is therefore $\Delta[D]_s$ and it can be written that:

$$\Delta[D]_s = -\frac{LR}{F}\frac{\partial[D]_s}{\partial t} \tag{5.4}$$

LR = Liquor ratio [$dm^3.kg^{-1}$]

F = Liquor flow rate [$dm^3.kg^{-1}.s^{-1}$]

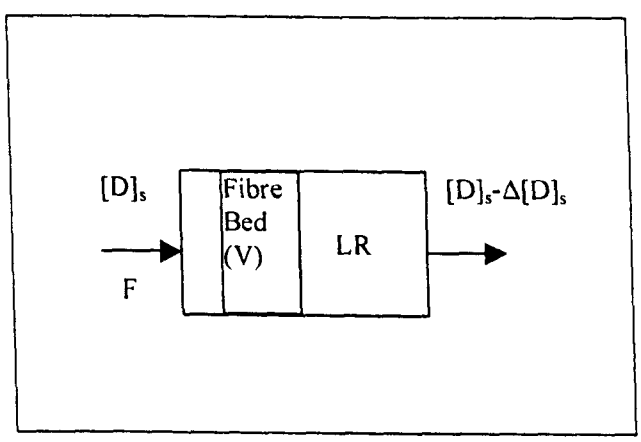

Figure 5.2: Simple Depletion Theory

The simple mass balance for the system is:

$$\frac{\partial [D]_f}{\partial t} = -\frac{M_0}{[D]_{s,0}} \frac{\partial [D]_s}{\partial t} \tag{5.5}$$

M_0 = Total amount of dye in the system [mol.kg^{-1}]

$[D]_{s,0}$ = Initial dyebath concentration [mol.dm^{-1}]

Substitution of 5.4 in 5.5 and rearrangement yields:

$$\frac{1}{M_0} \frac{\partial [D]_f}{\partial t} = \frac{F}{LR} \frac{\Delta [D]_s}{[D]_{s,0}} \tag{5.6}$$

In the simplest, idealised case the dye sorbs according to a Nernst isotherm on the fibre surface. This assumption leads to a dye uptake rate which is approximately proportional to the dyebath concentration. It may be then concluded that the fractional dye deposition error (DDE) between the entrance ($[D]_s$) and the exit of the package ($[D]_s$-$\Delta[D]_s$) is:

$$DDE \propto \frac{[D]_s - ([D]_s - \Delta [D]_s)}{[D]_s} = \frac{\Delta [D]_s}{[D]_s} \tag{5.7}$$

Let R be the specified tolerance for the dye deposition error that may not be exceeded during the dyeing process. The following condition may then be formulated:

$$-\frac{1}{[D]_{s,0}} \frac{\partial [D]_s}{\partial t} = \frac{1}{M_0} \frac{\partial [D]_f}{\partial t} \leq \frac{F}{LR} \frac{R}{[D]_{s,0}} [D]_s \tag{5.8}$$

Two important conclusions may be drawn from expression 5.8:

1) The permissible exhaustion speed is proportional to $F.LR^{-1}$, i.e. the bath circulation frequency. In other words, the higher the bath circulation frequency the higher the permissible exhaustion speed.

2) The permissible exhaustion speed must drop in line with $[D]_s$ if the DDE is to remain below the required level. As a consequence, the dye uptake rate would have to progressively decrease throughout the dyeing process.

In the more general case of a sorption behaviour that does not follow a Nernst isotherm the authors show that DDE is proportional to the following parameter:

$$DDE \propto \frac{[D]_s}{[D]_f} \frac{\partial [D]_f}{\partial [D]_s} \frac{\Delta [D]_s}{[D]_s} \tag{5.9}$$

The second part of this parameter, $d[D]_f.d[D]_s^{-1}$, describes the sensitivity of the dye fibre molality to changes in the dyebath concentration and may be interpreted in the special case of constant temperature as the slope of the sorption isotherm. Since this term usually

increases towards the end of the dyeing process, the required decrease in the exhaustion speed of equation 5.8 is even accentuated.

Based upon equation 5.8 it is suggested to use the following inequality as the central control parameter during the exhaustion phase:

$$Q = -\frac{1}{[D]_s}\frac{\partial [D]_s}{\partial t} \leq \frac{F}{LR} R \tag{5.10}$$

At constant bath circulation frequency, the result is a logarithmic profile of $[D]_s$ of the form $[D]_s = e^{-Qt}$ and an exponential profile of $[D]_f$ which are shown for arbitrary time units in figure 5.3.

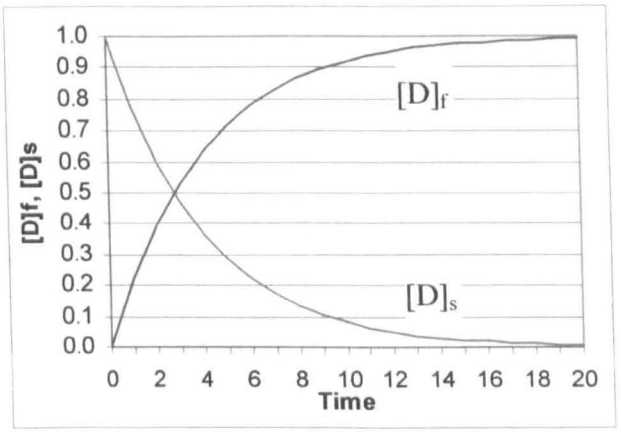

Figure 5.3: Schematic of Ideal Exhaustion Profile according to Simple Depletion Theory

5.1.3 Nobbs and Ren Model

One important purpose of the model developed by Nobbs and Ren (Ren 1985) is to quantify the dye deposition error in a yarn package as a function of the dyeing conditions during the process. The simulation of the kinetics is therefore kept fairly simple although it is more elaborate than in the model of Medley and Holdstock.

The model assumes that the dye uptake rate at any point inside the package follows first order kinetics:

$$\rho \frac{\partial [D]_{fi}}{\partial t} = \frac{\varepsilon}{1-\varepsilon} k_a [D]_s \tag{5.11}$$

ε = Voidage of the package [-]

k_a = Dyeing rate constant inside the package [s^{-1}]

A mass balance for an infinitely small element inside the yarn package yields:

$$\varepsilon \frac{\partial [D]_s}{\partial t} = -\frac{F}{2\pi r l} \frac{\partial [D]_s}{\partial r} - (1-\varepsilon)\rho \frac{\partial [D]_{fi}}{\partial t} \qquad (5.12)$$

F = Liquor flow rate [$m^3.s^{-1}$]

R = Radius of location inside the yarn package [m]

l = Package height [m]

Substitution of 5.11 in 5.12 and division by ε results in:

$$\frac{\partial [D]_s}{\partial t} = -\frac{F}{2\pi r l \varepsilon} \frac{\partial [D]_s}{\partial r} - k_a [D]_s \qquad (5.13)$$

In equation 5.13 k_a is the local rate constant of the dye uptake, not to be confounded with the overall, averaged rate of dye uptake of the entire package, K_a. A relationship between k_a and K_a has been derived based on the assumption of a first order dye uptake rate for the entire package. The resulting first order partial differential equation is then integrated by separation of variables so that the dye concentration can be predicted by applying suitable boundary conditions for any location inside the package at any moment during the dyeing process.

The incremental dye deposition error, DDE, is a function of time and is defined as the difference between the dye uptake rate at the inside of the package, $[D]_{fi,A}$, and at the outside of the package, $[D]_{fi,B}$:

$$DDE = \frac{\partial [D]_{fi,A}}{\partial t} - \frac{\partial [D]_{fi,B}}{\partial t} \qquad (5.14)$$

The overall dye deposition error, DDE_Σ, is the concentration difference at these two locations at the end of the process:

$$DDE_\Sigma = [D]_{fi,A} - [D]_{fi,B} = -(V - V_s)\frac{V}{V_s} \int \left[\frac{1}{F[D]_s} \left(\frac{d[D]_s}{dt} \right)^2 \right] dt \qquad (5.15)$$

The minimum of DDE_Σ is obtained by setting its time derivative equal to zero. The root of this time derivative equation is

$$\frac{1}{F[D]_s} \left(\frac{d[D]_s}{dt} \right)^2 = const \qquad (5.16)$$

The best exhaustion profile, i.e. the one giving the least overall dye deposition error, must therefore follow a quadratic profile. The dyebath concentration decreases according to equation 5.17, where $[D]_{s,0}$ is the initial dyebath concentration and t_d is the desired exhaustion time.

$$[D]_s = [D]_{s,0}\left(1 - \frac{t}{t_d}\right)^2 \tag{5.17}$$

Figure 5.4 shows a comparison of an exponential profile, as suggested by the model of Medley and Holdstock, with a quadratic profile as derived from the model of Nobbs and Ren.

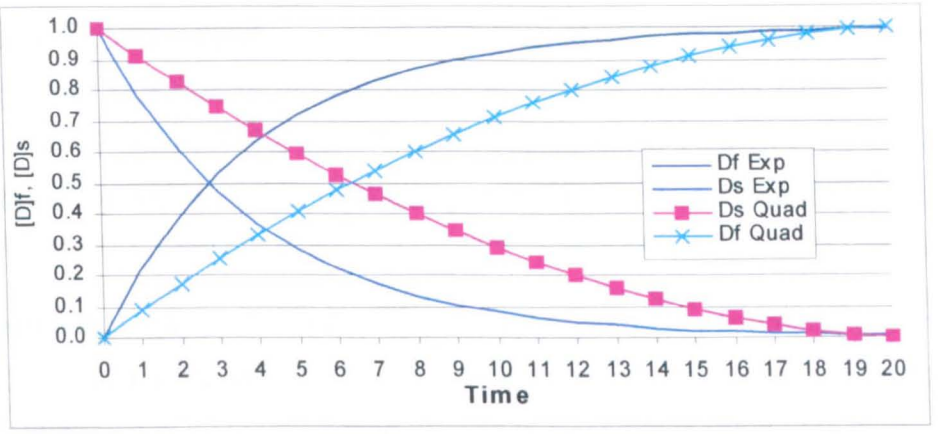

Figure 5.4: Comparison of Exponential and Quadratic Exhaustion Profile

In summary, all models emphasise the influence of the liquor flow rate on dye levelness. The models also suggest that the dye uptake rate at later stages during the process should be reduced since the dye fibre surface molality becomes more sensitive to changes in the dyebath concentration. Caution is warranted, however, in translating these results to the situation on a jet dyeing machine. First of all, a jet dyeing machine also involves the circulation of the substrate, which none of the models above include. Secondly, there is no easy way to geometrically describe the shape of the fabric load in a jet dyeing vessel since the fabric rope changes its form and its compression state continuously. Third, the liquor flow through the fabric rope does not follow any clear pattern. Part of the dyebath certainly penetrates the fabric almost perpendicularly to the direction of movement of the rope in the jet nozzle, but fabric-liquor interchange also occurs in the storage chamber where the flow pattern is anything but clear. Finally, none of the models uses assumptions about the dyeing rate and equilibrium sorption that would be generally realistic for direct dyeings of cotton. For these reasons building a mathematical model that would simulate unlevelness on a jet dyeing machines appears to be a very complex task and has not been attempted in this work. It is thought, however, that many valuable conclusions may be drawn from a closer analysis of experimental results of other researchers. They are reviewed in the next part of the chapter.

5.2 Controlled Sorption

Dye exhaust processes may be classified into two principal categories (Carbonell 1976):

1) Migration processes

2) Processes of controlled sorption

Migration processes achieve the required degree of dye levelness by relying on the migration properties of the dyes. Since the dye uptake rate is not controlled an initial unlevelness results that is subsequently gradually reduced by desorption and re-adsorption of the dyes. Dye migration is facilitated by high dyebath concentration, i.e. low exhaustion, and high temperature, which increases the dye desorption rate and the dye migration in the dyeliquor.

The aim of a controlled sorption is to limit the dye uptake rate at any stage during the process so that the tolerated degree of unlevelness is never exceeded. Control of the dye uptake rate is not limited to temperature control, but also includes dosing of dye, electrolyte, alkali, acids, etc. in short all the parameters that strongly influence the exhaustion speed for a particular dye fibre system (Carbonell 1987). Controlled sorption requires that the sorption speed is always smaller than the speed with which the dye is transported to the fibre. In other words: The demand of dye from the fibre has always to be smaller than the supply of dye from the dyebath. This is achieved by controlling the dye uptake rate during the sorption process accordingly. In a diffusion-controlled process such as polyester dyeing with disperse dyes, the temperature gradient is chosen such that the rate of dye uptake from the fibre does not exceed the supply from the dye bath at any moment during the exhaustion phase.. In a substantivity-controlled process like direct dyes on cotton the same is achieved by choosing a not too high salt dosing gradient.

There are several reasons why controlled sorption is superior over migration strategies. The most important one is that the migration strategy leads to poor colour reproducibility. This is the case because migration only occurs in a significant way at low levels of dye exhaustion. The higher the dye substantivity is the higher is the bath exhaustion and the lower is the migration tendency (Rattee 1974:281). At low bath exhaustion, process reproducibility is low because the exhaustion is sensitive to minor process variations (Carbonell 1982, Bradbury 1993). Since reproducibility is the key to the economic operation of a dyehouse under competitive conditions, the migration strategy is unacceptable for this reason alone. Controlled sorption also enhances reproducibility because it requires the automation not only of temperature control but also of salt, alkali and acid additions so that errors from manual interventions are minimised.

Second, dyes with high migration tendency inherently have low wet fastness (Breuer, Rattee 1974:281). Vice versa it is also true that dyes with high wet fastness tend to migrate very little. Since fastness requirements continue to increase, dye selection could exclude in many cases the application of the migration strategy. If, on the other hand, controlled sorption is used, then the dyes' low migration tendency does not negatively influence levelness (Hoffmann 1990:51).

Additionally, one disadvantage of the migration strategy is that it is not possible to improve the levelness of the dyeing through migration if the migration behaviour of each dyestuff in a multi-dyestuff recipe is different from one another (Leube 1978). The time necessary to compensate for initial unlevelness would also vary depending on substrate, style, dyestuff and dyeing conditions and if the migration time were adjusted for the worst case, resources would be wasted. Even for high migrating dyes a controlled sorption strategy is therefore advantageous, reducing the time required for dye levelling (Hoffmann 1990:51).

Finally, controlled sorption often leads to shorter process times. Batch time reductions of up to 40% are reported, additional benefit coming from a reduced percentage of additions and a diminished consumption of auxiliaries, mainly levelling agents (Carbonell 1984, Hoffmann 1998, Drechsel 1998).

Overall, it is therefore clear that controlled sorption is the preferred method of process control. Since its aim is to keep dye unlevelness within defined limits during the entire process two questions arise. They are: What is the tolerable level of unlevelness? And which parameters have to be controlled in order to achieve this goal. The parameters that could influence levelness are reviewed in the following sections.

5.2.1 Dye Uptake Rate, significant and critical Exhaustion Speed

It is known for over half a century that the dye uptake rate correlates with dye unlevelness (Boulton 1944): If the dye uptake rate was high, the result would be increased and often unacceptable unlevelness. Efforts to quantify the relationship between exhaustion speed and unlevelness lead to the development of the significant exhaustion speed, v_{sig} (Ruettiger 1972). Its authors claimed that, unlike previous attempts that were applicable only under a narrow range of conditions (Richter 1971, Mayer 1968, von der Eltz 1972, Beckmann 1968), v_{sig} would provide a means to compare the inherent tendency to unlevelness of process profiles for different dye-fibre systems. It can be interpreted as the weighted, average exhaustion speed.

For the calculation of v_{sig} the exhaustion curve is divided into around ten segments which approximate it in a linear fashion (figure 5.5). The values of the different segments, v_i, are then weighted to form v_i' by taking into account the fractional contribution of the segments to the exhaustion reached at the end of the process. As the reference value of the exhaustion is the endpoint of the particular dyeing, the total of all ΔEs always adds up to 100%.

The significant exhaustion speed is therefore

$$v_{sig} = \sum_{i=1}^{n} v_i' = \sum_{i=1}^{n} v_i \Delta E_i = \sum_{i=1}^{n} \frac{\Delta E_i}{\Delta t_i} \Delta E_i = \sum_{i=1}^{n} \frac{\Delta E_i^2}{\Delta t_i} \qquad (5.18)$$

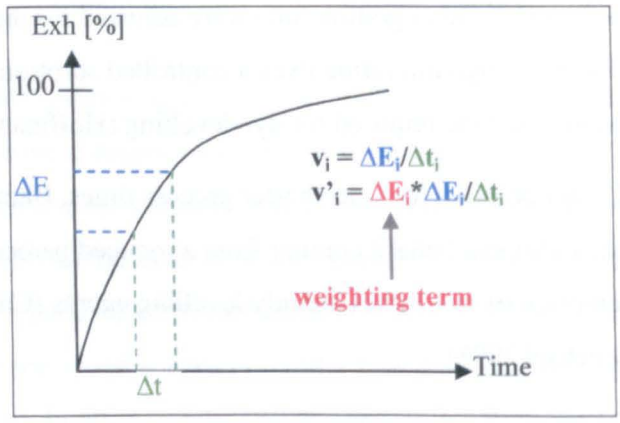

Figure 5.5: Calculation of v_{sig}

Experimental evaluations of different dyeings according to this method gave good correlation with unlevelness provided they were all undertaken on the same machine. When the same recipes were transferred to a different dyeing machine, the sequence of the dyeing samples in terms of their unlevelness remained the same but the absolute values of the levelness changed. The authors therefore concluded that for each dyeing machine there would be a critical exhaustion speed, v_{crit}, which, when exceeded, would lead to unacceptable results. v_{crit} is a value unique for a particular machine and depends on the liquor circulation rate, on the type of construction, on the geometry of the substrate and other factors. It is of course also a function of the tolerated degree of unlevelness. When the latter was set to a maximum concentration difference of 4%, the v_{crit} was found to be between 0.9 and 2.1%.min^{-1} for several production package dyeing machines.

5.2.2 Contact for Liquor and Fabric Flow

It soon became clear that the most important machine related factor is the bath circulation frequency or, more generally speaking, the dyeliquor-substrate interaction (Carbonell 1973). The suggestion was consequently made to express the exhaustion speed not in

exhaustion per time but in exhaustion per bath circulation. One bath circulation can be interpreted as one contact between a particular location on the substrate and the dyeliquor, hence the name exhaustion per contact.

In the case of a jet machine, as both fabric and liquor circulate, one circulation of the fabric is considered one contact as well as one circulation of the liquor, i.e. the contacts of dyebath and fabric are added (Hasler 1985). The contact is therefore a function of dyebath flow rate, dyebath volume, fabric speed and rope length. The faster liquor and fabric are turning, the higher is the interaction between fabric and liquor and the higher the number of contacts per minute. Subsequent experience showed that an additional factor is needed to take into account the geometrical design of the jet machine and its influence on the dyeliquor-substrate interaction (Carbonell 2002).

Since the introduction of the contact concept, many authors confirmed in laboratory tests and industrial-scale dyeings that a substrate is sufficiently level as long as a certain exhaustion per contact is not exceeded (Carbonell 1985, Bohrer 1990, Hoffmann 1989:385).

Experiments with reactant fixable dyes have shown that the maximum permissible relative bath exhaustion per contact ranges from 0.8 to 1.2 (Hasler 1987). For package dyed acrylic yarn acceptable unlevelness was achieved if the dyeing rate did not exceed 1.5% per contact (Gilchrist 1995:156). On a jet dyeing machine 4% per contact was seen as the limit value for disperse dyes on polyester (McCall 1979). It has also been claimed that it is generally recognised that in bulk production the dye uptake rate should be less than 2% per machine or process cycle in order to obtain commercially acceptable unlevelness (McGregor 1997).

The findings suggest that the maximum permissible exhaustion speed per contact is not a constant but varies between around 0.8% and 4.0%. Part of this variation is certainly due to different levelness requirements which are rarely disclosed in the cited literature. A variation in the limit value of a factor 5 indicates, however, that parameters other than the exhaustion speed and the circulation speeds of bath and fabric play an additional role in determining the levelness of the dyeing.

5.2.3 Shape of the Exhaustion Curve

One implication of the significant exhaustion speed is that a linear exhaustion results in the shortest exhaustion time for a certain value of v_{sig}. Consequently, a linear exhaustion profile has been advocated as the optimum (Schoenpflug 1975, Hasler 1975) and also featured prominently in the concept of isoreactive dyeing (Cegarra 1967, Carbonell 1968, Cegarra

1976, Cegarra 1979), developed independently of v_{sig}. A method to calculate the required temperature and salt dosing gradients for linear exhaustion per contact has been devised (Carbonell 1973). It was also realised that dye sorption has to be controlled only in a critical zone of exhaustion in order to achieve acceptable unlevelness. For nylon, it was found that uncontrolled dye sorption of the first approximately 20% did not adversely affect final unlevelness, especially when auxiliaries were used which improved the interfacial dye migration without affecting the final dye exhaustion (Annen 1979). The critical zone of exhaustion corresponds to a critical start and end temperature or acid concentration.

Starting in the mid-1970s some questions were raised as to whether a linear exhaustion profile is indeed the best option. One indication came from the analysis of the mode of action of levelling agents in the dyeing of wool with acid dyes (Brooks 1974). It was shown that unlevelness in the presence of certain levelling agents was significantly reduced at an exhaustion speed and profile identical to the reference without auxiliary. The effect could be explained in that the dye fibre surface molality in the presence of the levelling agent hardly changed during the final stages of the process whereas it sharply dropped without it. The conclusion was therefore that the sensitivity of concentration changes at the fibre surface to changes in the dyebath concentration played an important role in explaining unlevelness. It could also be derived that unlevelness created at later stages during the dyeing cycle contributed more to the final unlevelness than earlier stages.

These conclusions were tested in a subsequent series of experiments, again with an acid dye on wool (Brooks 1975). Different exhaustion profiles were compared and the best results were achieved with an exponential profile, closely followed by a profile in which the exhaustion was proportional to the square root of time. Linear exhaustion gave considerably worse unlevelness. The results are in good agreement with the predictions of the unlevelness model of Medley and Holdstock described above.

Other experimental evidence only partly supports these findings. The importance of the concentration changes at the fibre surface for unlevelness, and the significant role that levelling agents play in it, was confirmed in dyeings of acrylic with basic dyes and polyamide with acid dyes (Hoffmann 1989:385). Those dyeings with the smallest molality changes at the fibre surface had the lowest unlevelness. In dyeings of acrylic packages with a basic dye, the prediction of the model of Nobbs and Ren was confirmed that a quadratic exhaustion profile would give better results than either a linear or an exponential one (Gilchrist 1995). Experiments with direct dyes on cotton, however, could not find a significant difference in levelness between a linear salt dosing curve, i.e. a gradually decreasing exhaustion speed, and a progressive salt dosing curve that resulted in linear exhaustion (Luebbers 1990).

In all, there is convincing evidence that the shape of the exhaustion curve does play a part in determining unlevelness. It would therefore appear that the v_{sig}-concept, which favours linear exhaustion, is only a crude approximation and in many cases may not yield the best correlation between unlevelness and exhaustion speed. It is less clear which shape would be the optimum because the models that have derived a preferred shape, such as those of Medley et al. and Nobbs et al., are based on assumptions about dye sorption which are not accurate in many instances. But they probably correctly conclude that in the final stages of the exhaustion, when the dyebath concentration changes drastically for each percent of additional exhaustion, the exhaustion speed should be reduced compared to the early process stages. An additional reason in favour of this argument is the observation that the high dyebath molality at the start of the process encourages (interfacial) migration and reduces unlevelness (Annen 1980).

The question then remains how much the exhaustion speed should be reduced during the process. The likely answer is that it depends on the individual recipe and that there is no exhaustion profile which is universally better than any other. This would also explain why, as mentioned above, results from experiments on different dye-fibre systems and undertaken under particular conditions, do not converge. The preliminary conclusion is that the change in the dye concentration at the fibre surface per contact is a second parameter which needs to be taken into account when predicting unlevelness.

5.2.4 Auxiliaries

It was already pointed out that the addition of certain chemicals improves unlevelness. These chemicals are not necessarily levelling agents in the traditional sense because their positive effect is not due to their retarding action on the exhaustion speed. One principal reason for their effectiveness is their interaction with the dye reducing the concentration of monomolecular dye initially, e.g. by the formation of micelles, and then releasing dye molecules as the dyebath concentration drops (Brooks 1975). As a result the concentration of dye available for sorption on the fibre remains nearly constant during the process. Thus, these auxiliaries may in fact reduce the exhaustion speed under identical process conditions because the effective dyebath concentration is reduced, but even if this effect is compensated, e.g. by an increased temperature or salt dosing gradient, their beneficial influence on unlevelness is maintained. The contribution of these auxiliaries to a higher permissible exhaustion speed could thus at least partially be included under the more general heading of the influence of the change of the fibre surface molality on levelness.

The positive effect of certain chemicals was also noted early on by Carbonell and co-workers (Carbonell 1973, Carbonell 1976). They put emphasis on the fact that the auxiliaries that they found to be helpful for the dyeing of polyester, polyamide and acrylic did not necessarily coincide with the conventional notion of a levelling agent and referred to them as chemicals that "increase the mobility of the dyestuff". Addition of these chemicals allowed doubling the exhaustion speed per contact without impairing levelness. No detailed explanation of the supposed mechanism of action was given.

5.2.5 Other Factors

First and foremost are machine-related influences on unlevelness that are not taken into account by merely considering the machines' dyebath and fabric circulation speeds. The machine design influences the homogeneity of the dyebath in terms of temperature, dye and salt concentration. Even small gradients within the vessel are important as it was established in one case that a temperature difference of only 3K was found to produce an initial unlevelness of 10% (Hoffmann 1990:53). Features that contribute to dyebath homogeneity are the design of addition and dosing equipment, the vessel design, particularly its storage chamber, the design of the jet nozzle and others. Machines with the same dyebath and fabric circulation rates can therefore have a different maximum permissible exhaustion speed per contact ($\Delta E_{max}.c^{-1}$). In the early days of jet dyeing machines, $\Delta E_{max}.c^{-1}$ could vary by a factor of more than four between machines (Carbonell 1976). As the machine designs have matured, it is possible that these differences are smaller between modern machines.

For package dyeing machines, the frequency of flow reversals influences strongly dye unlevelness. Systematic investigations revealed that best results were achieved by changing the direction of liquor flow once every few contacts, the maximum frequency being once every circulation (Carbonell 1976). This method allowed the value of $\Delta E_{max}.c^{-1}$ to be quadrupled. Similar considerations apply to beam dyeing (Kretschmer 1991). What is best for dye levelness however may not be best for the substrate. Frequent changes in the liquor circulation cause, for example, an increase in yarn hairiness (Carbonell 1987). Compromises are therefore inevitable and many companies seem to have concluded that reversing the flow direction every two to three circulations is most suitable (Rouette 1995:674).

The properties and presentation of the substrate also plays a role. Loose fibre dyeing permits higher exhaustion speeds than tow dyeing and $\Delta E_{max}.c^{-1}$ is even smaller for yarn and fabric dyeing (Carbonell 1976). Most of the difference can be explained by varying

levels of tolerated unlevelness. Levelness requirements are least stringent in the case of loose fibre dyeing and most stringent for fabric and those yarn dyeings that will be employed for solid colours. An additional factor in this context is the accessibility of the fibre to the dye. In tightly woven fabrics, for example, the local liquor flow rate at the fibre intersections may be very low so that boundary layer effects could come into play and promote unlevelness (McGregor 1965:434, Hoffmann 1989:381). Along similar lines models have been developed particularly for jet dyeing machines that explain unlevelness by concentration differences in the fabric rope that emerge when parts of the rope twist, resulting in lower dye supply (Mizoguchi 1982a, Mizoguchi 1982b, Mizoguchi, Kawada 1985). Similarly, accessibility of the fibre may also be reduced for highly twisted yarns or when the fibre is under tension (Peters 1975:792). Under these difficult conditions a lower exhaustion speed (and an extended holding time at high temperature) might be required. Transitional kinetic models show that if a boundary layer exists, caused by insufficient liquor flow, the exhaustion speed of high exhausting dyes is more strongly affected by variations in liquor flow than the speed of dyes with a lower exhaustion (Etters 1991). Unfortunately, until now there seems to be no theory that would generally explain how differences in fibre morphology influence the levelness and how they can be overcome (Hoffmann 1990:53).

A further observation in relation to unlevelness was made in the application of reactant fixable dyes, when it was found that metering the salt during the heating phase – as opposed to a sequential process - had a positive effect (Hasler 1985). The authors did not put forward any explanation of the beneficial effect.

The levelling properties of the dyes would be of importance only if the process were not conducted by the principles of controlled sorption (Hoffmann 1990:51). It could be argued, for example, that highly migrating dyes permit a higher initial unlevelness since the dye deposition error would gradually disappear during the process. This approach is however hardly practical because the migration behaviour is very difficult to quantify and depends not only on a particular recipe but also on the machine characteristics (Fox 1968). For industrial applications, it therefore seems to be best to assume nil dye migration and to control the process to avoid unlevelness from the outset.

When dye mixtures are applied, the compatibility of the dyes must be taken into consideration. A pragmatic suggestion is to ensure that the target value of the exhaustion process, e.g. the $\Delta E_{max}.c^{-1}$, is complied with at all times for any dye in the system (Hasler 1987). The control parameters, e.g. the salt dosing gradient, would then be adjusted according to the dye with the highest exhaustion speed in a particular recipe taking into

account any differences in $\Delta E_{max}.c^{-1}$ between the dyes. Methods to quantify dye compatibility have been developed (Carbonell 1982, Hoffmann 1988, Bradbury 1995).

Finally it may be noted that the identification of the crucial parameters for dye levelness and the subsequent formulation of a recipe and process profile is greatly aided by the possibility of on-line process monitoring. The most important single parameter in the present context is the dye uptake rate which can be calculated from dyebath measurements. A number of tools have been developed on a research level and several of them are also available commercially (Carbonell 1991, Gilchrist 1995, Ferus-Comelo 2002). Other relevant parameters, in addition to the obvious temperature, include the fabric and dyebath circulation frequencies, conductivity (Luebbers 1990) and pH measurement (Shamey 1998).

5.3 References

1. Annen O, Carbonell J, Walliser R, Text. Ver. 14 (1979) 265
2. Annen O, Carbonell J, Walliser R, Text. Ver. 15 (1980) 296
3. Beckmann W, Glenz W, Mell. Textilber. 49 (1968) 1436
4. Bohrer E, Heetjans J H, Mell. Textilber. 71 (1990) 988
5. Boulton J, Crank J, J.S.D.C. 68 (1952) 109
6. Boulton J, J.S.D.C. 60 (1944) 5
7. Bradbury M J, Collishaw P S, Moorhouse S, AATCC International Conference, Book of Papers (1995) 268
8. Bradbury M, Collishaw P S, Moorhouse S, AATCC International Conference, Book of Papers (1993) 336
9. Breuer M M, Rattee I D, The Physical Chemistry of Dye Adsorption (London: Academic Press 1974)
10. Brooks J H, J.S.D.C. 90 (1974) 158
11. Brooks J H, J.S.D.C. 91 (1975) 394
12. Carbonell J, personnel communication, August 2002
13. Carbonell J, 37 ITB (2) (1991) 34
14. Carbonell J, Amer. Dye. Rep. 76 (3) (1987) 34
15. Carbonell J, Angehrn M, Heetjans J H, Mell. Textilber. 66 (1985) 58

16. Carbonell J, Hasler R, Walliser R, Knobel W, Mell. Textilber. 54 (1973) 68

17. Carbonell J, Hasler R, Walliser R, Text. Prax. Int. 31 (1976) 668

18. Carbonell J, Heetjans J H, AATCC International Conference, Book of Papers (1984) 70

19. Carbonell J, Merminod H, Hasler R, Bol. Inst. Inv. Text. 34 (1968) 23

20. Carbonell J, Puente P, Valldeperas J, Textilver. 17 (1982) 149

21. Cegarra J, Puente P, Text. Res. J. 37 (1967) 343

22. Cegarra J, Puente P, Valldeperas J, J.S.D.C. 92 (1976) 327

23. Cegarra J, Puente P, Valldeperas J, J.S.D.C. 95 (1979) 336

24. Drechsel B, Hoffmann F, Ottner S, Mell. Textilber. 79 (1998) 328

25. Etters J N, J.S.D.C. 107 (1991) 114

26. Ferus-Comelo M, Rev Prog Col. 32 (2002), in press

27. Fox M R, J.S.D.C. 84 (1968) 401

28. Gilchrist A, PhD Thesis, University of Leeds (1995)

29. Gilchrist A, Rev. Prog. Col. 25 (1995) 35

30. Hasler R, Palacin F, AATCC International Conference, Book of Papers (1985) 89

31. Hasler R, Palacin F, Int. Text. Bul. 33 (1) (1987) 27

32. Hasler R, Textile Chemist and Colorist 7 (2) (1975) 36

33. Hoffmann F, Mueller P F, J.S.D.C. 95 (1979) 178

34. Hoffmann F, Rev. Progr. Color. 18 (1988) 56

35. Hoffmann F, Textile Chemist and Colorist 30 (10) (1998) 19

36. Hoffmann F, Textilver. 24 (1989) 381

37. Hoffmann F, Textilver. 25 (1990) 49

38. Holdstock C R, PhD Thesis, University of Leeds (1988)

39. Kretschmer A, Text. Prax. Int. 46 (1991) 1226

40. Leube H, Ruettiger W, Mell. Textilber. 59 (1978) 836

41. Luebbers A, Souren I, Rouette H K, Mell. Textilber. 71 (1990) 371

42. Mayer et al., Mell. Textilber. 49 (1968) 145

43. McCall M T, Maslen S H, Sherill W T, Hipp J M, AATCC International Conference, Book of Papers (1979) 204

44. McGregor R, Manpreet S, Warren J, Text. Res. J. 67 (1997) 609

45. McGregor R, R H Peters, J.S.D.C. 81 (1965) 429

46. Medley J A, Holdstock C R, J.S.D.C. 96 (1980) 286

47. Mizoguchi K, Bulletin of Research Institute for Polymers and Textiles 132 (2) (1982a) 49

48. Mizoguchi K, K Kawada, Sen-i-Gakkaishi 41 (1985) 96

49. Mizoguchi K, Sen-i-Gakkaishi 38 (1982b) 259 & 500

50. Peters R H, Textile Chemistry, Vol. III, The Physical Chemistry of Dyeing (Amsterdam: Elsevier 1975)

51. Ren J, PhD Thesis, University of Leeds (1985)

52. Richter P, Vescia M, Textilind. 73 (1971) 25

53. Rouette H P, Lexikon der Textilveredlung, (Duelmen: Laumann Verlag 1995)

54. Ruettiger W, Ehlert J, Text. Praxis 17 (1972) 609

55. Schoenpflug E, Text. Prax. Int. 30 (1975) 1554

56. Shamey R, PhD Thesis, University of Leeds (1998)

57. Von der Eltz H U, Reuther A, Mell. Textilber. 53 (1972) 318

6 Methods for the Measurement of a Dye Amount in the Liquor and on the Fibre

6.1 Measurement in the Liquor

In batch dyeing, dyebath transmittance is the colour measurement method of choice for kinetic analysis because it difficult to measure the fibre colour directly in its wet state and relate the measurement results to the fibre colour when it is dry (Dalton 1995). Measurements in dyeliquor are based on the theory of the Beer-Lambert law which combines the two laws describing the absorption of light by coloured materials, Lambert's law and Beer's law (Vickerstaff 1954:30).

6.1.1 The Beer-Lambert Law

The law applies to the absorption of a monochromatic beam of light by a homogeneous material. Lambert's law states that the fraction of light absorbed by a substance is independent of the light's intensity. Consequently, if a solution transmits for example 50% of a monochromatic beam of light, it will still transmit the same percentage when the light intensity is changed. Lambert's law may be written as:

$$I_T = I_0 e^{-\alpha l} \tag{6.1}$$

I_T = Intensity of light transmitted [-]
I_0 = Intensity of light incident upon the absorbing body [-]
l = Thickness of the solution or substance [cm]
α = Constant [cm^{-1}]

Beer's law states that light absorption is proportional to the number of light absorbing molecules present in solution:

$$I_T = I_0 e^{-\beta c} \tag{6.2}$$

c = Concentration of the substance in solution [$mol.dm^{-3}$]
β = Constant [$dm^3.mol^{-1}$]

Combining the two laws yields:

$$I_T = I_0 e^{-\varepsilon c l} \tag{6.3}$$

ε = Molar extinction coefficient [$dm^3.mol^{-1}.cm^{-1}$]

Transmittance, T, is defined as the ratio of the transmitted to the initial intensity. Absorbance, A, is defined as the logarithm of the inverse of transmittance:

$$A = \ln\frac{1}{T} = \ln\frac{I_0}{I_T} = \varepsilon c l \tag{6.4}$$

Absorbance is additive for ideal solutions, which is important for the analysis of multiple dye solutions. Thus if the individual absorbance values of three dyes in solution are A_1, A_2 and A_3, then the total absorbance value, A_Σ, provided there is no interaction between the dyes, is:

$$A_\Sigma = A_1 + A_2 + A_3 \tag{6.5}$$

If a dye in solution conforms to the requirements of the application of the Beer-Lambert law, notably that it is in its monomolecular form in solution, then deriving the concentration from the absorbance value is very simple, once the dye's extinction coefficient has been determined from a calibration curve. Absorbance measurements are most accurate up to a maximum value of around 1.8 so that higher concentration solutions require appropriate dilution.

Unfortunately there are many circumstances when actual dye solutions deviate from the ideal behaviour postulated in the Beer-Lambert law. They are briefly described in the next section.

6.1.2 Dye Aggregation and other Measurement Difficulties

The list of factors that possibly influence a dye's molar extinction coefficient, ε, is long. Among the most prominent of them for direct dyes is dye aggregation. Dye aggregation can occur between identical dye molecules or between different dissolved dyes. Some consequences of dye aggregation for dye application properties have been mentioned in chapter two. The most important implication of dye aggregation for absorbance measurement is that the extinction coefficient is usually reduced and the wavelength of maximum absorbance experiences a hypsochromic shift, i.e. a shift to shorter wavelengths (Wang 2000, Coates 1969), although there are exceptions (Szadowski 1997). The fact that the presence of non-ionic surfactants based on ethoxylated fatty alcohols or polyglycol ethers can have an anti-agglomeration effect on direct dyes in solution is sometimes used to overcome measurement problems due to aggregation (Kuehni 1997).

Since dye aggregation is influenced simultaneously by many parameters, including the temperature, the dye and the electrolyte concentration of the solution, the effects on the extinction coefficient can be very complex.

Generally speaking, parameters with a possible influence on the measured absorbance value include (Commerford 1997):

1. pH of the solution (see also Navarro 1999)
2. Fluorescence of the dye, i.e. absorbed light is re-emitted and causes an erroneous reading
3. Photochromism, i.e. the sensitivity of the dye to irradiation, e.g. from sunlight. Photochromism is normally reversible so that an irradiated dye solution, kept sufficiently long in the dark, will yield the same reading as a sample not exposed to radiation.
4. Plating, i.e. the formation of a thin film on the window of the absorption cell. Plating does not alter the dye's extinction coefficient but gives erroneous instrument readings.
5. Temperature, including reversible and irreversible effects. A known cause for the influence of temperature is a change in the aggregation state of the dye but it is also possible that modifications of the dye structure occur that remain permanent even when the solution is cooled down again.
6. Additives to the commercial dye, which may be coloured and are used, for example, to standardise the dye's strength or to improve its application properties
7. Metal traces in the water, introduced for example by the water supply itself (copper or zinc pipes) or by the substrate (metal residues in cotton)

It is advisable to check a dye's sensitivity to some or to all of these parameters before quantitative work starts because the measurement method needs to be modified according to the dye's characteristics (Commerford 1997).

6.1.3 Measurement Methods for Dye Solutions

Generally speaking, two types of approaches have been developed to overcome the difficulties arising from non-ideal behaviour of the dye in the solution. The first approach attempts to bring the dyebath sample to standard conditions allowing an accurate and precise analysis before the absorbance measurement. This typically includes control of temperature, pH and dye concentration. The second approach aims at directly measuring the concentration in the dyebath during the process. The effects of temperature, pH and dye concentration on the extinction coefficient of the dye have therefore to be predicted and taken into account in the conversion from absorbance to concentration values.

The simplest method of kinetic analysis is to sample the dyebath at defined temporal intervals, to bring the sample to standard condition and then measure the absorbance on a

spectrophotometer at the wavelength of maximum absorbance. Detailed recommendations for transmission measurements of dye solutions have been published (ISCC 1972, Kuehni 1997). They cover the minimum amount of dye to be dispensed for the preparation of stock solutions, the conditioning of the dyestuff powder which is often hygroscopic in nature, the type of glassware to be used, the dissolution procedure for the dye and the possible addition of auxiliaries such as non-ionic surfactants to reduce dye aggregation and buffer solutions to stabilise the pH-value. In a series of inter-laboratory trials, the precision of the proposed method was found to be between +/- 1.7 and 4.5% (Sweeny 1976).

Luckily from a process control point of view, efforts of standardising the solution before spectrophotometric analysis are not limited to off-line methods of dyebath measurement. Flow Injection Analysis (FIA) exemplifies the standardising method for on-line measurements because its carrier stream can serve the multiple purposes of dilution, buffering and dissolution (in the case of disperse dyes). It has the additional advantage of a high dynamic range because the FIA signal can be quantitatively interpreted not only at the peak but also at the tail. Thus, if the dyebath sample is passed through a cooling device before it is injected into the carrier stream, fairly standardised measurement conditions can be obtained. FIA has been successfully employed for on-line monitoring of reactive (Lefeber 1994) and disperse dyes (van Delden 1996). FIA is capable of approximately one dyebath analysis per minute which is normally sufficient for control purposes under industry typical conditions. If applied to disperse dyes, water as the carrier has to be replaced by a solvent that dissolves both the non-polar disperse dye and the more polar dispersing agent because otherwise light scattered at the dispersed particles causes the absorbance readings to be erroneous. Good results were achieved with a 70/30 acetone/water blend (van Delden 1996).

Despite its accurate results, FIA is currently too expensive and complicated for widespread industrial use. A possibly cheaper and more robust alternative could be sequential injection analysis (SIA) (Draper 2001). The principle of operation of the two methods is similar, the major difference being that SIA uses a selection valve instead of an injection valve and therefore does not require a continuous carrier flow. Dyebath monitoring experiments with SIA yielded the same precision as those with FIA and overall correlation between the two methods was very good.

Even at constant pH and temperature, however, small variations in the dye concentration, especially if dye mixtures are employed, often lead to changes in the extinction coefficients. As a consequence, although the dye sample is diluted and brought to standard conditions, methods have to be developed that deal with deviations from the Beer-Lambert Law. Among the methods that have been used for dyebath analysis are multiple linear regression

(MLR) in different forms (Berkstresser 1993, Saus 1994), the partial least square (PLS) method (Lefeber 1994) and neural networks (Jasper 1993, Skelton 1997). Although neural networks have been shown to yield accurate predictions especially in the case of non-linear behaviour, their drawbacks are that they cannot predict outside the range of calibration data and that they employ a potentially enormous number of parameters. MLR and PLS appear to predict with sufficient accuracy if the significant interaction terms that describe the dyes' mutual effect on their absorbance values are included in the model.

As non-linearity of the extinction coefficient has to be taken into account anyway, it could be argued that direct dyebath monitoring has the advantage over methods such as FIA of requiring less hardware and maybe only little additional effort to compensate for temperature, pH and other effects. Changes in temperature and pH as they normally occur during the dyeing process, however, can have simultaneous and complex influences on the extinction coefficient of dyes alone and especially in a mixture. Temperature changes, as well as different electrolyte and auxiliary concentrations, may affect the dye aggregation state and therefore also its extinction coefficient (Wang 2000). The same also applies to different pH levels. Recent investigations into the aggregation behaviour of C.I. Direct Red 1, for example, showed that the dye is less aggregated at higher pH values because the dye's carboxylic group is dissociated, making it more polar and therefore hydrophilic (Navarro 1999).

Despite these difficulties, a group of researchers at Leeds University have shown that the deviations caused by temperature and pH effects can be taken into account so that direct dyebath measurements provide sufficiently accurate estimates. Empirical equations have been derived to describe the temperature-dependency of the absorbance of a basic dye during acrylic dyeing (Gilchrist 1995) and on-line monitoring was also found to be possible at varying pH values for a reactive dye (Shamey 1998). Fluctuations, as they inevitably occur especially in direct dyebath measurements, lead to corresponding variations in the calculation of the exhaustion rate but can be reduced to an acceptable level if time averaging methods are employed (Gilchrist 1998).

Another major obstacle in the use of direct dyebath monitoring is the limited concentration range that can be measured with transmission cells of a fixed path length. Dyebath concentrations in industrial batch dyeing machines can easily vary by a factor of 1000 considering the combined effects of high exhaustion values and of variations in the initial amount of dye. The simplest, and somewhat cumbersome, solution is to use a set of cells of different path lengths, each for an appropriate concentration range. Since the emergence of multiple input/output spectrophotometers, the set of cells can be used simultaneously (Arora 1999). A second possibility consists of a careful selection of the dye concentration

calibration range and exponential as well as step linear statistical models. Thus, dye concentrations for three commercial dyes of as low as 0.1ppm in mixtures could be determined with a 10mm cell with a maximum error of about 5% (Li 1996). A very promising third possibility employs multiple path length cells, i.e. cells in which the light simultaneously describes paths of different lengths (Wilkinson 1992). This path length distribution can be described mathematically by means of an inverse Laplace transform that relates dye absorbance and extinction coefficient. The method has been successfully used in a dyebath reflectance cell for the on-line monitoring of basic (Shamey 2001, Gilchrist 1997) and reactive dyes (Shamey 1999).

In the special case of monitoring reactive dyes it is not only important for the overall performance evaluation to measure the amount of sorbed dye but also the dye concentration that is covalently bonded to the fibre. Although it is currently impossible to measure on-line directly the dye fixed on or sorbed by the fibre, the ratio of non-hydrolysed to hydrolysed dye in the dyebath can be used as an indicator instead. As little hydrolysed dye as possible is desirable and a pre-requisite for high fixation levels. Absorbance measurement, however, normally cannot distinguish between hydrolysed and non-hydrolysed reactive dye in solution. In order to surmount this obstacle, FIA has been coupled with high performance liquid chromatography (HPLC) (Wallace 1997). In this method, a fraction of the combined dyebath-carrier sample that contained two reactive dyes was injected into the thermo-stabilised HPLC column. The total run time for one sample on the HPLC was around six minutes. Although the experiments were in principle successful, the fact that the whole system becomes complicated and expensive to run suggests unsuitability for routine operations. An alternative and cheaper method that has proved to be successful in the analysis of hydrolysed dye is capillary electrophoresis (CE) (Shamey 1998).

6.2 Measurement on the Fibre

Traditionally, two different methods have been employed to quantify the amount of dye on the fibre. The first one consists of dissolving the dye in a suitable solvent and then to measure the absorbance of the obtained solution according to the methods described in the previous section. The second method uses reflectance spectrophotometry.

6.2.1 Extraction of Dye on the Fibre

Extraction with 25% pyridine solution is a standard method for many direct dyes (Vickerstaff 1954:48). Alternative solvents such as DMF (N,N-Dimethlyformamide) and

cellosolve (ethylene glycol monoethyl ether) are also frequently used. Two criteria have to be fulfilled in order for the method to be suitable:

1. quantitative extraction of the dye from the fabric, i.e. no dye must be left on the fibre
2. stability of the extracted dye solution to boiling

The dissolution of the dye occurs normally with a Soxhlet apparatus under reflux conditions until no more dye dissolves. A simpler method is to add the fibre to the boiling solvent in a beaker and replace the solution until no more dye dissolves. Once all dye is extracted the amount of dye is calculated from transmission measurement of the obtained solution.

The major potential drawback of this method in its application to direct dyes on cotton is that removal from the fibre is sometimes not complete (Vickerstaff 1954:49; Willis 1945, Kulkarni 1969). It is not entirely clear why the problem arises. One possible explanation is that a limited number of sites on the cotton fibre entertain stronger dye-fibre interactions especially with high affinity dyes. A second disadvantage concerns the health risks associated with some of the solvents such as DMF and pyridine.

As a result of these disadvantages but mainly because reflectance spectrophotometers have become more affordable, reliable and accurate, usage of these instruments enjoys increasing popularity for the determination of dye amounts on the fibre.

6.2.2 Light Reflectance

The conversion of reflectance data to a parameter that can be easily related to the amount of dye on the substrate is often achieved by the Kubelka-Munk function (McDonald 1987). It predicts the reflectance of a substrate that has both absorbing and scattering power and is valid only for monochromatic light. In the special case that the reflecting material is opaque the following simple relationship is obtained:

$$\frac{K}{S} = \frac{(1-R)^2}{2R} \tag{6.6}$$

K = Absorption coefficient of the material [-]
S = Scattering coefficient of the material [-]
R = Fractional reflectance of material

Over small concentration ranges, $K.S^{-1}$ increases linearly with the dye amount, $[D]_f$, making it an easy to interpret parameter for predictions (Stearns 1969:222, Bridgeman 1987). Even if the relationship becomes non-linear, functions can often be found that approximate the behaviour close enough for accurate, quantitative work (Gilchrist 1995). Whatever the relationship, once a suitable function has been found the dye amounts on different fibre

samples may be compared by analysing their $K.S^{-1}$-values at the wavelength of minimum reflectance. The ratio of the samples' $K.S^{-1}$-values is often referred to as relative dye strength (Garland 1997).

The accuracy of the prediction can often be increased if the $K.S^{-1}$-values are compared not for only wavelength but for multiple wavelengths. This is easily achieved since most modern spectrophotometers output a reflectance value at every 10 or 20 nm in the visible spectrum from 400 to 700 or 800nm, depending on the device. The 20 or more $K.S^{-1}$-values thus obtained are added up for each measurement, giving K_Σ, and K_Σ of the first sample is then compared to the K_Σ of the second sample.

Another convenient feature of the function is that, like the absorbance value in the Beer-Lambert law, $K.S^{-1}$ is additive when several colorants are present. Since textile dyes can be considered to be dissolved in the fibre they have no scattering power and all light scattering is therefore attributed to the substrate, S_f. Under these circumstances, and assuming that there are three dyes, $K.S^{-1}$ becomes:

$$\frac{K}{S} = \frac{[D]_{f1}K_1 + [D]_{f2}K_2 + [D]_{f3}K_3 + K_f}{S_f} = [D]_{f1}\frac{K_1}{S_f} + \ldots + \frac{K_f}{S_f} \qquad (6.7)$$

State-of-the-art spectrophotometers are very precise and accurate. Frequently errors are therefore not the result of limited instrumental capabilities but a result of erroneous handling of the sample. For experimental work, the following aspects need to be considered:

1) The sample needs to be opaque. This can be checked by comparing the reflectance values of the sample before a white with those before a black background. If the sample is opaque, the two values must not differ by more than the experimental error of the measurement.

2) The reflectance value is affected by the texture of the sample and its orientation on the sampling port. The sample should therefore be measured several times by changing the orientation of the texture and by moving the measurement location slightly. The number of required measurements for a precise value increases with the size of the sample and the degree of unlevelness of the dye. The surface of the sample should not be touched.

3) As the fabric not only scatters but also absorbs light, the $K.S^{-1}$-value of the substrate must be measured independently and subtracted from the $K.S^{-1}$-value of the dye. Before the measurement the undyed fibre should be treated in a mock dyebath, i.e. a dyebath containing all the chemicals used in the

dyeing process except the dyes, at the employed dyeing conditions. This precaution is necessary because the process and its chemicals might affect the $K.S^{-1}$-value.

4) The reflectance values are affected by the light source of the spectrophotometer and the size of its aperture. For comparisons, the same light source and aperture must therefore be employed.

5) The reflectance values are also affected by the temperature and moisture content of the sample. Therefore the sample should be conditioned before measurement, e.g. in an atmosphere of 65% at 20°C.

6.3 Methods employed in this Work

6.3.1 Liquor Measurements

Before calibration, preliminary tests were carried out analysing the sensitivity of the absorbance value of Optisal Yellow 2 RL (C.I. Direct Yellow 162) to various parameters. They yielded the following results:

1) **pH**: The absorbance value is not sensitive to pH-changes in the range of values encountered in un-buffered dyebaths.

2) **Electrolyte concentration**: At 20°C the addition of 2.5 to 15g.dm^{-3} sodium chloride, compared to no salt, shifted the wavelength of maximum absorbance by 11nm from 399nm without salt to 410nm with salt and reduced the absorbance at λ_{max} by approximately 6%. Changes in the salt concentration between 2.5 and 15g.dm^{-3} did not result in statistically significant variations in the extinction coefficient.

3) **Non-ionic surfactant**: Addition of 1 cm^3.dm^{-3} of an alkyl amine polyglycol ether as a non-ionic surfactant (ALBEGAL W of CIBA SPECIALTY CHEMICALS) increased the wavelength of maximum absorbance at 20°C from 399nm without surfactant to 416nm with surfactant. Also, the addition of the surfactant increased the absorbance value of the solution at 20°C by about 20% at λ_{max}. The new equilibrium was established two minutes after the addition of the surfactant (figure 6.1).

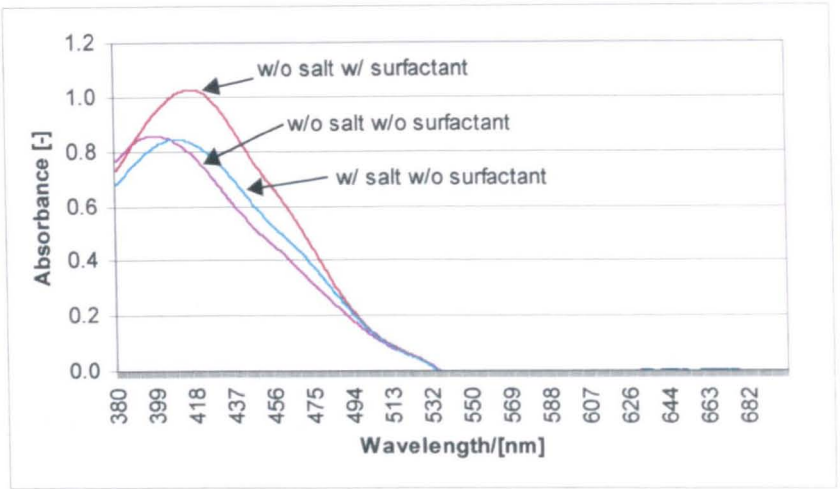

Figure 6.1: Influence of Electrolyte and Surfactant on the Absorbance Value

4) **Temperature**: When no surfactant was present, the absorbance value increased with temperature up to a maximum value at 90°C, the highest temperature tested. When $1cm^3.dm^{-3}$ surfactant was present, the absorbance value decreased with temperature. The temperature effect was reversible in all cases, so that the solution regained its original absorbance value after cooling down to room temperature (table 6.1).

	Max. Absorbance [-] @ 20°C	λmax/ [nm] @ 20°C	Max. Absorbance [-] @ 90°C	λmax/ [nm] @ 90°C
W/o surfactant w/o added electrolyte	0.849	399	0.916	395
W/o surfactant w/ 15g.dm^{-3} electrolyte	0.801	410	0.867	399
W/ surfactant w/o added electrolyte	1.021	416	0.950	408
W/ surfactant w/ 15g.dm^{-3} electrolyte	0.972	418	Not tested	Not tested

Table 6.1: Influence of Temperature on A and λmax on Absorbance Value

5) **Light exposure**: A dye solution in the measurement cell was held for one minute next to a 100W light bulb and re-measured (table 6.2). Afterwards, it was left over night in the dark and re-measured the next morning.

Absorbance Value	Condition
1.219	Fresh solution
1.078	After light exposure
1.216	Following morning

Table 6.2: Influence of Light Exposure on Absorbance Value

A more detailed investigation of the dye's photochromism indicated that it took the absorbance value around 30 minutes to recover after light exposure.

5) **Ageing of Solution**: A freshly dispensed dye solution was re-measured after 4, 6 and 7 days (table 6.3).

Absorbance Value	Age of Solution	Change [%]
1.259	Fresh	
1.251	4 Days	-0.6
1.241	6 Days	-0.8
1.225	7 Days	-1.3

Table 6.3: Ageing Effect on Absorbance Value

7) **Metals in Solution**: A solution containing several metal salts was added to the dye solution so that the following metal concentrations were obtained [$mg.dm^{-3}$]: Calcium: 41, Magnesium: 35, Iron: 0.5, Copper: 0.2. There was no significant effect on the absorbance value.

8) **Tap water**: The dye precipitated from solution when it was attempted to dissolve it in tap water instead of distilled water.

6.3.1.1 Adopted Measurement Method

The sensitivity tests showed that distilled water had to be used in the preparation of the dye solution and that its extinction coefficient as well as λ_{max} were a function of electrolyte concentration and temperature and also changed after addition of a non-ionic surfactant. Taking additionally into account the dye's photochromaticity, the following measurement method was adopted:

1) All measurements were made in a room without daylight and minimal artificial illumination.

2) Calibration solutions were prepared for three situations: dye only, dye and electrolyte, dye and surfactant and used distilled water as solvent. The three extinction coefficients were determined in each case from at least five absorbance values at 410 nm by linear regression.

3) All measurements were made at room temperature within 24 hours of sampling.

The measurements were made on a K-Tron UVICON 860 Dual Beam spectrophotometer using glass cells of 10mm pathlength. The precision of the thus defined method was determined by three repeat dyeings (exhaustion in each case higher than 90%) at four different temperatures. The variation coefficient, v.c. of the exhaustion value was in all cases less than 0.5% (table 6.4).

Temperature/[°C]	43	65	90	100
V.C. [%]	0.30	0.18	0.11	0.40

Table 6.4: Precision of Exhaustion Value by Dyebath Measurement

The precision of this method increases with the exhaustion value since measurement variations hardly affect the exhaustion value when the fractional dye amount in the dyebath is very low. The average v.c. of a larger number of dyeings, some of them with exhaustion values of less than 50%, was 1.2%.

6.3.1.2 The Dye's State in Solution

The transmission measurements give some indication about the dye's states in solution under different conditions. The observed shift of λ_{max} and the reduction in the absorbance value of a solution when electrolyte was added are, for example, fairly typical for changes that occur upon dye aggregation. Increase in temperature reduces aggregation and therefore increases the absorbance, an effect which has been confirmed in the present experiments. The observed variations support the view that some dye aggregation has already occurred when no electrolyte is added but is further increased by salt additions.

When a non-ionic surfactant is added, the dye-aggregates probably disappear completely because it was observed that the absorbance value became independent of the electrolyte concentration and did not increase when the solution was heated. In fact, the absorbance

value was reduced at elevated temperature, mainly due to the volume expansion of the water. The results indicate, however, that the state of the dye in solution in the presence of the surfactant is different to that without surfactant, even at temperatures close to the boil, because the values of λ_{max} and of ε remained distinctly different. The difference can be explained by the formation of temperature-stable dye-surfactant micelles in the presence of surfactant, i.e. the dye is not in its monomolecular form. Not only are polyglycol ethers known to form such micelles, leading to higher extinction coefficients and a bathochromic shift (Peters 1975), but separately carried out equilibrium dyeings showed a notable reduction in dye sorption when the surfactant was present. This would be expected since the dye-surfactant micelles reduce the effective dye concentration in solution that is available for dye sorption.

6.3.2 Fabric Measurements

Early tests compared the results of dye estimation by extraction with those of reflectance measurements.

6.3.2.1 Extraction

The cotton fabric was dyed with 3% (omf) C.I. Direct Yellow 162 at 80°C in the presence of 15g.dm^{-3} sodium chloride. The extraction was attempted with three different solvents, pyridine, DMF and Cellosolve.

Pyridine: Aqueous pyridine solutions of 25% or more were used. About 1.5g of fabric was placed directly in the pyridine solution and boiled for 10 to 15 minutes before the solution was exchanged with new liquor. This process was repeated until no more colour could be removed from the fabric. Finally, 100% pyridine was added and boiled again for around 15 minutes. The solutions were collected into a single container.

DMF: 0.6g of fabric were boiled in a 250cm^3 flasks with condenser so as to avoid evaporation losses in 100cm^3 of 50/50 DMF/distilled water solution. Every 45 minutes the solution was decanted and replenished with a fresh 100cm^3 solution of the same solvent. After the second replenishment, i.e. a total solvent volume of 300cm^3, no more dye was extracted from the fibre.

Cellosolve: 0.7g of fabric were boiled in a 250cm^3 flasks with condenser so as to avoid evaporation losses in 100cm^3 of 50/50 Cellosolve/distilled water solution. Every 60 minutes the solution was decanted and replenished with a fresh 50cm^3 solution of the same solvent. After the second replenishment, i.e. a total solvent volume of 200cm^3, no more dye was extracted from the fibre.

In all three cases, the fabric retained a yellowish tint after the end of the extraction, indicating that not all of the dye had been removed. A quantitative comparison with the (more accurate) exhaustion values obtained from dyebath measurements showed that the solvents removed only between 87 and 90% of the dye (table 6.5).

	Pyridine	DMF	Cellosolve
Amount of dye on the fibre by extraction [% omf]	Not calculated	2.20	2.31
Amount of dye on the fibre by bath exhaustion [%]		2.51	2.58
Extraction/Bath Exhaustion [%]		87.40	89.50

Table 6.5: Results of Dye Extraction Tests

6.3.2.2 Reflectance

All measurements were done on a DATACOLOR SF500 SPECTRAFLASH, using a 30mm aperture, a Xenon flash light source and included specular reflectance. The UV-filter was switched on so that the UV section of the illuminating spectrum was excluded.

Opacity

The scoured, undyed fabric samples were measured with the fabric face to the light source against a white and a black background in 1 to 16 layers (table 6.6). The reflectance value of each sample was the average of six measurements. The difference in colour represented by the reflectance values was expressed in $\Delta E_{(CMC)(2,1)}$ calculated under D65 and 10° observer conditions. The sample was considered to be opaque if an increase in the number of layers did not yield a reduction in the $\Delta E_{(CMC)}$-value. The table 6.6 below shows that opacity required a minimum of six fabric layers. All subsequent measurements were made with eight layers of fabric.

No. of Layers	ΔE(CMC)
1	4.70
2	1.90
4	0.18
6	0.05
8	0.06
16	0.07

Table 6.6: Determination of the Number of Layers required for Opacity

Precision of various Preparation Methods

Several ways in which the fabric could be prepared for the reflectance measurement after the end of the dyeing cycle were studied. Rinsing of the sample with cold tap water is one option. As some of the adsorbed dye can possibly desorb during the rinsing, it has been suggested to use cold concentrated salt solution of tap water instead so that the tendency of the dye to desorb is minimised (Willis 1945). A third possibility would be to squeeze the fabric after the dyeing without rinsing and subtract the amount of dye deposited on the fibre surface due to adhering liquor.

For a comparison of the three methods' precision, the samples, of mass of around seven gram each, were all dyed in the same dyebath of a 1000cm^3 beaker on a Roaches Ballotini machine at a liquor ratio of 8:1 until equilibrium. After the dyeing the samples were removed from the beaker and treated in the three different ways explained below. Four samples were obtained for each method, all stemming from the same dyebath.

One set of samples was rinsed for two minutes with cold, running tap water. Another set was rinsed with concentrated sodium chloride solution. The third set of samples was squeezed, put into a sealable plastic bag and weighed. The fabric was then removed from the plastic bag and air-dried over night. The plastic bag was weighed, with the difference between the mass of the bag with fabric and without fabric giving the mass of the wet fabric. The air-dried fabric was then oven-dried at 125°C for three hours, put into a plastic bag of known mass and weighed to give the mass of the bone-dry fabric. The difference between wet and bone-dry fabric gave the mass of the adhering liquor. Assuming that the dye concentration in the adhering liquor was equal to the dyebath concentration, the amount of dye in the liquor could be calculated.

Each sample was measured at seven arbitrary locations on the face of the fabric to give an average $K.S^{-1}$-value. The measurements were corrected by the $K.S^{-1}$-value of the substrate ("mock dyeing").

Rinsing with concentrated salt solution led to salt deposits after drying on the fabric surface. This method was therefore discarded. The average $K.S^{-1}$-values of the rinsed and squeezed samples are shown in table 6.7 before and after correction for the dye in the adhering liquor.

	Rinsed	**Squeezed w/o correction**	**Squeezed w/ correction**
K/S @ 400 nm	20.17	20.22	20.19
K/S @ 420 nm	22.55	22.86	22.62
K/S @ 440 nm	20.77	21.27	20.79
V.C [%]	1.3	0.6	0.6

Table 6.7: Precision of Different Sampling Techniques for Reflectance Measurement

The table shows a higher precision for the samples prepared by squeezing. A statistical evaluation of the difference in the variation coefficient between the squeezed and the rinsed samples was inconclusive. An F-test showed that the difference was significant at 440nm and insignificant at 400nm. The difference at 420nm was at the border between significant and insignificant. As expected, the $K.S^{-1}$-values of the squeezed samples are slightly higher than for the rinsed samples because dye from previously adhering liquor was deposited on the fibre surface. It is interesting to note, however, that the difference in the $K.S^{-1}$-values between rinsed and squeezed samples is higher than what can be explained by dye from adhering liquor because the corrected values in the third column are all slightly higher than those in the first column. This indicates that some of the adsorbed dye has desorbed during the rinsing. Both facts, the consistently lower variation coefficient and the measurement of total adsorbed dye, lead to the conclusion that the squeezing method is most suitable for the purposes of this research project.

Adopted Sample Preparation Method for Reflectance Measurements

After the end of the dyeing, the fabric sample obtained from the small laboratory machine (around 7g) was squeezed without rinsing. The amount of dye in the adhering liquor and the $K.S^{-1}$-value of the mock-dyed substrate were taken into account when correlating $K.S^{-1}$-values with dye amounts on the fabric values.

For the reflectance measurements the fabric was folded to give eight layers and at least seven measurements were averaged for each sample.

6.4 References

1. Arora M, Koch T, Int. Pat. WO 99/66117 (1999)
2. Berkstresser G A, Beck K R, Smith C B, McGregor R, Jasper W, AATCC International Conference, Book of papers (1993) 108
3. Bridgeman I, in Colour Physics for Industry (Bradford: SDC 1987) 1
4. Coates E, J.S.D.C. 85 (1969) 355
5. Commerford T R, in Color Technology in the Textile Industry (Research Triangle Park: AATCC 1997)
6. Dalton P M, Nobbs J H, Rennell R W, J.S.D.C. 111 (1995) 285
7. Draper S L, Beck K R, Smith B, AATCC Review 1 (1) (2001) 24
8. Garland C E, in Color Technology in the Textile Industry (Research Triangle Park: AATCC 1997)
9. Gilchrist A, J.S.D.C. 113 (1997) 327
10. Gilchrist A, J.S.D.C. 114 (1998) 247
11. Gilchrist A, PhD Thesis, University of Leeds (1995)
12. ISCC Committee, Text. Chem. Col. 4 (5) (1972) 25
13. Jasper W J, Kovacs E T, Berkstresser G A, Text. Res. J. 63 (1993) 545
14. Kuehni R G, in Color Technology in the Textile Industry (Research Triangle Park: AATCC 1997)
15. Kulkarni G G, PhD Thesis, University of Leeds (1969)
16. Lefeber M R, Beck K R, Smith C B, McGregor R, Text. Chem. Col. 26 (5) 1994 30
17. Li S, White B, Tincher W C, AATCC International Conference, Book of papers (1996) 58
18. McDonald R, in Colour Physics for Industry (Bradford: SDC 1987) 116
19. Navarro A, Sanz F, Dyes and Pigments 40 (1999) 131
20. Peters R H, Textile Chemistry, Vol. III, The Physical Chemistry of Dyeing (Amsterdam: Elsevier 1975)

21. Saus W, Cleve E, Denter U, Duffner H, Schollmeyer E, Textilver. 29 (1/2) (1994) 13

22. Shamey R, Nobbs J H, Gilchrist A, Colour Science 98, Volume III, Leeds (2001) 172

23. Shamey R, PhD Thesis, University of Leeds (1998)

24. Shamey R, Text. Chem. Col. 31 (2) (1999) 35

25. Skelton H, PhD Thesis, University of Leeds (1997)

26. Stearns E I, The Practice of Absorption Spectrophotometry (New York: Wiley-Interscience 1969)

27. Sweeny C D (ISCC Committee), Text. Chem. Col. 8 (2) (1976) 31

28. Szadowski J, Niewiadomski Z, Dyes and Pigments 33 (1997) 97

29. van Delden T, Beck K R, Smith C B, AATCC International Conference, Book of papers (1996) 369

30. Vickerstaff T, The Physical Chemistry of Dyeing, 2nd edition (London: Oliver and Boyd 1954)

31. Wallace M L, Beck K R, Smith C B, AATCC International Conference, Book of papers (1997) 307

32. Wang J C, Advances in Colour Science and Technology 3 (2000) 20

33. Wilkinson D, MSc Thesis, University of Leeds (1992)

34. Willis H F, Warwicker J O, Standing A, Urquhart A R, Trans. Far. Soc. 41 (1945) 506

7 Pilot-scale Jet Dyeing Machine

The pilot-scale jet dyeing machine was a MATHIS JFO purchased by the Department of Colour Chemistry during the duration of the project and delivered to the department in December 2000.

The Swiss manufacturer gives the specifications reported in table 7.1 for the machine (Mathis 1995, Mathis 1998):

Parameter	Value
Dyebath Volume/[dm^3]	6-20
Liquor ratio/[$dm^3.kg^{-1}$]	5:1 to 50:1
Liquor flow rate/[$dm^3.min^{-1}$]	10 to 300
Fabric content/[kg]	0.1 to 1.2
Fabric speed/[$m.min^{-1}$]	1 to 30
Volume preparation tank/[dm^3]	40
Volume pressurised add tank/[dm^3]	0.5
Volume circulation add tank/[dm^3]	1
Flow rate addition pump/[$dm^3.min^{-1}$]	0 to 3
Maximum temperature/[°C]	140
Maximum pressure/[bar]	3
Maximum heating gradient/[$°C.min^{-1}$]	5
Maximum cooling water flow/[$dm^3.min^{-1}$]	10
Range of conductivity probe/[$mS.cm^{-1}$]	0.1 to 200
Max. capacity of liquid dosing pump/[$cm^3.min^{-1}$]	210
Power heating elements/[kW]	9
Power main circulation pump motor/[kW]	2.3
Dimensions (H * W * D)/[m]	1.57 * 1.20 * 0.85

Table 7.1: Specifications MATHIS JFO

Figure 7.1 is a schematic of the machine which is shown in figure 7.2

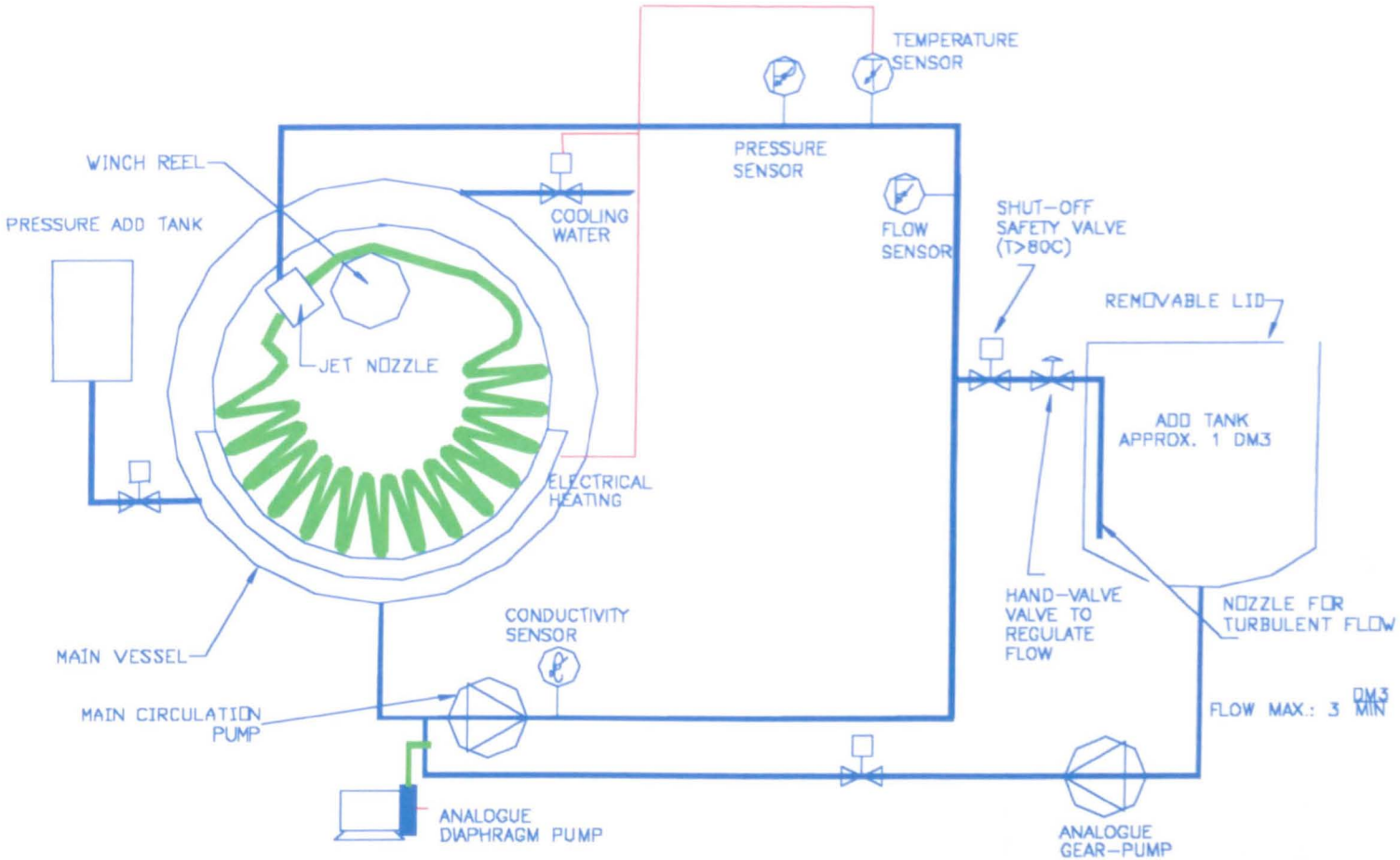

Figure 7.1: Schematic of Pilot-scale Jet Dyeing Machine

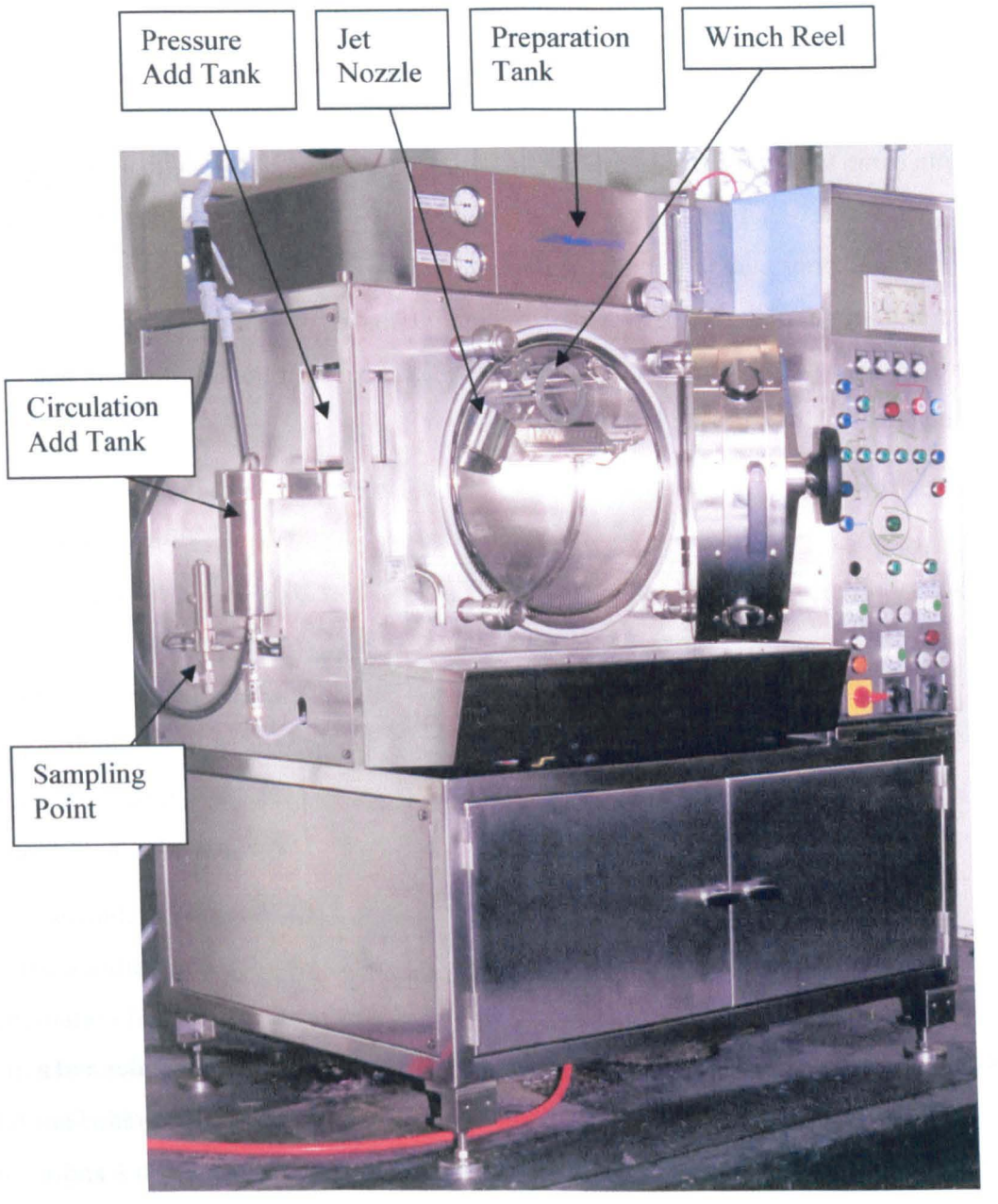

Figure 7.2: Pilot-scale Jet Dyeing Machine

Some of the machine features, which are explained in detail in the next section, were unique and made to the specification devised as part of this study. They were:

1) a second addition tank that could draw liquor from the main dyebath and fitted with a separate, speed-controlled pump
2) a connector for a conductivity probe welded into the main circulation line
3) a detector for the fabric circulation frequency
4) process control by a tailor-made IBM-PC based system

7.1 Machine Features

7.1.1 Jet Nozzle, Winch Reel and Treatment Chamber

The machine came with three differently sized jet nozzles that could be easily exchanged by loosening two screws attaching the nozzle to the vessel housing. They all had the same length (75mm) and approximately the same slit width for the liquor of around 3mm but varied in their nominal diameter between 40, 55 and 90mm to accommodate ropes from fabrics of different widths or constructions (figure 7.3). The maximum fabric width that can be processed with a 90mm nozzle is around 1.5m.

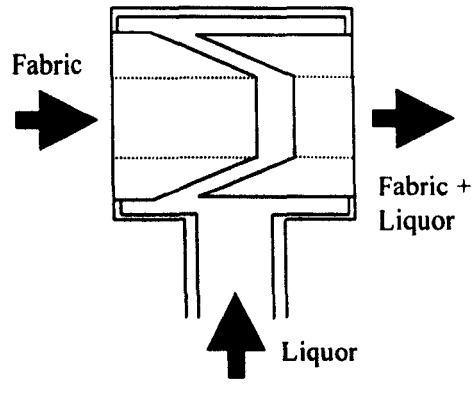

Figure 7.3: Schematic Pilot-scale Nozzle

The winch reel consists of four regularly spaced stainless steel rods. A cloth guider and a feeding plate installed immediately before the reel ensures that the fabric is centred. The reel is driven by a DC motor the speed of which can be varied smoothly between 1 and 30m.min^{-1}.

After passage through the nozzle, the fabric falls onto a freely rotating (not-driven), perforated basket, 20cm deep and with a diameter of around 45cm, which is several millimetres smaller than the inner diameter of the treatment chamber. Thus direct contact between the fabric and the heated walls of the chamber is prevented. In this respect, the design resembles that of the Thies Roto-Stream (Ratcliffe 1978) and, as a result, the fabric piled up in the drum barely touches the dyebath liquor level at low liquor ratios and the packing density is reduced.

The treatment chamber can be pressurised up to a maximum of 3bar by injection of air.

7.1.2 Main Circulation Pump

The main circulation pump, a SAWA ZA 17/32-M1 centrifugal pump, is bolted immediately under the treatment chamber and delivers a flow rate of between 10 and 300$dm^3.min^{-1}$. The pump speed and therefore also the flow rate are controlled by means of a frequency inverter that allows any setting between 0 and 50Hz. Pump efficiency, i.e. the efficiency of the conversion of electric to kinetic energy, ranged from 30 to 45% (Sawa 1998).

7.1.3 Addition Tanks

The standard addition tank has a volume of 0.5dm^3. Liquid transfer, e.g. of solutions containing dyes or chemicals, to the treatment chamber is controlled by an adjustable pressure gradient. The maximum pressure of the tank is 3.5bar so that additions can even be made when the treatment chamber is under pressure, e.g. due to process temperatures above 100°C. When the pressure gradient is reversed, i.e. the pressure in the treatment chamber is higher than that in the addition tank, liquid can be transferred from the chamber to the tank. A solenoid-controlled sampling port then allows liquor to be drawn from the treatment chamber into the tank.

The second, tailor-made addition tank with a volume of 1dm^3 operates in a similar manner to the addition tank found on bulk-scale machines, since it draws liquor from the main circulation line which, after passage through the addition tank, re-enters the main circulation line at the suction side of the main circulation pump (figure 7.4). The tank has a lid to avoid evaporation losses at higher temperatures. Two solenoid valves at the tie-in locations with the main line allow the tank to be isolated. The flow entering the tank can be manually controlled by an infinitely adjustable valve. The flow from the tank is controlled by a GATHER variable speed magnetic coupling gear pump which delivers a maximum flow rate of 3$dm^3.min^{-1}$. As the tank is open to the atmosphere, additions are limited for safety reasons to dyebath temperatures of less than 80°C. In order to protect the gears of the pump against mechanical damage, a stainless-steel NUPRO in-line filter with a mesh size of 90µm is installed between the tank and the pump. The wire mesh of the filter can be removed for cleaning purposes.

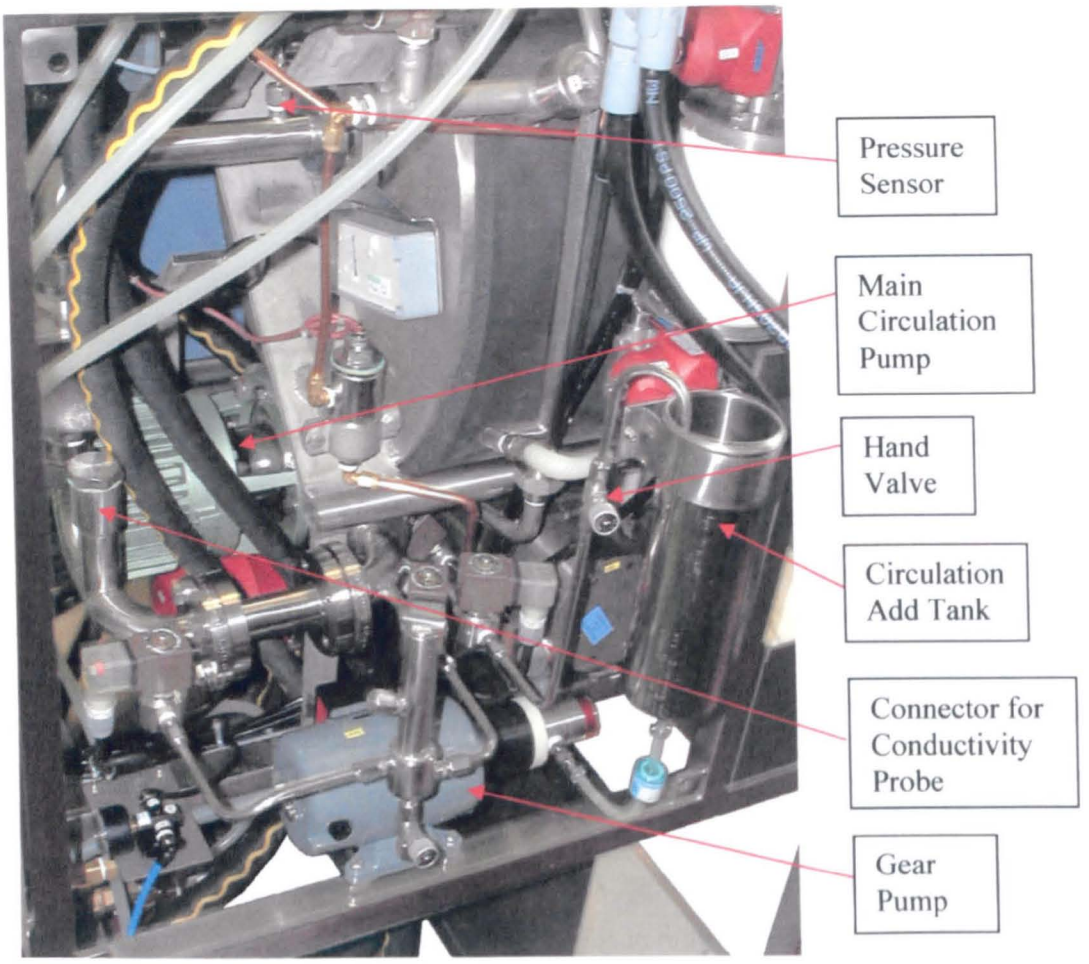

Figure 7.4: JFO Interior

7.1.4 Heating and Cooling

Heating of the treatment chamber is achieved by a water jacket surrounding the entire chamber that can be heated with electrical elements switching in two steps. Each element has 4.5kW so that the possible settings of the system are 0kW (heating switched off), 4.5kW and 9kW (Mathis 2000). When both elements are switched on the maximum temperature gradient obtained at a liquor ratio of 8:1 is around $5°C.min^{-1}$. Due to the large heat capacity of the system, first requiring the water in the jacket to heat up which then increases the temperature of the steel of the main vessel in order to finally augment the dyebath temperature, the time delay before reaching the maximum gradient is several minutes.

Cooling of the machine is made possible by a second jacket at the back of the treatment chamber in which cooling water with a maximum flow rate of around $10dm^3.min^{-1}$ can be introduced. The volume flow of the cooling system can be adjusted manually by a hand valve. At maximum flow, the cooling rate is around $4°C.min^{-1}$ close to the boil and less than $1°C.min^{-1}$ for temperatures of less than 40°C.

7.1.5 Liquid Dosing

Liquids such as dye or electrolyte solutions can be dosed into the suction side of the main circulation pump with a magnetically driven PROMINENT GAMMA G/4a diaphragm dosing pump (figure 7.5, Prominent 1995, Vetter 2001). The flow rate of this pump type is a function of the stroke length and the stroke frequency. The stroke length can be adjusted manually with a knob between 0 and 100%. The frequency of the pump can be varied either manually or via an analogue signal between 0 and 120Hz. At maximum stroke length and frequency, the pump delivers around $210cm^3.min^{-1}$ when there is no counter pressure. The flow rate varies in good approximation linearly with both stroke length and frequency. Thus, keeping the stroke frequency constant, halving the stroke length results in half the flow rate. When properly primed, the pump's precision was better than +/- 5%. An error could be introduced, however, at speeds of more than 50% of the main circulation pump because the suction created was then sufficiently high to draw in liquor even when the dosing pump was not in operation.

Figure 7.5: Liquid Dosing Pump

7.1.6 Filling and Emptying of the Main Vessel

The main treatment chamber is filled with liquor by transfer from the preparation tank, which has hot and cold water connections. As the preparation tank is open to the atmosphere, it is also possible to use distilled water instead of tap water and to dissolve additions such as electrolyte prior to transfer. By pressurising the treatment chamber, it is possible to reverse the flow direction and transfer liquor from the chamber to the preparation tank. This is a useful feature when a fabric entanglement needs to be cleared during the process. This requires removing the liquor from the treatment chamber and opening the front door. Without this feature the dyebath liquor would be lost to the drain.

Draining the chamber occurs by gravity through a pipe located at the bottom of the chamber. It is possible to increase the speed with which the chamber is drained by applying air pressure to the chamber.

7.1.7 Fabric Rinsing

The conventional technique to rinse a fabric is the fill-and-drop-method in which case the treatment chamber is filled with rinse water that is subsequently heated to the desired temperature and circulated for a number of minutes together with the fabric. As an additional feature of the machine used for this project, it is possible to employ controlled rinsing and rinse-to-drain, i.e. to have filling and draining valves simultaneously open while dyebath and fabric are both circulating. This enables much faster cooling gradients and largely prevents fabric contamination by deposition of impurities during the draining step (also discussed in chapter one).

7.1.8 Dyebath Sampling

A possible method to sample the dyebath is to use the sampling port connected to the standard 0.5dm^3 addition tank described in section 7.1.3. The disadvantage of this method is that the sample volume could not be accurately controlled and is relatively high. Moreover, after the first sample, some liquor is likely to remain in the pipe work leading to the sampling port, thereby contaminating subsequent samples.

A second, more suitable method consists of using a small hand-valve in the pH-metre by-pass of the circulation line. Sampling by this method takes less than five seconds, including rinsing, and the volume of the sample can be accurately controlled. Initial tests showed that

after the end of a dye addition, a homogeneous and representative sample of the dyebath was attained after around two minutes circulation time.

7.1.9 Process Control

Contrary to the standard machine, the machine delivered to the Department of Colour Chemistry is equipped with a custom-made PC controller from ADAPTIVE CONTROL SOLUTIONS (Adaptive 2002). It controls all the variables and devices mentioned in the subsection above, i.e. temperature, reel and main circulation pump speed, additions via the two tanks, filling and draining of the main vessel, rinsing mode and liquid dosing. Values of these and other parameters are logged every 10 seconds and can be viewed during and after the process or exported to a CSV-file for analysis with spreadsheet software.

Process profiles and parameter settings can be stored in individual programs. One type of graphical window allows the display and analysis of all the valve positions and the status of the heating and the cooling system during the process (figure 7.6). A second window shows which program steps have already been completed, which step is currently in operation and which steps have yet to be completed.

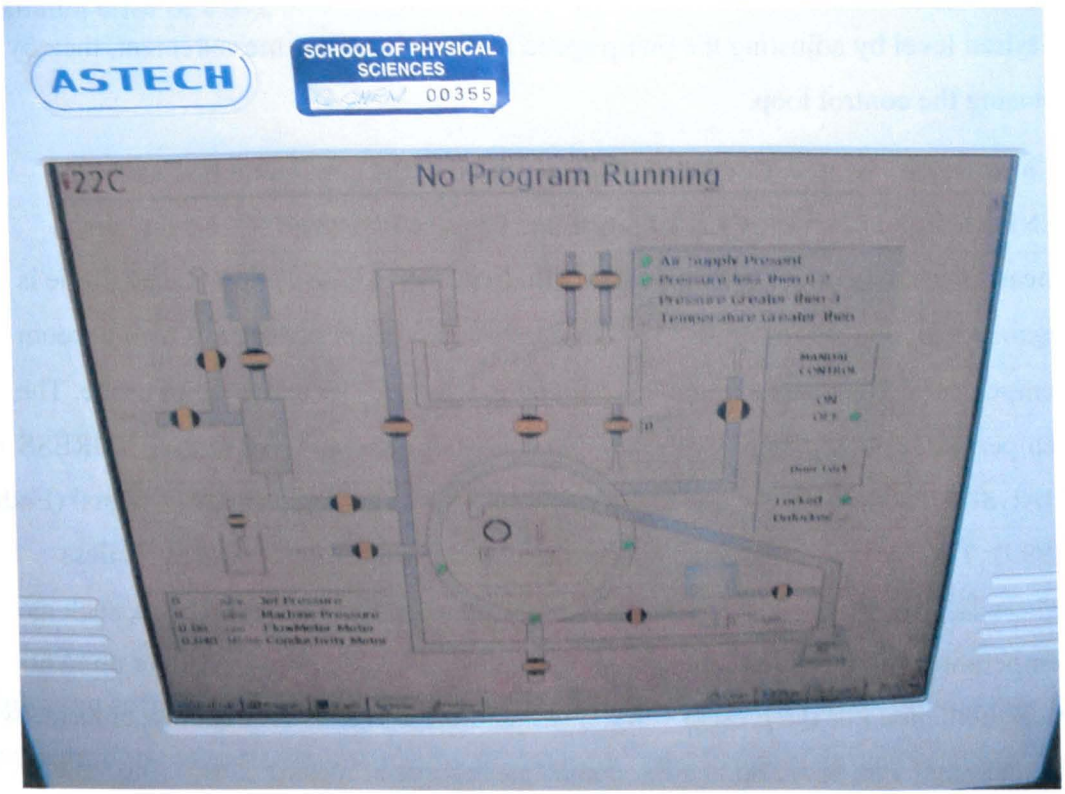

Figure 7.6: Machine Status Window of PC Controller

A number of process parameters are measured on-line so that the possibility for closed-loop control is given. They are:

1) **Temperature**: The Pt-100 temperature sensor is located at the connection between the bottom of the main treatment chamber and the circulation line.

   PID control algorithms for temperature control are available but simple on/off control of the two heating elements was found to be sufficiently accurate for the purposes of the present work, yielding the desired temperature within +/- 0.5°C.

2) **Flow Meter and Bath Circulation Frequency**: An ENDRESS + HAUSER DOSIMAG, an electromagnetic flow meter with a nominal diameter of 25mm, is installed in the main circulation line. Its accuracy is better than 1% and the sensor can tolerate temperatures of up to 130°C at a pressure of up to 30bar (Endress 2000). The measurement signal is converted into an analogue 0-20mA signal with 20mA equalling a flow velocity of $10m.s^{-1}$ and a flow rate of $295dm^3.min^{-1}$ (Mathis 2000). The software allows entering the dyebath volume of a particular batch so that the dyebath circulation frequency can be calculated at each moment during the process. The values of the frequency, as well as that of the flow rate, are logged and displayed on the controller screen.

   During the experiments carried out in this work the flow meter was used solely for monitoring purposes but it would, in principal, be possible to control the flow rate at a desired level by adjusting the pump speed based on the flow measurement, thereby closing the control loop.

3) **Conductivity Meter**: Conductivity is measured in the circulation line with an ENDRESS + HAUSER CLS 30 probe that has a cell constant of $10.5cm^{-1}$ and a measuring range of 0.1 to $200mS.cm^{-1}$ (Endress 1997). The Teflon-coated probe is inert against temperatures of up to 135°C and bore a maximum pressure of 6bar at room temperature. The measurement head contains also a Pt 100 temperature probe. The temperature and conductivity measurement signals are converted by an ENDRESS + HAUSER LIQUISYS S CLM 223 transmitter into an analogue 4-20mA signal (Endress 1999). The value at 20mA can be user-defined and was set to $20mS.cm^{-1}$ unless otherwise mentioned. The transmitter possessed numerous useful features, such as temperature correction of the conductivity value and value averaging over up to 60 measurements. For the present work, a temperature correction for sodium chloride was selected that was based upon a fixed non-linear curve according to IEC 746. The averaging value was set to one, i.e. no signal damping occurred.

   The probe was initially calibrated twice at 25°C with a solution containing 7.419g potassium chloride per kg of water. The results of the calibration are shown in the table 7.2:

Literature Value (Weast 1989:D164)/[mS.cm^{-1}]	Experimental Value/[mS.cm^{-1}]	Error [%]
12.85	12.67	-1.4
12.85	12.96	+0.9

Table 7.2: Calibration Data for Conductivity Probe

The slight difference between reference value and measured value was almost certainly due to inaccuracies in the temperature control during the experiment. The temperature was controlled to +/- 0.2°C but the conductivity value is very sensitive to temperature variations.

In a second test the linearity of the conductivity signal was examined in distilled water at 25°C for common salt concentrations between 0 and 15g.dm^{-3}. The results showed that the signal was approximately linear although the prediction error based upon a linear regression curve was high for concentrations of up to around 1g.dm^{-3} (figure 7.7). For concentrations between 2 and 15g.dm^{-3} the average prediction error was 1.9% with a maximum error of 4.0%.

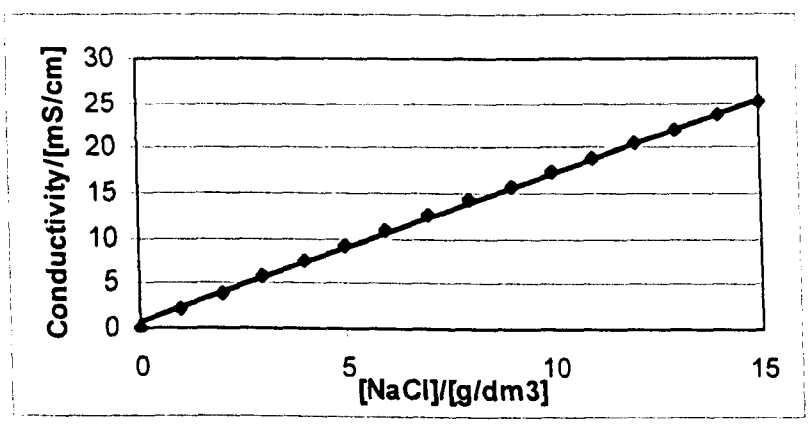

Figure 7.7: Linearity of Conductivity Signal

Third, the accuracy of the built-in temperature correction function was examined for the concentrations of common salt of 0.5g.dm^{-3}, 5g.dm^{-3} and 10g.dm^{-3} at temperatures between 40°C and 80°C. Table 7.3 shows the change of conductivity indicated by the probe when the temperature was increased from 40° to 80°C.

[NaCl]/[g.dm^{-3}]	Change in compensated Conductivity [%]
0.5	+10
5	+4
10	+/-0

Table 7.3: Precision of Temperature Compensation

The compensation was found to be satisfactory at concentration of around 5g.dm^{-3} or higher but deficient at low concentrations. It was also noted that the probe had a significant heat capacity so that around five minutes were required until the integrated temperature sensor of the probe reached equilibrium with the surrounding solution. When a temperature gradient was applied to the dyebath, an overshoot of the conductivity-value could therefore be noted at the end of the heating ramp. The overshoot was caused by the different time constants of the conductivity and the temperature measurement: While the conductivity sensor reacted instantaneously to changes, the temperature probe reacted belatedly. At the end of the temperature ramp the conductivity value therefore reached its maximum several minutes before the in-built temperature probe recorded a steady value.

Even though the meter had been found to be accurate, variations of up to 30% around the true value arose under practical dyeing conditions. It is believed that the most important single reason was the development of foam in the dyebath, caused by the un-intentional introduction of residual surfactant contained in the fabric due to insufficient rinsing during bulk pretreatment. Foam formation was expedited by the high liquor agitation introduced by the jet nozzle. The presence of foam then disturbed the current flow between the two elements of the conductivity cell, which should be entirely immersed in water. The problem was aggravated by the low liquor ratio of 8:1 used in the experiments. As cotton fabric retains around 300% of its own weight in water, the effective free liquor ratio was 5:1, leaving very little dyebath in the treatment chamber.

As the accuracy of the dosing pump was higher than that of the conductivity probe under conditions employed in the experiments, the control loop was not closed and the dosing pump frequency followed a pre-determined profile.

5) **Fabric Circulation Frequency**: The machine is fitted with a MAGNETECT magnetic detector from ADAPTIVE CONTROL SOLUTIONS, located on the front side of the

machine immediately above the treatment chamber (figure 7.8, Adaptive 2000). The sensor is based on the Hall-effect and reacts to the presence of a magnetic field by sending a pulse to the controller. Its sensitivity can be adjusted by a knob accessible when the front panel of the sensor is removed.

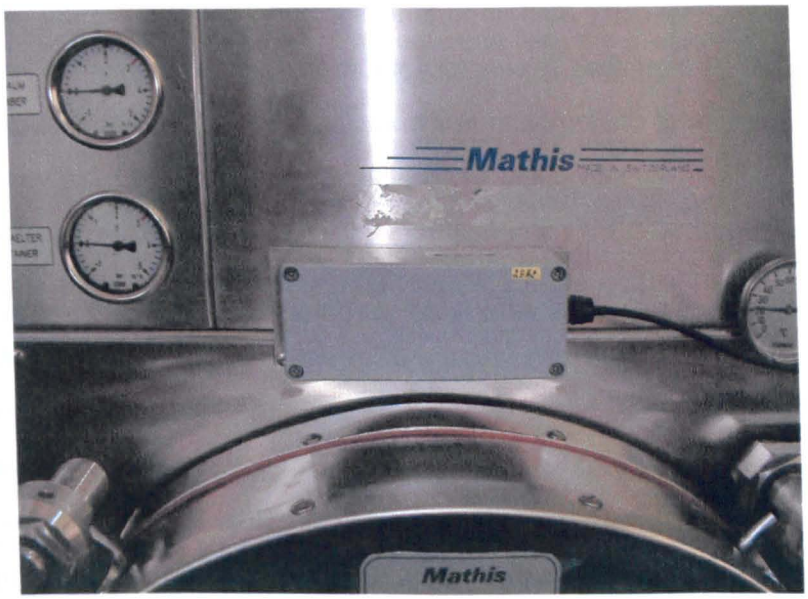

Figure 7.8: Magnetic Detector

For the dyeing experiments, a magnet with a length of around 5cm was sewn into the fabric. The sensitivity was adjusted such that the sensor picked up a signal each time the sewn-in magnet passed over the winch. The controller then counted the time between passages to give the fabric circulation frequency. At very slow fabric speeds of around $2m.min^{-1}$ or less, the detector initially noticed the magnet twice during one passage, so that a dead time after a signal was introduced during which the controller ignored any signal coming from the detector. In this set-up, the controller registered approximately nine out of ten fabric passages correctly.

The controller also allows closing the control loop by adjusting the winch speed according to the measured fabric circulation time to give the desired fabric speed. In order to avoid wild swings in the winch speed introduced by erroneous signals from the detector, the controller would change the winch speed by only 1%, i.e. $0.3m.min^{-1}$, in case of a deviation. The feature was not used, however, for the present experiments because the fabric length of 6.25m remained identical in all experiments and the reproducibility of the fabric circulation time was better than 5s in all cases even without feedback control.

5) **Liquor Pressure in Circulation Line**: Like many production machines, a pressure transmitter, manufactured by WIKA, is located in the main liquor circulation line close to the jet nozzle. Its measurement range is from –1bar (4mA) to 5bar (20mA) (Mathis

2000). The value is displayed during the process on the controller screen and logged to the database for future reference.

7.2 Jet Hydrodynamics

Control of the fluid velocity is an important aspect of the overall control of the dyeing process because, as explained in chapter four, it possibly influences the exhaustion speed as well as the levelness of the application. On the other hand, excessive fluid velocities can abrade the surface of the fabric and result in an unnecessarily high consumption of electricity. Some jet machine manufacturers therefore vary the flow rate during the process, in some cases as a function of the dyeliquor temperature (Bohrer 1990, Carbonell 1990).

As the liquor flow rate in the circulation pipe of production machines is not usually measured, the jet nozzle speed is normally adjusted to the desired value by referring to a differential pressure gauge that is installed in the circulation line. The pressure is then correlated by empirical formulae to the nozzle fluid velocity. The questions that therefore arose concerned the basis for this conversion and the accuracy of the assumptions for the conversion.

The pressure drop in the pipe system of a machine, i.e. the circulation pipe with its valves, bends and the nozzle etc., generally increases with the flow rate. The functional relationship between flow rate and pressure drop, Δp, is given by the following equation (Schade 1989:115):

$$\Delta p = \rho g(z_{ex} - z_{en}) + p_{ex} - p_{en} + \left(\frac{1}{A_{ex}^2 - A_{en}^2} + \sum_{v=1}^{m} \lambda_v \frac{L_v}{D_v A_v^2} + \sum_{t=1}^{n} \zeta_t \frac{1}{A_t^2} \right) \frac{\rho}{2} \dot{V}^2 \qquad (7.1)$$

ρ= density of liquid [kg.m^{-3}]

g = gravitational constant [m^2.s^{-1}]

z_{ex} = height of pipe exit (= nozzle) [m]

z_{en} = height of pipe entrance (= pressure sensor) [m]

p_{ex} = pressure at pipe exit [N.m^{-2}]

p_{en} = pressure at pipe entrance [N.m^{-2}]

A_{en} = pipe cross-sectional area entrance [m^2]

A_{ex} = pipe cross-sectional area exit [m^2]

λ_v = pressure loss coefficient of pipe [-]

L_v = length of pipe [m]

D_v = diameter of pipe [m]

A_v = cross-sectional area of pipe [-]

ζ_t = pressure loss coefficient of fitting [-]

A_t = cross-sectional area of fitting [-]

$\dot{V}$ = volumetric flow rate [m^3.s^{-1}]

Ideally, the pressure sensor would be installed immediately before the nozzle, so that there is no potential energy difference between the liquid at the nozzle and at the sensor. For this machine the pipe entrance and the pipe exit, i.e. the suction pipe of the centrifugal pump and the jet nozzle, are both to the main vessel and as a consequence there is no pressure difference between entrance and exit. If the pressure loss coefficients of the pipe and of the fittings are independent of the flow rate, then the equation is of the general type:

$$\Delta p = A_0 \dot{V}^2 = A_1 v_{nozzle}^2 \tag{7.2}$$

The constants A_0 and A_1 depend on the size of the entrance and exit flow cross-sectional areas and on the design of the pipe system (bends, nozzle design etc.). If the sensor is mounted next to the nozzle, i.e. the pipe length is very short, then the pressure drop is mainly caused by the difference in the flow areas and the obstruction caused by the nozzle itself. For the pilot-scale machine, a calculation showed that the pressure loss due to the nozzle's obstruction was around 15 times higher than that caused by pipe friction.

In a series of experiments on the pilot-scale machine, the pressure drop for different liquor flow speeds and nozzle diameters was determined at 30°C and 8dm^3 of water in the machine without fabric. The coefficient A_1 of equation 7.2 was then calculated by linear regression. These values were compared with the results of a calculation that assumed that all the pressure energy measured by the differential pressure gauge were converted into kinetic energy (table 7.4). The latter method is sometimes used to provide an estimate for the nozzle fluid velocity based upon pressure measurements (Thies 2001).

Table 7.4 lists three nozzle velocities, which were derived in different ways. The first one, named "measured", was derived from the measured flow rate in the circulation pipe of the pilot scale machine by taking into account the surface area of the liquid outlet of the nozzle. The second one, named "regression", was predicted from v_{nozzle} using an equation based upon a linear regression fit of the measured velocity values of the general form of equation 7.2. The third flow rate, named "kinetic energy conversion", was calculated based upon the assumption that all the pressure energy was converted to kinetic energy.

Nozzle Diameter /[mm]	Pump Speed [%]	Nozzle Pressure /[mbar]	Measured /[m/min]	Regression /[m/min]	Kinetic Energy Conversion /[m/min]
40	37	30	137	127	147
	53	75	204	201	232
	70	130	267	264	306
	86	205	329	332	384
	100	235	356	355	411
55	37	30	134	129	147
	53	70	200	197	224
	70	130	265	269	306
	86	205	336	338	384
	100	270	389	387	441
90	37	0	104	0	0
	53	15	153	117	104
	70	35	183	178	159
	86	55	220	223	199
	100	75	250	261	232

Table 7.4: Correlation Pump Speed and Nozzle Velocities

If the 55mm nozzle results are taken as an example, which was the most suitable nozzle for the narrow fabric used in the experiments, the linear regression fit yielded a good estimate of the measured flow rate in the nozzle. The estimate based on the pressure conversion over-estimated the velocity by around 20%.

Once the relationship between nozzle pressure and fluid velocity in the nozzle had been established, the next question was, how the pressure would have to be adjusted to the desired value. On older types of production machine, the pressure can be varied by means of a flap valve in the circulation line. Newer types of machine, that also includes the pilot-scale machine, regulate the pressure by changing the frequency of the electrical supply to

the pump motor, and therefore change the speed of the centrifugal pump in the circulation line. The flow rate created by a centrifugal pump is, for a wide range of flow rates, directly proportional to the applied frequency.

$$\dot{V} \propto f \tag{7.3}$$

$\dot{V}$ = flow rate [$dm^3.min^{-1}$]

f = applied frequency to AC pump drive [$dm^3.s^{-1}$]

For a centrifugal pump, increasing the rotation speed not only increases the flow rate but also the pressure created by the pump. Thus, at a certain rotation speed, both, the necessary flow rate and the necessary pressure are produced. This is the desired operating condition of the pump for a given pipe system (figure 7.9).

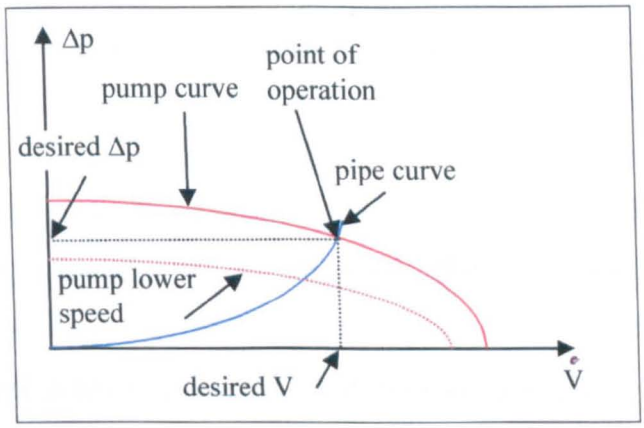

Figure 7.9: Characteristic Pump Curve

The individual characteristics of the pump determine the rotation speed that is needed to reach the point of operation. For the pilot-scale machine, the following relationships between applied frequency, differential pressure at the nozzle and nozzle flow speed were determined for a nozzle diameter of 55mm:

Applied Frequency /[Hz]	**Differential Pressure/[mbar]**	**55mm Nozzle Flow Speed/[m/min]**
17	30	134
25	70	200
33	130	265
41	205	336
47	270	389

Table 7.5: Pump-Pipe System Characteristics Pilot-Scale Jet

The experiments confirmed the linear relationship between pump drive frequency and flow rate.

7.3 Scaling of Dyeing Equipment

The ultimate objective of carrying out sample colorations in a textile dyehouse is to simulate the results obtained under production-scale conditions. For this purpose a number of types of machine of different sizes are available which fall broadly speaking into the three categories of pure laboratory machines, pilot-scale equipment and production machines. The smallest size type is for laboratory-scale fabric dyeing and is often a rotating beaker-type machine with beakers holding 100cm^3 dyebath. A typical sample size for this size of beaker would be around 5g. If larger samples are required, then the beaker size on many machines can be increased up to a maximum of 500 or even 1000cm^3.

On the next size level, there are machines that circulate the dyebath and therefore more closely simulate the conditions of production machines. These machines could be termed summarily as pilot-scale type equipment even though the size varies widely from machines for around 10g of fibre to those holding several kilogram. There are pilot-scale versions available of all the major types of batch machine such as jiggers, beam and package as well as jet dyeing machines.

Finally, there are sampling type machine that very closely resemble true production machines in size and design. In the case of jet dyeing machines, for example, identical nozzles to those employed in bulk would be used. They usually have only one fabric rope and the capacity of the treatment chamber may or may not be smaller than that of some full-fledged production vessels.

One important consideration in the context of the present work is whether results obtained on one machine type can be transferred to another machine type. The focus in this analysis is here only on those aspects related to the reproduction of the dyes' exhaustion behaviour and the dye distribution on the fabric. Issues that may well be important in other contexts, like the tension and surface abrasion that the fabric undergoes in each machine type, will not be considered. Since equilibrium uptake is by definition independent of the machine type, provided the liquor ratio stays constant, and as rotating beaker machines are not suited to analyse the influence of process conditions on dye levelness, because there is no liquor circulation, the list of relevant questions may be reduced to:

1) Can the hydraulic conditions of a bulk jet dyeing machine be simulated on a pilot-scale machine?

2) Do the exhaustion kinetics on bulk and on pilot-scale machines vary with fabric and dyebath circulation speeds?

3) Are the exhaustion kinetics on a rotating-beaker type machine identical to those found on pilot-scale or bulk machines?

The issue of the scaling of test equipment correctly so that experimental results are transferable is a familiar one in many engineering disciplines and falls under the category of similarity and dimensional analysis. Therefore, a brief review of their methods follows next. Subsequently, the identified theoretical considerations are applied to the particular case of the jet dyeing machine and to the extraction of a set of parameters that could be used to evaluate scaling effects. Then the pilot-scale parameter settings are established that would most closely simulate bulk-scale conditions. Finally, the exhaustion kinetics of a rotating beaker laboratory machine are compared to the situation on the pilot-scale machine.

7.3.1 Dimensional Analysis and Physical Similarity

Dimensional analysis is a method to reduce the number of variables in a system in order to reduce the number of necessary experiments and to facilitate a mathematical description (Schade 1989:276). It is frequently used in chemical and hydraulic engineering, e.g. to analyse transport phenomena (Darby 1996, Deen 1998, Taylor 1974).

Any mathematical equation that describes a physical system must be dimensionally homogeneous, i.e. its individual terms must have the same dimension, so that for example a force [N] cannot be equal to but only proportional to a mass [kg]. This requirement is used in dimensional analysis in order to express the desired entity, A, as a function of m dimensionless parameters, P, instead of n dimension-containing variables E ($n \geq m$):

$$A = f(E_1, E_2 \ldots E_n) \Rightarrow f(P_1, P_2 \ldots P_m) \tag{7.4}$$

The parameters P are the dimensionless products of the variables E:

$$\begin{aligned} P_1 &= a_1 E_1^{b1} E_2^{c1} \ldots E_n^{o1} \\ P_2 &= a_2 E_1^{b2} E_2^{c2} \ldots E_n^{o2} \\ &\ldots \\ P_m &= a_m E_1^{bm} E_2^{cm} \ldots E_n^{om} \end{aligned} \tag{7.5}$$

where b_1 to o_m are coefficients ensuring dimensional homogeneity.

The method can be explained by using an example. The flow resistance, R_F [kg.m.s^{-2}], of a sphere can be described as a function of the sphere diameter, D [m], the fluid velocity, c [m.s^{-1}], the fluid density, ρ [kg.m^{-3}], and the kinematic viscosity of the fluid, ν [m^2.s^{-1}]:

$$R_F = f(D, c, \rho, \nu) \tag{7.6}$$

A closer analysis reveals that in its dimensionless form, R_F may be written as:

$$\frac{R_F}{\rho \nu^2} = f\left(\frac{cD}{\nu}\right) \tag{7.7}$$

Instead of requiring four variables, the dimensionless flow resistance ($R_F.\rho^{-1}.\nu^{-2}$) can thus be expressed as a function of one parameter only ($c.D.\nu^{-1}$).

Dimensionless parameters are not only useful to reduce the number of necessary experiments for the characterisation of a given system but they also relay valuable information for the scaling of test equipment. They need to retain their value, independent of the equipment size, if the two systems are to be physically similar. This means that, continuing the example above, the situations in two different flow channels would be hydrodynamically identical if the value of their dimensionless flow resistance ($R_F.\rho^{-1}.\nu^{-2}$) was the same. It also becomes clear that geometrical similarity does not necessarily lead to physical similarity. In the example, if the diameter of a circulation pipe of a pilot-scale equipment had a quarter of the size of the production equipment, the flow velocity would have to be quadrupled if the same liquid were used in order to generate the same flow resistance for a spherical object in the flow. It would therefore not have been enough to merely reduce the diameter of the pipe and leave the fluid velocity unaltered!

7.3.2 Parameters influencing Dye-uptake and distribution on a Jet Dyeing Machine

Based upon the general description of the machine operation forwarded in chapter one, it would be expected that the following machine parameters could influence a dye's exhaustion speed and its distribution on the fabric:

1. **Jet nozzle size and design**, i.e. their influence on fluid velocity and fabric-liquor interchange: Higher fluid velocities and a more intense fabric-liquor interchange could increase the exhaustion per unit time if boundary layer phenomena played a role in the kinetics, i.e. if the process were liquid diffusion controlled.

2. **Fabric-liquor interchange in the storage chamber**: Here the same argument as in the jet nozzle applies: Higher dyebath flow rates could also increase the exhaustion per unit time in the storage chamber as the liquid travels over and through the piled up fabric. In fact it would be expected that variations in the flow rate would more easily influence the dye uptake per unit time in the storage chamber compared to the nozzle because flow rates are much lower in the chamber. The packing density presumably plays a role, too. At higher densities the fibre surface becomes less accessible but on the other hand a higher pressure increases the dye transfer between the wet, compressed fabric layers and the degree of de-watering is also higher. The latter additionally contributes to a better fabric-liquor interchange by increasing the pick-up of fresh dyebath in the nozzle. The degree of de-watering also depends, of course, on the level of the dyebath in the vessel which in turn depends on machine design as well as on the machine load. The overall situation is therefore very complex and could affect both the exhaustion per unit time as well as the time required to obtain a given dye levelness.

3. **Fabric circulation frequency**: The possible influence of the fabric circulation frequency on the uptake rate is related to the fact that the fabric looses some of the adhering water on its way from the storage chamber to the nozzle. Experimental work on winch dyeing machines has shown that the dye molality on the fibre surface decreases on the way from the storage chamber to the reel and, as a consequence, the dye uptake rate is influenced by the fabric circulation frequency (Wyles 1983). The main reason for this decrease is gravitational drainage of the dyebath from the fabric once the fabric has left the dyebath at the bottom of the machine (Fox 1968). When fresh dye solution is supplied in the nozzle, the dye concentration rises again. A similar effect has been found for continuous contacting treatment with squeezing rollers (Burley 1970). These experiments showed that the fabric-fluid interaction is limited to the moments immediately before and after the squeezing when the dyebath is forced out of the fabric or is replenished. This effect is qualitatively depicted for jet dyeing in figure 7.10. It shows a decreasing dyebath concentration in the nozzle, arbitrarily chosen to diminish linearly with time. The dye solution concentration at the fibre surface will be identical to the nozzle concentration until the fabric is lifted out of the dyebath if it is assumed that no diffusional boundary layer exists. The

concentration then drops, indicated by the blue line in figure 7.10, until the solution is replenished in the nozzle. At half the fabric speed, the concentration drop occurs only half as often but its duration is twice as long and the concentration drop is also deeper (red dotted line). The lower the fabric circulation frequency, it could therefore be argued, the lower the average dye solution concentration at the fibre surface and the lower the dye uptake rate.

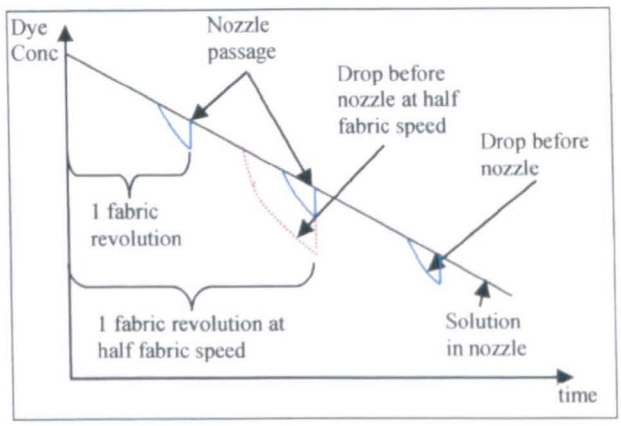

Figure 7.10: Influence of fabric circulation frequency on exhaustion speed

The influence of the fabric circulation frequency on dye levelness has been described in chapter five and is expressed in the contact-concept.

4. **Dyebath circulation frequency**: A higher dyebath circulation frequency, all other machine parameters remaining unchanged, would result in a higher flow rate in the jet nozzle and in the storage chamber. The possible effect of such an increase on kinetics has been described above. Its influence on dye distribution is expressed in the contact-concept, described in chapter five.

5. **Liquor ratio**: Another, fifth factor that is influenced by the machine design and that is potentially of importance is the liquor ratio. It is especially significant in cotton dyeing, as the liquor ratio can strongly influence the degree and the rate of exhaustion.

It should be noted that these considerations apply to machines with hydraulic jets. In jet dyeing machines that use air or air and water to propel the fabric there is virtually no fabric-liquor interchange in the storage chamber. Additionally, in this type of machine an air/water mixture is applied in the jet nozzle. As a consequence, the considerations expressed here apply only partly, if at all, to these machine types.

7.3.3 Derivation of Dimensionless Parameters

7.3.3.1 Influence on Exhaustion Kinetics

From the qualitative analysis in the previous section, it would appear that as far as the dye uptake rate is concerned the central issue is whether boundary layer phenomena exert any influence in any part of the machine. This observation includes questions of fabric-liquor interchange in the nozzle as well as in the storage chamber and also affects the depletion of dye in solution near the fibre surface between the storage chamber and the jet nozzle. A suitable dimensionless parameter, L, to quantify the influence of the boundary layer on the exhaustion kinetics has already been introduced in chapter four, equation 4.31. For a Langmuir isotherm, L becomes

$$L = \frac{D_s l}{D_f \delta K}\left(\frac{[D]_{sat}}{[D]_{sat} - [D]_{f,eq}}\right) \tag{7.8}$$

It could therefore be argued that the exhaustion kinetics on different machines would only be identical if they had the same L-value or if the L-value was high enough not to influence the exhaustion speed. Of all the variables in the equation, only the boundary layer thickness, δ, the partition coefficient, K, and the equilibrium dye uptake, $[D]_{f,eq}$, could possibly change with the machine scale. K and $[D]_{f,eq}$ would only be affected if the liquor ratio, LR, changed. A major difficulty is the determination of δ for the situation found in a dyeing machine. If the simplest case of a plain sheet with parallel flow is assumed, δ is, as explained in chapter four equation 4.33, proportional to the inverse of the square root of the fluid velocity, v_0, and to the square root of the length of the laminar flow in flow direction, l.

$$\bar{\delta} = 1.47\left(\frac{D_s}{\nu}\right)^{\frac{1}{3}}\sqrt{\frac{\nu l}{\upsilon_0}} \tag{7.9}$$

In other systems, the following general relationship holds (McGregor 1965):

$$\delta \propto \frac{1}{\upsilon_0^n} \tag{7.10}$$

where the exponent n is an empirically determined coefficient that assumes a value ranging normally from 0.33 to 1.

It can be easily seen that v_0 could vary with the scale of a machine, typically assuming larger values with increasing machine size. But even l could change with the machine

design, depending for example on the nozzle length and on the size of and flow patterns in the storage chamber.

In summary, it may be concluded that the key dimensionless parameters for the scaling of dyeing equipment are L and LR with respect to exhaustion kinetics. L is mainly influenced by the flow velocity in the vicinity of the fibre surface but could also be affected by geometrical machine differences, especially in the storage chamber.

7.3.3.2 Influence on Unlevelness

Unfortunately, one of the prerequisites in the application of dimensional analysis and similarity is not fulfilled in this case as not all the major factors influencing unlevelness can be expressed mathematically or are even known. There is some link to the parameters influencing the dye uptake rate because it is different dye uptake rates at different locations in the machine that cause unlevelness. But the varying uptake rates could be caused not only by boundary layer effects but also by concentration differences in the dyebath. These are particularly likely to occur in the storage chamber with its relatively low flow rates and high packing densities.

Despite these uncertainties the models and experimental results detailed in chapter five lead to the conclusion that, with respect to the question of scaling, three dimensionless parameters play an important role even though they do not cover all influences. They are the exhaustion per contact, $\Delta E.c^{-1}$, the sensitivity of the dye fibre surface molality to changes in the dyebath molality, $\Delta[D]_{fs}.\Delta[D]_s^{-1}$ [g dye.g fabric^{-1}/(g dye.g water^{-1})] and the liquor ratio [kg water.kg fabric^{-1}], LR. If the LR remained unaffected by the scaling, $\Delta[D]_{fs}.\Delta[D]_s^{-1}$ would not change either. Under this condition $\Delta E.c^{-1}$ becomes the only significant parameter. Consequently, processes on different scales would be directly comparable (i.e. one minute on the first scale would be equivalent to one minute on the second scale) if they had the same number of contacts per minute. For dyeings with identical exhaustion per contact, the same degree of unlevelness would be expected.

7.3.4 Simulation of Production-Scale Conditions on Pilot-Scale

From the previous discussion, the following parameters appear to be central to the scaling of dyeing equipment:

1) Liquor ratio (LR)
2) Number of total contacts per minute ($\Delta E.c^{-1}$)
3) L, more specifically the fluid velocity in the vicinity of the fibre surface (v_0) and the length of laminar flow conditions near the fibre surface (l)

7.3.4.1 Liquor Ratio

Many dyehouses in the UK employ a liquor ratio of 8:1 for the dyeing of cotton but it can be as low as 5:1 on the most modern equipment. Achieving the same low liquor ratio as on production machines is a major challenge for pilot-scale jet machine designers (Smith 1983). The main reason for the difficulty lies in the higher proportion of dyeliquor contained in the pipe work of the pilot-scale machine. The pipe size cannot be scaled down proportionally because the pilot machines are usually specified to run normal width fabric. Therefore, the nozzle and also the attached pipe have to be of a similar size as the production unit. Inquiries with several manufacturers of pilot-scale dyeing machines and test runs at various facilities carried out during the period of this work confirmed the difficulty of achieving low liquor ratios. In most instances a liquor ratio of 12:1 was the lowest attainable value.

The designers of the MATHIS JFO machine tried to circumvent this problem by limiting the pipe lengths to the absolute minimum. This was achieved by eliminating the heat exchanger and by bolting the circulation pump directly onto the main vessel. Thanks to these features the pilot-scale unit required only around 3.5dm^3 of free water (i.e. without fabric in the machine) for the main circulation pump to run properly. Assuming a machine load of 0.85kg of fabric and a water retention of the fabric of around 3dm^3.kg^{-1}, the minimum dyebath volume calculated to a little over 6dm^3. This translated into a minimum required liquor ratio of 7.1:1. When it was additionally taken into account that foam formation increased the risk of pump cavitation, the minimum liquor ratio under practical conditions was 8:1 when the fabric was loaded dry before dyeing. Under industrial conditions cotton is normally pretreated in the same vessel before dyeing. The minimum liquor ratio, even of very efficient machines running at a ratio of 5:1, is effectively 8:1 on a dry-fabric-basis. The important criteria of identical liquor ratio between pilot-scale and production-scale was therefore fulfilled.

7.3.4.2 Fabric and Dyebath Contacts

Fabric

Bulk-scale jet dyeing machines typically run at speeds between 150 and 600m.min^{-1}, resulting in a fabric rope circulation time of 60 to 180s or 0.3 to 1.0 contacts per minute (c.min^{-1}), depending on the length of fabric rope. The 850g of fabric used on the pilot-scale machine had a length of 6.25m. Therefore, if the same fabric circulation times were to be achieved on the pilot-scale jet, a fabric speed of between 2 and 6m.min^{-1} would seem appropriate.

Dyebath

Dyebath circulation times on jet production machines vary between 30s and 360s or between 0.2 and 2.0c.min^{-1} (Rouette 1995:922, Carbonell 2002). A typical value for a modern jet dyeing machines would be between 30s and 60s. With a typical load of 850g on the pilot-scale jet and a liquor ratio of 8:1, the average dyebath volume calculates to around 7dm^3. If the same dyebath circulation times were to be achieved on the pilot-scale, the dyebath flow rate would therefore have to be between 1 and 14dm^3.min^{-1}.

7.3.4.3 Liquor Velocities in Storage Chamber and in the Jet Nozzle

Storage Chamber

The average fluid velocity in the storage area of a production machine is estimated to be around 1.5m.min^{-1} (Kaup 2001). If it is assumed that on the pilot-scale machine the dyebath flows through an area of 5cm by 15cm then the equivalent required flow rate would calculate to 11dm^3.min^{-1}. This is obviously only a very crude estimate because the assumption of the flow area for the pilot-scale jet machine may not be true. This is because some of the flow through the nozzle does not attain the fabric in the storage chamber at all and because there may be significant speed differences within the chamber liquor at different locations.

Additionally, the packing density of a rope in a bulk machine is much higher. The fabric in the pilot-scale machine should therefore be more accessible for the dyebath, but the influence of this effect might be compensated for by a reduced level of dye transfer between fabric layers. The lower compression and the much-reduced acceleration within the pilot-scale machine lead to less de-watering of the fabric before it enters the nozzle. It is difficult to derive theoretically the overall effect of these different parameters. Experience indicates that the fabric-liquor interchange on a pilot-scale machine is often bigger than that on a production machine (Carbonell 2002).

Jet Nozzle

Production-scale jet machines are reported to have a liquor speed in the nozzle between 200m.min^{-1} on soft flow machines and up to 1400m.min^{-1} on pure jets i.e. between 1.5 to 3 times higher than the fabric speed (Cegarra 1992:215). The liquor speed in the pilot jet nozzle would therefore have to reach a speed of between 3 and 18m.min^{-1} for fabric speeds of 2 and 6m.min^{-1}.

The pilot-scale machine came with three different circular nozzles. They all had the same length (75mm) and a similar slit width for the liquor of between 2.75 and 3.75mm but varied in their nominal diameter between 40, 55 and 90mm. As the slit area of each nozzle

was known, the average liquor speed in the nozzle could be calculated as a function of the dyebath flow rate (table 7.6).

Nozzle Diameter (nominal)/[mm]	Dyebath Flow Rate/[$dm^3.min^{-1}$]	Liquor Speed in Nozzle/[$m.min^{-1}$]
40	1	2
55	1	2
90	1	1
40	7	12
55	7	12
90	7	9
40	200	360
55	200	350
90	200	240

Table 7.6: Liquor speed in different jet nozzles

7.3.4.4 Suggested Parameter Settings Pilot-scale Jet

All in all, in order to get the same number of contacts per minute it would therefore appear that the settings given in table 7.7 on the pilot machine appropriately scaled-down the conditions in production equipment. The dyebath flow rates were calculated for a liquor ratio of 8:1 and for the weight of fabric used in the experiments, i.e. $136g.m^{-1}$.

	Fabric Contacts /[min^{-1}]	Fabric Speed /[$m.min^{-1}$]	Dyebath Contacts /[min^{-1}]	Dyebath Flow Rate /[$dm^3.min^{-1}$]	Nozzle Liquor Speed/ [$m.min^{-1}$]
Low Dynamic	0.32	2 (P) 150 (B)	0.14	1 (P) 71 (B)	2 (P) 225 (B)
High Dynamic	0.96	6 (P) 400 (B)	1.03	7 (P) 470 (B)	12 (P) 1200 (B)

Table 7.7: Pilot scale settings for the Simulation of Bulk-scale Conditions (P = pilot-scale, B = bulk-scale)

Two important differences between the pilot and the production jet, however, have to be noted.

First, and most importantly, a dyebath flow rate scaled-down to match the number of bath contacts per minute of a production machine leads to a much lower velocity in the nozzle and therefore to a possibly significantly thicker boundary layer. An estimate for the changes in δ can be based upon the following general relationship:

$$\frac{L_{pilot}}{L_{bulk}} \propto \frac{\delta_{bulk}}{\delta_{pilot}} \propto \frac{v_{0,pilot}^{n}}{v_{0,bulk}^{n}} \tag{7.11}$$

Table 7.8 shows that the ratio of the L-values varies between a factor of 0.01 (for n = 1) and a factor of 0.22 (for n = 0.33). It is therefore clear that different flow regimes in pilot and bulk machine result in significant differences of the boundary layer thickness and possibly also of the dye uptake per unit time.

	Bulk	**Pilot-scale**
Liquid speed [$m.min^{-1}$]	800	8
L_{pilot}/L_{bulk} (n = 0.33)	0.22	
L_{pilot}/L_{bulk} (n = 1)	0.01	

Table 7.8: Ratio of L-values pilot-scale to bulk

This calculation shows that although the cycle times for both dyebath and fabric might be appropriately scaled-down, the kinetics could change from a film-diffusion controlled system in the production machine to a liquid-diffusion controlled system in the pilot-scale machine.

A second important difference is that, unlike on a production machine, the jet of the pilot machine is not able on its own to provide enough force to propel the fabric but it has to rely heavily on the winch. In a conventional production jet dyeing machine the fabric rope is transported mostly by the liquor from the jet nozzle with a minor contribution from the winch reel. How much each of them contributes to the overall force depends on the machine design as well as the fabric and liquor speeds. The total force required to transport the fabric can be divided into two parts (Boehnke 1998): the force necessary to lift the wet fabric from the dyeing chamber to the highest point in the machine (F_l) and the force necessary to accelerate the fabric (F_a):

$$F_{\Sigma} = F_l + F_a = mgh_l + mv^2 \tag{7.12}$$

m = specific mass of wet fabric [kg.m^{-1}]

g = gravitational constant [m.s^{-2}]

h_l = lifting height of fabric[m]

v = fabric speed [m.s^{-1}]

The force exerted by the winch reel, F_r, can be approximated by:

$$F_r = F_d e^{\mu\alpha} = mgh_d e^{\mu\alpha} \tag{7.13}$$

F_d = force of wet fabric at exit of winch [N]

h_d = dropping height of fabric from winch to storage chamber [m]

μ = friction factor [-]

α = angle described by fabric as it passes around the winch [-]

The force applied by the jet, F_j, can be calculated if the fabric rope is idealised as a pipe with a fairly rough surface and with liquid flowing around it (not inside it). In this case, the force is entirely due to friction losses at the rope surface. Common pipe friction models, such as the one developed by Nikuradse, can be used if it is further assumed that the friction loss is the same for a fluid flow around the outside of a pipe (situation in jet nozzle) as for a fluid flow inside a pipe (normal tube) (equation 7.14, Boehnke 1998).

$$F_j = \frac{(v_0 - v)^2 l \rho \pi d}{8\left(2\lg\left(\frac{d}{k}\right) + 1.138\right)^2} \tag{7.14}$$

v_0 = fluid velocity [m.s^{-1}]

v = fabric rope velocity [m.s^{-1}]

l = effective length of nozzle [m]

ρ = density fluid [kg.m^{-1}]

d = diameter fabric rope [m]

k = roughness rope surface [m]

Based upon equations 7.12 to 7.14, the mechanics of the fabric transport on a typical bulk machine can be compared with the situation on the pilot-scale machine. The calculations in the table 7.9 assume for both machines a wet fabric mass, m, of 560g.m^{-1} (i.e. approximately 300% pick-up), a rope diameter, d, of 4cm, a friction factor, μ, of 0.1 and a fabric roughness, k, of 0.003m.

	Pilot-scale	Bulk	Parameters Pilot-scale	Parameters Bulk
Winch/[N] (eq. 7.13)	1.8	9.6	l: 0.05m α: 90° v: 6m.min^{-1} v_{fl}: 8dm^3.min^{-1} h_l: 0.3m h_d: 0.3m	l: 0.5m α: 180° v: 400m.min^{-1} v_{fl}: 800dm^3.min^{-1} h_l: 1.5m h_d: 1.5m
Jet/[N] (eq. 7.14)	0.04	30		
Total/[N] (eq. 7.12)	1.7	33		
Winch [%]	108	29		

Table 7.9: Forces on Fabric Rope in Pilot-scale and Bulk Machine

The winch and the jet contributions data in table 7.9 do not add up to the total because of inaccuracies in the underlying assumptions but the results are qualitatively instructive. On production machines less than a third of the total force required to move the fabric is contributed by the winch. The winch is almost entirely responsible for fabric transport on the pilot-scale machine. The much weaker force exerted by the jet points to a lower fabric-liquor interchange for the pilot-scale machine compared to the production machine. This is mainly due to the lower nozzle velocity but is also a consequence of the short ring style of jet nozzle that lacks the attached tube often employed in production machines.

For both reasons, the reduced fabric-liquor interchange and the thicker diffusional boundary layer, it therefore seemed better to adjust the flow rate on the pilot machine such that the absolute speed difference between the liquid and the fabric in the jet nozzle was approximately equal to the speed difference on the bulk machine. This leads, however, to a much shorter dyebath circulation time, expressed in the higher number of dyebath contacts per minute, in the pilot-scale machine (table 7.10).

	Fabric Contacts /[min^{-1}]	Fabric Speed /[$m.min^{-1}$]	Dyebath Contacts /[min^{-1}]	Dyebath Flow Rate /[$dm^3.min^{-1}$]	Nozzle Liquor Speed /[$m.min^{-1}$]
Low Dynamic	0.32	2 (P) 150 (B)	5.88 (P) 0.14 (B)	40 (P) 71 (B)	70 (P) 225 (B)
High Dynamic	0.96	6 (P) 400 (B)	29.41 (P) 1.03 (B)	200 (P) 470 (B)	350 (P) 1200 (B)

Table 7.10: Modified Pilot-scale Settings for the Simulation of Bulk-scale conditions

Table 7.10 shows that the pilot scale fluid velocity in the nozzle does not reach the very high speeds of certain types of production units. Nevertheless, it should be possible to simulate the hydrodynamic characteristics of "gentler" bulk jets. As the fabric speed is much smaller than the liquid speed in the nozzle it would be expected that changes in the fabric speed, e.g. from 2m.min^{-1} to 6m.min^{-1}, would not have a significant influence on the thickness of the boundary layer. It is conceivable, however, that changes in the liquor speed in the jet nozzle, e.g. from 70 to 350m.min^{-1}, could have an influence on the exhaustion kinetics.

Since the number of dyebath contacts per minute under the modified conditions is drastically increased compared to a production machine, process profiles cannot be compared directly on a time-basis but need to be converted to a contact-basis. This is particularly relevant for the transfer of results for experiments designed to investigate dyeing unlevelness.

Another consequence of the higher bath circulation frequency is that the liquor flow rate in the storage chamber could be higher than that on a production machine but, as pointed out in section 7.3.4.3, grounds for an accurate calculation do not exist.

7.3.5 Exhaustion Kinetics of Pilot-scale and Rotating-beaker Machines

Having established the range of parameter settings that most closely simulate bulk conditions on the pilot-scale machine, the remaining questions to be answered are whether changes within this range affect the exhaustion kinetics and whether there are any significant differences between results obtained using a rotating-beaker machine and a

pilot-machine. The experiments reported in this section were carried out to answer these questions.

7.3.5.1 Experimental

The standard nozzle diameter for the tests of this section was 55mm but some tests used a 90mm nozzle, which is specifically mentioned. All the experiments were carried out under standard conditions, i.e. at a liquor ratio of 8:1 and with a fabric load of around 850g (fabric mass: 136g.m^{-1}). The experiments took place at 65°C and used 0.45% (omf) dye as well as 10g.dm^{-3} sodium chloride unless otherwise mentioned. These conditions create a high substantivity environment which previous considerations had shown to be most favourable for the detection of boundary layer influences on the dye uptake rate (chapter 4.3). All the salt was added to the solution at the beginning and dyeliquor addition occurred by using either the pressurised 0.5dm^3 tank or the 1dm^3 open tank. Time started counting from the moment when the dye was added. Samples were normally taken after 3, 5, 15, 30, 45, 60, 90 and 120 minutes. In some instances, the intervals were changed to 3, 5, 7, 10, 15, 30, 60 and 120 minutes. The dye exhaustion was determined indirectly via analysis of the dyebath as described in chapter six. Three repeat dyeings yielded a variation coefficient in the averaged exhaustion values of less than 1%.

Initial tests had shown that after each addition a small percentage of the dyeliquor (around 6% in case of the pressure addition and around 3% in case of the pumped addition) remained in the tanks and their adjacent pipes. In the calculations these dye losses have been taken into account.

In the experiments the fabric speed was between 2 and 9m.min^{-1} and the dyebath flow rate was between 10 and 80dm^3.min^{-1}. Flow rates higher than around 80dm^3.min^{-1} lead to pulsations in the flow as the circulation pump started to temporarily suck in air. At higher liquor ratios higher flow rates would have been possible but at the preferred liquor ratio of 8:1, 80dm^3.min^{-1} constituted the maximum value for stable running conditions.

A second set of experiments was carried out on a MATHIS LABOMAT infrared rotating beaker machine containing a maximum of 16 100cm^3 beakers. In order to examine whether the rotation speed of the lab dyeing machine had an influence on the exhaustion speed, experiments were repeated at three different settings: the minimum possible setting of 5 revolutions per minute, 25 revolutions per minute and the maximum possible setting of 65 revolutions per minute. Two series of three dyeings were conducted at 65°C, one under low substantivity conditions (4% dye, 0g.dm^{-3} salt) and one under high substantivity conditions (0.45% dye, 10g.dm^{-3} salt). The high substantivity conditions were thus identical to the conditions of the pilot-scale experiments.

7.3.5.2 Influence of Fabric Speed and of Liquor Speed on Exhaustion Kinetics

It was found that variations in fabric and liquor speed within the limits of scaled-down bulk conditions did not affect the uptake rate, which is reported in figure 7.11 as per cent of equilibrium exhaustion. If it is additionally considered that processes in industry usually have a much lower uptake rate, because the exhaustion speed is controlled by temperature and/or by gradual salt addition, it is safe to conclude that fabric speed and liquor speed do not affect the exhaustion kinetics for values within the normal industrial range.

It was found that when the dyebath flow rate was further reduced (at a fabric speed of $2m.min^{-1}$), the exhaustion speed started to drop (figure 7.12). At flow rates lower than approximately $30dm^3.min^{-1}$, the nozzle action reduced visibly. Instead of providing a full, even water jet, most of the water exited the nozzle at the bottom and barely touched the fabric rope. Unfortunately, the experimental error increased at low flow rates as the frequency supply to the main centrifugal pump was at the lower limit of its spectrum and the flow rate became susceptible to minor pressure variations in the circulation line. Pressure variations occurred when dye was transferred by a pressure gradient from the addition tank to the main vessel, so that fluctuations in the flow rate during processing could not be avoided. Nevertheless, the data shown in figure 7.12 indicate a clear tendency.

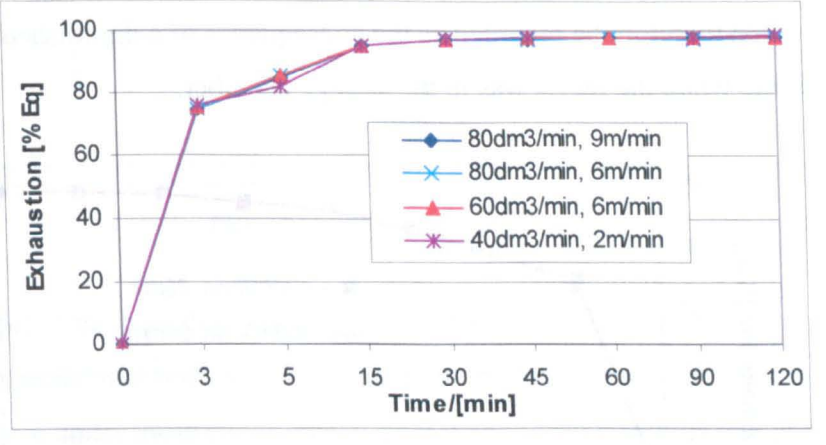

Figure 7.11: Influence of Fabric and Liquor Speed under scaled-down Bulk Conditions

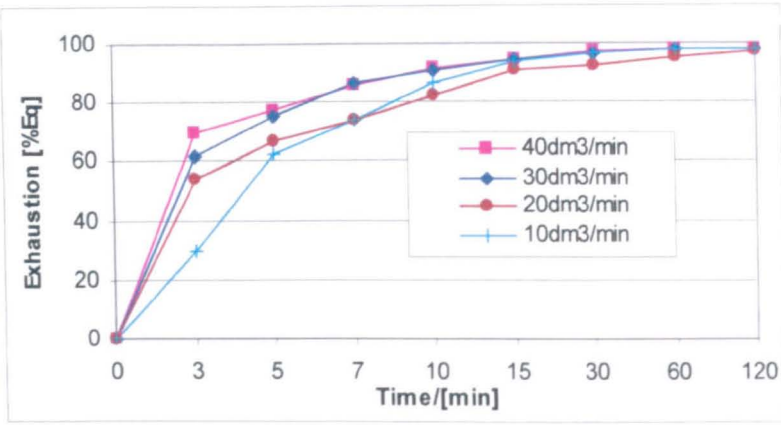

Figure 7.12: Influence of Liquor Speed at low Levels, 2m.min^{-1} Fabric Speed

7.3.5.3 Influence of Nozzle Diameter on Exhaustion Kinetics

In order to find out whether the reduced dye uptake rate at low liquor speeds was caused by a diminished level of fabric-liquor interaction in the nozzle, the nozzle diameter was increased from 55mm to 90mm (the fabric speed remained 2m.min^{-1}). With the large diameter, the fabric rope did not touch the nozzle walls and the fabric-liquor interaction in the jet nozzle was thus reduced to a minimum, even at flow rates of 40dm^3.min^{-1} and more. Surprisingly, the exhaustion speed did not become smaller (figure 7.13). This indicated that the interaction in the nozzle had less of an influence on the exhaustion speed than the fabric-liquor interchange in the storage area. The drop in the exhaustion rate shown in figure 7.12 could therefore be regarded as the consequence of a diminished dye supply within the fabric while the fabric was in the storage chamber.

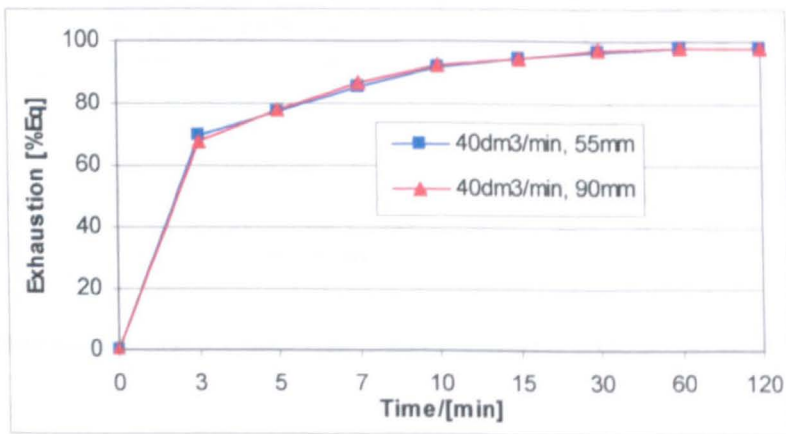

Figure 7.13: Influence of Nozzle Diameter, 2m.min^{-1} Fabric Speed

The importance of the flow through the storage chamber for the overall dye uptake rate would also explain why the fabric speed did not influence the exhaustion speed. If dye supply to the fabric occurred mainly in the nozzle it would be expected that a higher fabric speed also led to a higher uptake rate as postulated in section 7.3.2. If however the dye

supply were essentially uniform around the machine, the influence of the fabric circulation frequency would vanish.

The fact that increases in the flow speed beyond $40dm^3.min^{-1}$ did not increase the uptake rate implied that any influence of a diffusional boundary layer was eliminated. Consequently, the exhaustion speed was solely determined by the dye "demand" from the fibre, not by the dye "supply" from the dyebath.

7.3.5.4 Comparison of Rotating Beaker with Pilot-scale Jet Machine

The experimental results expressed in figure 7.14 show that the rotation speed in the rotating beaker machine generally did not influence the exhaustion speed, implying that the dyeing process was not liquid-diffusion limited. The only exception appeared to be the early stages of the high substantivity dyeing at low rotation speed when a small but significant drop in the exhaustion value was observed. For all subsequent dyeings a rotation speed of 25 revolutions per minute was selected as the standard setting.

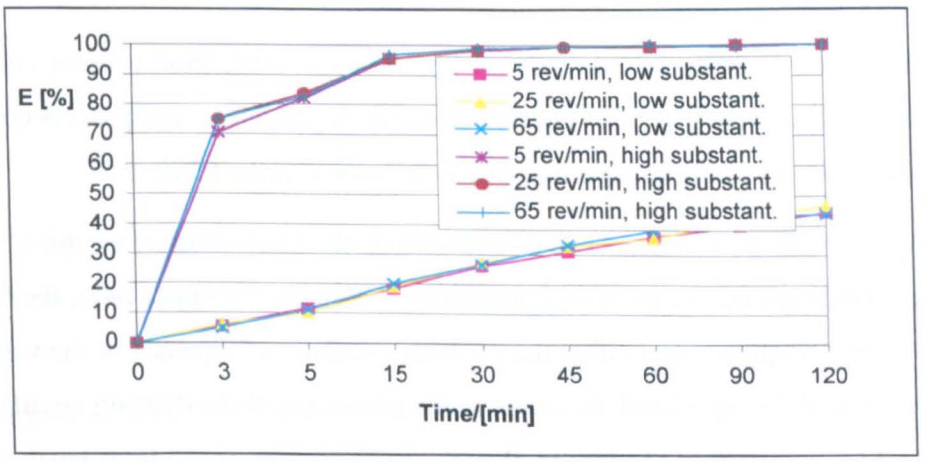

Figure 7.14:Influence of Rotation Speed

Since any effect of the boundary layer vanished at sufficiently high flow or agitation rates, it would be expected that both types of equipment, beaker and jet, yield the same exhaustion curve under these conditions. Figure 7.15 indeed confirms this prediction, within the margins of experimental error.

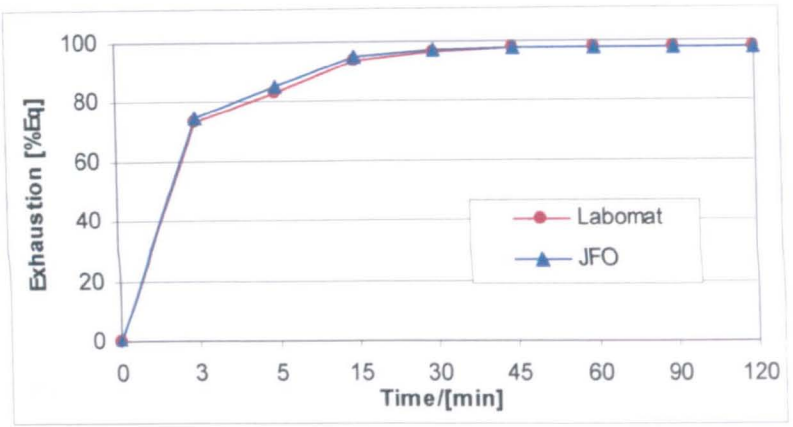

Figure 7.15: Influence of Equipment-type

7.3.6 Conclusions Concerning the Scaling of Dyeing Equipment

In summary, the following conclusions may be drawn:

1. Liquor ratio, dyebath and fabric circulation times, average fluid velocity (v_0) and flow pattern (l) are parameters that characterise a dyeing machine and process conditions in terms of exhaustion behaviour and dye distribution on the fabric.

2. Three of the five parameters can be adjusted on the pilot-scale jet machine to match the corresponding parameters of bulk machines. These are the liquor ratio, the fabric circulation frequency and either the dyebath circulation frequency or the velocity difference of the liquid and the fabric in the jet nozzle. If the dyebath circulation time is adjusted to match bulk conditions, then the fluid velocity in the jet is much smaller. On the other hand, if the fluid velocity is increased then the dyebath circulation time is shorter than on industrial machines.

   The situation could be improved if nozzles on the pilot-scale machine were designed with a smaller slit width, yielding higher velocities at the same dyebath circulation rate. In any case, the fabric-liquor interchange in the pilot-scale nozzle remains weaker. The conditions in the storage chamber, affecting v_0 as well as l, are also very different, but competing influences make a prediction of a beneficiary or adversary impact on exhaustion kinetics and dye distribution difficult.

3. Exhaustion kinetics are independent of the fabric and liquor flow conditions under industry-typical parameter settings in a jet machine. Only when the dyebath flow rate drops to low levels is the exhaustion rate reduced, at least under high substantivity conditions.

4. If the exhaustion speed is essentially independent of the fabric and liquor speeds, then the dye supply at the fibre surface must be at least equal to the amount being taken up the fibre at any moment in the entire machine. If it were different, i.e. if the dye supply were for example reduced in the storage chamber, the fabric speed would have an influence on the overall exhaustion speed because the more frequently the fabric passes through the nozzle, the more often the dye would be replenished. Therefore boundary layer effects appear to be negligible not only in the in the jet nozzle but also in the storage chamber and, as a result, the exhaustion speed is independent of the fabric circulation rate in the range studied.

5. The fact that the fabric speed does not play a role in the exhaustion kinetics on a jet machine marks a difference to the older winch dyeing machine. The difference must be due to a better fabric-liquor interchange in the jet machine. One contributor to the better exchange is of course the jet nozzle which has no equivalent on a winch dyeing machine. But based upon this investigation it would appear that the major distinction lies in the higher interchange in the storage chamber because the dyebath is flowing quite rapidly over the stacked fabric to the suction side of the main circulation pump. On a winch machine, on the other hand, a slow moving fabric rests in a non-circulating bath, thus creating a fairly static situation.

6. Exhaustion kinetics on a rotating beaker machine are independent of the beaker rotation speed, indicating that boundary layer effects are not significant for the rotation speeds studied.

7. Exhaustion kinetics were identical on the pilot-scale jet and the rotating beaker machine even under high substantivity conditions when boundary layer effects are most likely to influence the dye uptake rate. This further confirms the assumption that boundary layer effects are negligible.

8. From a process modelling point of view, the findings lead to the (welcome) conclusion that simulation models of the exhaustion kinetics do not have to take into account liquor and fabric flow conditions. The same is not true, of course, for their effect on dye levelness. Here it would be expected that liquor flow and fabric flow do play an important role in the dye distribution on the fabric.

7.4 References

1. Adaptive Control Solutions, http://www.adaptivecontrol.com, last access date: 10.May 2002

2. Adaptive Control Solutions, Technical Information Magnetect Seam Detection (2000)

3. Boehnke B, Mell. Textilber. 79 (1998) 346

4. Bohrer E, Heetjans J H, Mell. Textilber. 71 (1990) 988

5. Burley R, Textile Manufacturer 96 (1970) 332

6. Carbonell J, Int. Text. Bul. 36 (1) (1990) 7

7. Carbonell J, personnel communication, August 2002

8. Cegarra J, Puente P, Valldeperas J, The Dyeing of Textile Materials (Biella: Texilia 1992)

9. Darby R, Chemical Engineering Fluid Mechanics (New York: Marcel Dekker 1996)

10. Deen W M, Analysis of Transport Phenomena (New York: Oxford University Press 1998)

11. Endress + Hauser, Calibration Protocol Dosimag A, 28.02.2000

12. Endress + Hauser, Technical Information Conductivity Measuring Cell CLS 30, TI 086C/07/en (1997)

13. Endress + Hauser, Technical Information Liquisys S CLM 223/253, BA 193C/07/en (1999)

14. Fox M R, J.S.D.C. 84 (1968) 401

15. Kaup S, personnel communication, July 2001

16. Mathis AG, Electro Drawings, JFO 15000, Zurich (2000)

17. Mathis AG, Operating Instruction Jet Dyeing Apparatus Type JFO, Zurich (1998)

18. Mathis AG, Technical Information Laboratory Overflow Jet Type JFO, Zurich (1995)

19. McGregor R, Peters R H, J.S.D.C. 71 (1965) 393

20. ProMinent, Operating Instructions Metering Pump Gamma G/4a, (1995)

21. Ratcliffe J D, Rev. Prog. Col. 8 (1978) 58

22. Rouette H P, Lexikon der Textilveredlung, (Duelmen: Laumann Verlag 1995)

23. Sawa Pumpen, Technical Information ZA17-50/40 (1998)

24. Schade H, Kunz E, Stroemungslehre, 2nd edition (Berlin: de Gruyter 1989)

25. Smith S S, in: C Duckworth (Ed.), Engineering in Textile Coloration (SDC: Bradford 1983)

26. Taylor E S, Dimensional Analysis for Engineers (London: Clarendon Press 1974)

27. Thies, Technical Information Sheet (2001)

28. Vetter G, Handbuch Dosieren, 2nd edition (Essen: Vulkan Verlag 2001)

29. Weast R C, Astle M J, Beyer W H, Handbook of Chemistry and Physics (CRC: Boca Raton 1988)

30. Wyles D H, in C Duckworth, (Ed.) Engineering in Textile Coloration (Bradford: SDC 1983)

8 Development of an Equilibrium Sorption Model

In this chapter, the first section is devoted to answering the question of the maximum dye deposition error that is still visually acceptable. This is necessary in order to specify the required accuracy of any equilibrium sorption model. Afterward, the performance of the five different equilibrium sorption models introduced in chapter three is compared. The five models are:

1) 2-phase Donnan
2) 3-phase Donnan
3) 3-phase Donnan with variable internal volume V
4) Gouy-Chapman
5) Gouy-Chapman with fibre saturation value $[D]_{sat}$

Based upon the results of their evaluation, a model is then developed that is shown to predict the experimentally observed results of this study with sufficient accuracy.

8.1 Experimental

Dye equilibrium sorption tests with 0.2, 0.45, 1.35 and 4% (omf) dye were performed on a Roaches Pyrotec S infrared laboratory dyeing machine using 275cm^3 beakers. Each dye concentration was used at three temperatures, 65°C, 90°C and 100°C – and six different concentrations of common salt, 0, 2.5, 5, 7.5, 10 and 15g.dm^{-3}. Initial attempts to include 43°C as a fourth temperature were not successful because the equilibrium dyeing time was found to be more than three weeks and dye and fabric degradation significantly biased the experimental results. A liquor ratio of 8:1 was used, calculated from the fabric weight in its bone-dry state. The following times were found sufficient to reach equilibrium conditions: 72 hours at 65°C, 8 hours at 90°C and 6 hours at 100°C. The dye exhaustion was determined indirectly via analysis of the dyebath at the end of the dyeing process as explained in chapter six. The experimental error lead to a variation coefficient of the measured exhaustion value of 1.2% on average. The largest observed fluctuation between experiments in absolute terms was 4%.

Close analysis revealed that each gram of fabric contributed electrolyte to the dyebath solution. Atomic Absorption Spectroscopy measurements gave a sodium concentration of 2.10^{-5}mol.g^{-1} fabric. Conductivity measurements indicated that some other sources of ions were present on the fabric, too. If those unknown ions had an identical conductivity to

sodium chloride, then the total equivalent sodium concentration would equate between 2.5 and $3.5.10^{-5}$mol.g^{-1}fabric. A value of $3.5.10^{-5}$mol.g^{-1} sodium chloride was taken into account in all the calculations.

In order to evaluate the different models to calculate affinity more thoroughly, experimental results of other authors' sorption isotherms were also analysed. Sometimes assumptions, e.g. about the dyebath pH, had to be made because the published experimental conditions did not contain this information. For the studies mentioned in table 8.1 it was felt, however, that inaccuracies introduced by these estimates would not have significantly changed the results. In the case of pH, for example, the range of typical pH values for direct dyeings is fairly narrow (6.5 – 8.0) and therefore hardly affects the ionisation degree of the hydroxyl and carboxyl groups of the cotton.

Table 8.1 summarises the experiments that were included in the analysis.

Willis et al.'s experiments were chosen because their experiments covered a wide range of dye and salt concentrations and were also conducted at different temperatures. In the analysis, experiments were not included that had a salt concentrations of less than 2g.dm^{-3} because the sodium contributions of the dye, which were not known, might have become significant. Gerber's experiments were of interest because he used a commercial, as opposed to a purified, dye in his experiments with a purity of 50%. For the calculations, the diluent was assumed to be only sodium sulphate. Neale et al.'s experiments analysed the influence of different carboxyl-concentrations of the cotton fibre on the dye sorption. It had been previously shown that the Donnan method can take into account their electrostatic effect (Porter 1992) but no comparison with the Gouy-Chapman method was available. Peters et al.'s isotherms were included in this investigation because they analysed the influence of pH on the partition coefficient of a vat dye on cupro, a member of the cellulosic fibre family. Whereas the carboxyl-group is mostly ionised at pH-values above 7, the hydroxyl-group only ionises at higher pH levels. If the equilibrium sorption model were correct, it would compensate for the effect of changing pH-values and would nevertheless yield a constant affinity.

All calculations were performed using MS Excel on a standard Pentium PC.

Source (Name of Dataset)	Dye	Experimental Conditions
Willis 1945 (DY12)	Direct Yellow 12 (Crysophenine G) on cellophane	Temperatures: 40, 60, 80 and 97.5°C Salt concentrations: 2 – 40g.dm^{-3} NaCl Dye concentrations on fibre: 0.01 – 0.19mol.dm^{-3} internal phase pH = 7.2 (estimate)
Gerber 1990 (DB106)	Direct Blue 106 on cotton	Temperature: 98°C Salt concentrations: 5, 15, 45g.dm^{-3} Na_2SO_4 Dye concentrations on fibre: 0.002 – 0.02mol.dm^{-3} internal phase pH = 4.5
Neale 1940 (DB1)	Direct Blue 1 on high carboxyl-cotton	Temperature: 90°C Salt concentration: 5g.dm^{-3} NaCl Dye concentrations on fibre: 0.005 – 0.02mol.dm^{-3} internal phase pH = 6.2
Peters 1954 (VR35)	Vat Red 35 (Caledon Red BN) on cupro	Temperature: 40°C Salt concentration: 5.8 - 35.1g.dm^{-3} NaCl Dye concentrations on fibre: 0.03 – 0.4mol.dm^{-3} internal phase pH = 12 – 13.3
This study (DY162)	Direct Yellow 162 (Optisal Yellow 2RL) on cotton	Temperatures: 65, 90 and 100°C Salt concentrations: 0, 2.5, 5, 10 and 15g.dm^{-3} NaCl Dye concentrations on fibre: 0.003 – 0.06mol.dm^{-3} internal phase pH = 7.2 – 8.0

Table 8.1: Experiments included in Affinity Calculations

8.2 Required Precision of Dye on the Fibre Prediction

The reflectance values of a number of dyeings, the dye amounts of which were known from dyebath measurements, were determined according to the method described in chapter six. After arbitrarily designating one sample in a pair of fabric samples as the standard, the reflectance values were then converted into a $\Delta E_{(CMC\ 2:1)}$-colour difference number by using the algorithms in the DATACOLOR software of the spectrophotometer. If a $\Delta E_{(CMC\ 2:1)}$-value of 1.0 is taken as the limit of what is visually acceptable, then the data of table 8.2 indicates that a dye deposition error, DDE, of approximately 10% would be the maximum dye deposition error that is visually acceptable. The DDE appeared to be independent of the

average dye amount on the fabrics. In view of the fact that the acceptable variation might be reduced by a factor of 2 for combination dyeings, a 5% target value for the DDE was chosen for the subsequent model evaluation. This implies that the affinity model would have to predict the dye amount on the fabric correctly within +/- 5%.

Dye Concentration Standard [% omf]	Dye Deposition Error Sample (DDE) [%]	$\Delta E_{(CMC\ 2:1)}$ [-]	ΔE/DDE [-]	Average ΔE/DDE [-]
0.19	-11.2	0.75	6.6	
0.19	-6.8	0.79	11.5	
0.20	-3.9	0.43	11.1	**10**
0.43	-13.1	1.65	12.6	
0.44	-19.2	1.45	7.6	**10**
1.3	-11.1	0.89	8.1	
1.3	-8.6	0.79	9.2	
1.3	-4.1	0.46	11.3	**10**
3.5	-15.2	0.89	5.8	
3.5	-22.1	1.39	6.3	
3.9	-10.1	1.05	10.4	**8**

Table 8.2: Influence of Dye Deposition Error on Colour Difference

It should be noted that there is not a linear relationship between a variation in the affinity value and the resulting change in the predicted dye fibre molality. How much the predicted dye fibre molality deviates for a change in the affinity will also depend on the application conditions. In order to identify how much the affinity value could vary before the dye fibre prediction error would exceed 5%, some ranging calculations were made with a 2-phase Donnan model. The results are presented in table 8.3.

Conditions (Temp, Dye, Salt)	Calculated Affinity /[kJ.mol^{-1}]	Delta Affinity [%]	DDE [%]
100°C, 4%, 15g.dm^{-3}	-21.14	-8.3	-5.0
100°C, 4%, 0g.dm^{-3}	-18.24	-4.5	-5.0
100°C, 0.2%, 15g.dm^{-3}	-20.50	-64.0	-5.0
100°C, 0.2%, 0g.dm^{-3}	-24.68	-6.2	-5.0

Table 8.3: Influence of Affinity Variations on Final Dye Amount Predictions on the Fibre, 2-phase Donnan Model

The calculations show that at low dye and high salt concentrations, i.e. very high exhaustion values, a 64%-change in the affinity value resulted in a prediction difference of only 5%. At high dye and low salt concentrations, however, a 5% prediction difference is caused by only a 4.5% change in the affinity value. For a prediction of the dye fibre molality within +/- 5%, the calculated affinity values should thus ideally be accurate to within +/- 5%. It should be noted however that under high substantivity conditions, larger variations in the affinity value can be tolerated.

8.3 Application of Donnan and Gouy-Chapman Models

8.3.1 Donnan Models

For the present work, all the Donnan equations took into account carboxyl and hydroxyl groups of the cotton fibre, hydroxyl ions in the water and, where necessary, impurities in the dye. As the degree of ionisation of the fibre groups is pH-dependent, the equations took this effect into account, too, following the methods outlined in chapter three. The substrate specific constants included the fibre concentrations of the hydroxyl and carboxyl groups and their dissociation constants as well as the volume term. The calculations used a volume term of 0.22dm^3.kg^{-1} for cotton, 0.33dm^3.kg^{-1} for cellophane and 0.65dm^3.kg^{-1} for cupro. The substrate specific constants were adopted from the publications of the original works where available or, when that was not the case, were taken from values published in the standard literature mentioned in chapter three.

The 3-phase Donnan calculations used the same substrate specific constants as the 2-phase model and its fibre saturation value was chosen so as to give the least variation coefficient of the affinity values for a given set of experiments.

The 3-phase model with variable internal volume used surface areas of 204 000$m^2.kg^{-1}$ for cotton, 400 000$m^2.kg^{-1}$ for cellophane and 480 000$m^2.kg^{-1}$ for cupro in the calculations (Bredereck 1996).

In the application of the Donnan model, it is required to use the dyebath concentrations, e.g $[Na]_{s,eq}$, $[OH]_{s,eq}$, $[Cl]_{s,eq}$, $[SO_4]_{s,eq}$ and $[D]_{s,eq}$, at equilibrium conditions. It is quite clear that $[OH]_{s,eq}$ can be easily calculated from pH measurement of the final dyebath, and that $[D]_{s,eq}$ can be determined by the methods described in chapter six. The electrolyte concentrations of $[Na]_{s,eq}$, $[Cl]_{s,eq}$ and $[SO_4]_{s,eq}$ differ from the initial solution because their distribution between bulk and internal phase depends on the equilibrium conditions. Therefore, it would have been necessary to measure these concentrations in the final dyebath, too. As this would have been laborious, a preferred method was to estimate the final dyebath concentrations of the electrolytes from the amounts of $(Na)_{s,0}$, $(Cl)_{s,0}$ and $(SO_4)_{s,0}$ initially added to the dyebath.

The calculation of the ions' concentrations in the final dyebath based on the initially added amounts involved two equation systems (Sumner 1986:394). The first one calculated the total quantities of ions in the initial dyebath and the second one determined the distribution of the ions between fibre phase and dyebath phase. Equations 8.1 and onwards assume that a commercial dye of purity, p, with (1-p) sodium sulfate impurities, is used. The equations are equally valid for a purified dye, with p being unity.

Total Quantities of Ions [mol] in Initial Dyebath (subscript 0):

$$(Na)_{s,0} = L\left(\frac{2[Na_2SO_4]}{M_{Na_2SO_4}} + \frac{[NaCl]}{M_{NaCl}} + \frac{z[D]_{comm,0}\,p}{M_D} + \frac{2[D]_{comm,0}(1-p)}{M_{Na_2SO_4}}\right) \quad (8.1)$$

L = Total volume of dyebath [dm^3]

$[Na_2SO_4]$ = Initial concentration of sodium sulfate [$g.dm^{-3}$]

M_{Na2SO4} = Molecular weight sodium sulfate [$g.mol^{-1}$]

p = Purity of dye, i.e. fractional weight of dye anion of commercial dye [-]

z = Number of charges on dye anion [-]

$[D]_{comm,0}$ = Initial dye concentration in commercial form [$g.dm^{-3}$]

The first two expressions in the brackets of equation 8.1 refer to the added electrolytes, NaCl and Na_2SO_4 where the electrolyte concentrations may be calculated by dividing the amount of electrolyte added by the volume of the dyebath, i.e. by ignoring any Donnan membrane effects. The added electrolyte may include any electrolyte contributions from the fibre. The third expression refers to the sodium coming from the dye molecule, assuming that the dye is of the form Na_zD. The fourth expression refers to the sodium coming from the diluent in the commercial dye, assuming that the diluent is Na_2SO_4.

$$(SO_4)_{s,0} = L\left(\frac{[Na_2SO_4]}{M_{Na_2SO_4}} + \frac{[D]_{comm,o}(1-p)}{M_{Na_2SO_4}}\right) \tag{8.2}$$

The first expression in brackets of equation 8.2 refers to the added Na_2SO_4, including any contributions from the fibre. The second expression refers to the sulphate coming from the diluent in the commercial dye.

$$(Cl)_{s,0} = L\left(\frac{[NaCl]}{M_{NaCl}}\right) \tag{8.3}$$

In equation 8.3 chloride is assumed to be coming solely from the added electrolyte and here, too, the added electrolyte may include any contributions from the fibre.

$$(D)_{s,0} = L\left(\frac{[D]_{comm,o}\,p}{M_D}\right) \tag{8.4}$$

Distribution of Ions between Dyebath and Fibre Phase

Assuming the following Donnan relationships:

$$\begin{aligned}
\frac{[Na]_l}{[Na]_s} &= \frac{[H]_l}{[H]_s} \\
\frac{[SO_4]_l}{[SO_4]_s} &= \left(\frac{[H]_s}{[H]_l}\right)^2 \\
\frac{[Na]_l}{[Na]_s} &= \frac{[Cl]_s}{[Cl]_l}
\end{aligned} \tag{8.5}$$

the total amounts may be written as:

$$\begin{aligned}
(Na)_{s,0} &= V[Na]_{l,eq} + (L-V)[Na]_{s,eq} = V[Na]_{l,eq} + (L-V)[Na]_{l,eq}\frac{[H]_{s,eq}}{[H]_{l,eq}} \\
(SO_4)_{s,0} &= V[SO_4]_{l,eq} + (L-V)[SO_4]_{s,eq} = V[SO_4]_{l,eq} + (L-V)[SO_4]_{l,eq}\left(\frac{[H]_{l,eq}}{[H]_{s,eq}}\right)^2 \\
(Cl)_{s,0} &= V[Cl]_{l,eq} + (L-V)[Cl]_{s,eq} = V[Cl]_{l,eq} + (L-V)[Cl]_{l,eq}\frac{[Na]_{l,eq}}{[Na]_{s,eq}}
\end{aligned} \tag{8.6}$$

where V is the internal volume of the fibre phase in dm^3.

Rearranging equations 8.6 for the dye molalities on the fibre and inserting the molalities in the electric neutrality equation then yields:

$$[H]_{i,eq}+[Na]_{i,eq}=\frac{K_W}{[H]_{i,eq}}+\frac{[H]_{s,eq}[Cl]_{s,0}}{V[H]_{s,eq}+(L-V)[H]_{i,eq}}+2\frac{[H]^2_{s,eq}[SO_4]_{s,0}}{V[H]^2_{s,eq}+(L-V)[H]^2_{i,eq}}$$
$$+\frac{z[D]_{comm,0}pEL}{M_D V}+\frac{K_{COOH}Q_{COOH}\dfrac{K_W}{[H]_{i,eq}}}{K_{COOH}+[H]_{i,eq}}+\frac{K_{OH}Q_{OH}\dfrac{K_W}{[H]_{i,eq}}}{K_{OH}+[H]_{i,eq}} \qquad (8.7)$$

where E is the fractional dye exhaustion.

If $[H]_{f,eq}$ in equation 8.7 is substituted by the equation 8.8 (derived from equation 8.6)

$$[H]_{i,eq}=\frac{[Na]_{i,eq}(L-V)[H]_{s,eq}}{[Na]_{s,0}-[Na]_{i,eq}V} \qquad (8.8)$$

then only $[H]_{s,eq}$, i.e. the pH of the final dyebath, and $[D]_{s,eq}$, to calculate the exhaustion value, E, have to be measured and equation 8.7 can be solved by iteration for $[Na]_{i,eq}$.

8.3.2 Gouy-Chapman Models

The equations for the simple Gouy-Chapman model used here followed the method developed by Gerber and outlined in chapter three.

For the model with saturation value, the Gerber method was slightly modified. Contrary to his method, which calculates the fibre saturation value based upon geometrical considerations of the dye molecule, a saturation value was used that gave the least overall variation coefficient for the affinity values.

Note: The ionic strength in the Gouy-Chapman model refers to the ionic concentration in solution at infinitely large distance from the fabric surface, i.e. when cationic and anionic concentrations are equal, due to the requirement of electric neutrality. Thus, contrary to the Donnan model, the ionic concentrations in solution at equilibrium can easily be determined by dividing the total amount of initially added electrolyte by the total volume of dyebath.

The standard heat of dyeing was obtained in all cases by plotting $\Delta\mu.T^{-1}$ against T^{-1} and subsequent linear regression as explained in chapter three.

8.4 Overall Performance of the Different Models

On average, the various models were found to yield significantly different variation coefficients of the affinity values (table 8.4). Best results were obtained with the Gouy-Chapman model with saturation value, the least accurate results with the variable volume 3-phase Donnan model. It was shown that inclusion of saturation effects also improved the prediction of the Donnan model by 1.4% on average. Model performance varied considerably depending on the individual dye and the particular dyeing conditions. The Donnan models predicted the influence of changes in the degree of ionisation of the hydroxyl and carboxyl groups better than the others and the Gouy-Chapman models gave better results at predicting the influence of temperature and electrolyte concentration.

Dye (parameters varied)	2-Phase Donnan	3-Phase Donnan	3-Phase Donnan variable V	Gouy-Chapman	Gouy-Chapman w/ Sat. Value
DY 12 (NaCl & T)	4.4	4.4	12.9	3.5	2.8
DB 106 (Na_2SO_4)	12.1	7.2	13.4	3.0	2.1
DB 1 (CellCOOH)	2.9	1.6	1.6	8.8	3.4
VR 35 (CellOH)	2.6	2.7	6.7	5.2	2.8
DY 162 (NaCl & T)	11.9	11.3	7.6	7.6	5.6
Average	**6.8**	**5.4**	**8.4**	**5.6**	**3.3**

Table 8.4: Average Variation Coefficient of the Affinity Values [%]

A comparison of the values for the heat of dyeing, which could of course only be calculated for those experiments that were conducted at different temperatures, showed that while all models calculated similar values for DY162, large differences existed for DY12 (table 8.5). This was in part due to the sensitivity of the regression method to minor changes in the affinity value and the fact that experiments at only four different temperatures constituted the database. Additionally, the regression method used here for the Gouy-Chapman models only minimised the error at one particular temperature and not over a range of temperatures, which would have improved the estimate for the heat of dyeing (Gerber 1996). Therefore, the results of the Donnan models appear to be more reliable.

	2-Phase Donnan	3-Phase Donnan	3-Phase Donnan variable V	Gouy-Chapman	Gouy-Chapman w/ sat. value
DY162					
Heat of Dyeing /[kJ.mol^{-1}]	-38.7	-41.4	-36.6	-35.8	-35.9
Correlation Coefficient [-]	0.989	0.990	0.985	0.959	0.995
DY12					
Heat of Dyeing /[kJ.mol^{-1}]	-57.9	-59.6	-34.2	-40.2	-42.3
Correlation Coefficient [-]	0.999	0.999	0.936	0.929	0.934

Table 8.5: Heat of Dyeing Predictions

8.5 Varying Carboxyl Molalities

In this case only the results of Neale's experiments were compared to the models' predictions, DB1 in tables 8.1 and 8.4. As Neale's experiments were conducted at only one salt concentration (5g.dm^{-3} NaCl), the coefficients A_1 and A_2 in the Gouy-Chapman model could not be determined by multiple linear regression. Instead they were calculated from the initial charge density of the fibre surface, σ_0, which was derived from the following equation:

$$\sigma_0 = \frac{F\left([CellCOO]_f + [CellO]_f\right)}{A} \tag{8.9}$$

F = Faraday Constant [C.mol^{-1}]

$[CellCOO]_f$ = Molality of ionised carboxyl-groups on the cotton fibre [mol.kg^{-1}]

$[CellO]_f$ = Molality of ionised hydroxyl-groups on the cotton fibre [mol.kg^{-1}]

A = Specific fibre surface area accessible to the dye [m^2.kg^{-1}]

The value of A was assumed to be 204 000m^2.kg^{-1}, $[CellCOO]_f$ was calculated from the carboxyl content of the cotton fibre assuming complete ionisation and $[CellO]_f$ was taken to be negligibly small. The value of A_1 was then calculated using equation 3.32. As the surface area was assumed to be independent of the carboxyl

molality, A_2 was constant for all calculations, whereas A_1 increased proportionally to the carboxyl content.

The results shown in table 8.6 show that the Gouy-Chapman models, especially the simple one, yielded in this case a considerably higher variation coefficient than the Donnan models. The variation arose from an increase in the affinity values with an increase in the carboxyl concentration, that either indicates that the Gouy-Chapman model is not satisfactory or that the carboxyl groups are actually less ionised than was assumed for the Donnan model. If, for example, a dissociation constant of the carboxyl group of $0.80.10^{-6}$ was used instead of $1.35.10^{-6}$ then the variation coefficient of the simple Gouy-Chapman model dropped to 3.0%, a value similar to the value of the 2-phase Donnan model.

Carboxyl Molality /[mol.kg^{-1}]	**Donnan 2P** KCOOH = $1.35.10^{-6}$	**Gouy-Chapman** KCOOH = $1.35.10^{-6}$	**Gouy-Chapman** KCOOH = $0.80.10^{-6}$
0.000	-24.11	-20.32	-20.32
0.010	-24.02	-20.51	-19.65
0.019	-24.28	-21.18	-19.55
0.030	-24.42	-22.11	-19.32
0.035	-24.74	-22.92	-19.60
0.046	-25.92	-25.51	-20.90
Variation Coefficient [%]	2.9	8.8	3.0

Table 8.6: Affinities [kJ.mol^{-1}] and Variation Coefficient for Varying Carboxyl-Group Contents of the Fibre

8.6 Varying Hydroxyl Molalities

The evaluation of the model in this case was solely based upon the experimental results of Peters et al., VR35 in tables 8.1 and 8.4. For the comparison, only the results at pH 12 and 13 were considered because at these pH levels there were numerous enough values available to warrant the application of the regression methods for solution of the Gouy-Chapman model. Since the degree of ionisation of the hydroxyl groups changes from pH 12 to pH 13, one regression was made at each pH-value, yielding a value for the initial surface charge density (σ_0) for each pH in case of the Gouy-Chapman model.

By comparing the variation coefficients in table 8.2 with those in table 8.4, it can be seen that all models with the exception of the 3-phase Donnan model with variable V achieved acceptable results. A closer analysis revealed that they differed in their prediction of the degree of ionisation of the hydroxyl and carboxyl groups of the fibre as a function of the pH value. A comparison between the Donnan and the Gouy-Chapman models can be made if the $[CellO]_f$ and $[CellCOO]_f$-molalities of the Donnan models are converted to a surface charge density by equation 8.9.

Table 8.7 shows that while both models correctly predicted an increase in the surface charge density with pH, the underlying σ_0 was much higher in the Gouy-Chapman model. The surface charge density of the Donnan model varied even at constant pH because the different salt and dye concentrations of the experiments affected the degree of ionisation. Due to its reliance on physico-chemical constants that can be verified in independent experiments, the values of the Donnan model are probably closer to the true situation. This indicates that the substrate specific coefficients of the Gouy-Chapman models do not necessarily represent the true situation if they are determined by regression.

	Gouy-Chapman σ_0/[C.m^{-2}]	**2-P Donnan σ_0/[C.m^{-2}]**
pH 12	0.074	0.0100-0.0197
pH 13	0.157	0.0570-0.0880

Table 8.7: Surface Charge Densities for different pH-values

When the σ_0-value determined from the Donnan model was used in the Gouy-Chapman model to calculate the affinity, the variation coefficient increased significantly (table 8.8). Thus, the overall better performance of the Gouy-Chapman models was at least partially a result of the fact that its substrate specific coefficients had here been calculated by linear regression and were not derived from independent measurements.

	Gouy-Chapman w/ Regression	**Gouy-Chapman w/ Donnan coefficients**
Variation Coefficient [%]	5.2	10.7

Table 8.8: Influence of the Method of determining the Substrate Coefficients on the Variation Coefficient of the Affinity with the Gouy-Chapman Model

8.7 Varying Electrolyte Concentration

The results obtained showed that two aspects are of interest. First, the results explained why the variable volume Donnan model was generally the least accurate. As the electrolyte concentration (and the ionic strength) increases, the volume term shrinks so much that the affinity value grows, too (table 8.9). In other words, the model seems to over-estimate the effect of the salt concentration on the volume term. The only two datasets when it outperformed the simple 2-phase Donnan model was at constant electrolyte concentration (DB1) and varying but low electrolyte concentrations (DY162).

Ionic Strength of Dyebath [-]	Volume Term /[$dm^3.kg^{-1}$]	Affinity /[$kJ.mol^{-1}$]
0.11	0.18	-24.5
0.11	0.18	-23.2
0.12	0.17	-21.8
0.13	0.16	-21.3
0.32	0.10	-27.6
0.33	0.10	-26.1
0.33	0.10	-25.6
0.34	0.10	-25.0
0.96	0.06	-30.0
0.97	0.06	-30.6
0.97	0.06	-31.2
0.98	0.06	-30.8

Table 8.9: Results for different Salt Concentrations with 3-P Donnan Model with variable V (DB106)

The good performance at low and varying salt concentrations pointed to the second interesting aspect, i.e. the relative failure of the Donnan models at low dye and zero added salt concentrations. The calculation revealed dramatically increased affinity values under these conditions. The effect was most pronounced in the case of the 2-phase Donnan model when the affinity value doubled but the Donnan 3-phase model yielded only a slight

improvement. The results for 100°C are shown in table 8.10. Calculations at 65°C and 90°C showed very similar results.

100°C	Dye [% omf]			
Salt conc [g.dm^{-3}]	0.20	0.45	1.35	4.00
0.0	-31.23	-30.30	-26.66	-19.15
2.5	-21.79	-24.17	-24.04	-20.01
5.0	-21.10	-22.32	-22.77	-20.52
7.5	-20.70	-22.24	-22.55	-21.30
10.0	-20.61	-22.13	-22.52	-20.32
15.0	-20.71	-21.75	-22.38	-21.36

Table 8.10: Affinity Values [kJ.mol^{-1}] 2-Phase Donnan (DY 162) with Common Salt

As all possible sources of electrolyte, i.e. salt, dye, fabric and water, had been taken into account, this deviation was not due to unaccounted for electrolyte. Furthermore, reflectance measurements of the fabric showed that the indirectly calculated amount of dye on the fabric was correct and therefore did not cause erroneously high affinity values. That left the following five possible explanations.

1) There could be a significant number of adsorption sites of higher and of lower affinity on the cotton surface. At low dye concentrations and in the absence of salt, more dye would therefore go on the fabric than expected. An indication, though no proof, of this effect would be an increasing heat of dyeing at low dye concentrations (Daruwalla 1963). Analysis of the heat of dyeing for the various dye concentrations present in dataset DY162, however, indicated that the heat of dyeing did not change systematically with dye concentration (table 8.11).

Dye [% omf]	0.08	0.20	0.45	1.35	4.00
Heat of dyeing at 0g.dm^{-3} salt	-37.6	-35.4	-58.4	-41.0	-39.8
Heat of dyeing at 15g.dm^{-3} salt	Not calc.	-40.7	-34.8	-32.0	-45.0

Table 8.11: Heat of Dyeing for various Dye Amounts, DY162

It has to be noted that the heat of dyeings were calculated based on only three temperatures, 65°C, 90°C and 100°C and that the calculation is sensitive to minor changes in the affinity value. The experimental determination of the exhaustion value at very low dye concentrations was complicated by the fact that the absorbance of the equilibrium dye solution was very close to that of the blank dyebath after dyeing, thereby increasing the experimental error. Therefore, the data in table 8.11 should only be interpreted with caution.

2) Aggregation of the dye in solution with increasing dye and salt concentrations could mean that some parts of the fibre surface become inaccessible for the dye. It was pointed out in chapter two that the accessible area on cellulosics is a function of the molecule size. The dyeings without added salt would show a higher affinity because more surface area is available to the low-aggregated dye in solution. Similarly, it could be argued that aggregation decreases the hydrophobicity of the dye due to micelle formation (Yeung 1999). This decrease in hydrophobicity would lead to a lower affinity of the dye to the fabric (Daescu 2000). In the Donnan approach this effect could be simulated with a variable volume term that is a function of the dye and salt concentration. In the Gouy-Chapman approach it would result in the surface area being a function of the dye and salt concentration. A requirement for this hypothesis to be possibly true is that the aggregation number increases with increase in dye and salt concentration. Experiments described in chapter six indicated that this was probably the case for the dataset DY162. At low concentrations, the dye was mono-disperse at temperatures of 70°C and higher if no salt was added. In the presence of salt, the dye remained aggregated at least up to 90°C even at low dye concentrations.

   However, the observed affinity discrepancies did not decrease at higher temperatures, as might be expected from the fact that the aggregation number decreased with increasing temperature. Some doubt is also cast on this explanation because dyeings in the presence of a non-ionic surfactant showed the same tendency of much higher affinity values when no electrolyte was added. The surfactant should, as explained in chapter six, cause the break-down of the dye aggregates and the formation of a dye-micelle complex that appeared to be stable also at high salt concentrations. As the dye state in solution was therefore in this case unaffected by salt concentration, affinity differences would have been expected to be diminished.

3) Increasing the salt concentration is known to reduce the surface area accessible to the dye (Schaumann 1996). For viscose fibres and modal fibres reductions in the swelling of about 30% and 40% respectively have been reported for a pH value of 7 when the sodium sulphate concentration was increased from 0 to 50g.dm^{-3} . The result would be

similar to that indicated in 2) above, i.e. the dyes would only be able to access a reduced fibre surface volume at higher electrolyte concentrations. Table 8.12 indicates how much the internal volumes would have to change, taking a volume term of $0.22dm^3.kg^{-1}$ as reference, in order to lead to a constant affinity when no common salt was added.

Dye [%omf]	0.20	0.20	0.20	0.45	0.45	0.45	1.35	1.35	1.35
Temp/[°C]	65	90	100	65	90	100	65	90	100
V 2-P Donnan /[$dm^3.kg^{-1}$]	0.73	0.67	0.64	0.62	0.50	0.46	0.32	0.29	0.31

Table 8.12: Internal Volume required in order to yield a constant Affinity Values (DY162)

The data in table 8.12 show that the volume term would have to change by a factor of around three to maintain the same affinity, which is far more than any reported effects of electrolyte on cellulose. Moreover, the jump in the affinity value at low dye amounts occured for datasets at 0 and only $2.5g.dm^{-3}$ salt, so that this explanation can be safely discarded as a major contributing factor.

4) As the diluent of the commercial dye was mostly sodium sulphate, it could be argued that the high affinity without added sodium chloride was caused by the stronger hydrophobic effect of sulphate compared to chloride (Yang 1992). With increasing chloride addition, according to this hypothesis, the hydrophobic interaction is reduced and therefore a smaller than expected fraction of dye would be sorbed by the substrate. Dyeings in which sodium sulphate replaced sodium chloride as electrolyte so as to give the same sodium concentration, showed indeed a somewhat diminished jump in affinity values at low dye amounts (table 8.13). The hydrophobic effect of the sulphate contained in the commercial dye could therefore have contributed to the phenomenon seen in table 8.10.

100°C	Dye [% omf]			
Equivalent Common Salt Conc./[g.dm^{-3}]	0.20	0.45	1.35	4.00
0.0	-31.23	-29.54	-25.59	-19.62
2.5	-24.68	-23.74	-22.30	-19.64
5.0	-24.65	-22.75	-21.82	-19.10

Table 8.13: Affinity Values 2-Phase Donnan w/ Sodium Sulphate (DY162)

5) The increase in affinity could also reflect a limitation in the applicability of the Donnan membrane theory. Direct measurements on the fibre surface, for example, indicated that the ion distribution between fibre and bulk solution of simple electrolytes, such as sodium chloride, was not constant and did not obey the Donnan relationship, particularly at low ionic concentrations (McGregor 1972). The poor performance of the Donnan model at solutions of low ionic strength has also been noted elsewhere when it was found that under these conditions the Gouy-Chapman model yielded more accurate results (Rattee 1974:14). Evidence was also found that dye-fibre interactions of an unspecified nature increased at low dye concentrations (Daruwalla 1963, McGregor 1972). The increase of dye-fibre interactions is possibly due to a non-linear relationship between the dye concentration in the internal solution and in the fibre phase. As a consequence, the affinity would not remain constant at constant temperature but increase at low dye concentrations.

Overall, it seems to be possible to explain the high affinity values of DY162 at low dye and electrolyte concentrations, at least partially, by solution effects such as aggregation and hydrophobic interaction. The substrate appears to have little influence. Additionally, the experiments may have exposed the limits of the Donnan membrane theory in their application to textile dyeing processes.

8.8 Gouy-Chapman Model with Variable Saturation Value

For the experimental dataset DY162 obtained as part of this study, the Gouy-Chapman models yielded lower variation coefficients of the affinity values than the Donnan model (table 8.4). This can be attributed to two characteristics. Firstly, because of the variable

thickness of the double layer (being equivalent to the internal volume in the Donnan models) expressed by the Debye-length, the Gouy-Chapman models were more suitable to describe the quantities of dyes sorbed on the fibre when no electrolyte was added. As a consequence the affinity values showed only a smaller increase when no electrolyte was added compared to the Donnan models. The increased volume-term is equivalent to an increased distribution coefficient for the inorganic ions at low dye concentrations in the Donnan model (i.e. a higher fraction of ions sorb on the fibre), a fact that has been confirmed experimentally as mentioned above.

Secondly, as the initial charge density of the substrate and the fibre surface area accessible to the dye were determined by regression, better correlation was achieved than by taking literature values, as was the case for the Donnan model. The values of the coefficients A_1 and A_2 of the simple Gouy-Chapman model without saturation value as determined by linear regression, translated into an average surface area of 220,000 $m^2.kg^{-1}$ fabric (different values were obtained for different temperatures) and an average surface charge density of 0.0025 $C.m^{-2}$. The first figure was close to literature values for cotton (Bredereck 1996) but the surface charge density was approximately 3 times higher than that assumed by the Donnan models. As it is unlikely that the carboxyl-content of the cotton used was particularly high, the fabric had not been treated with oxidizing chemicals like hydrogen peroxide, the value was probably not physically realistic. As the Gouy-Chapman model makes simplifying assumptions (e.g. dyes as point charges) - like all of the models examined - and as there were indications that dye aggregation occurred but changed with dye and salt concentration, it seemed extremely difficult to build a model that would accurately take into account all the parameters involved in the practical dyeing situation.

Nevertheless it was desirable to further reduce the variation coefficient of the affinity values for the Gouy-Chapman model with saturation value. Although the variation coefficient was the lowest among all the models tested, it would still have resulted occasionally in a prediction error of more than the targeted value of five per cent. It was decided to introduce a variable saturation value in the Gouy-Chapman model. In agreement with the findings outlined in chapter three, the saturation value was taken to be dependent on the ionic strength of the dyebath (representing the influence of electrolyte) and the equilibrium dye concentration in solution (representing the influence of the dye amount):

$$[D]_{sat} = B_0 + B_1 I + B_2 I^2 + B_3 [D]_{s,eq} + B_4 [D]_{s,eq}^2 \qquad (8.10)$$

B_0, B_1, B_2, B_3, B_4, B_5: coefficients

I = Ionic strength of solution [-]

The coefficients B_0 to B_4 in equation 8.10 were chosen so as to give a small variation coefficient of the affinity values. Figure 8.1 shows the $[D]_{sat}$-values obtained from equation 8.10, using coefficient values of $B_0 = 0.0026$, $B_1 = 0.129$, $B_2 = -0.14$, $B_3 = 2.10^5$, $B_4 = -5.6.10^{-4}$. With these coefficients, the predicted saturation value increased with salt concentration and with dye amount - possibly due to the combined effects of dye aggregation and multi-layer formation (figure 8.1).

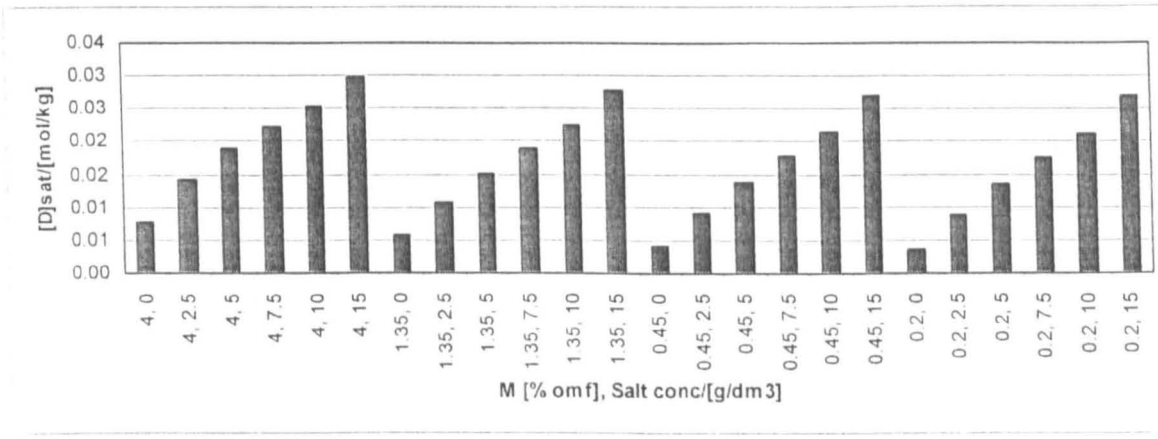

Figure 8.1: $[D]_{sat}$ as a Function of Dye Amount and Salt Concentration

The average variation coefficient for the affinity values using the newly defined $[D]_{sat}$-values was 3.0% (table 8.14). The heat of dyeing was calculated to 36.2kJ.K^{-1}.mol^{-1}.

	65°C				90°C				100°C			
	Dye [% omf]											
Salt conc. [g.dm^{-3}]	0.20	0.45	1.35	4.00	0.20	0.45	1.35	4.00	0.20	0.45	1.35	4.00
0.0	-30.0	-31.0	-28.5	-29.7	-30.4	-29.6	-27.7	-29.7	-29.2	-28.8	-27.8	-29.7
2.5	-30.4	-29.9	-30.8	-29.3	-30.6	-30.5	-29.9	-28.2	-29.7	-30.9	-29.6	-27.1
5.0	-30.1	-29.0	-30.1	-30.2	-30.0	-29.9	-30.3	-28.1	-29.1	-29.4	-29.2	-27.8
7.5	-29.6	-29.3	-29.7	-30.0	-29.6	-29.8	-29.8	-28.6	-28.4	-28.9	-29.1	-28.9
10.0	-29.5	-29.2	-29.4	-30.3	-29.1	-29.3	-29.6	-29.2	-28.0	-29.0	-29.0	-27.9
15.0	-29.1	-28.8	-29.1	-30.7	-28.7	-29.2	-29.1	-29.2	-27.7	-28.1	-28.7	-29.2
	Average: -29.7				Average: -29.4				Average: -28.8			

Table 8.14: Affinities [kJ.mol^{-1}] Gouy-Chapman Model with Variable Saturation Value (DY162)

Using the parameter settings described above, the Gouy-Chapman model with variable saturation value was used to back-predict the dye fibre amounts for dataset DY162. The results are compiled in table 8.15 and show an average prediction error of 1.7% with a maximum error of 11.6%. The results were deemed satisfactory for the purposes of this work.

	65°C				90°C				100°C			
	Dye [% omf]											
Salt conc. [g.dm^{-3}]	0.20	0.45	1.35	4.00	0.20	0.45	1.35	4.00	0.20	0.45	1.35	4.00
0.0	-0.7	-3.7	6.5	0.0	-4.0	-2.1	10.5	-1.8	-0.7	1.3	8.2	-2.7
2.5	-0.5	-0.2	-1.6	1.5	-1.9	-2.3	-2.5	5.3	-1.4	-4.0	-2.3	11.6
5.0	-0.2	0.5	-0.5	-1.9	-0.8	-0.9	-2.3	5.8	-0.1	-0.6	-0.6	6.8
7.5	0.1	0.2	-0.7	-0.9	-0.3	-0.5	-1.0	2.9	0.8	-0.1	-0.3	0.8
10.0	0.1	0.2	0.2	-1.5	0.1	0.0	-0.6	0.1	1.1	0.0	0.0	5.0
15.0	0.1	0.3	0.3	-1.5	0.3	0.0	0.1	0.1	1.3	1.0	0.5	-0.6
	Average: 1.0				Average: 2.2				Average: 1.9			

Table 8.15: Dye on Fibre Back-prediction Error [%], Gouy-Chapman Model with variable Saturation Value (DY162)

8.9 References

1. Bredereck K, Gruber M, Otterbach A, Schulz F, Textilver. 31 (1996) 194
2. Breuer M M, Rattee I D, The Physical Chemistry of Dye Adsorption (London: Academic Press, 1974)
3. Daescu C, Hadaruga D, J.S.D.C. 116 (2000) 48
4. Daruwalla E H, D'Silva A P, Text. Res. J. 33 (1963) 40
5. Gerber H, J.S.D.C. 112 (1996) 153
6. Gerber H, Textilver. 25 (1990) 207
7. McGregor R, Text. Res. J. 42 (1972) 536
8. Neale S M, Stringfellow W A, J.S.D.C. 56 (1940) 17

9. Peters R H, Simons J, J.S.D.C. 70 (1954) 557

10. Porter J J, Text. Res. J. 62 (1992) 236

11. Schaumann W, Lenzinger Berichte 75 (1996) 81

12. Sumner H H, J.S.D.C. 102 (1986) 301 (part I), 341 (part II) and 392 (part III)

13. Willis H F, Warwicker J O, Standing A, Urquhart A R, Trans. Far. Soc. 41 (1945) 506

14. Yang Y, AATCC International Conference, Book of Papers (1992) 266

15. Yeung K W, Shang S M, J.S.D.C. 115 (1999) 228

9 Development of a Dye Sorption Model

From the literature review of sorption models presented in chapter four, it appeared that although a fair number of models of exhaustion kinetics have been developed, few of them, if any, have been tested over the wide range of application conditions that are found in industrial practice. The range includes changes in dye and electrolyte amounts as well as variations in liquor ratio and temperature. Moreover, the majority of the models have been tested using experimental data obtained from dyeing systems with a considerably longer liquor ratio than that encountered in industry. This is particularly relevant for testing a model's ability to describe the dyeing of cotton with direct dyes because it is the first strike of the dye that is difficult to model and the first strike is more pronounced at short liquor ratios.

It was therefore decided to test the model developed during this study over a range of conditions that approximate the situations found in industry. This also meant that data was recorded for experimental dyeings carried out with varying dyeing conditions, in this case an electrolyte dosing gradient was used. There still remained a major and significant simplification compared to industrial systems, i.e. the use of a one-dye solution instead of dye mixtures. It therefore remains to be seen if a model similar to the one suggested in this study would make correct predictions for the dyeing of fibre with a dye mixture under dynamic conditions, i.e. truly industrial conditions.

Considering that the complex interactions between substrate, dye, salt and water during the dyeing process are not even nearly fully understood, it was accepted that some of the model parameters and coefficients would have to be adjusted empirically in order to fit the experimental results rather than being derived from independently verifiable measurements. Nevertheless the attempt was made to use fundamental laws of physical chemistry such as Fick's Second law of diffusion or Langmuir sorption kinetics as the basis for the model. This approach, it was hoped, would facilitate the future application of the model to dye-fibre systems other than that examined in this investigation. The approach could also help to clarify which types of information (and experiments) are needed in order to predict the exhaustion kinetics under industrial conditions.

9.1 Experimental

For the investigation the dyeings were made with the fabric described in section 2.1.6 at a liquor ratio of 8:1 and carried out on a MATHIS LABOMAT infrared rotating beaker

laboratory machine using 100cm^3 beakers and around 7g of fabric unless otherwise mentioned. A first series of experiments was carried out under isothermal conditions with 15g.dm^{-3} common salt at the temperatures of 43°C, 65°C, 90°C and 100°C, and four different dye amounts of 0.2%, 0.45%, 1.35% and 4% (omf). In addition, dyeings were carried out using electrolyte concentrations of 0g.dm^{-3}, 5g.dm^{-3} and 10g.dm^{-3} at each of the four dye amounts at 65°C.

In order to evaluate how the kinetic model developed in this section coped with changes in liquor ratio, dyeings of 0.45% (omf) were performed at a liquor ratio of 65:1, instead of 8:1, at temperatures of 40°C, 65°C and 90°C with 15g.dm^{-3} common salt and at 90°C with no added common salt. This is a much wider variation in conditions than would be expected under normal industrial conditions and therefore represented a worst-case scenario. If the model predicted with satisfactory accuracy in the worst-case scenario, liquor ratio variations as they typically occur in industry could probably also be compensated for.

A third series involved the direct measurement of dye adsorption constants at different temperatures, which required short time interval sampling of the dyebath in the initial phase of the dyeing process. This could not be achieved with the rotating beaker-type machine and a temperature-controlled, double-walled 500cm^3 glass vessel was used instead. The fabric was attached to a shaft rotating with approximately 100 revolutions per minute. Absorbance measurements were made at 6 seconds intervals with a HELLMA 10mm pathlength quartz immersion probe that was connected via fibre optical cables to a single-beam ZEISS SPECORD S 100 spectrophotometer. The absorptivity was determined at the wavelength of maximum absorption. Due to the comparatively long pathlength of the immersion probe, only low concentrations could be measured so that a long liquor ratio of 65:1 was employed. The adsorption constants were determined for a dye amount of 0.45% (omf) at five different temperatures: 40, 50, 65, 80 and 90°C and two different electrolyte concentrations, 0 and 15g.dm^{-3}.

For the fourth type of experiment, two dyeings were carried out on the pilot-scale jet dyeing machine using the dosing of common salt to control the exhaustion rate. Both dyeings used 0.3% (omf) dye and were conducted at isothermal conditions at 80°C. The final electrolyte concentration was 17g.dm^{-3}. Dye addition occurred at 80°C via the open-air addition tank over a period of 80s. Salt dosing started 60s after the beginning of the dye addition with the PROMINENT dosing pump, i.e. 20s before the dye addition was over. The total salt dosing time was in both cases 8 minutes, but the dosing profiles were different (table 9.1).

Time/[min]	1	2	3	4	5	6	7	8
#1	8	5	7	8	11	43	81	82
#2	4	3	3	7	55	103	45	30

Table 9.1: Dosing Pump Frequencies/[min^{-1}] of Pilot-scale Tests

The liquor flow in the main circulation line was both times 40$dm^3.min^{-1}$, high enough to ensure adequate dye supply at the fibre surface. The fabric speed was 2$m.min^{-1}$.

Stock solutions for the experiments on the rotating beaker machine were used up to an age of three days in the case of 5$g.dm^{-3}$ dye or more and up to an age of seven days in the case of 1$g.dm^{-3}$ dye or less. Dye solutions for the jet dyeing experiments were always freshly prepared. The minimum dispensed volume was 1.5cm^3. All pipettes of 25cm^3 or less were of class A grade. The experiments determined the dye quantity on the fibre with an average precision of +/- 1.2%, the maximum error being 5.3%.

Model calculations were performed using MS Excel on a standard Pentium PC.

9.2 Application of Diffusion Models

9.2.1 Diffusion Only: Finite and Infinite Bath

In a first step, the experimental results were compared to existing analytical solutions of the diffusion equations for a finite and for an infinite dyebath. For finite bath, Crank's diffusion equation for a cylinder was used (Crank 1975:78). For high exhaustion values the error function used in this equation was asymptotically expanded to obtain higher accuracy as suggested by Crank. For an infinite dyebath, Hill's equation for a cylinder was used [Crank 1975:73]. The first 21 roots of the relevant Bessel functions were taken into account. Figure 9.1 compares the experimental with the predicted results for two dye amounts, 4% and 1.35%, at 65°C and 15$g.dm^{-3}$ electrolyte. In the calculations the diffusion coefficient in Crank's and Hill's equations was adjusted so as to fit the experimental exhaustion after 3 minutes. The exhaustion is expressed in per cent of equilibrium exhaustion.

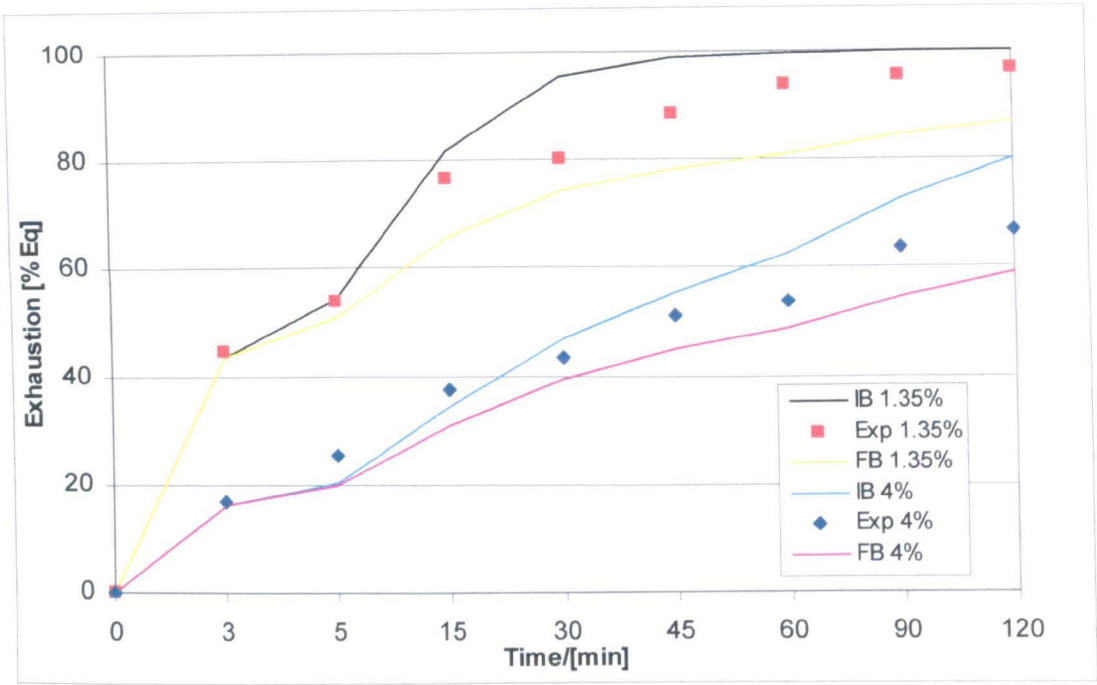

Figure 9.1: Diffusion only Models for the Exhaustion from a finite Bath (FB) and an infinite Bath (IB). "Exp" = experimental values

It is clear from the data shown in figure 9.1 that the experimental values were between the predicted results of the finite and the infinite dyebath equations. An explanation for this behaviour was easily found: An assumption of the finite bath model is that the partition coefficient remains constant during the process. As with most direct dyes, however, experiments described in chapter eight had clearly shown this not to be the case with Direct Yellow 162 when the partition coefficient decreased considerably at higher dye amounts. As a consequence, as the exhaustion proceeds and the dyebath concentration dropped, the partition coefficient increased and led to a higher fibre surface molality of the dye than that used in the finite bath model. An increased dye molality at the fibre surface in turn would lead to a higher measured diffusion speed into the fabric and therefore a higher measured exhaustion speed than that predicted by a fixed partition coefficient model.

For the same reason, an assumption of the infinite bath condition equations, i.e. a constant fibre surface molality, was to be rejected. Provided that the diffusion coefficient is independent of sorbed dye molality, the solution for an infinite bath predicts that the fraction of sorbed dye, M_t/M_∞, at a certain time is independent of the dye concentration in solution in the bath. A calculation shall illustrate that this assumption was not justifiable for the present case:

The equilibrium dye quantity on the fibre, M_∞, at 4%, was experimentally determined to be 2.9 times higher than M_∞ at 1.35%. At any time under infinite bath conditions, the dye quantity on the fibre, M_t, would therefore be expected to be 2.9 times higher for a 4%

dyeing compared to a 1.35% dyeing. In reality, however, the dye uptake after three minutes at 4% was only 10% higher than at 1.35%, indicating that the dye surface molalities in both cases were almost identical during the first minutes of the exhaustion.

Due to the failure of both the finite and infinite bath models to adequately predict the exhaustion behaviour under the conditions of the experiments, a different way to describe the fibre surface molality had to be developed. This description built on the fact that the adsorption speed of the dye at the fibre surface is high compared to the diffusion speed. It may therefore be assumed that at each moment during the dyeing process the equilibrium dye molality is rapidly established at the fibre surface. In previous experiments described in chapter eight, the equilibrium sorption for Direct Yellow 162 had been quantitatively described with a model based on the Gouy-Chapman theory. The predictions of this equilibrium model were used here to calculate the fibre surface molality. A similar approach, using empirical equations for the equilibrium uptake instead of the Gouy-Chapman model, has been successful to simulate the exhaustion of direct dyes on cotton (Reddy 1997).

The results given in table 9.2 calculations showed that the changes at the fibre surface calculated from the Gouy-Chapman sorption isotherms (columns 2 and 4) were less pronounced than those based upon a constant partition coefficient (columns 3 and 5), especially in the case of the 4% dyeing. This suggested that the infinite bath model, as well as the finite bath model, did not satisfactorily describe the situation during the dyeing process. It also explained the fact that the absolute dye quantities on the fibre found in the experiments after 3 minutes for 4% and 1.35% dyeings were much closer than the total dye amounts suggested.

Time /[min]	Based on Isotherm 4% Dye	Finite Bath 4% Dye	Based on Isotherm 1.35% Dye	Finite Bath 1.35% Dye
0	0.0241	0.309	0.0201	0.107
3	0.0233	0.286	0.0182	0.093
5	0.0232	0.275	0.0175	0.087
15	0.0227	0.240	0.0150	0.072
30	0.0222	0.212	0.0141	0.061
45	0.0218	0.194	0.0123	0.054
60	0.0215	0.181	0.0103	0.050
90	0.0208	0.162	0.0096	0.043
120	0.0202	0.149	0.0088	0.039

Table 9.2: Calculated Dye Molalities/[mol pure dye.kg^{-1}] at the Fibre Surface

9.2.2 Diffusion Only: Analytical Solution for a Linearly Decreasing Surface Concentration

As can be seen from table 9.2, the dye surface molality as calculated from the sorption isotherms decreased in the particular experiments in fair approximation linearly with time in the interval from 3 minutes to 60 minutes. An analytical solution for a surface molality that is non-zero initially and then changes linearly with time can be derived by the superposition of the analytical solutions for a constant surface molality and for a linearly decreasing surface molality (Crank 1975:76). This superposed analytical solution was used in figure 9.2 to compare the experimental results with calculations assuming a linearly changing surface molality for a 1.35% dyeing.

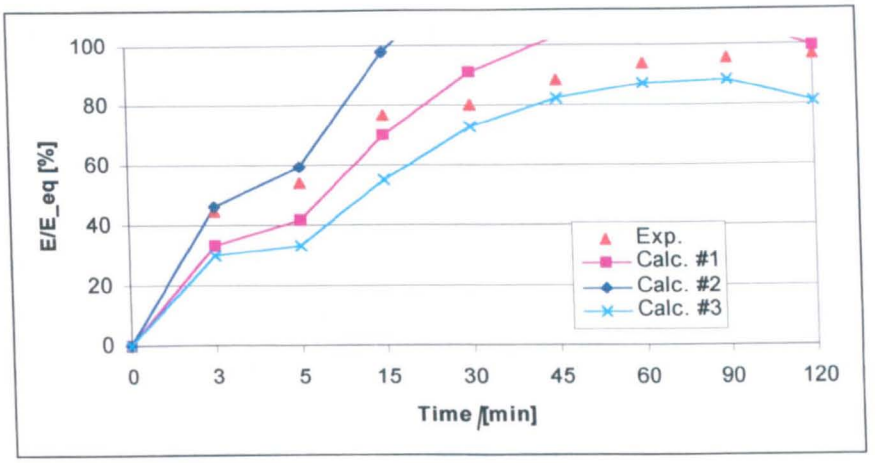

Figure 9.2: Diffusion with a linearly decreasing Dye Surface Molality

Interestingly, it proved to be impossible to fit the experimental data satisfactorily. If the diffusion coefficient was adjusted so as to yield a good fit of the experimental results early in the process (calculation #2), then the theoretically predicted exhaustion occurred much faster than the actual exhaustion at later times in the process. If, on the other hand, the diffusion coefficient was adjusted so as to yield a reasonable fit of the experimental results later in the process (calculations #1 & 3), then the theoretically predicted exhaustion early on in the process occurred much slower than in the experiments. Another noteworthy aspect of the model prediction is that the exhaustion value in calculations #1 and #2 peaked after approximately 60 minutes before dropping to the final equilibrium value, i.e. after 60 minutes the dyestuff would have to be transferred from the fibre back to the dyebath. This is the case because the calculated diffusion speed in these two cases was so high that an inversion of the concentration gradient between the interior of the fibre and the surface occurred as the dyebath concentration fell. The decline in the predicted exhaustion value between 90 and 120 minutes in calculation #3 was caused by the difference in the linearly approximated and the actual surface molality when the linear fit yielded a relatively poor result for the last 30 minutes of the process.

The most likely explanation of these results would be that the exhaustion speed was not only determined by diffusion but also by adsorption. Thus, the exhaustion speed during the first several minutes of the process would be mainly determined by the fast adsorption of the dye while the diffusion would be more important in the later stages of the exhaustion. Evidence for the relevance of adsorption in the initial exhaustion phase can be found in the data of table 9.2, where it can be seen that the diffusion-only models required a dye fibre surface molality much higher than that obtained from calculations based upon experimental results (e.g. 0.107 instead of 0.0192mol.kg^{-1} at 1.35%). At the lower, more realistic dye fibre surface molalities, the predicted dye uptake of a diffusion-only model would have

been much lower than the experimentally found uptake values. This difference can be attributed to rapidly adsorbed dye (First Strike).

As the adsorption speed is much higher than the diffusion speed, the initial rise in the dyebath exhaustion would be steep and then flatten with increasing process time as the diffusion becomes more important. This prediction coincides well with the shape of the exhaustion profile of figure 9.2. The exhaustion model subsequently developed was therefore based on a combined adsorption-diffusion mechanism.

9.3 New Adsorption-Diffusion Model

The exhaustion model developed in this study divides the fibre into two phases, the fibre surface layer and the fibre interior. In the model, the dye adsorbs rapidly at the surface layer and then moves slowly into the fibre interior by diffusion (figure 9.3).

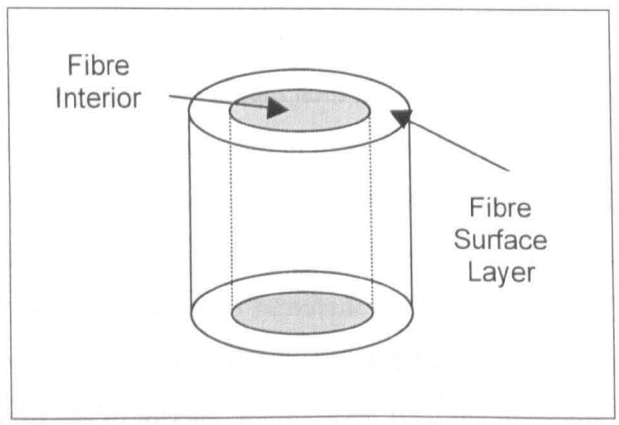

Figure 9.3: Fibre Regions in the Adsorption-Diffusion Exhaustion Model

Details of the mathematical model are described next.

9.3.1 Fibre Surface Layer

The dye molality in the fibre surface layer, $[D]_{fs}$, is assumed to be homogeneous, i.e. there is no molality gradient within the surface layer. The molality is in a dynamic equilibrium with the dyebath according to Langmuir kinetics, taking into account additionally the amount of dye which is continuously transferred between the surface layer and the fibre interior (equation 9.1).

$$\frac{d[D]_{fs}}{dt} = k_a[D]_s\left([D]_{sat} - [D]_{fs}\right) - k_d[D]_{fs} - \frac{dM_{fi}}{dt}\frac{1}{V} \qquad (9.1)$$

$[D]_{fs}$ = Dye molality in the fibre surface [mol.kg fibre surface^{-1}]

$[D]_s$ = Dye concentration in solution [mol.dm^{-3}]

$[D]_{sat}$ = Dye saturation molality [mol.kg fibre surface^{-1}]

k_a = Dye adsorption constant [dm^3.mol^{-1}.min^{-1}]

k_d = Dye desorption constant [min^{-1}]

M_{fi} = Dye quantity in fibre interior [mol.kg fibre^{-1}]

V = Fractional surface layer [kg fibre surface.kg fibre^{-1}]

The saturation molality, $[D]_{sat}$, is dependent on the application conditions and is calculated based upon the formula employed in the Gouy-Chapman model described in chapter eight (equation 8.10), using identical values for the coefficients B_0 to B_4. The saturation concentration is calculated once in the beginning of the process for equilibrium conditions with equation 8.10 and is assumed to be constant during the process. This assumption was made because the coefficients of equation 8.10 had been derived for a maximum equilibrium dyebath concentration of around 2.5g.dm^{-3}. Since initial dyebath concentrations were in some experiments up to twice as high, extrapolation would have been required and that led in some cases to inconsistent results. It could happen, for example, that $[D]_{sat}$ was calculated to be smaller than the equilibrium dye molality on the fibre surface $[D]_{fs,eq}$.

The dye concentration in solution, $[D]_s$, in equation 9.1 is derived from the mass balance for the entire fibre:

$$[D]_s = \frac{M_0 - [D]_{fs}V - [D]_{fi,av}(1-V)}{LR} \qquad (9.2)$$

M_0 = Total dye quantity [mol.kg fibre^{-1}]

LR = Liquor ratio [dm^3.kg fibre^{-1}]

$[D]_{fi,av}$ = Average dye molality in the fibre interior [mol.kg fibre interior^{-1}]

The values for the desorption constant, k_d, and the fraction of the surface layer, V, in equation 9.1 were chosen so as to give the best fit of the experimental values. The adsorption constant, k_a, is derived from the relationship between k_a and k_d (equation 9.3) which is based upon the fact that the dyeing has achieved a dynamic equilibrium, i.e. the dye adsorption speed must equal the dye desorption speed under equilibrium conditions (subscript "eq").

$$\frac{k_a}{k_d} = \frac{[D]_{fs,eq}}{[D]_s\left([D]_{sat} - [D]_{fs,eq}\right)} \qquad (9.3)$$

It is important to note that in equation 9.3, the dye equilibrium molality on the fibre surface, $[D]_{fs,eq}$, is not the equilibrium concentration at the end of the dyeing process but the fibre surface molality that would be established if the conditions at a specific moment were held for an infinite time. $[D]_{fs,eq}$ therefore has to be calculated for each moment during the process, in this case based upon the prediction of the Gouy-Chapman model with variable saturation value derived in chapter eight:

$$-\ln\frac{[D]_{fs,eq}}{[D]_s}+\frac{\Delta\mu}{RT}+\ln\left([D]_{sat}-[D]_{fs,eq}\right)+A_1r_D+A_2r_D\sum z_i[D]_{fs,eq}=0 \quad (9.4)$$

Equation 9.4 was solved in the present case with the solver tool in MS Excel. As $[D]_s$ drops during the process, $[D]_{fs,eq}$ and with it the ratio of k_a and k_d change, too.

The final term in equation 9.1, $dM_{fi}.dt^{-1}.V^{-1}$, describes the dye quantity that is transferred from the surface layer to the fibre interior.

9.3.2 Fibre Interior

The dye molality in the fibre interior, $[D]_{fi}$, is modelled as a one-dimensional, radial diffusion into a cylinder:

$$\frac{\partial[D]_{fi}}{\partial t}=\frac{1}{r}\frac{\partial}{\partial r}\left(rD\frac{\partial[D]_{fi}}{\partial r}\right) \quad (9.5)$$

$[D]_{fi,i}$ = Dye molality in fibre interior layer [mol.kg interior fibre^{-1}]

r = Fibre radius [cm]

D = Diffusion coefficient [cm^2.min^{-1}]

The following boundary conditions apply:

$$[D]_{fi,(t=0)}=0;\left.\frac{\partial[D]_{fi}}{\partial r}\right|_{(r=0)}=0;[D]_{fi,(r=a_{fi})}=[D]_{fs} \quad (9.6)$$

The first boundary or initial condition states that the fibre is initially free of dye. The second condition implies that there is no molality gradient at the fibre centre and the third condition says that the dye molalities of surface layer and interior are identical at their boundary ($r = a_{fi}$).

As the radius of the fibre interior, a_{fi}, changes with the fractional surface layer, V, a_{fi} is smaller than the fibre radius, a, and has to be calculated as a function of V. Since

$$V=\frac{V_{fibre}-V_{fi}}{V_{fibre}}=\frac{\pi a^2l-\pi a_{fi}^2l}{\pi a^2l}=1-\frac{a_{fi}^2}{a^2} \quad (9.7)$$

it follows for a_{fi}:

$$a_{fi} = a\sqrt{(1-V)} \tag{9.8}$$

The value of "a" was calculated from the information provided about the yarn. The yarn had a fineness of 38 count. This equated to a weight of 0.016g per metre yarn (Grover 1960:327). Assuming a cotton density of 1.35g.cm^{-3} (Morton 1986:156), the volume per metre yarn was $1.2.10^{-8}$m^3. The radius was then calculated to be 0.06cm. SEM-Analysis of yarn cross-sections showed a radius of approximately 0.08cm. A radius of 0.06cm was used for further mathematical treatments.

9.3.3 The Numerical Solver

Due to the model's complexity, no analytical solution of the equations is available and a numerical procedure had to be employed instead. The numerical solution was achieved in several steps. In the first calculation step, the dyebath concentration was calculated with equation 9.2. In the second calculation step, the differential equation for the fibre surface layer was solved by the finite difference method as a backward difference approximation in its explicit form (Lapidus 1982:38) (equation 9.9). The superscript j indicates the j-th time step, the superscript j-1 indicates the j-1-th time step and the superscript j+1 indicates the j+1-th time step.

$$[D]_{fs}^{j+1} = [D]_{fs}^{j} + \Delta t\left\{k_a^j [D]_s^j \left([D]_{sat} - [D]_{fs}^{j}\right) - k_d^j [D]_{fs}^{j}\right\} - \frac{M_{fi}^{j} - M_{fi}^{j-1}}{V} \tag{9.9}$$

In this equation, the $[D]_s$-value previously calculated in the first step was used. The values for fractional surface layer, V, and the desorption constant, k_d, were constant during the process and were determined so as to give the best overall fit of the experimental data. The adsorption constant, k_a, is calculated with equation 9.3, where $[D]_{fs,eq}$ was determined previously as described above.

In the third calculation step, the diffusion equation was solved by the Crank-Nicolson implicit method in time steps of 0.5 min (Crank 1975:144). For the calculation, the fibre interior was sliced into twenty layers of equal thickness. As fibre geometry and dye distribution are assumed to be symmetrical, only half of the 20 layers are needed for a complete description of the dye distribution in the fibre interior. The numerical solution therefore yielded ten dye molalities, one for each layer of one fibre-half, at every time step (figure 9.4).

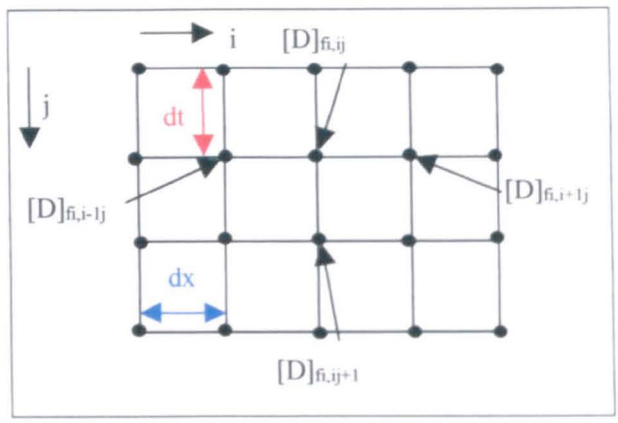

Figure 9.4: Time-space Grid for Fibre Interior

Written in its dimensionless form, the implicit method for diffusion in a cylinder uses the following finite-difference approximation for the second order partial differential equation:

$$\frac{c_{fi,ij+1}-c_{fi,ij}}{\delta T}=\frac{1}{2}\left\{\begin{array}{l}\dfrac{(2i+1)c_{fi,i+1j}-4ic_{fi,ij}+(2i-1)c_{fi,i-1j}}{2i(\delta R)^2}\\ +\dfrac{(2i+1)c_{fi,i+1j+1}-4ic_{fi,ij+1}+(2i-1)c_{fi,i-1j+1}}{2i(\delta R)^2}\end{array}\right\} \qquad (9.10)$$

$c_{fi} = [D]_{fi}.M_0^{-1}$ [-]

$T = Dt.a^{-2}$ [-]

$R = r.a^{-1}$ [-]

Rearrangement and making use of the substitution of $\delta T.(\delta R)^{-2} = r$ yields:

$$\begin{aligned}&\frac{-(2i-1)}{2i}rc_{i-1j+1}+(2+2r)c_{ij+1}-\frac{r(2i+1)}{2i}rc_{i+1j+1}\\&=\frac{(2i-1)}{2i}rc_{i-1j}+(2-2rc_{ij})+\frac{(2i+1)}{2i}rc_{i+1j}\end{aligned} \qquad (9.11)$$

Written in this form, equation 9.11 contains all unknown values at time j+1 at the left side of the equation and all known values at time j at the right side of the equation. The result is a set of equations in which at any moment the molality at any location depends upon the molality of its two neighbours.

Inserting values for i results in the following equations for different locations in the fibre (only exemplified for i = 0 to 2).

i = 0 (fibre centre):

$$c_{0j+1}=(1-4r)c_{0j}+4rc_{1j} \qquad (9.12)$$

i = 1:

$$-\frac{1}{2}rc_{0j+1}+(2+2r)c_{1j+1}-\frac{3}{2}rc_{2j+1}=\frac{1}{2}rc_{0j}+(2-2r)c_{1j}+\frac{3}{2}rc_{2j} \qquad (9.13)$$

i = 2:

$$-\frac{3}{4}c_{1j+1}+(2+2r)c_{2j+1}-\frac{5}{4}rc_{3j+1}=\frac{3}{4}c_{1j}+(2-2r)c_{2j}+\frac{5}{4}rc_{3j} \qquad (9.14)$$

etc.

Thus, a total of ten equations is obtained with the ten unknown concentration c_{0j+1} to c_{9j+1}. The equations can be solved by step-by-step elimination, i.e. c_{0j+1} is calculated from the first equation and then substituted in the second equation, which can then be solved for c_{1j+1}. c_{1j+1} is then substituted in the third equation and so on so that the grid of values is progressively filled, figure 9.5.

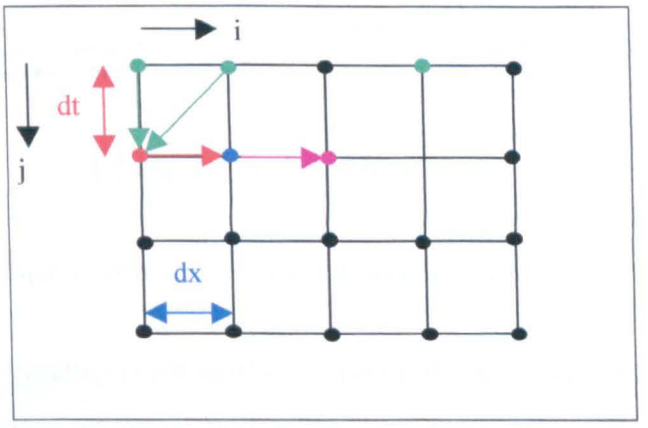

Figure 9.5: Progression of Implicit Method

In order to calculate the total amount of dye in the fibre interior at any one time, M_{fi}, the dye molalities in the interior, $[D]_{fi}$, have to be integrated over the entire fibre diameter. There are several integration methods available for this purpose, among them the trapezoidal method and Simpson's rule. The trapezoidal rule for the ten layers is based on the following algorithm:

$$M_{fi}=\frac{1}{10}\left([D]_{fi,0}r_0+2\sum_{i=1}^{9}[D]_{fi,j}r_i+[D]_{fi,10}r_{10}\right) \qquad (9.15)$$

r_i = Fractional distance of layer from fibre centre, ranging from 0 to 1 [-]

The algorithm for Simpson's rule is:

$$M_{fi}=\frac{2}{3}\frac{1}{10}\left([D]_{fi,o}r_0+4[D]_{fi,1}r_1+2[D]_{fi,2}r_2+..+4[D]_{fi,9}r_9+[D]_{fi,10}r_{10}\right) \qquad (9.16)$$

The accuracy of the two integration methods of the diffusion equation can be quantified if boundary conditions are selected for which an analytical solution of the diffusion equation exists. In figure 9.6 infinite bath conditions, i.e. constant surface molality, were used to compare the numerical solutions obtained by the two integration methods and the accurate, analytical solution of the diffusion equation.

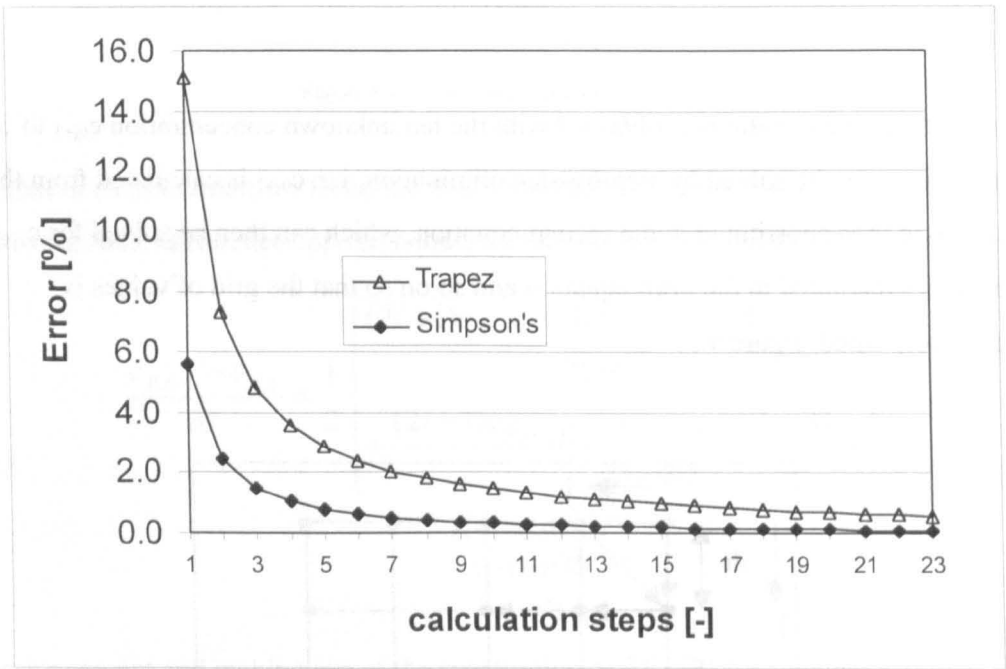

Figure 9.6: Accuracy of numerical Solutions of the Diffusion Equation

The initial error of the numerical solutions results from the singularity at time equal to zero, when there is no dye in the first nine layers of the fibre (counting from the centre of the fibre outwards) but the layer in contact with the dyebath contains the equilibrium dye amount. From figure 9.6 it is clear that Simpson's rule yielded more accurate results and that after three calculation steps, i.e. after 1.5 minutes, the error was under 2% and after four steps the error dropped to 1%. Simpson's rule was therefore used in all further analysis as the integration method of choice.

9.3.4 Forward and Central Difference versus Backward Difference Approximation

The backward difference approximation method described in the previous section was generally used to solve the fibre surface molality equation because it had the advantage of showing fairly high stability and of requiring only one iteration per time step for $[D]_{fs,eq}$, thus enabling a rapid progress of the solver in time. It had two disadvantages, though. First,

it was of limited accuracy and second, the solver became unstable under certain conditions. The numerical solution became unstable for values of the fractional volume of less than around 0.07. For these low values, the dye amount transferred in each iteration step from the surface layer to the interior, $\Delta M_{fi}.V^{-1}$, became large compared to the total amount of dye in the surface layer, $M_{fs} = V.D_{fs}$. The small fractional volume and, as a second factor, the singularity at time zero caused, in these cases, fluctuations in the dye amount of the surface layer that increased with simulation time.

The limited accuracy could be improved by employing a central difference approximation around the time level $j+^1/_2$ (Lapidus 1982:41, Vosoughi 1993) (equation 9.17). The Crank-Nicolson method of solving the diffusion equation was unaffected by this modification.

$$\frac{[D]_{fs}^{j+1}-[D]_{fs}^{j}}{\Delta t}=\alpha\left\{k_a^{j+1}[D]_s^{j+1}\left([D]_{sat}-[D]_{fs}^{j+1}\right)-k_d^{j+1}\right\}$$
$$+(1-\alpha)\left\{k_a^{j}[D]_s^{j}\left([D]_{sat}-[D]_{fs}^{j}\right)-k_d^{j}\right\}-\left(\alpha\frac{M_{fi}^{j+1}-M_{fi}^{j}}{V\Delta t}+(1-\alpha)\frac{M_{fi}^{j}-M_{fi}^{j-1}}{V\Delta t}\right) \quad (9.17)$$

The coefficient α is a weighting term that when set to 0.5 yields equal weight for the forward and the backward step. Here, an alpha-value of 0.5 was used for the calculations.

Rearrangement of equation 9.17 gives:

$$[D]_{fs}^{j+1}=\frac{\Delta t\left\{\alpha\left(k_a^{j+1}[D]_s^{j+1}[D]_{sat}^{j+1}+\frac{M_{fi}^{j+1}-M_{fi}^{j}}{V\Delta t}\right)+(1-\alpha)\left(k_a^{j}[D]_s^{j}[D]_{sat}^{j}+\frac{M_{fi}^{j}-M_{fi}^{j-1}}{V\Delta t}\right)\right\}}{1+\Delta t\alpha\left(k_a^{j+1}[D]_s^{j+1}k_d^{j+1}\right)}$$
$$+\frac{[D]_{fs}^{j}\left\{1-\Delta t(1-\alpha)\left(k_a^{j}[D]_s^{j}+k_d^{j}\right)\right\}}{1+\Delta t\alpha\left(k_a^{j+1}[D]_s^{j+1}k_d^{j+1}\right)} \quad (9.18)$$

Since $[D]_{fs}^{j+1}$ depends not only on parameter values of the past iteration step j but also on those of the present iteration step j+1, it becomes necessary to determine it by iteration at each time step. This was achieved by using the solver tool in MS Excel until the following condition was fulfilled:

$$[D]_{fs}^{j+1}-[D]_{fs}^{estimate}<10^{-10} \quad (9.19)$$

The second downside of the backward difference solver, its stability, could be improved by employing a forward difference approximation (equation 9.20). Its accuracy was of the same order as that of the backward approximation.

$$[D]_{fs}^{j+1} = [D]_{fs}^{j} + \Delta t\left\{k_a^{j+1}[D]_s^{j+1}\left([D]_{sat} - [D]_{fs}^{j+1}\right) - k_d^{j+1}[D]_{fs}^{j+1}\right\} - \frac{M_{fi}^{j+1} - M_{fi}^{j}}{V}$$

(9.20)

Here, too, $[D]_{fs}$ had to be determined at each time step by iteration.

Figure 9.7 shows the results obtained by the three approximation methods for a 4% dyeing at 90°C with 15g.dm^{-3} electrolyte.

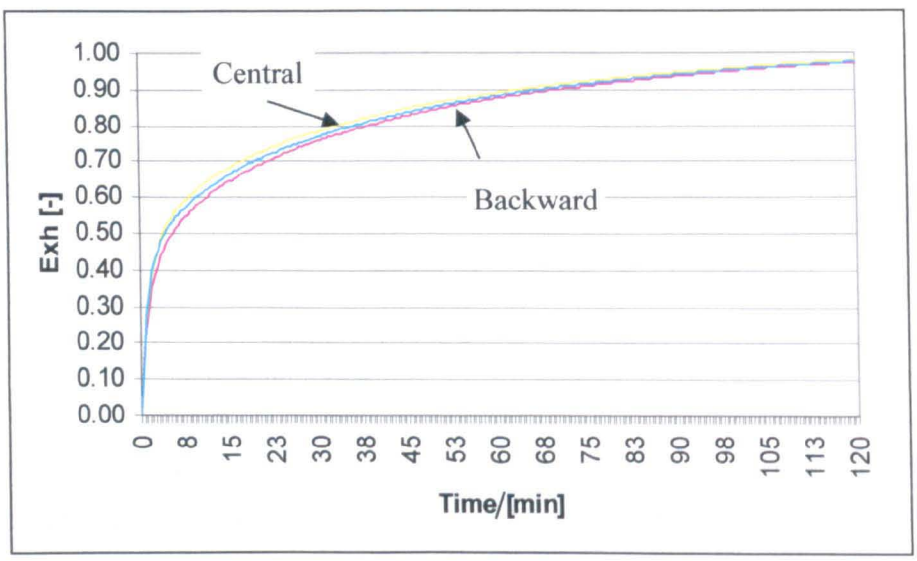

Figure 9.7: Simulation Results for backward, forward and central Difference Approximations

Compared to the more accurate central difference approximation, exhaustion values determined by the backward difference approximation were on average 2.0% lower, with a maximum difference of 4.9%. The forward difference approximation yielded exhaustion values that were on average 0.9% lower with a maximum difference of 1.5%. The increased accuracy of the central and forward difference approximations came at the expense of considerably higher calculation time due to the necessity of calculating $[D]_{fs}$ by iteration at each time step.

9.4 Modelling the Influence of the Boundary Layer

In a second development step, the model was extended to take into account boundary layer effects. A quantitative treatment of their influence on the dye uptake rate is possible if it is assumed that the key influencing parameter is the diffusional boundary layer thickness, δ (McGregor 1965). The boundary layer thickness is the distance between the fibre surface and the point in the dyebath where 99% of the average bulk concentration is reached (figure 9.8). In this case, a description of the boundary layer is necessary that shows how much the dye fibre surface molality changes as a function of the boundary layer thickness. Once the

dye solution concentration at the fibre surface, $[D]_s'$, is known the exhaustion speed can be predicted with the 2-phase adsorption-diffusion model described in the previous section.

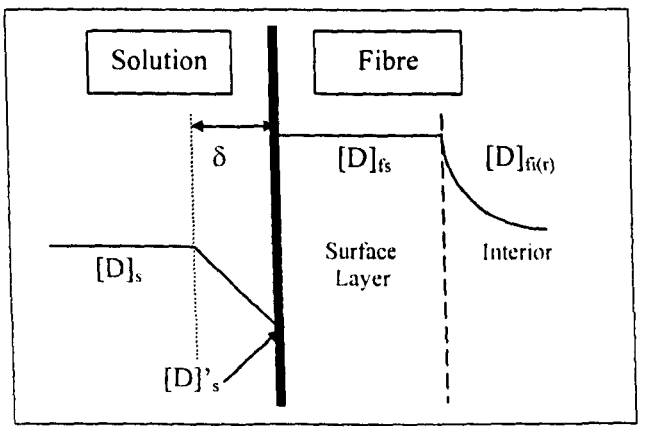

Figure 9.8: Diffusional Boundary Layer and 2-phase Adsorption-diffusion Model

The flux of dye through the boundary layer, under steady-state conditions, can be derived from Fick's first law:

$$J_{BL} = -D_s \frac{([D]_s' - [D]_s)}{\delta} \qquad (9.21)$$

J_{BL} = Rate of diffusion through boundary layer [mol.m.s^{-1}.dm^{-3}]

D_s = Diffusion coefficient of the dye in water [m^2.s^{-1}]

$[D]'_s$ = Dye concentration in solution at the fibre surface [mol.dm^{-3}]

δ = Boundary layer thickness [m]

The amount of dye transferred from the solution to the fibre, i.e. the adsorption process, can be described in the form of Langmuir kinetics during the early stages of the dyeing process when the diffusion into the fibre interior may still be neglected. This simplification may be justified because, as will be seen later on, the influence of the boundary layer is more pronounced under high substantivity conditions and early on in the process.

$$\frac{d[D]_{fs}}{dt} = k_a[D]_s([D]_{sat} - [D]_{fs}) - k_d[D]_{fs} \qquad (9.22)$$

$[D]_{fs}$ = Dye molality in the fibre surface [mol.kg fibre surface^{-1}]

$[D]_s$ = Dye concentration in solution [mol.l^{-1}]

$[D]_{sat}$ = Dye saturation molality [mol.kg fibre^{-1}]

k_a = Dye adsorption constant [l.mol^{-1}.min^{-1}]

k_d = Dye desorption constant [l.min^{-1}]

It may be further assumed that the amount of dye transferred to the fibre (equation 9.22) is equal to that transported through the boundary layer (equation 9.21). Before the two equations can be equated, it is necessary to convert the dye flux through the boundary layer from a flux per surface area to a flux per mass unit (equation 9.23).

$$J_{BL}\frac{A_F}{V_F}LR = J_{BL}\frac{2\pi al}{\frac{\pi a^2}{2}l}LR = J_{BL}\frac{4LR}{a} = \frac{d[D]_{fs}}{dt} \qquad (9.23)$$

A_F=Surface area fibre [m^2]

V_F=Volume fibre [m^3]

LR = Liquor ratio [$dm^3.kg^{-1}$]

a = Fibre radius [m]

l = Fibre length [m]

The boundary condition now becomes:

$$J_{BL}\frac{4LR}{a} = -D_s\frac{4LR([D]'_s - [D]_s)}{a\delta} = k_a[D]_s([D]_{sat} - [D]_{fs}) - k_d[D]_{fs} = \frac{d[D]_{fs}}{dt} \qquad (9.24)$$

Rearrangement of Eqn 9.24 for [D]'$_s$ yields

$$[D]'_s = [D]_s\left(\frac{1}{1+\frac{\delta k_a a}{4D_s LR}([D]_{sat} - [D]_{fs})}\right) + \frac{\delta a k_d[D]_{fs}}{4D_s LR + \delta a k_a([D]_{sat} - [D]_{fs})} \qquad (9.25)$$

which can be written as

$$[D]'_s = [D]_s\left(\frac{1}{1+L}\right) + \frac{L}{K}\frac{[D]_{fs}}{([D]_{sat} - [D]_{fs})} \qquad (9.26)$$

with the dimensionless group L

$$L = \frac{\delta a k_a}{4D_s LR}([D]_{sat} - [D]_{fs}) \qquad (9.27)$$

and the constant K [$dm^3.mol^{-1}$]

$$K = \frac{k_a}{k_d} \qquad (9.28)$$

For δ equal to zero, [D]'$_s$ becomes equal to [D]$_s$. In this case the exhaustion speed is at its maximum. It reduces as the ratio of [D]'$_s$.[D]$_s^{-1}$ becomes smaller. The first term of Eqn 9.26 shows an inverse relationship between [D]'$_s$ and the composite parameter L. The second

term of the equation can be interpreted as the fraction of already occupied adsorption places on the surface layer to those still available. Thus, the influence of the boundary layer on $[D]'_s$ and therefore also on the exhaustion speed will be high if

- L is big
- K is big and
- $[D]_{fs}.([D]_{sat} - [D]_{fs})^{-1}$ is small

This is the case when

- high substantivity conditions prevail (high $[D]_{sat}$, high K, low LR, small D_s)
- the dyeliquor velocity is low relative to the fibre surface (high δ)
- the dyeing process is in its early stages {small $[D]_{fs}.([D]_{sat}-[D]_{fs})^{-1}$}

Note: The last conclusion only applies to constant dyeing conditions. If the substantivity increases during the dyeing process, e.g. due to salt dosing, the process is not necessarily more sensitive to boundary layer effects during its early stages.

At the end of chapter 9.5, equation 9.26 is used to predict the critical boundary layer thickness below which the dye uptake rate becomes dependent on the flow rate. It is also used to analyse experimental data obtained on the pilot-scale jet machine under conditions when the flow rate influenced the dye uptake rate. The value of δ is estimated as a function of the flow velocity.

9.5 Model Prediction versus Experimental Results

9.5.1 Constant Dyeing Conditions

9.5.1.1 Liquor Ratio 8:1

The adsorption-diffusion model uses three parameters, which were adjusted empirically so as to fit the experimental results. They are:

- the desorption constant, k_d, as a function of temperature
- the diffusion coefficient, D, as a function of temperature, salt and dye concentration
- the fractional surface layer, V, as a function of temperature, salt and dye concentration.

All model calculations at 65°C, 90°C and 100°C used the backward difference approximation method. Model calculations at 43°C were carried out using the forward difference approximation method because of its increased numerical stability. Tables 9.3 to 9.5 show the parameter settings that were needed to satisfactorily simulate the experimental results.

		V/[kg surface.kg fibre^{-1}]			
Dye [% omf]	**Salt conc./[g.dm^{-3}] (Dyeing temp.)**	**43°C**	**65°C**	**90°C**	**100°C**
0.20	5 (65°C), 10 (65°C), 15	0.070	0.180	0.25	0.25
0.45	5 (65°C), 10 (65°C), 15	0.060	0.155	0.25	0.25
1.35	5 (65°C), 10 (65°C), 15	0.040	0.130	0.25	0.25
4.00	5 (65°C), 10 (65°C), 15	0.030	0.090	0.25	0.25
0.20	0		0		
0.45	0		0		
1.35	0		0		
4.00	0		0		

Table 9.3: The fractional Surface Layer, V, as a Function of Temperature, Salt and Dye Amount

The tendency of the fractional surface layer (V, table 9.3) to increase with temperature and decrease with dye amount could be explained by changes in the aggregation state of the dye molecules in solution. Experiments described in chapter six had shown that aggregation in the presence of electrolyte slowly decreased up to a temperature of 90°C, which coincides well with the increase in the fractional volume from 43°C to 90°C. Dye aggregation could also be the reason why V was lower at higher dye amounts. On the other hand, dye uptake without common salt could be best described with a diffusion-only process, implying that the first strike is closely linked to the presence of higher electrolyte concentrations – and therefore also higher aggregation. Considering this result it would be anticipated that the model of Reddy et al., which as outlined in chapter four successfully employed a diffusion-only system, would fail at steeper electrolyte dosing gradients and higher salt concentration. It was also striking that the V-value at temperatures close to the boil was, maybe coincidentally, very close to the typical value of the internal volume for cotton in the Donnan membrane theory.

The complex relationship between the fractional volume, the amount of dye and the temperature could be approximated with a non-linear equation:

$$V = a_0 + a_1 M_0 + a_2 M_0^2 + a_3 T + a_4 MT \qquad (9.29)$$

$a_0 - a_4$ = Regression coefficients [-]

M = Total amount of dye [% omf]

T = Temperature [°C]

Equation 9.29, together with the knowledge that the fractional volume was zero when no common salt was present (in the case of C.I. Direct Yellow 162) and that it was independent of temperature and dye amount at temperatures beyond 90°C led to an average prediction error in the fractional volume of 6%.

		k_d/[min^{-1}]			
Dye [% omf]	**Salt conc./[g.dm^{-3}] (Dyeing Temp.)**	**43°C**	**65°C**	**90°C**	**100°C**
0.20	0 (65°C), 5 (65°C), 10 (65°C), 15	0.10	0.15	0.25	0.36
0.45	0 (65°C), 5 (65°C), 10 (65°C), 15	0.10	0.15	0.25	0.36
1.35	0 (65°C), 5 (65°C), 10 (65°C), 15	0.10	0.15	0.25	0.36
4.00	0 (65°C), 5 (65°C), 10 (65°C), 15	0.10	0.15	0.25	0.36

Table 9.4: The Desorption Constant, k_d, as a Function of Temperature

The desorption constant was a function of temperature only in accordance with experimental evidence that the desorption constant is independent of dye concentration (table 9.4, Snyder 1997). A simple approximation of the temperature-dependency of k_d, which yielded an average prediction error of 5.5%, is expressed in equation 9.30.

$$k_d = a_0 a_1^T \qquad (9.30)$$

a_0, a_1 = Regression coefficients

		D/[cm^2.min^{-1}]			
Dye [% omf]	**Salt conc./[g.dm^{-3}] (Dyeing Temp.)**	**43°C**	**65°C**	**90°C**	**100°C**
0.20	5 (65°C), 10 (65°C), 15	$2.5.10^{-09}$	$1.0.10^{-08}$	$3.0.10^{-08}$	$6.0.10^{-08}$
0.45	5 (65°C), 10 (65°C), 15	$2.5.10^{-09}$	$1.0.10^{-08}$	$3.0.10^{-08}$	$6.0.10^{-08}$
1.35	5 (65°C), 10 (65°C), 15	$2.5.10^{-09}$	$1.0.10^{-08}$	$3.0.10^{-08}$	$6.0.10^{-08}$
4.00	5 (65°C), 10 (65°C), 15	$2.5.10^{-09}$	$1.0.10^{-08}$	$3.0.10^{-08}$	6.0.10-08
0.20	0		4.0.10-09		
0.45	0		7.0.10-09		
1.35	0		8.0.10-09		
4.00	0		1.7.10-08		

Table 9.5: The Diffusion Coefficient, D, as a Function of Temperature, Salt and Dye Amount

The true physico-chemical relationship between the diffusion coefficient and the salt and dye concentration is very complex, as was pointed out in chapter four. However, in the model calculations satisfactory results were achieved with a diffusion coefficient independent of dye and salt concentration when at least 5g.dm^{-3} electrolyte were present (table 9.5). This was partly due to the limited role the diffusion plays in determining the exhaustion profile under high substantivity conditions when changes in the diffusion coefficient have very little effect on the dye uptake rate. The values of the diffusion coefficient used here were at the lower end of those for other direct dyes (Jones 1989). This would be expected as the dye under investigation, C.I. DY162, has a particularly high molecular weight and a high affinity for cotton. Both characteristics imply a comparatively low diffusion coefficient.

The temperature-dependency of the diffusion coefficient is usually expressed through an Arrhenius equation:

$$D = D_0 e^{-\frac{E_A}{RT}} \tag{9.31}$$

The apparent activation energy was determined by linear regression from the experimental values by using equation 9.32.

$$\ln D = \ln D_0 - \frac{E_A}{R}\frac{1}{T} \tag{9.32}$$

Application to the data of table 9.5 gave a correlation coefficient of 0.99, a standard diffusion coefficient, D_0, of $1cm^2.min^{-1}$ and an apparent activation energy of $53kJ.mol^{-1}$ which is in good agreement with other direct dyes (Jones 1989).

When no salt was added to the dyebath, a constant diffusion coefficient no longer yielded acceptable results. Instead, the diffusion coefficient had to be increased approximately linearly with the dye amount. Experimental evidence indicates that this assumption of an increasing diffusion coefficient could reflect a true physico-chemical phenomenon (Peters 1975:453).

Using the parameter settings of tables 9.3 to 9.5 for k_d, V and D, the model predicted the experimental exhaustion value of all the isothermal experiments with an average (absolute) accuracy of +/- 2.3%. The highest single prediction error was 4.2%. The model performance was thus satisfactory.

Two examples shall illustrate the modelling results. One example, a 1.35% dyeing at 65°C in the presence of $5g.dm^{-3}$ salt, represents conditions under which both diffusion and adsorption play an important role (figure 9.9). The second example, 0.45% dye, 100°C, $15g.dm^{-3}$ salt, represents conditions under which the exhaustion is mostly determined by adsorption in the fibre surface layer (figure 9.10). In both figures, the experimentally measured exhaustion values are labelled "Exp.". The exhaustion values are expressed as a fraction of equilibrium exhaustion.

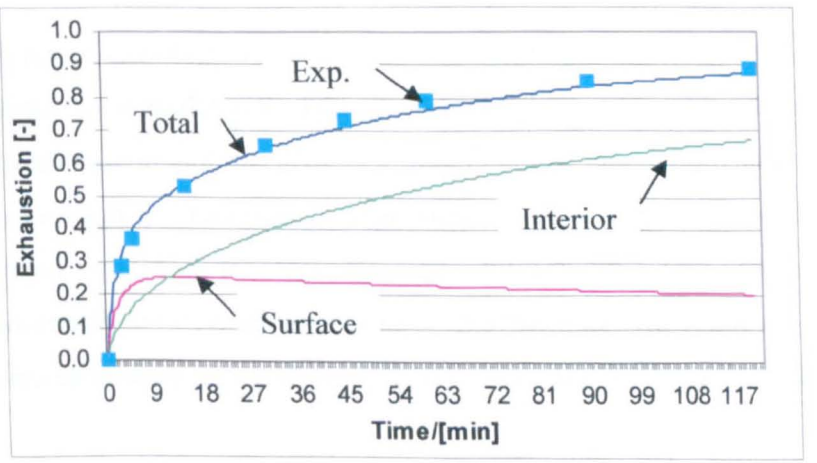

Figure 9.9: Modelling Results for moderate Substantivity Conditions

In figure 9.9, the surface layer adsorbs at the peak about 25% of the total dye. As the surface layer accounts for only 13% of the total fibre, it can be seen that even under

moderate substantivity conditions, the dye is concentrated in the surface layer during the early exhaustion stages. From there it gradually diffuses into the fibre interior, leading to a slow decrease of the amount of dye in the surface layer.

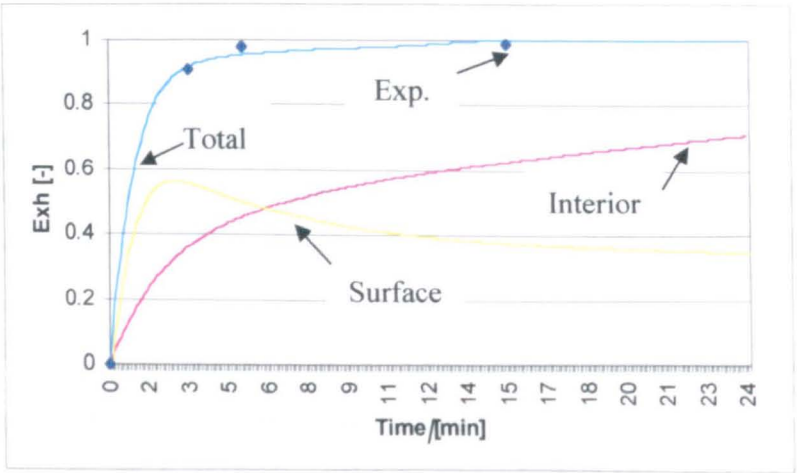

Figure 9.10: Modelling Results for high Substantivity Conditions

Figure 9.10 shows that dye exhaustion is almost complete within only five minutes. This, however, does not mean that the exhaustion process reached equilibrium within the fibre as more than half of the total equilibrium dye fibre amount is concentrated in the surface layer. It takes a further 30 minutes before that percentage drops by internal re-distribution of the dye to the equilibrium value of 25%. The model thus describes correctly the well-known effect that the dye is concentrated in a narrow ring at the fibre surface in the early stages of the dyeing process under high substantivity conditions (Vickerstaff 1954:150).

9.5.1.2 Liquor Ratio 65:1

Dyeing machines employed in bulk production of textiles run at different liquor ratios, depending on the machine type, the fabric type and the machine load. An important feature of a useful exhaustion model would therefore be to accurately predict the exhaustion profile for different liquor ratios. For the comparison, the parameter settings for k_d, D and V were identical to those of a 8:1 liquor ratio. The coefficients for the Gouy-Chapman model, which were needed to predict the dye fibre surface molality, were determined from a series of isothermal dyeings at a liquor ratio of 65:1 according to a method described in chapter eight.

The table below lists the prediction error of the adsorption-diffusion model for these experiments.

Temperature [°C], Salt Conc. [g.dm^{-3}]	Average Dye Fibre Prediction Error [%]
40, 15	2.2
65, 15	4.9
90, 15	6.6
90, 0	5.2

Table 9.6: Model Accuracy at a Liquor Ratio of 65:1

The data indicate that the prediction accuracy decreased to approximately +/- 5% on average. This error would not yet necessarily lead to a perceptible colour difference if the results of chapter eight are taken into account. The model therefore appeared to yield accurate enough predictions for changes in the liquor ratio as they are encountered in practice without requiring adjustment of its coefficients.

9.5.2 Electrolyte Dosing Gradient

For the simulation of the process with electrolyte dosing, the values for k_d, V and D were based on the values tabled in the previous section and calculated from the regression equations 9.29 to 9.31. An additional assumption had to be made for V because an interpolation was needed between its value at zero salt concentration, when V was zero, to its value at 5g.dm^{-3} salt, when the regression equation 9.29 applied. The following interpolation equation for V was chosen:

$$V' = V\left\{0.15 + 0.85\left(1 - e^{-[NaCl]}\right)\right\} \tag{9.33}$$

where V' is the interpolated value for the fractional volume of the surface layer. This equation resulted in a steep rise of V' towards V (figure 9.11).

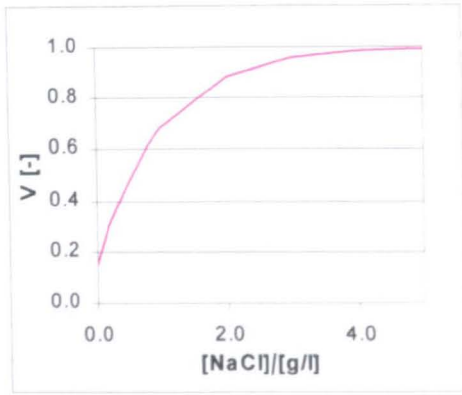

Figure 9.11: Interpolation for V at low Salt Concentrations

The figures 9.12 and 9.13 show the modelling results. They include not only the dye amounts in the surface layer and in the fibre interior but also the dye fibre surface molality corresponding to equilibrium conditions, $[D]_{fs,eq}$.

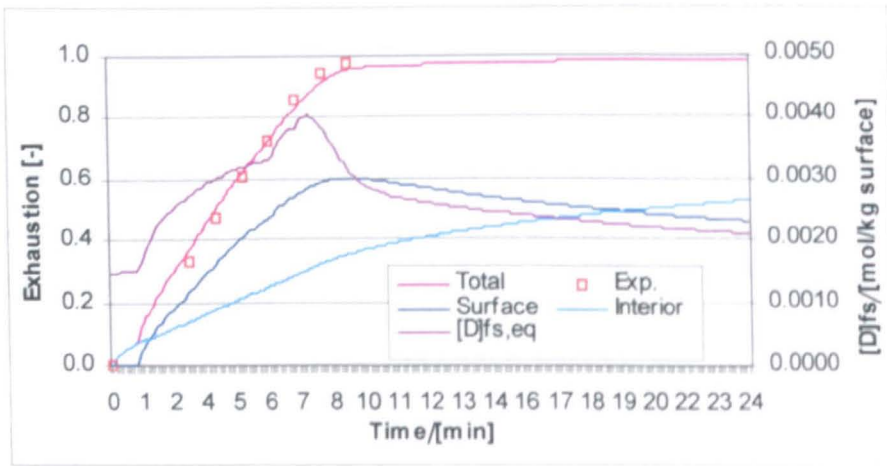

Figure 9.12: Modelling of Salt Dosing Experiment #1

The prediction of the exhaustion and the experimental data for the first experiment are in good agreement as shown in figure 9.12. During the first minute of the process, there was no dye in the surface layer because the electrolyte concentration was zero. As soon as the salt dosing started, $[D]_{fs,eq}$ and V increased and as a result so did the dye amount in the surface layer. It is also noticeable that $[D]_{fs,eq}$ rose more rapidly after around six minutes when the salt dosing gradient increased. An increased $[D]_{fs,eq}$ thus compensated for the factors that tended to reduce the uptake rate, notably a diminishing dyebath concentration, and an overall linear exhaustion profile with time was obtained.

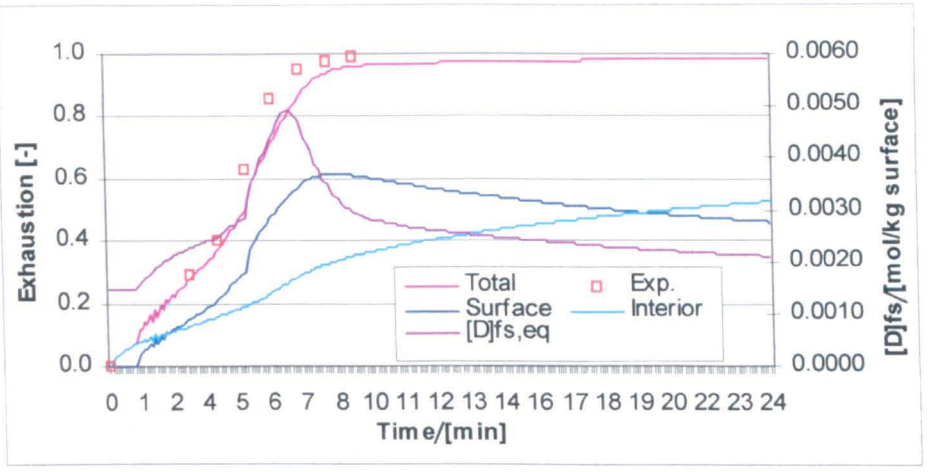

Figure 9.13: Modelling of Salt Dosing Experiment #2

A comparison between prediction of exhaustion and the measurements for the second experiment, depicted in figure 9.13 shows that considerable differences arose once the salt dosing gradient increased after five minutes. Even though the model predicted qualitatively correctly the increase in the uptake rate once the dosing gradient got steeper, the actual response of the system was faster and more pronounced. The fit could be improved by doubling the Langmuir kinetic constants k_a and k_d, leading to a quicker establishment of equilibrium conditions in the fibre surface layer (figure 9.14).

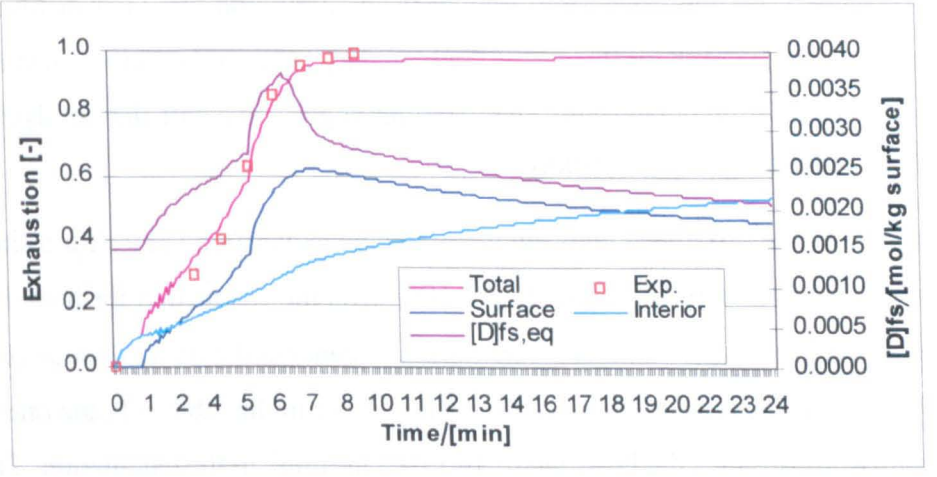

Figure 9.14: Modelling of Salt Dosing Experiment #2 with modified k_d-value

The fluctuations of $[D]_{fs}$ that can be observed in figures 9.13 and 9.14 between the first and second minute are due to stability problems of the backward difference solver which was at the border of becoming unstable when V assumed low values in the initial moments of the salt dosing.

9.5.3 Influence of the Boundary Layer

With the help of equation 9.26 to determine $[D]'_s$ from $[D]_s$, it is possible to predict the maximum permissible boundary layer thickness in order to avoid any significant influence on the dye uptake rate. If the effect of the boundary layer on the exhaustion kinetics in an early process stage, i.e. $d[D]_{fs}.dt^{-1}$, is to be evaluated with equations 9.22 and 9.26, k_a and k_d can be determined experimentally, either directly or indirectly as is the case for the adsorption-diffusion model. The diffusion coefficient of the dye in water (D_s) must be known in order to use equation 9.26. As no specific data was available for C. I. DY162, D_s was estimated from literature values. Diffusion coefficients of dyes in water are generally in the range between 10^{-4} and 10^{-6} $cm^2.min^{-1}$ (Zollinger 1991:284), which has been confirmed specifically for direct dyes, too (McGregor 1965, Inglesby 2001). Additionally, it is known that the diffusion coefficient of direct dyes in water is 1,000 to 10,000 times higher than in the fibre (Jones 1989, Vickerstaff 1954:124). Based on this information, the lower estimate at 65°C was taken to be $5.10^{-6}cm^2.min^{-1}$, i.e. 500 times higher than the apparent, modelled diffusion coefficient in the fibre, and the higher estimate was $100.10^{-6}cm^2.min^{-1}$, i.e. 10,000 times higher.

The influence of the boundary layer thickness on the exhaustion rate was modelled once for high substantivity [0.45% (omf) dye, $10g.dm^{-3}$ salt, 65°C, $t_{1/2}$[8] = 1.7min], once for medium [0.45%, $2g.dm^{-3}$, 65°C, $t_{1/2}$ = 5min] and once for low substantivity conditions [0.45%, $0.5g.dm^{-3}$, 65°C, $t_{1/2}$ = 22min]. The low substantivity conditions could probably serve as a conservative estimate of the influence of the boundary layer under industrial standard conditions, as data from the dyestuff manufacturer suggested a half-time of dyeing of between 30 and 40min (Sandoz 1986).

Table 9.7 shows the difference between the predicted exhaustion values for a situation when there is no boundary layer, i.e. $[D]_s' = [D]_s$, with the exhaustion for boundary layers of different thicknesses, δ. Numbers were normally generated with a D_s-value of $5.10^{-6}cm^2.min^{-1}$. In the cases where there is a second number in the table cell, the one shown after the forward slash used a D_s-value of $100.10^{-6}cm^2.min^{-1}$ in the calculation. Thus, for example, the model predicted that the exhaustion value after 3 minutes under high substantivity conditions is 2% lower when δ is 1μm and D_s is $5.10^{-6}cm^2.min^{-1}$. That value drops to zero when the D_s-value is equal to 100.10^{-6} $cm^2.min^{-1}$.

---

[8] $t_{1/2}$ is the half-time of dyeing, i.e. the time after which 50% of equilibrium exhaustion is attained.

Time /[min]	Dyeing condition	δ = 1 μm	δ = 4 μm	δ = 16 μm	δ = 64 μm	δ = 256 μm
3	High Substantivity	2 / 0	6 / 0	13 / 1	23 / 4	32 / 11
	Medium Substantivity	1	2	6	12	18
	Low Substantivity	0 / 0	1 / 0	2 / 0	5 / 1	9 / 2
5	High Substantivity	1 / 0	3 / 0	8 / 1	15 / 3	23 / 7
	Medium Substantivity	0	2	5	11	17
	Low Substantivity	0 / 0	1 / 0	2 / 0	5 / 1	9 / 2
15	High Substantivity	0 / 0	0 / 0	0 / 0	1 / 0	1 / 0
	Medium Substantivity	0	1	2	5	8
	Low Substantivity	0 / 0	0 / 0	1 / 0	3 / 0	6 / 1
30	High Substantivity	0	0	0	0	0
	Medium Substantivity	0	0	1	2	4
	Low Substantivity	0 / 0	0 / 0	1 / 0	2 / 0	4 / 1
45	High Substantivity	0	0	0	0	0
	Medium Substantivity	0	0	1	1	2
	Low Substantivity	0 / 0	0 / 0	1 / 0	2 / 0	3 / 1

Table 9.7: Predicted Difference in Exhaustion values in % for different δ compared to δ = 0

Table 9.8 shows the influence of the boundary layer thickness on the half-times of dyeing.

Dyeing Condition	δ = 1 μm	δ = 4 μm	δ = 16 μm	δ = 64 μm	δ = 256 μm
High Substantivity	1.4	1.6	2.0	2.7	3.4
Medium Substantivity	4.5	5.0	5.5	7.0	8.5
Low Substantivity	22.0	22.0	23.0	25.5	28.0

Table 9.8: Calculated Half-times of Dyeing [min] for different δ, $D_s = 5.10^{-6}$ $cm^2.min^{-1}$

The data in tables 9.7 and 9.8 confirmed that deviations from the ideal flow condition of low boundary layer thickness can most easily be detected under high substantivity conditions during the first several minutes of the dyeing process. If the substantivity was reduced, the peak deviation was smaller but persisted for a longer period of time. The data also showed that under industry-typical, low substantivity conditions the boundary layer started to exercise a detectable influence only for values of higher than 16μm. This is in good agreement with the results of previous researchers (McGregor 1965:400). If the high estimate of the diffusion coefficient in water was used, then even a boundary layer thickness of 256μm did not significantly alter the exhaustion speed under low substantivity conditions.

The fluid velocity that corresponds to a particular boundary layer thickness can be estimated from the model of a plane sheet immersed in a flow parallel to its axis. Under this assumption, it can be written (McGregor 1965:400):

$$\upsilon_0 = 1.47^2 \left(\frac{D_s}{\nu} \right)^{\frac{2}{3}} \frac{\nu\lambda}{\delta^2} \qquad (9.34)$$

Table 9.9 shows the minimum fluid velocity for which the boundary layer has no significant influence on the uptake rate, $v_{0,crit}$ for different D_s-values and dyeing conditions. The calculations used a kinematic viscosity-value of $4.4.10^{-3}cm^2.s^{-1}$, the value for water at 65°C (Weast, 1989 F-38). The two parameters λ and D_s were not known but were estimated. A plausible value for λ in the case of the pilot-scale machine could be 5cm, i.e. the effective length of the jet nozzle. For D_s, the same estimates were used as above, i.e. $5.10^{-6}cm^2.min^{-1}$ as the lower estimate and $100.10^{-6}cm^2.min^{-1}$ as the higher estimate. The boundary layer thickness used in the calculation was the critical value, δ_{crit}, such that beyond this value the exhaustion speed started to be significantly influenced. The value varied therefore depending on the diffusion coefficient and on the substantivity (table 9.7). Thus a value of δ_{crit} equal to 30μm was used in conjunction with a low diffusion coefficient estimate under low substantivity dyeing conditions.

Dyeing Condition	D_s/[$cm^2.min^{-1}$]	δ_{crit} /[μm]	$v_{0,crit}$ /[$m.min^{-1}$]
Low Substantivity	high (100.10^{-6})	300	0.15
High Substantivity		60	4
Low Substantivity	Low (5.10^{-6})	30	3
High Substantivity		4	130

Table 9.9: Critical Fluid Velocities

According to table 9.9, the critical main stream fluid velocity under conditions of a low diffusion coefficient and low substantivity, a worst case estimate for bulk industrial conditions, is around $3m.min^{-1}$. That implies that for fluid velocities of more than around $3m.min^{-1}$, the boundary layer effect on the exhaustion speed on the pilot-scale dyeing machine should be negligible. This is in fairly good agreement with experimental evidence using Direct Blue 1, when it was concluded that "good stirring" conditions in the dyebath correspond to an apparent boundary layer thickness of 30μm and a fluid velocity parallel to the fibre surface of around $6m.min^{-1}$ (McGregor 1965:400). Under high substantivity conditions a fluid velocity of up to $130m.min^{-1}$ could be required in order to eliminate an influence of the boundary layer on the exhaustion speed. On bulk machines under low affinity conditions, assuming a low diffusion coefficient in water and a value for λ of 50cm, the critical flow rate would be $30m.min^{-1}$, dropping to $1.5m.min^{-1}$ for a high D_s-value.

The calculations showed that the flow rates in the nozzle of pilot-scale and production jet are generally high enough to eliminate any influence of the boundary layer. The overall exhaustion speed in a jet dyeing machine is, however, also influenced by the fabric-liquor interchange in the storage chamber, where flow rates are much lower. The average fluid velocity in the storage area of a production machine is estimated to be around $1.5m.min^{-1}$ (Kaup 2001). In certain areas the velocity might even be lower because access of the dyeliquor is impaired by densely piled fabric. Depending on the value of λ, the influence of the boundary layer might in this case therefore become significant. These locations of reduced dye uptake are unlikely to influence noticeably the overall exhaustion speed under controlled sorption conditions, as the experiments of chapter seven showed, but they provide a qualitative explanation for the creation of unlevelness.

The experimental data of chapter seven that used low flow rates provide an opportunity to estimate δ as a function of the flow rate. To this end, the adsorption-diffusion model,

extended to include boundary layer effects, was used to determine the δ-values that yielded the best match of the experimental results presented in figure 7.12 (figure 9.15).

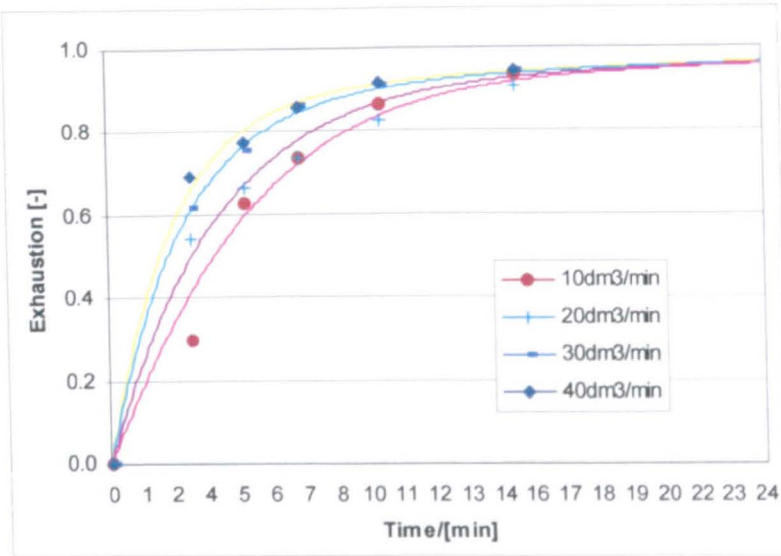

Figure 9.15: Modelling the Boundary Layer Thickness, δ

The calculations assumed that no boundary layer existed at a flow rate of $40dm^3.min^{-1}$. The experimental data for 30, 20 and $10dm^3.min^{-1}$ were fitted with δ-values of 0.008, 0.06 and 0.22cm (80, 600 and 2200μm) and D_s equal to $100.10^{-6}cm^2.min^{-1}$.

The absolute value of δ is of little significance as the influence of the boundary layer also depends on the fibre radius, a, the adsorption constant, k_a, the diffusion coefficient in water, D_s, and the liquor ratio, LR. It is more useful to utilise the before mentioned composite and dimensionless parameter L.

$$L = \frac{\delta a k_a}{4 D_s LR}\left([D]_{sat} - [D]_{fs}\right) \qquad (9.35)$$

The value of k_a increases and that of $([D]_{sat} - [D]_{fs})$ decreases during the exhaustion, as the dyebath concentration diminishes. Therefore L is not a constant during the dyeing process and was averaged for the present calculation over the first 24 minutes, the period of time after which the influence of the boundary layer could no longer be detected. The results for δ and for L, shown in figure 9.16, were qualitatively very similar but the L-value increased slightly more than δ at low flow rates because the product $k_a([D]_{sat} - [D]_{fs})$ was bigger due to the smaller value of $[D]_{fs}$.

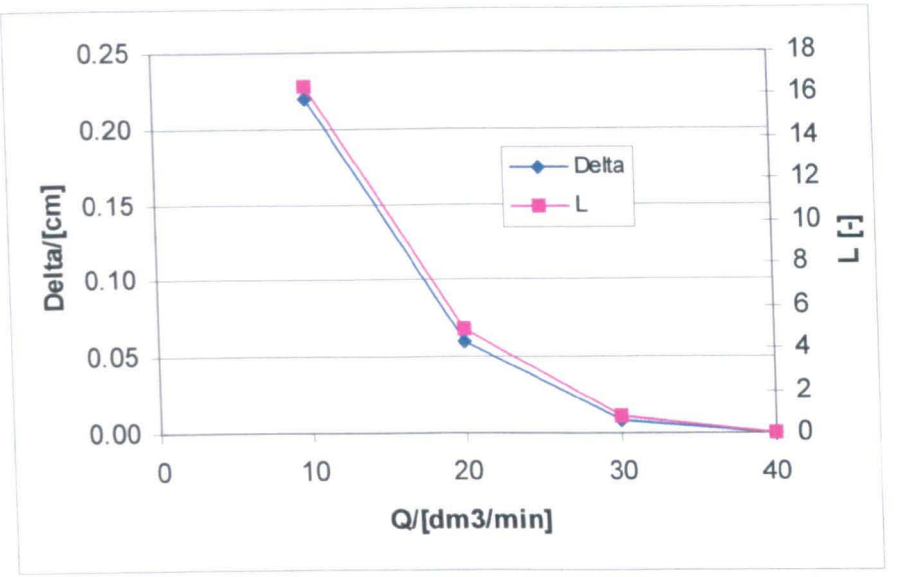

Figure 9.16: δ and L as a Function of the Dyebath Flow Rate, Q

It is noteworthy that δ appeared to increase exponentially as the flow rate was reduced, which is in contrast to the situation of a plane sheet immersed in a flow parallel to its axis when the boundary layer thickness is proportional to the inverse of the square root of the flow rate.

9.6 Experimental Adsorption Constant versus Model estimated Constant

The values for the adsorption and desorption constants in the model were, as mentioned before, adjusted so as to give the best fit between the model predictions and experimental data. Since the underlying Langmuir equation aimed at reproducing the true physico-chemical situation, the values of the constants can be compared with those determined directly from experiments. This section compares the adsorption constant, k_a, as required by the adsorption-diffusion model with the adsorption constant measured during the first several seconds of the exhaustion process.

From the model of dye adsorption at the surface layer, it follows that during the first several seconds of the dyeing process, when there is no or almost no dye on the fibre, the dye uptake rate can be approximated by:

$$\frac{d[D]_{fs}}{dt} = k_a[D]_s[D]_{sat} \tag{9.36}$$

Since $d[D]_{fs}.dt^{-1}$ is the dye uptake rate which can be derived for example from dyebath absorbance analysis, measurement of the change of $[D]_s$ early in the exhaustion phase makes it thus possible to determine $k_a.[D]_{sat}$ experimentally. Using the experimental set-up described in chapter 9.1, the $[D]_s$-values without salt were averaged over the first 90

seconds while the values with 15g.dm^{-3} salt were averaged over a period of only 30 seconds, as in this case the exhaustion speed dropped quickly (table 9.10). The table also shows $k_a.[D]_{sat}$ as predicted by the adsorption-diffusion model with forward approximation 30 seconds after the start of dyeing. Not all of the experimental conditions were predicted by the adsorption-diffusion model, so that some fields in the fourth column do not contain values.

Temperature /[°C]	**Salt Conc. /[g.dm^{-3}]**	**Measured** $k_a.[D]_{sat}$ **/[dm^3.min^{-1}.kg surface^{-1}]**	**Ad-Diff Model** $k_a.[D]_{sat}$ **/[dm^3.min^{-1}.kg surface^{-1}]**
40	0	0.7	7
50	0	0.7	-
65	0	0.7	6
80	0	0.5	-
90	0	0.4	4
40	15	20	90
50	15	14	-
65	15	20	100
80	15	20	-
90	15	30	80

Table 9.10: Comparison of Adsorption Constants

It is evident that the constant required by the model was considerably higher than that obtained experimentally. The reason was at least partly that the process in the glass vessel was partially liquid diffusion limited, i.e. the dye supply at the fibre surface was less than in the rotating-beaker machine or on the pilot-scale jet vessel. This was confirmed by a comparison of the exhaustion values after 3 and 5 minutes of the glass vessel and the rotating-beaker-type machine (table 9.11).

Temperature [°C], Salt Conc./[g.dm^{-3}]	Time /[min]	Exhaustion Rotating-Beaker Machine [%]	Exhaustion Reaction Vessel [%]
65, 0	3	6.1	1.4
	5	6.9	2.1
65, 15	3	44	39
	5	56	49

Table 9.11: Influence of Dyeing System on Exhaustion Values

If it is assumed that $[D]_{sat}$ was independent of temperature, then the data in table 9.10 suggest that the adsorption constant decreased with temperature when no salt was present. In the presence of electrolyte, the adsorption-diffusion model yielded an essentially invariable adsorption constant. The increase in the experimentally determined adsorption constant at 90°C in the presence of electrolyte might not be adsorption related but due to the onset of dye diffusion, which becomes more significant at higher temperatures and when there is a steep concentration gradient within the fibre.

To examine the question whether a change of k_a with temperature would be expected, equation 9.37 may be analysed:

$$\frac{k_a}{k_d} = \frac{[D]_{fs,eq}}{[D]_s\left([D]_{sat} - [D]_{fs,eq}\right)} \tag{9.37}$$

When the temperature increases the equilibrium molality at the fibre surface, $[D]_{fs,eq}$, decreases due to the exothermic nature of the sorption process. Assuming that $[D]_{sat}$ is independent of temperature, $k_a.k_d^{-1}$ becomes smaller as $[D]_{fs,eq}$ drops. This could mean that either k_a becomes smaller or that k_d increases or that a combination of both factors is at work. The experimental data can therefore be interpreted satisfactorily with the assumption of Langmuir kinetics.

As a whole, the results indicate that the values for the adsorption constant used in the adsorption-diffusion model reflect well the qualitative changes in the values obtained directly from experiments at different temperatures and salt concentrations but they also show that there is no quantitative agreement. The Langmuir model is thus a useful

contribution to explaining the dye uptake rate, even though it does not quantitatively represent the physico-chemical reality.

9.7 References

1. Crank J, The Mathematics of Diffusion, 2nd Edition (Clarendon Press: London 1975)
2. Grover E B, Hamby D S, Handbook of Textile Testing and Quality Control (New York 1960)
3. Inglesby M K, Zeronian S H, Dyes and Pigments 50 (2001) 3
4. Jones F in Johnson A (Ed.): The Theory of Coloration of Textiles, 2nd edition (Bradford: SDC 1989) 373
5. Kaup S, personnel communication, July 2001
6. Lapidus L, Pinder G F, Numerical Solution of Partial Differential Equations in Science and Engineering (New York: Wiley 1982)
7. McGregor R, Peters R H, J.S.D.C. 71 (1965) 393
8. Morton W E, Hearle J W S, Physical Properties of Textile Fibres (Manchester: Textile Institute 1986)
9. Peters R H, Textile Chemistry, Vol. III, The Physical Chemistry of Dyeing (Amsterdam: Elsevier 1975)
10. Reddy M, Jasper W J, McGregor R, Lee G, Text. Res. J. 67 (1997) 109
11. Sandoz, Technical Information, Indosol SF (1986)
12. Snyder W, Berkstresser G, Smith B, Beck K, McGregor R, Jasper W, Text. Res. J. 67 (1997) 571
13. Vickerstaff T, The Physical Chemistry of Dyeing, 2nd Edition (London: Oliver and Boyd 1954)
14. Vosoughi M, PhD Thesis, Heriott-Watt University, Edinburgh (1993)
15. Weast R C, Astle M J, Beyer W H, Handbook of Chemistry and Physics (CRC: Boca Raton 1988)
16. Zollinger H, Colour Chemistry, 2nd edition (Weinheim: VCH 1991)

10 Development of a Statistical Model for Unlevelness

The literature review indicated that many factors could influence the degree of dye unlevelness. It also became clear that building a mathematical model to describe the dye distribution on the fabric rope as a function of time and location would be very complex because the rope changes its shape during one revolution and liquor flow conditions vary considerably depending on the location within the vessel. The decision was made to break down the influences on unlevelness into key factors and analyse these aspects individually by a series of experiments. These factors were:

1) the influence of **fabric and liquor circulation rate**: These experiments were interpreted using the contact-concept.

2) the influence of **dye amount**: The literature review had given some indication that higher dye amounts have a tendency to result in lower unlevelness when all other factor remained equal.

3) the influence of certain **non-ionic surfactants**: It was to be examined if the presence of surfactants reduced unlevelness at a given dye uptake rate. Only those types of surfactant were selected that had no negative influence on equilibrium sorption for reasons of reproducibility and environmental performance.

4) the influence of the **shape of the exhaustion profile**: The performance of a linear exhaustion profile was to be compared to various other profiles, notably to a profile resulting from a linear salt dosing gradient.

5) control by **dye dosing** instead of electrolyte dosing: Dye dosing may be required in the case of a high First Strike of the dye, in line with the principles of controlled sorption. The intention here was two-fold. First, one of the axioms of controlled sorption was to be tested, namely that it is better to control the substantivity of the dye for the fibre by electrolyte dosing than it is to control the supply of dye by dye dosing. Second, it would greatly enhance the possibilities for dyebath recycling, which usually leads to high electrolyte concentrations, if a method were found to control dye unlevelness by dye dosing into a dyebath already containing high amounts of salt.

The overriding aim of the investigations described in this chapter was to identify and describe the major influencing factors for unlevelness. Target values for the important parameters would be derived that could be used by a control algorithm in order to guide the dyeing process such that the user-defined degree of unlevelness would be achieved in the shortest possible time.

10.1 Experimental

The set-up of the experiments is described below according to the five factors for investigation stated in the introduction of this chapter. Some of the features shared by all tests are described first. The tests had in common a jet nozzle diameter of 55mm and that the dye exhaustion was determined indirectly via analysis of the dyebath as described in chapter six. The fabric mass was, as usual, 136g.m^{-1} fabric and the jet vessel was loaded with on average 850g, or 6.25m, of fabric. The liquor ratio was 8:1. Small dye losses during the transfer of dye from the addition tanks to the main vessel were taken into account as explained in chapter seven. At the end of the dyeing process, the dyebath was immediately dropped and the fabric was rinsed with cold water with the drain valve open for five minutes while the fabric circulated. This process step was automated and since the cold water flowed into the vessel from the preparation tank which was always pre-filled to the same level, a high degree of reproducibility was obtained. At the end of the rinsing cycle, the fabric was sequeezed manually and cut into three strips of approximately the same width to ensure that the fabric could be dried in a single layer in the pad-dry unit depicted below (figure 10.1). Before cutting, the strips were marked appropriately in order to ensure that like ends could be identified later on. The strips were then manually batched onto a roll one after the other, sewn together at the end, in random sequence. This roll was used to feed a MATHIS pad-dry unit with the set-up shown in figure 10.1.

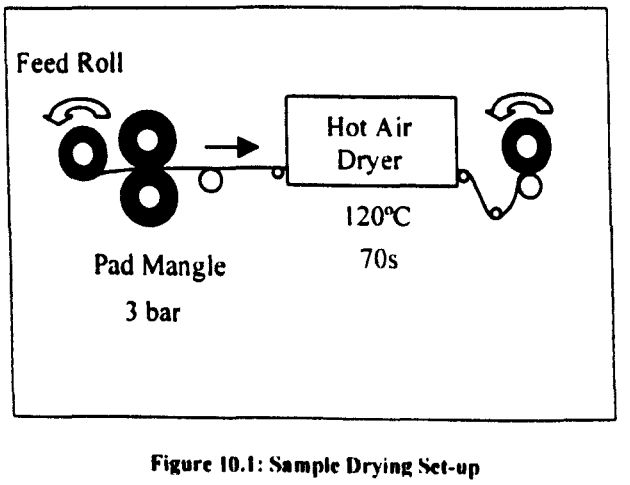

Figure 10.1: Sample Drying Set-up

A rubber coated pad mangle was used to remove excess liquor before entering the dryer. At the dryer's exit, the fabric was dry to the touch. The tension during the drying process stretched the fabric by between 7 and 8%. Drying the fabric took a total time of around 30 minutes and the fabric was always dried immediately following the end of the dyeing/rinsing process in order to minimise dye migration due to uncontrolled pre-drying of the fabric.

10.1.1 Evaluation of Unlevelness

The basis for the evaluation of unlevelness was a statistical interpretation of the variation in the dye amount at different locations on the fabric, which were determined by reflectance measurements according to the method outlined in chapter six. On each of the three fabric strips obtained per dyeing, seven locations were measured, each one metre apart from the other so that values were obtained for a total of 21 locations per sample (figure 10.2).

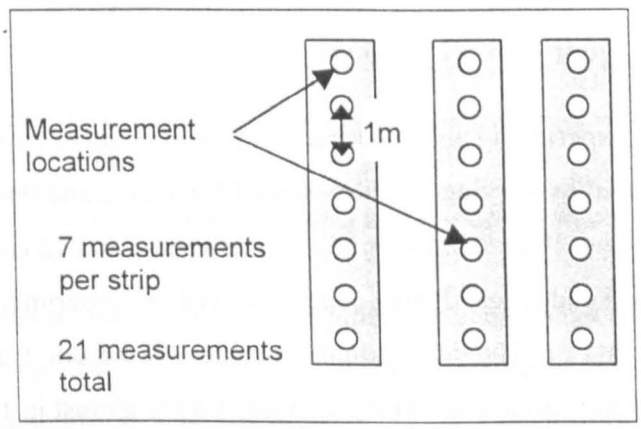

Figure 10.2: Pattern of Positions for Reflectance Measurements for Unlevelness Evaluation

At each location, ten measurements were made on the folded fabric because initial tests had shown that this number was needed in order to obtain an average, constant value independent of the number of measurements. The reflectance values were converted into colour strength with the DATACOLOR software, using the wavelength range from 400 to 700nm as basis. The colour strength was corrected for the absorbance of the mock-dyed cotton substrate and used the average colour strength of the first strip as reference strength, which was arbitrarily set equal to 100%. The reference strength was calculated based upon a total of seventy measurements using the locations shown in figure 10.2. Thus, a colour strength of for example 96.5% indicated that the particular location had 96.5% of the colour strength of the averaged first strip. Since colour strength differences were mostly less than +/- 15%, a linear relationship between colour strength and dye amount on the fabric was

assumed. In other words, to continue the example, it was assumed that the location had 3.5% less dye on the fabric than the strip one average.

For a quantitative comparison between samples, the variation coefficient, expressed in per cent, of the 21 measurements was used. The variation coefficient is defined as the standard deviation of the sample values divided by their average. A higher variation coefficient therefore indicated a higher degree of unlevelness.

Three repeat measurements of the variation coefficient of the colour strength of the same strip of fabric on three different days resulted in a maximum (absolute) difference in the variation coefficient of 0.3%. Several repeat dyeings under conditions thought to be identical showed that the maximum (absolute) difference in the variation coefficient was around 3%. This considerable experimental error calls for caution when comparing the results of individual dyeings.

10.2 Description of Test Series

10.2.1 Fabric and Liquor Flow Conditions

During the first set of experiments the influence of fabric and liquor flow conditions on unlevelness was analysed by varying the fabric speed between 2 and 9m.min^{-1} and the dyebath flow rate between 10 and 80dm^3.min^{-1}, i.e. between 1 and 12 contacts per minute (c.min^{-1}), under otherwise identical dyeing conditions. All the experiments took thus place at 65°C with 0.45% (omf) and 10g.dm^{-3} sodium chloride. All the salt was added to the dyeliquor at the beginning and dye addition occurred at 65°C almost instantaneously by using the pressure tank. Time started counting from the moment when the dye was added and liquor samples were taken after 3, 5, 15, 30, 45, 60, 90 and 120 minutes.

10.2.2 Dye Amount

The second test series analysed the influence of the dye amount on unlevelness. In order to take into account industrial requirements for high process reproducibility, it was decided that equilibrium adsorption should be no less than 97.5% at a temperature of 80°C. At temperatures lower than 80°C higher equilibrium exhaustion values would have been possible but the diffusion speed became so low that sufficient fibre penetration was only achieved after long dyeing times that would be uneconomical in industry. 80°C was therefore regarded as the best compromise between the aims of high equilibrium exhaustion and short dyeing times. This requirement (97.5% exhaustion at 80°C) and the observation that 20g.dm^{-3} constituted the maximum concentration of common salt at room temperature

before the dye started to precipitate, even at moderate dye concentrations, limited the maximum dye amount. Screening tests showed that the highest dye amount which still achieved 97.5% exhaustion at 20g.dm^{-3} was 0.4% (omf). The other dye amounts chosen were 0.05, 0.1, 0.2 and 0.3% (omf). For each dye amount, the final salt concentration was adjusted so that the equilibrium uptake would also be 97.5% because the degree of exhaustion was to be excluded as a parameter in the tests. Experiments on a rotating beaker machine at 80°C gave the following results:

Dye Amount [% omf]	**Common Salt Concentration for 97.5% Exhaustion/[g.dm^{-3}]**
0.05	0.2 (1)
0.1	4
0.2	14
0.3	17
0.4	20

Table 10.1: Salt Concentrations for the second Test Series

For 0.05% dye, the concentration used in the experiments on the jet dyeing machine was actually 1g.dm^{-3} instead of 0.2g.dm^{-3} because the latter concentration was too low to control the exhaustion speed by electrolyte dosing. Thus, the final exhaustion at the end of the process when using 1g.dm^{-3} was 99% instead of 97.5% but the uptake rate was identical to those used for the other four dye amounts.

The temperature was held constant at 80°C. The choice of isothermal conditions had two reasons. First, the salt dosing gradient and not the temperature gradient was the main parameter controlling the exhaustion speed. Second, the long time constant of the pilot-scale machine's heating system meant that the temperature could be raised at the most by about 30°C over a period of nine minutes. A complete exhaustion in nine minutes, i.e. around 11% per minute, was necessary in order to achieve uptake rates in the critical range of between 1 and 2% per theoretical contact, i.e. without considering the influence of the machine design. Thus, for the particular conditions of the pilot-scale machine, it appeared to be best to vary only the salt dosing profile and the dye addition time. For each of the five dye amounts, these two parameters were therefore adjusted to give a linear exhaustion with time over a period of nine minutes (figure 10.3).

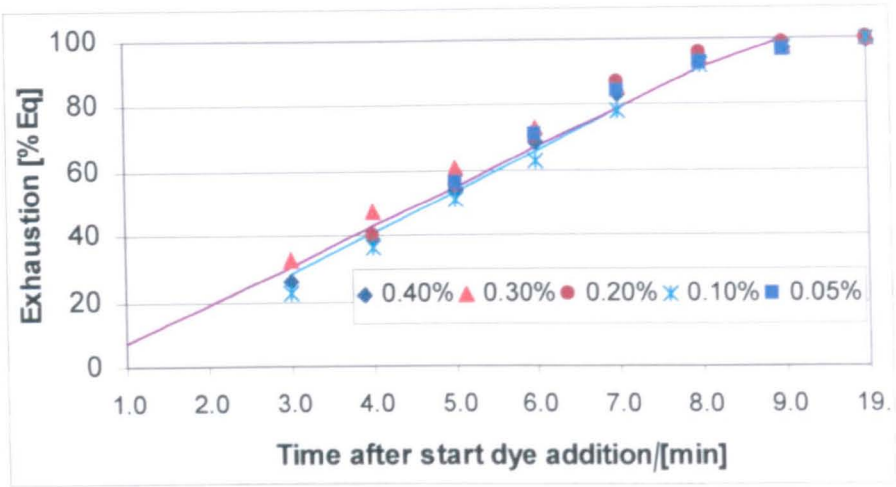

Figure 10.3: Exhaustion Profiles obtained when analysing the Influence of Dye Amount on Unlevelness

The salt dosing profile was exponential in nature but varied for each dye amount. The dye addition time was selected such that the exhaustion at the end of the dye addition period corresponded to an exhaustion rate of around 11% per minute. Since the relative dyebath exhaustion (as per cent of the total dye amount) at the end of the dye addition decreased with increase in the dye amount, the addition time also decreased with increase in the dye amount (table 10.2). Electrolyte dosing commenced after the end of the dye addition.

Dye Amount [% omf]	Exhaustion at End of Dye Addition [%]	Dye Addition Time/[s]
0.05	42	230
0.1	25	135
0.2	22	120
0.3	14	75
0.4	9	50

Table 10.2: Dye Addition Times for analysing the Influence of Dye Amount on Unlevelness

All in all, the result was, as shown in figure 10.3, an exhaustion profile independent of the dye amount[9] so that any significant difference in unlevelness could not have been due to variations in the exhaustion speed or to the exhaustion at the end of the dyeing cycle.

[9] The dye uptake rate during the dye dosing time was not measured and thus may have differed for each of the dyeings. Since the dye exhaustion at the end of the dye dosing

After the end of the salt dosing period, the dyeing was continued for another ten minutes before the dyebath was dropped and the fabric rinsed in the usual way (figure 10.4). The holding time was limited to ten minutes only, in order to reduce any contribution of dye migration to producing a lower unlevelness.

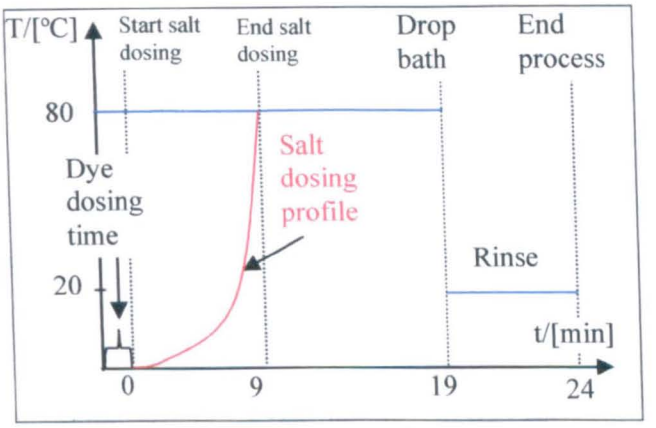

Figure 10.4: Schematic Process Profile second Test Series

For each dye amount, the identical salt and dye dosing profiles were used at three different fabric speeds and dyebath flow rates:

1) Fabric speed 2m.min^{-1} and dyebath flow rate 40dm^3.min^{-1} (ca. 6c.min^{-1})
2) Fabric speed 4m.min^{-1} and dyebath flow rate 50dm^3.min^{-1} (ca. 8c.min^{-1})
3) Fabric speed 8m.min^{-1} and dyebath flow rate 60dm^3.min^{-1} (ca. 10c.min^{-1})

The dye uptake rate varied therefore between around 1 and 2% per contact.

10.2.3 Surfactants

The third series of experiments analysed the influence of non-ionic surfactants in the dyeliquor on the unlevelness. The initial selection included four commercial products all having polyglycolethers as their main constituent. They were SANDOGEN EDP and EKALINE F from CLARIANT as well as the ALGEGAL FFA and CIBAFLOW JET from CIBA SPECIALTY CHEMICALS. CIBAFLOW JET was eliminated after initial tests when it was found that it caused turbidity in the dyeliquor which made accurate measurements of the dye amount in the liquid impossible. Then equilibrium dyeings (80°C, 0.2% dye, 14g.dm^{-3} common salt) with the three remaining surfactants were conducted and

---

phase was less than or equal to 25% for all dye amounts except 0.05%, it is thought that this difference did not significantly influence the final levelness of the dyeings.

it was confirmed that none of them influenced the final exhaustion when the concentration of EKALINE F and SANDOGEN EDP was 1g.dm^{-3} and that of ALBEGAL FFA was 0.6g.dm^{-3}. When applied on the pilot-scale jet vessel EKALINE F lead to excessive foam development and tests with this product were therefore also abandoned. The two remaining products, SANDOGEN EDP and ALBEGAL FFA, did not influence the exhaustion kinetics compared to the process when no surfactant was used and the degree of foam development was similar, too, if not less. To evaluate their influence on unlevelness, the same process profile as in the second test series was employed. The dye was thus exhausted linearly over nine minutes by dosing electrolyte at a constant temperature of 80°C at three different dyebath and fabric circulation rates, equating to around 6, 8 and 10c.min^{-1}. The concentration of SANDOGEN EDP was 1g.dm^{-3}, the concentration of ALBEGAL FFA was 0.6g.dm^{-3}. Both concentrations fell into the range recommended for application by the manufacturers which were 0.5 to 1g.dm^{-3} for SANDOGEN EDP and 0.2 to 2g.dm^{-3} in the case of ALBEGAL FFA (Ciba 1997, Clariant 1999). The resulting unlevelness was compared to a fabric processed in an identical manner with the only exception that no surfactant was added. Since neither dye uptake rate nor equilibrium exhaustion were affected by the surfactants, any difference in the unlevelness would have been attributable to the effect of the surfactants.

10.2.4 Shape of Exhaustion Profile

The fourth test series analysed the influence of the shape of the exhaustion profile on unlevelness. Three different control strategies were pursued:

1) Controlling the salt dosing gradient to give a linear dye exhaustion per contact
2) Linear salt dosing profile with time
3) Controlling the salt dosing gradient to give a linear change of the dye fibre surface molality per contact ($\Delta[D]_{fs}.contact^{-1}$ = constant).

The experiments of the first strategy corresponded to those described in the second test series, i.e. five dye amounts (0.05, 0.1, 0.2, 0.3 and 0.4%) were used at three different exhaustion speeds per contact. For the second control strategy, the same five dye amounts were applied and the electrolyte was dosed linearly for a duration of five minutes. The starting temperature was 30°C when dye addition occurred gradually over 3.5 minutes (0.2 to 0.4% dye) or 7 minutes (0.05 to 0.1% dye). At the end of the dye addition, the salt dosing started and the temperature was raised as fast as possible to the final temperature of 80°C.

The high time constant of the heating system meant that at the end of the salt dosing, the temperature had reached only around 45°C (figure 10.5). Once 80°C was reached after a further 7 minutes, (i.e. 12 minutes total since start of salt dosing), the temperature was kept at that level for 10 minutes before the dyebath was dropped and the fabric was rinsed in the usual way. These tests were conducted at 2m.min^{-1} fabric speed and 40dm^3.min^{-1} dyebath flow rate.

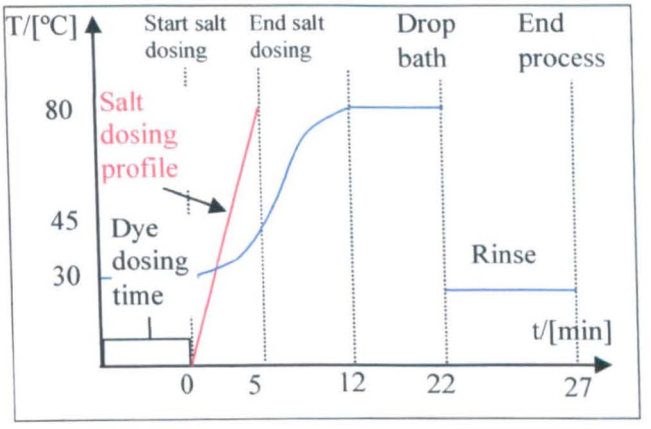

Figure 10.5: Schematic Process Profile second fourth Test Series

The third control algorithm was aimed at achieving a process profile that would yield a linear change of the dye fibre surface molality, $[D]_{fs}$. The algorithm was derived by assuming that $[D]_{fs}$ was in equilibrium with the dyebath concentration, $[D]_s$, at each moment during the process. Details of the methods used to calculate an appropriate dosing profile are explained below in the subsection of 'Results and Discussion'. Three experiments were made with 0.3% dye (omf) at a constant temperature of 80°C, a fabric speed of 2m.min^{-1} and a dyebath flow rate of 40dm^3.min^{-1}. The steps in the process profile were in principle identical to those shown in figure 10.4, the only difference being that the salt dosing profile was not exponential with time.

10.2.5 Dye Dosing

In the fifth series of experiment the entire dye amount was dosed in a controlled way into the dyebath which already contained the final common salt concentration (14g.dm^{-3}) and which had reached the final temperature (isothermal conditions, 80°C). The dye dosing settings are summarised in table 10.3. After the end of the dye addition, the process was continued for another ten minutes before the dyebath was dropped and the fabric was rinsed in the usual way.

Parameter	Exp. #1	Exp. #2	Exp. #3	Exp. #4	Exp. #5
Temperature/[°C]	65	80	80	80	80
Dye Amount [% omf]	0.45	0.20	0.20	0.20	0.20
[NaCl]/[g.dm^{-3}]	10	14	14	14	14
Fabric Speed/[m.min^{-1}]	2	6	6	6	8
Dyebath Flow Rate /[dm^3.min^{-1}]	40	40	40	40	60
Dye Addition Time/[s]	20	20	60	180	480
Dye Addition Time /[fabric contacts]	0.1	0.3	1.0	3.0	11.0
Holding Time/[min]	110	10	10	10	10

Table 10.3: Dye Dosing Settings

10.2.6 Minimum Unlevelness

In addition to the five test series, two isothermal dyeings were made in order to establish the minimum dye unlevelness that could be achieved on the pilot-scale machine for C. I. DY 162 using a dye amount 0.4% (omf). Neither experiment included any common salt and the dye was added during around 50 seconds at 60°C in the first and at 80°C in the second experiment. The dyeing was carried out for two hours, after which the dyebath was dropped and the fabric was rinsed by the standard method. Since no salt was added, the exhaustion speed was very low and 40% or more of the dye remained in the dyebath at the end of the two hours, both circumstances favouring low unlevelness (figure 10.6). For a comparison, the unlevelness of two air-dried 7g fabric samples dyed to equilibrium at 90°C with 0.2% dye and 0g.dm^{-3} sodium chloride on a rotating beaker machine was also measured. Their variation coefficient of colour strength was calculated based upon ten single measurements at different locations.

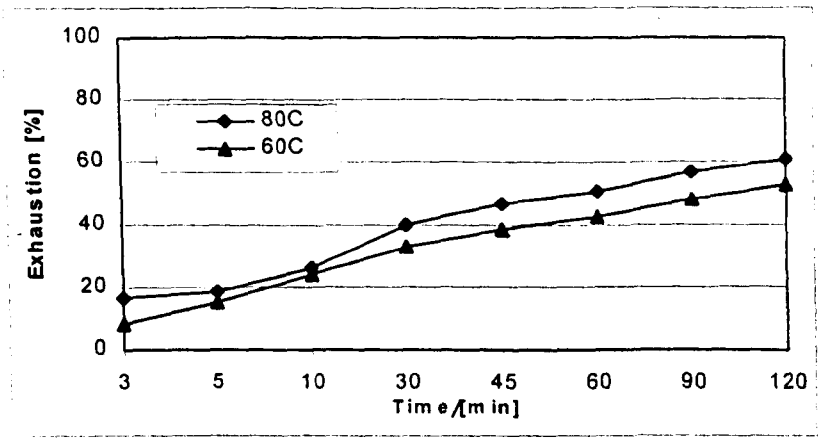

Figure 10.6: Exhaustion Profile of Minimum Unlevelness Tests

10.3 Results and Discussion

10.3.1 Minimum Unlevelness

The results of the experiments described in section 10.2.6 showed that the lower limit of unlevelness achievable on the jet vessel, expressed as the variation coefficient (v.c.) of the colour strength in per cent, appeared to be around 3% (table 10.4).

Experiment	Pilot-scale 60°C	Pilot-scale 80°C	Beaker #1	Beaker #2
Unlevelness [%]	3.2	2.4	3.7	5.5

Table 10.4: Minimum Unlevelness

The fabric samples of the rotating beaker machine showed, surprisingly, a higher unlevelness than the jet machine samples. This could be due to either dye migration during the drying period which was extended compared to the samples of the pilot-scale machine or dye photochromaticity. The latter effect could play a role because multiple measurements on a small sample result in overlapping measurement areas and with each measurement, the dye's extinction coefficient is reduced (table 10.5).

	Reference	1min later	2min later	15min later	25min later	40min later	70min later
Colour Strength [%]	100.0	99.1	98.3	97. 6	97.1	96.6	97.0

Table 10.5: Repeat Measurements of identical Location

This would also explain why the observed v.c. of the beaker samples was higher than expected based upon research papers cited in chapter one. Photochromatic effects occurred during measurements of the fabric rope from the pilot-scale machine, but since the effect takes place at each measurement location and as different locations far away from each other were compared, the effect would be expected to cancel out within the variation coefficient calculation.

Under the assumption of a Student "t" distribution of the measurement variation and taking into account that the v.c. was the result of 21 measurements, the 95%-confidence interval of the colour strength, CI_{95} is

$$CI = \pm 2.09 SE \tag{10.1}$$

where SE is the standard error (Nobbs 1999). Using the relationships between the standard deviation of the samples, s, v.c. and SE yields:

$$SE = \frac{s}{\sqrt{n}} = \frac{\bar{X} v.c.}{\sqrt{n}} = \frac{100 v.c.}{\sqrt{21}} \tag{10.2}$$

where $\overline{X}$ is the average colour strength in per cent.

Assuming a v.c. of 3% as the minimum obtainable on the pilot-scale machine (table 10.4), it follows that

$$CI_{95\%} = \pm 2.09 \frac{3}{\sqrt{21}} = \pm 1.4 . \tag{10.3}$$

The true value for the average colour strength of the fabric rope was with a 95% probability within +/- 1.4% of the averaged, measured value.

An estimate for the range in which 95% of the individual location colour strength values would fall can be obtained from a statistical calculation if it is assumed that the 21 colour

strength values follow a normal distribution around the average of 100% with a v.c. of 3%. The requirement for an estimate for the colour strength range can be written as:

$$X_{low(P=0.025)} < \overline{X} < X_{high(P=0.975)} \qquad (10.4)$$

yielding

$$94\% < \overline{X} < 106\% \qquad .(10.5)$$

The same calculation carried out for a 99% range gave:

$$93\% < \overline{X} < 107\% \qquad (10.6)$$

It would therefore be estimated that 5% of all colour strength values fell more than +/- 6% from the average and only 1% within +/- 7% from the average colour strength. The calculation showed that the minimum unlevelness obtainable under practical conditions was under the limit of what would be perceivable to the human eye of around +/- 10%. While it was thus clear that the quality criteria of an acceptable unlevelness could be fulfilled, it also became evident that this limit lay only narrowly above what was technically feasible or, in fact, coincided with the technical limit if it was taken into account that the threshold for dye mixtures would probably be lower still.

10.3.2 Fabric and Liquor Circulation

The results of the experiments described in section 10.2.1 suggested that there was a linear relationship between the significant exhaustion speed per theoretical contact ($v_{sig(c)}$) and the resulting unlevelness when all other parameters stayed constant (figure 10.7). Since fabric speed and dyebath flow rate were changed independently from each other and entered the calculation of the number of theoretical contacts per minute with equal weight, it was also confirmed that both contributed to the same extent to unlevelness.

Three repeat experiments under supposedly identical conditions at 2% exhaustion per contact gave v.c.-values of 2.5, 3.6 and 5.0%, a variation high enough to underline that process evaluations based upon a single dyeing would imply considerable uncertainty, especially when close to the lower limit of unlevelness.

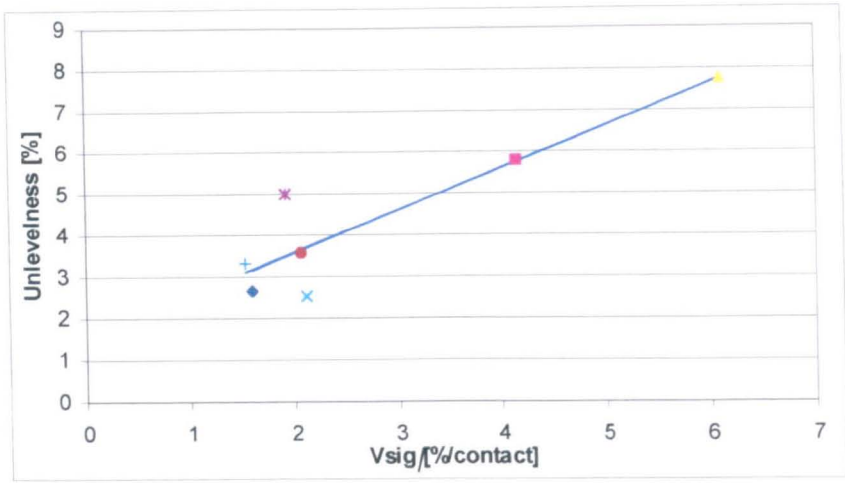

Figure 10.7: Correlation between v_{sig} and Unlevelness for varying Contact-values

10.3.3 Dye Amount

A comparison of the dyeings with different dye amounts (section 10.2.2) showed that the dye amount did not influence unlevelness (figure 10.8). The variation in $v_{sig(c)}$ between the dye amounts at any given fabric and dyebath circulation speed (e.g. between 1.45 and 1.65%.c^{-1} at 50dm^3.min^{-1} and 6m.min^{-1}) was caused by deviations from the targeted linear exhaustion profile. The major reason for these deviations was the fluctuation of the dye addition time at constant pump settings which was mainly due to the tendency of the gear pump's filter to become clogged with lint from the fibre or other impurities.

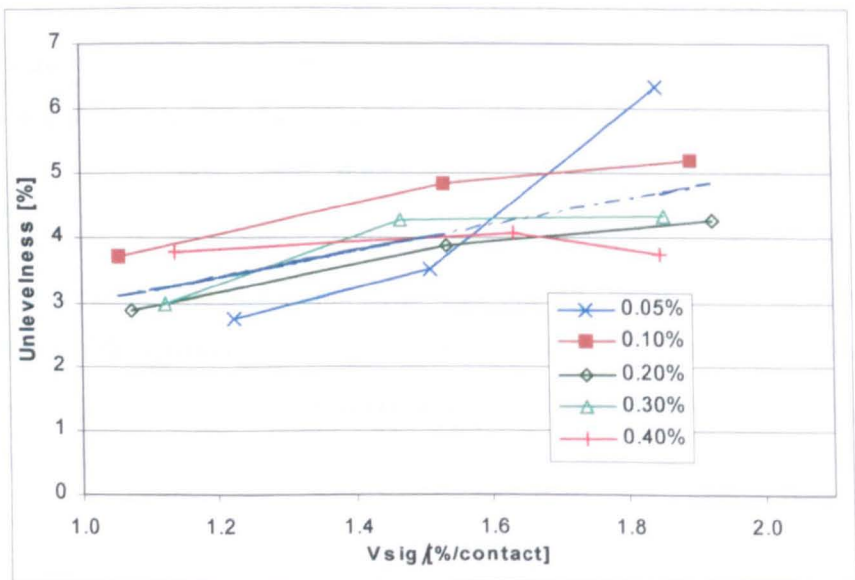

Figure 10.8: Influence of Dye Amount on Unlevelness

Assuming a critical unlevelness-value, u_{crit}, of 3% it was also noteworthy that the critical exhaustion speed per contact, v_{crit}, appeared to be different for data in figure 10.7 compared to figure 10.8. A linear regression of the data gave a lower v_{crit}-value for the all-in process than for the linear exhaustion process (table 10.6).

Process-Type	v_{crit}/[%.contact^{-1}]
All-in (figure 10.7)	1.4 ± 0.9 (std. error)
Linear exhaustion (figure 10.8)	1.0 ± 0.8 (std. error)

Table 10.6: Comparison of v_{crit}-values

This difference could possibly be explained by differences in the shape of the exhaustion curve. Compared to the linear-exhaustion process, the all-in process has a steep initial slope and a small slope towards the end of the process, a fact that could be favourable for reducing unlevelness as explained in chapter five. But it is also possible that the difference was due to the experimental set-up as the all-in process included a wider range of v_{sig}-values. It could be argued that the inclusion of high v_{sig}-values led to a steeper slope of the regression curve as the influence of experimental fluctuations became less pronounced. If for example only the unlevelness-values of dyeings with a v_{sig}-value between 1 and 2%.c^{-1} were taken into account, figure 10.7 suggests that v_{crit} would have been lower. Even if it were true that the all-in process performed better in the tests than the linear exhaustion process, it should not be inferred that all-in processes would be advantageous under industrial conditions. In the all-in process the dye exhausted to around 75% in only three minutes (figure 9.10), i.e. 25% per minute. In order to reduce the uptake rate to around 1.4% per contact, 18 contacts per minute are required, which is clearly impossible on a production machine without damaging the dyed goods. Under the high initial substantivity of the all-in process, it was only thanks to the high dyebath and fabric circulation frequencies possible on the pilot-scale jet that the unlevelness could be brought to an acceptable level.

10.3.4 Non-Ionic Surfactants

The results of the experiments described in section 10.2.3 suggested that the addition of non-ionic surfactants did not reduce unlevelness, if all other factors remained constant (figure 10.9). Although there are clearly differences in the unlevelness shown figure 10.9 it is thought that they were the result of (unwanted) variable experimental conditions. As was

pointed out in section 10.1, the experimental error could contribute to differences in the variation coefficient of the colour strength values from dyelot to dyelot of up to 3%.

Since equilibrium experiments with the two commercial products used in this investigation had shown no difference to the reference dyeing without surfactant, it may be concluded that the fibre surface molalities remained unaltered. This indicated that the effects of surfactants reported in literature and reviewed in chapter five could have been mainly due to their influence on the fibre surface molality. If the main mechanism of action were the effect on the surface molality, it would therefore be expected that ALBEGAL FFA and SANDOGEN EDP did not affect unlevelness. The two surfactants appeared to not influence the interfacial migration of the dyes on the fibre surface either. The use of the two surfactants therefore does not permit to increase the maximum permissible exhaustion rate per contact.

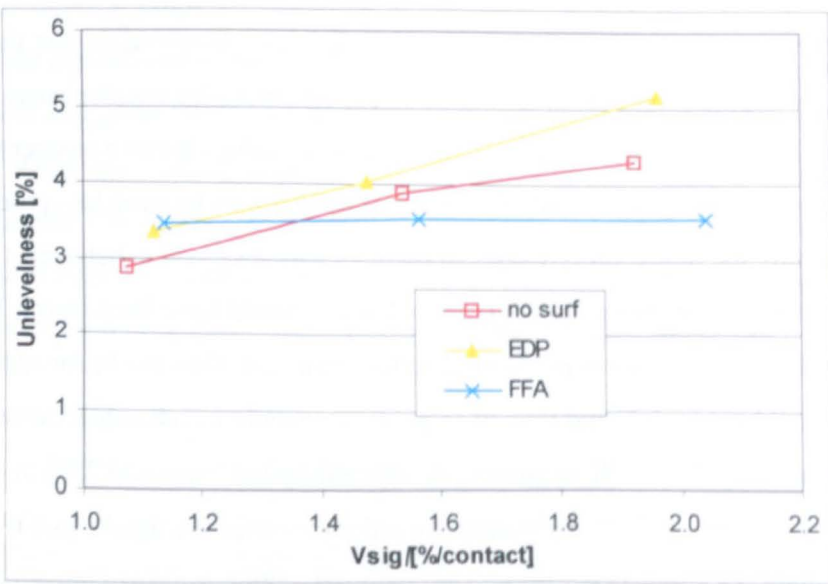

Figure 10.9: Influence of Surfactants on Unlevelness

10.3.5 Shape of the Exhaustion Curve

Figure 10.10 compares the unlevelness obtained from dyeings with linear exhaustion with those using linear electrolyte dosing and those attempting a linear change of the fibre surface molality (section 10.2.4).

There appeared to be a lower unlevelness in the case of dyeings with linear salt dosing. An evaluation of the data aiming at a linear fibre surface molality change requires a more detailed analysis which follows at the end of this section.

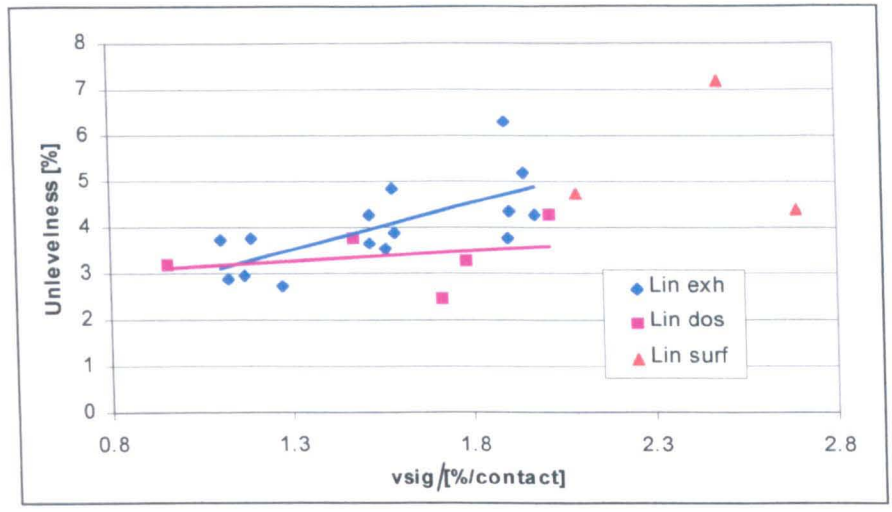

Figure 10.10: Influence of Exhaustion Profile on Unlevelness

In order to find out possible reasons for the better performance of the linear salt dosing processes, the exhaustion profiles were compared with those of the linear uptake processes (figure 10.11). As can be seen in the figure, the profiles of linear salt dosing were characterised by a steeper initial rise and a lower final uptake rate than the linear exhaustion profile. This difference at the end of the exhaustion phase between the two types of control was more pronounced at higher dye amounts as the exhaustion at the end of the salt dosing phase was lower. The exception to this general tendency was the 0.05% dyeing which was unusual because its uptake rate was determined to an important part by the dye diffusion speed and not by the electrolyte dosing gradient.

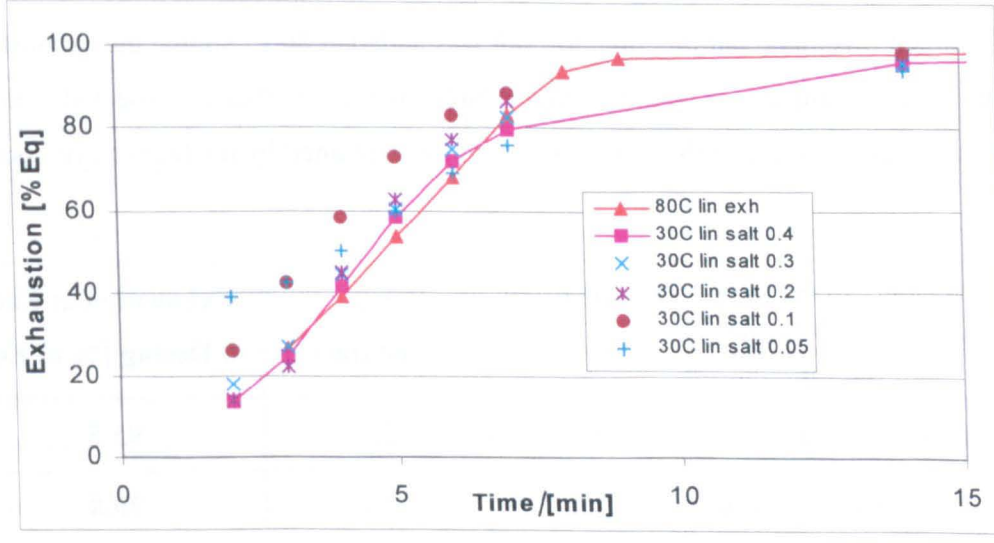

Figure 10.11: Comparison of Exhaustion Profiles

If the exhaustion level at the end of the salt dosing period played a crucial role in determining unlevelness, then a correlation between the two parameters would be expected.

Figure 10.12 indeed shows that, when the salt was dosed linearly, the unlevelness (indicated by the first column in each series), tended to be lower when the exhaustion at the end of the dosing phase was lower (triangles). The situation was different for the linear exhaustion processes when the exhaustion at the end of the salt dosing phase was generally close to 100% (circles) and showed no correlation with unlevelness (third solid column in each series). The presumed correlation between the exhaustion value at the end of the salt dosing phase and unlevelness was weak, however, if it existed at all.

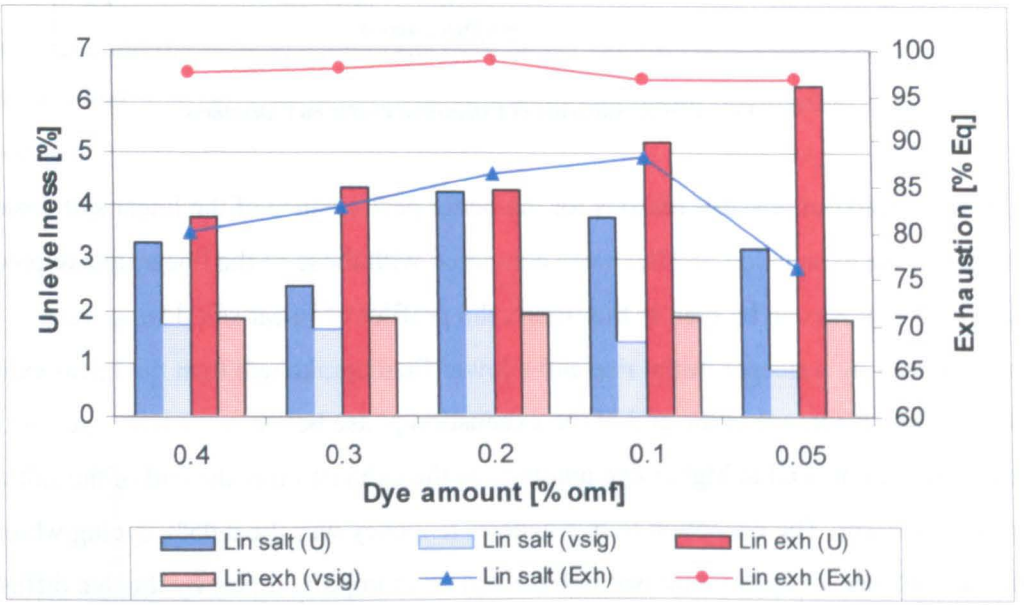

Figure 10.12: Correlation of Unlevelness and Exhaustion at the End of the Salt Dosing Phase

In order to further examine the correlation, a 0.4% dyeing (omf) with linear salt dosing over four minutes was made but this time the salt was added at 80°C, so that the exhaustion at the end of the dosing phase would be high. Table 10.7 shows that, as expected, unlevelness was much higher, an effect that could not alone be explained by the higher dye uptake rate.

Temp. at start salt dosing, salt dosing profile, dye amount	Unlevelness [%]	v_{sig} /[%.contact^{-1}]	Exhaustion at End of Dosing [% of Eq]
80°C, lin. salt, 0.4%	11.7	2.5	95.5
30°C, lin. salt, 0.4% (section 10.2.4)	3.3	1.7	79.8
80°C, lin. exh, 0.4% (section 10.2.2)	3.8	1.8	97.3

Table 10.7: Influence of Exhaustion at the End of the Salt Dosing Phase

The evidence that unlevelness was reduced when the dye uptake rate was slowed during the last approximately 20% of exhaustion pointed to the importance of the rate of change in dye fibre surface molality. As explained in chapter five, the surface molality tends to drop more quickly towards the end of the process because of an increase in the partition coefficient at low dyebath concentrations. The better performance of a process with reduced uptake rate during the final phase could be understood. Accepting this line of argument, it would then follow in analogy to the significant exhaustion speed, v_{sig}, that the optimum process would see a linear change in the dye fibre surface molality per contact. This requirement (assuming full differentiality; an assumption which may not be true) may be written as

$$\frac{\Delta[D]_{fs}}{\Delta c} = const = \left(\frac{\Delta[D]_{fs}}{\Delta[D]_s}\right)\left(\frac{\Delta[D]_s}{\Delta c}\right) = \left(\frac{\Delta[D]_{fs}}{\Delta[NaCl]}\right)\left(\frac{\Delta[NaCl]}{\Delta[D]_s}\right)\left(\frac{\Delta[D]_s}{\Delta c}\right) \quad (10.7)$$

where $\Delta[D]_s.\Delta c^{-1}$ is proportional to the exhaustion speed per contact and $\Delta[D]_{fs}.\Delta[D]_s^{-1}$ is the sensitivity of $[D]_{fs}$ to changes in $[D]_s$. Thus, if $\Delta[D]_{fs}.\Delta[D]_s^{-1}$ is constant (constant partition coefficient), then the equation coincides with the requirement of constant exhaustion speed, i.e. linear exhaustion. A constant partition coefficient is not normally true for cotton dyeing, therefore the exhaustion speed has to be adjusted such that changes in $\Delta[D]_{fs}.\Delta[D]_s^{-1}$ are compensated for in order for $\Delta[D]_{fs}.\Delta c^{-1}$ to be constant.

The term $\Delta[NaCl].\Delta[D]_s^{-1}$ in equation 10.7 can be interpreted as the inverse sensitivity of the exhaustion speed to the electrolyte, i.e. it quantifies how much salt is needed to exhaust a certain amount of dye. The term rises monotonously during the process, usually in exponential form and therefore requires a slower exhaustion speed towards the end of the process in order for $\Delta[D]_{fs}.\Delta c^{-1}$ to be constant. The term $\Delta[D]_{fs}.\Delta[NaCl]^{-1}$, the sensitivity of the fibre surface molality to changes in the electrolyte concentration, is much more complex to describe because there are two competing trends. An increase in the salt concentration at constant $[D]_s$ pushes $[D]_{fs}$ and also increases the exhaustion and thus reduces $[D]_s$, the net result may be an increase or decrease in the value. If the term is initially negative and then becomes positive (that seemed to be generally true in the present case unless the dye amount was very low), the result is a phase in the process when $\Delta[D]_{fs}.\Delta[NaCl]^{-1}$ becomes zero, i.e. $[D]_{fs}$ becomes insensitive to changes in the electrolyte concentration. In other words: even a steep increase in the amount of added salt does not cause a sudden change in $[D]_{fs}$ so that high exhaustion speeds are possible without causing unlevelness. Overall, an S-shaped exhaustion profile would therefore be the result (figure 10.13).

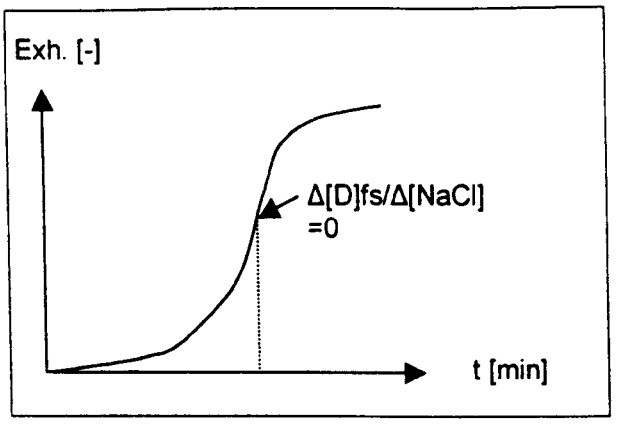

Figure 10.13: S-shaped Exhaustion Curve

The hypothesis that a linear drop in $[D]_{fs}$ with time would result in the optimum profile with respect to unlevelness was tested with a series of dyeings aiming at achieving a linear fall of the dye fibre surface molality.

In order to derive the required salt dosing profile two assumptions were made:

1) The fibre surface is in equilibrium with the dyebath, so that $[D]_{fs}$ can be calculated using the Gouy-Chapman model with variable $[D]_{sat}$.

2) The exhaustion speed is principally influenced by the electrolyte dosing gradient, so that the influence of temperature can be neglected.

As a consequence of the second assumption, the exhaustion at any moment could be predicted as a function of the salt concentration. Taking for example the exhaustion profile of a 0.3% dyeing with linear exhaustion as reference, the exhaustion, $[D]_f \cdot [D]_{f,eq}^{-1}$, was approximated as:

$$\frac{[D]_f}{[D]_{f,eq}} = -52.4 + 1.25[NaCl] + 218\frac{[NaCl]}{(1+[NaCl])} - 26.4\ln([NaCl]+1) \quad (10.8)$$

This function was obviously purely empirical and applied only to a particular range of salt concentrations, in this case 0.9 to 17g.dm^{-3}, from which extrapolations may not be made. With the amount of dye on the fibre thus defined, it was possible to calculate the amount of salt required to achieve a desired dye molality on the fibre surface, $[D]_{fs}$, using the Gouy-Chapman model with variable $[D]_{sat}$ described in chapters three and eight (equation 10.9).

$$\Delta\mu^0 = -RT\left[\ln\left(\frac{[D]_{fs}}{[D]_s}\right) - \ln([D]_{sat} - [D]_{fs}) + A_1 r_D + A_2 r_D \sum z_i [D]_{fs}\right] \quad (10.9)$$

This equation was solved by iteration with the salt concentration being the manipulated parameter, adjusted to give the desired value of the controlled parameter $[D]_{fs}$. Solutions at

several points in time yielded therefore a salt dosing curve for a desired linear change of $[D]_{fs}$. In the case of the example above for 0.3% dye, an S-shaped instead of an exponential salt dosing profile resulted (figure 10.14). The figure also shows the salt dosing profile ("Lin exh-[NaCl]") and the values for $[D]_{fs}$ ("Lin exh-$[D]_{fs}$") when the exhaustion profile was linear as well as the predicted $[D]_{fs}$-values for the new process profile ("Lin $[D]_{fs}$-$[D]_{fs,pred}$").

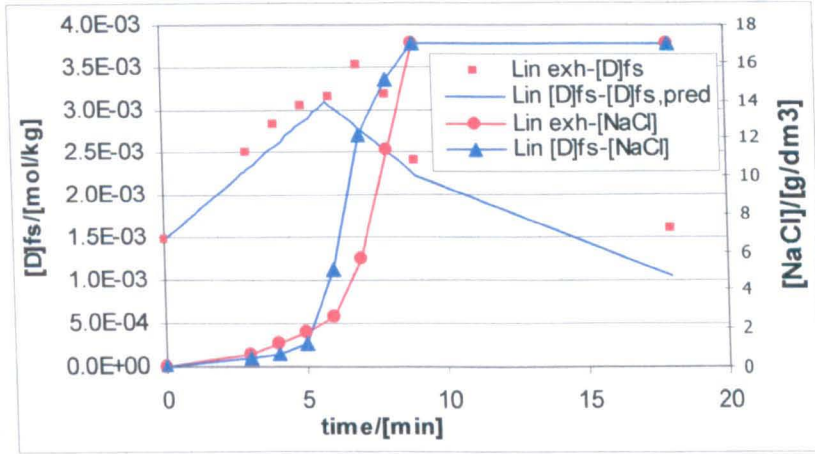

Figure 10.14: Comparison of Salt Dosing Profiles and $[D]_{fs}$

A dyeing carried out on the pilot-scale jet dyeing machine with the new salt dosing profile showed that, unexpectedly, unlevelness using this new process profile was found to be higher compared to the linear profile (table 10.8).

Profile	Unlevelness [%]	v_{sig} /[%.contact^{-1}]
lin $[D]_{fs}$, 0.3%	7.2	2.4
lin exh, 0.3%	4.3	1.9

Table 10.8: Performance Comparison of linear Exhaustion vs. linear change in $[D]_{fs}$

When the $[D]_{fs}$-values were recalculated from the experimental data and compared with the predicted $[D]_{fs}$-values it became clear that the salt dosing gradient did not yield the expected exhaustion profile and therefore the $[D]_{fs}$-values also deviated from the prediction. Figure 10.15 shows that the inferior unlevelness could be explained by the sudden increase in $[D]_{fs}$ between the 5th and 6th minute. Thus the rate of change of $[D]_{fs}$ proved indeed to be a valuable tool in explaining unlevelness a posteriori but the model, i.e. equation 10.8, failed in predicting $[D]_{fs}$ a priori. The deficiency lay clearly in the empirical equation

linking dye exhaustion to salt concentration which was not sufficiently accurate in predicting the effect of altering the salt dosing gradient.

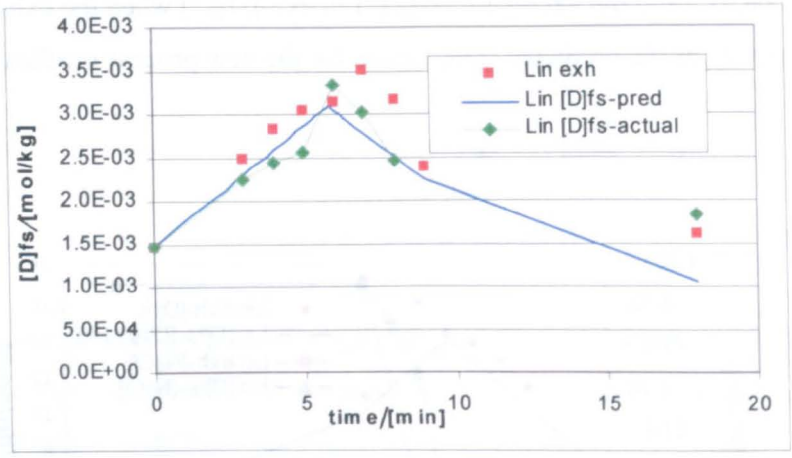

Figure 10.15: Predicted and actual $[D]_{fs}$-values

In a second attempt, the newly found correlation between the exhaustion and the electrolyte concentration was empirically fitted using the same functionality as equation 10.8 but resulting in different coefficients. The equation was then employed to predict a new dosing profile for a linear change in $[D]_{fs}$ which, when tested, had performed no better than the first dosing profile and confirmed that a one-parameter (NaCl) exhaustion model was not sufficiently accurate (figure 10.16).

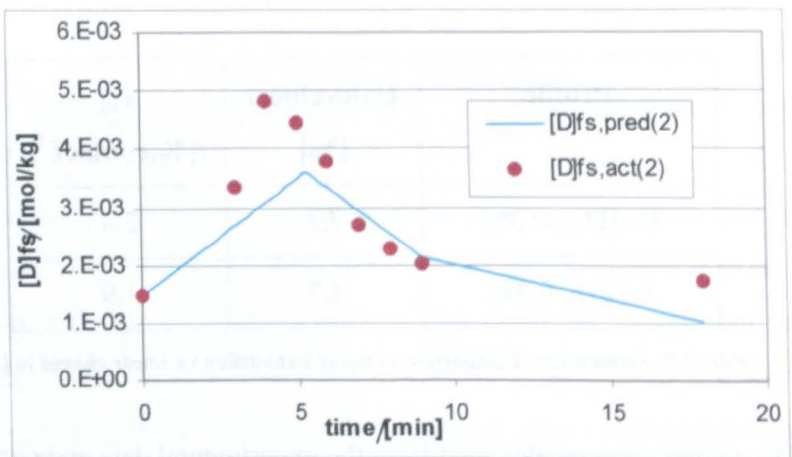

Figure 10.16: Second Test comparing actual with predicted $[D]_{fs}$

For the final test, it was therefore decided to use the newly developed adsorption-diffusion model described in chapter nine for the prediction of the exhaustion value. The method to derive the required salt dosing profile was analogous to the one-parameter model, i.e. at

each time step the salt concentration was calculated iteratively that would result in the desired value for $[D]_{fs}$, using equation 10.9. However, this time the values related to the exhaustion such as $[D]_s$ were calculated not by the empirical equation 10.8 but by the adsorption-diffusion model using the coefficient-values compiled in tables 9.3 to 9.5. The new salt dosing profile was then tested on the pilot-scale jet dyeing machine.

Figure 10.17 shows that the actual and the predicted $[D]_{fs}$-values were in good agreement during the first seven minutes of the process. Subsequently the model predicted values were greater than the "actual" values of $[D]_{fs}$, indicating that the actual diffusion speed within the fibre was higher than the modelled diffusion speed. The figure also makes clear that $[D]_{fs}$ was fairly insensitive to errors in $[D]_s$ in the early process stages when $[D]_{fs}$ was high, as the model gave accurately enough predictions for $[D]_{fs}$ even though it had over-estimated the dye uptake rate. The situation changed in the later phase of the process when even a minor prediction error in the dye exhaustion caused a serious deviation in $[D]_{fs}$.

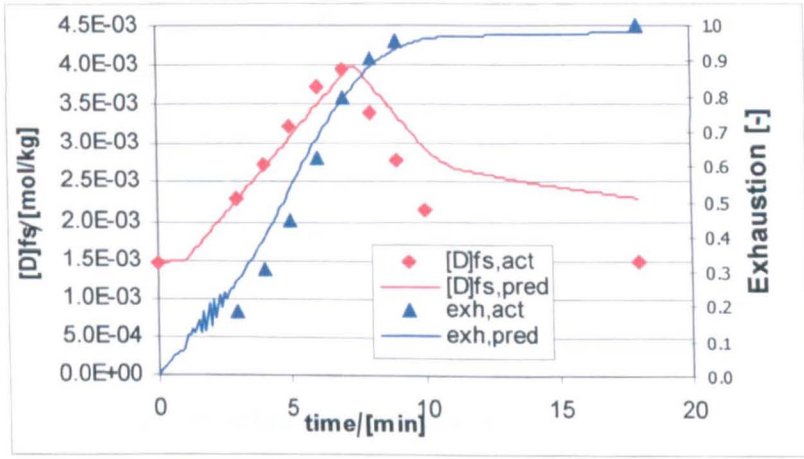

Figure 10.17: Comparison of Prediction with Adsorption-diffusion Model and Experiment

Unlevelness was 4.7% at a $v_{sig(c)}$-value of 2.0%, a result that did not appear to be different from that obtained with a linear exhaustion speed. Due to the fairly large experimental error mentioned in section 10.1, however, it is unsafe to draw conclusions based upon a single test are prone to error. An evaluation including consideration of a larger number of tests is summarised in chapter 10.2.7.

Overall, it would appear that the adsorption-diffusion model predicted fairly successfully the salt dosing gradient that would be required in order to obtain a linear change of the dye fibre surface molality. Since small prediction errors in the dye uptake rate at the end of the

process may already cause significant deviations from the expected fibre surface molality further experiments would however be required to verify the model's suitability.

10.3.6 Dye Dosing versus Electrolyte Dosing

When the dye was dosed into the dyebath containing the full amount of electrolyte as described in section 10.2.5, the dye in experiments #2, 3 and 4 was almost completely sorbed by the fibre at the end of the dye dosing time (figure 10.18). Despite an equally quick initial dye addition, the uptake rate in experiment #1 was reduced due to the lower temperature, the higher dye amount and the lower salt concentration. In case of experiment #5, the exhaustion followed in good approximation the linear dosing profile of the pump, i.e. most of the dye dosed was immediately sorbed by the fibre. The dyebath concentration reached equilibrium after around five minutes, then dropped when dye dosing stopped after eight minutes (figure 10.19).

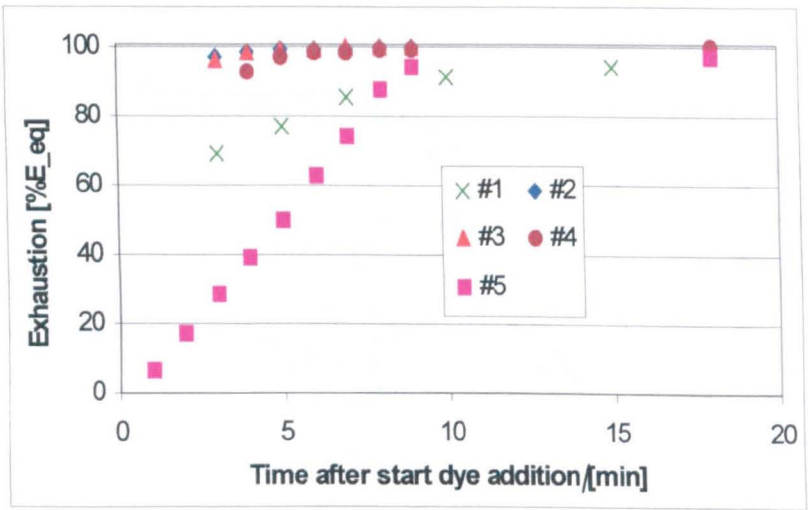

Figure 10.18: Exhaustion Profiles of Dye Dosing Tests

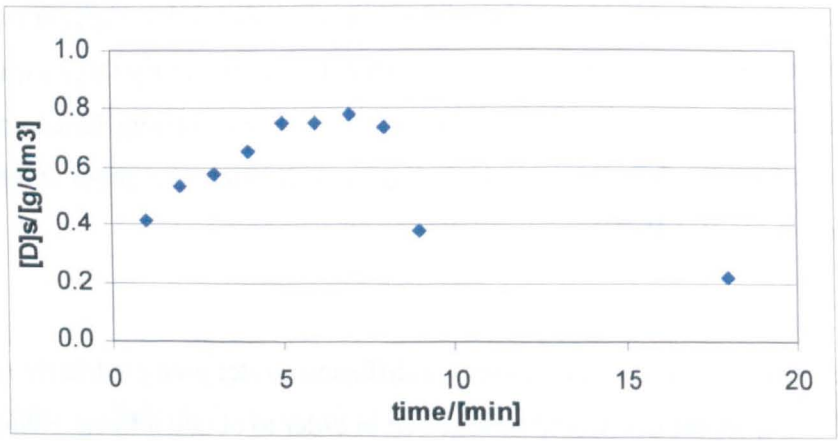

Figure 10.19: Dyebath Concentration Experiment #5

A comparison of experiment #5 with the equivalent linear process profile obtained from electrolyte dosing instead of dye dosing showed that unlevelness was much higher (table 10.9). It was thus clearly confirmed that controlling the substantivity of the dye for the fibre is a more efficient dyeing method than controlling the dye supply. When the dye supply is the rate-limiting factor, it is more likely that variations in the local dye supply occur due to differences in fibre accessibility (e.g. caused by twists of the fabric rope) or dyebath inhomogeneity (e.g. higher dye concentration at the dye dosing point) because the uptake rate is so high. In other words: The "demand" of dye from the fibre is so high that the fibre sorbs all dye that is available in the entrained liquor, emphasising the risk of local concentration differences. When electrolyte is dosed, on the other hand, the dye "demand" of the fibre is controlled such that the demand never outstrips dye supply from the dyebath.

Process Description	**Unlevelness [%]**	**v_{sig} /[%.contact^{-1}]**
Dye dosing, 0.2% (exp. #5) (section 10.2.5)	8.3	1.0
Electrolyte dosing, 0.2% (section 10.2.4)	2.9	1.1

Table 10.9: Performance Comparison of Dye Dosing vs. Electrolyte Dosing

Although it is therefore clearly desirable to control the electrolyte and not the dye amount, optimising dye addition techniques becomes important when dyebaths are to be recycled. For cost and environmental reasons, the recycled dyebath normally still contains much of the electrolyte (some is lost with the fabric) so that electrolyte dosing is not an option. One question is how dye additions should be made into a dyebath of high salt content.

One control parameter available for dye additions to a dyebath containing electrolyte is the dye dosing time. Reducing the dye dosing time led to even higher unlevelness as shown in table 10.10, where it can be seen that reduction in the dosing time from 8 minutes (experiment #5), to 3 minutes (#4), to 1 minute (#3) and to 20 seconds (#2) increased unlevelness from 8.3% to 13.7%. Remarkably good results were however obtained when the dye was dosed rapidly at a lower temperature and higher dye amount (#1).

Process Description (section 10.2.5)	**Unlevelness [%]**	**v_{sig} [%.contact^{-1}]**
Dye dosing exp. #1	3.8	2.3
Dye dosing exp. #2	13.7	4.7
Dye dosing exp. #3	12.8	4.5
Dye dosing exp. #4	9.5	3.2
Dye dosing exp. #5	8.3	1.0

Table 10.10: Performance Comparison of Dye Dosing vs. Electrolyte Dosing

It would therefore appear that the best levelness results can be obtained from dye dosing into a cold dyebath, the temperature of which is only raised once the dye addition is completed. In this case, rapid dye addition may be preferential because it could lead to a situation when dye supply from the dyebath is high enough to equate the sorption speed of the fibre, even under high substantivity conditions.

During the addition, fabric and dyebath circulation speeds should be sufficient to keep the dye uptake per contact below the critical value. In case of experiment #1, for example, the machine ran at around 6 theoretical contacts per minute, yielding nearly acceptable unlevelness (3.8%). A typical production machine running at 1.5 theoretical contacts per minute would thus require only a quarter of the uptake rate in experiment #1 to achieve the same result. It is clear that this would be difficult to achieve even if the temperature was lowered as far as possible.

One contributing factor to the better performance of experiment #1 was certainly the higher dye amount (0.45% as opposed to 0.2%). The positive influence of the dye amount could be used beneficially in industrial applications because it is normal practice to arrange the colour sequence for dyeing on any particular machine so that lighter shades are dyed first and then subsequent dyelots become gradually darker. The darker colour of the subsequent process requires higher electrolyte concentrations than the preceding batch so that the ratio of dye amount to initial salt concentration increases from one batch to the next batch.

10.3.7 Summary of Experimental Findings

The analysis of the results described in this section led to several conclusions:

1) It was confirmed that the dye uptake rate by the fabric on a jet dyeing machine should refer to the dyebath and fabric circulation, i.e. uptake per (theoretical) contact rather than uptake per minute.

2) Neither the total dye amount nor the use of the two tested non-ionic surfactants appeared to influence unlevelness in a significant way.

3) A curved exhaustion profile with a lower exhaustion speed towards the end of the dyeing process appeared to yield favourable results compared to a linear exhaustion profile. If a variation coefficient of 3% was taken as the limit for acceptable unlevelness, the critical uptake rate per contact lay between 1.0% (linear exhaustion) and 1.4% (regressive profile). It was thought that the positive influence of a decreasing exhaustion speed could be explained with the rate of change of the dye molality at the fibre surface per contact, $\Delta[D]_{fs}.contact^{-1}$.

4) Using the previously developed adsorption-diffusion model, it was possible to derive a salt dosing gradient that yielded in good approximation constant $\Delta[D]_{fs}.contact^{-1}$ during the entire process.

5) Electrolyte dosing gave a much lower unlevelness than dye dosing into a bath containing electrolyte, all other factors being equal.

For the next and final step it was decided to use statistical tools to consolidate these findings by analysing all of the experiments carried out on the pilot-scale machine, with the exception of the dye dosing experiments #2, 3, 4 and 5 with their extremely high dye uptake rates, rather than looking at individual sets of data as previously.

10.4 Multiple Linear Regression of Major Factors

It was assumed for the statistical analysis that the following factors could influence unlevelness:

1) the significant exhaustion speed per contact, $v_{sig(c)}$ [$\%.c^{-1}$]

2) the significant speed of the dye molality change at the fibre surface per contact, $v_{sig,surf(c)}$ [$\%.c^{-1}$]

3) the dye amount, M_0 [% omf]

4) the dye addition time, t_{ad} [c]

5) the holding time at maximum temperature, t_{hold} [c]

The method used to calculate $v_{sig,surf(c)}$ was similar to the one suggested by Ruettiger for v_{sig} described in chapter five, but instead of normalising the value with the dye amount exhausted at the end of the process the value was derived by dividing by the difference between the maximum and the minimum fibre surface molality for that particular dyeing process. Equations 10.10 to 10.12 in combination with figure 10.20 illustrate how $v_{sig,surf(c)}$ was derived for an arbitrary profile of $[D]_{fs}$.

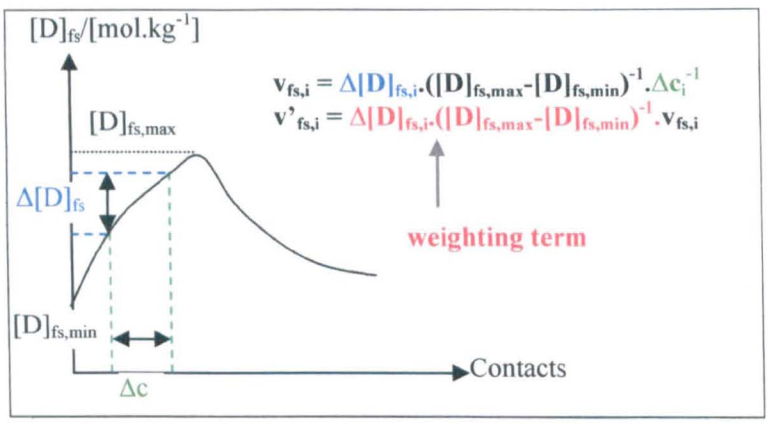

Figure 10.20: Calculation of $v_{sig,surf(c)}$

From figure 10.20 the analogy between $v_{sig(c)}$ (see section 5.2.1), which sets the equilibrium exhaustion as 100%, and $v_{sig,surf(c)}$, which sets the maximum fibre surface molality difference as 100%, becomes clear. The formulae to calculate $v_{sig,surf(c)}$ were accordingly:

$$v_{sig,surf(c)} = 100\sum_{i=1}^{n} v'_{fs,i} = 100\sum_{i=1}^{n}\left\{ v_{fs,i}\frac{\Delta[D]_{fs,i}}{\left([D]_{fs,\max}-[D]_{fs,\min}\right)}\right\} \qquad (10.10)$$

$$v_{sig,surf(c)} = 100\sum_{i=1}^{n}\left\{\frac{\Delta[D]_{fs,i}}{\left([D]_{fs,\max}-[D]_{fs,\min}\right)\Delta c_i}\frac{\Delta[D]_{fs,i}}{\left([D]_{fs,\max}-[D]_{fs,\min}\right)}\right\} \qquad (10.11)$$

$$v_{sig,surf(c)} = 100\sum_{i=1}^{n}\frac{\Delta[D]_{fs,i}^{2}}{\left([D]_{fs,\max}-[D]_{fs,\min}\right)^{2}\Delta c_i} \qquad (10.12)$$

The factor 100 was introduced to yield values in the same order of magnitude as $v_{sig(c)}$. For the calculation of $[D]_{fs}$ it was assumed, as previously, that the fibre surface was in equilibrium with the dyebath so that equation 10.9 applied.

There are other possibilities to normalise the change in $[D]_{fs}$, i.e. to make it a dimensionless value, notably by including M_0. Among the alternatives tested in this investigation were

$$\frac{\Delta[D]_{fs}}{M_0} \tag{10.13}$$

$$\frac{\Delta[D]_{fs}}{[D]_{fs,\max}} \tag{10.14}$$

$$\frac{\Delta[D]_{fs}}{[D]_{fs,\min}} \tag{10.15}$$

$$\frac{\Delta[D]_{fs}}{[D]_{fs,\max} M_0} \tag{10.16}$$

None of these parameters however achieved equally as good a correlation with the observed unlevelness. This was interesting because it suggests that it does not matter how much dye is initially present but the range of $[D]_{fs}$-values is important. $[D]_{fs,max}$ of course can be influenced by the process profile and as $v_{sig,surf(c)}$ decreases with higher values of $[D]_{fs,max}$, it becomes understandable why the processes with linear salt dosing into the cold dyebath, with their fairly high initial salt concentration, showed better performance.

The statistical evaluation used multiple linear regression (MLR) that was developed stepwise in order to determine the significant parameters (Nobbs 1999). Stepwise development of a multiple linear regression fit means that only one parameter is added to the model at a time and after each addition it is determined whether this parameter made any statistically significant contribution to the explanation of the variation in the observed effect, in the present case unlevelness. The sequence of the parameter addition depended on the value of their correlation coefficient, higher correlating parameters being added first. The application of MLR requires, among others, that the amount of random variation of the response variable, in this case unlevelness, is normally distributed around the "true" value and that it is independent of the size of the variable. It was not known whether these requirements were actually fulfilled but there was no evidence either that they were not complied with. MLR additionally demands that there be no random error in the predictor variables, such as $v_{sig(c)}$. This was not strictly true but as the random error was small compared to the value changes between different experiments, it was felt that the regression method could nevertheless be applied.

A first MLR fit gave the the results in table 10.11, in order of parameter addition:

Parameter	% of Variation	P-value	R^2 (adj)
$v_{sig(c)}$	51.6	0.00	0.25
$v_{sig,surf(c)}$	11.2	0.00	0.37
t_{ad}	6.1	0.01	0.45
M_0	2.4	0.11	0.47
t_{hold}	0.0	0.85	0.46

Table 10.11: First MLR-fit

The second column in table 10.11 shows how much of the overall observed variation in the unlevelness value was explained by the particular parameter. The third column shows the probability with which the hypothesis had to be rejected that the parameter contributed significantly to unlevelness. For example, the probability that M_0 had to be rejected as a significant parameter was 0.11 or 11%. It is often assumed that any probability higher than 5% indicates that the parameter contribution has not been significant and that the parameter should therefore be discarded in the MLR. Another way to determine the statistical significance of a parameter is the adjusted R^2-value, which tends to rise as long as significant parameters are added to the MLR equation. It can be seen from table 10.11 that the two methods do not necessarily agree which parameters are significant. According to the P-value, only $v_{sig(c)}$, $v_{sig,surf(c)}$ and t_{ad} were significant, whereas the R^2-value suggested that all parameter except t_{hold} played a significant role.

The data proved that $v_{sig,surf(c)}$ indeed was a suitable way of expressing the influence of the situation at the fibre surface on dye levelness and that its inclusion provided information in addition to $v_{sig(c)}$. The analysis also confirmed that the dye amount played only a minor role, if any. A small but significant contribution to unlevelness appeared to have been made by the dye addition time. The rejection of the holding time as significant parameter would be expected under a high-substantivity regime since there is very little dye left in the dyebath at the end of the exhaustion phase so that migration is very small. Judging conservatively and including only $v_{sig(c)}$, $v_{sig,surf(c)}$ and t_{ad} around 69% of the overall variation could be explained.

In order to improve the accuracy of the predictions, two modifications were made. The first regarded the method of calculation of $v_{sig(c)}$ and $v_{sig,surf(c)}$ and the second affected the method to calculate t_{ad}. It was pointed out in chapter five that the work of Carbonell had shown that the sorption of the first approximately 20% of dye did not affect final unlevelness.

Consequently, it would seem more appropriate for the calculations of $v_{sig(c)}$ and $v_{sig,surf(c)}$ to disregard this initial sorption. This was achieved by converting $v_{sig(c)}$ into $v_{sig(c),25}$:

$$v_{sig(c),25} = \frac{1}{1-0.25}\left\{\frac{\Delta E_1}{\Delta c_1}(E_1 - 25) + \sum_{i=2}^{n}\left(\frac{\Delta E_i}{\Delta c_i}\Delta E_i\right)\right\} \qquad (10.17)$$

where $E_1 > 25\%$ and where all E_i-values smaller than 25% were ignored. The factor $(1-0.25)^{-1}$ merely served to ensure that the new $v_{sig25(c)}$-value was not systematically smaller than the old $v_{sig(c)}$-value.

Similarly, $v_{sig,surf(c),25}$ was defined as:

$$v_{sig,surf(c),25} = 100\left[\frac{\Delta[D]_{fs,1}\, abs\left([D]_{fs,1} - [D]_{fs,25\%}\right)}{\left([D]_{fs,max} - [D]_{fs,min}\right)^2 \Delta c_1} + \sum_{i=2}^{n}\left\{\frac{\Delta[D]_{fs,i}^2}{\left([D]_{fs,max} - [D]_{fs,min}\right)^2 \Delta c_i}\right\}\right] \qquad (10.18)$$

where $[D]_{fs,25\%}$ was the fibre surface molality at 25% exhaustion. As $[D]_{fs,25\%}$ could be smaller or bigger than $[D]_{fs,1}$ the absolute difference was taken. Changes in $[D]_{fs}$ during the first 25% of the exhaustion were ignored.

It was also found that better predictions could be obtained when t_{ad} included information about the dye amount and the first strike, FS, at that amount. The reason for the better fit can easily be seen as a dye addition time of, for example, five contacts would be appropriate at a dye amount of 0.45% with a low first strike of around nine per cent but insufficient at a dye amount of 0.05% with a first strike of over forty per cent. The modified addition time $t_{ad,2}$ therefore became

$$t_{ad,2} = 10 t_{ad} M_0 FS \qquad (10.19)$$

The calculation used the FS-values listed in table 10.2 for 80°C without electrolyte.

With these modified parameter definitions, the MLR yielded the equation

$$U = 2.7 + 0.54 v_{sig(c),25} + 0.44 v_{sig,surf(c),25} - 0.10 t_{ad,2}\,. \qquad (10.20)$$

It gave the following results:

Parameter	% of Variation	P-value	R^2 (adj)
$v_{sig(c),25}$	54.8	0.00	0.29
$v_{sig,surf(c),25}$	20.4	0.00	0.55
$t_{ad,2}$	3.9	0.01	0.60
M_0	0.5	0.30	0.60
t_{hold}	0.4	0.35	0.60

Table 10.12: Second MLR-fit

Table 10.12 shows that the fit was considerably improved. As expected, both $v_{sig(c),25}$ and $v_{sig,surf(c),25}$ accounted for more of the variation in the experimental findings than $v_{sig(c)}$ and $v_{sig,surf(c)}$. The regression confirmed that the dye addition time, $t_{ad,2}$, had a significant influence on unlevelness. It could also be concluded that M_0 did not constitute an important parameter other than through $t_{ad,2}$ because both the probability and the R^2-test assigned no significant influence. The second MLR explained 79% of the total variation.

It could be argued that later stages in the process contribute more to the final unlevelness than earlier stages because less time is available for dye relocation and because the dyebath concentration is lower. According to this argument if there were some unlevelness early in the process, it would be more likely to diminish than unlevelness later in the process. In order to test this suggestion, the exhaustion sequence was divided into intervals of ten per cent each and then assigned a weighting factor that increased with the exhaustion value (table 10.13).

Exh. [%]	0-25	25-30	30-40	40-50	50-60	60-70	70-80	80-90	90-100
Weight [-]	0	1	2	3	4	5	6	7	8

Table 10.13: Weighting Factors for $v_{sig,surf(c),25}$

The weighting factor was then taken into account when calculating $v_{sig,surf(c),25}$. Different weighting functions were explored besides the one shown in table 10.13, such as 0.5 increments from interval to interval or a 10% increase at each step, but all of them yielded

an inferior accuracy of prediction. *This, together* with the conclusion that t_{hold} was not a significant parameter, indicated that dye migration contributed little to reduce unlevelness even when the sorption was not controlled, e.g. in case of the all-in processes.

Using the second MLR-model unlevelness could be predicted for varying values of $v_{sig(c),25}$, $v_{sig,surf(c),25}$ and $t_{ad,2}$. Table 10.14 summarises some calculation results over a typical range of values for each parameter.

$v_{sig(c),25}$ /[%.c^{-1}]	$v_{sig,surf(c),25}$ /[%.c^{-1}]	$t_{ad,2}$ /[c]	U [%]
0.5	**0.5**	**10**	**2.1**
	1.0	10	2.3
	1.0	1	3.3
	5.0	10	4.1
1	**0.5**	**10**	**2.4**
	1.0	10	2.6
	1.0	1	3.5
	5.0	10	4.3
1.5	**0.5**	**10**	**2.6**
	1.0	10	2.9
	1.0	1	3.8
	5.0	10	4.6
2	**0.5**	**10**	**2.9**
	1.0	10	3.1
	1.0	1	4.1
	5.0	10	4.9

Table 10.14: Prediction of Unlevelness, U, as a Function of significant Parameters

When interpreting table 10.14, at least two things should be considered. First, predictions of an unlevelness-value of less than around 3% merely contain the qualitative information that unlevelness would be as low as practically possible on the machine. Second, while $t_{ad,2}$ can

be freely adjusted under practical conditions, $v_{sig(c),25}$ and $v_{sig,surf(c),25}$ are not entirely independent from each other. A rapid dye uptake rate for example would usually imply high values for both parameters. The table therefore does not imply that the all combination can be achieved for a particular process.

On a more general note, it is noteworthy that although the inclusion of $v_{sig,surf}$ yielded a much better prediction of the unlevelness, it was equally clear that the main parameter was the significant exhaustion speed. Theoretical considerations, outlined earlier in this chapter, would lead one to predict that the rate of molality change at the fibre surface includes the influence of v_{sig} so that the latter would not need to be included in the list of significant parameters in addition to $v_{sig,surf}$. There are a number or possible explanations why this has proved to be incorrect.

First, there are inaccuracies in the $[D]_{fs}$-prediction by the Gouy-Chapman model. When the model predicted $[D]_{fs}$ not based upon M_0 (see equation 3.36 for comparison) but on $[D]_s$ (see equation 3.33 for comparison), as was the case for the prediction during the process, the accuracy dropped significantly. The first method can be applied only if the exhaustion at the end of the process is to be predicted, i.e. under equilibrium conditions for the whole dye-fibre system. During the process, it is necessary to use the second method. While, as reported in chapter eight, the accuracy of the first method was better than 2%, the back prediction error in the second case was 11.4% for the same data set.

Second, the calculation of $v_{sig,surf}$ assumed that equilibrium at the fibre surface is instantaneously established. Although adsorption takes place rapidly, this assumption may be an over-simplification so that the actual changes at the fibre surface are less pronounced than anticipated.

Third, the calculation interpolated linearly between any two measurements. Since $[D]_{fs}$ normally underwent a maximum during the process, it is quite likely that the actual maximum value was not taken into account properly (see figure 10.21). This deficiency could be minimised if the time interval between measurements could be shortened, e.g. through on-line dyebath monitoring.

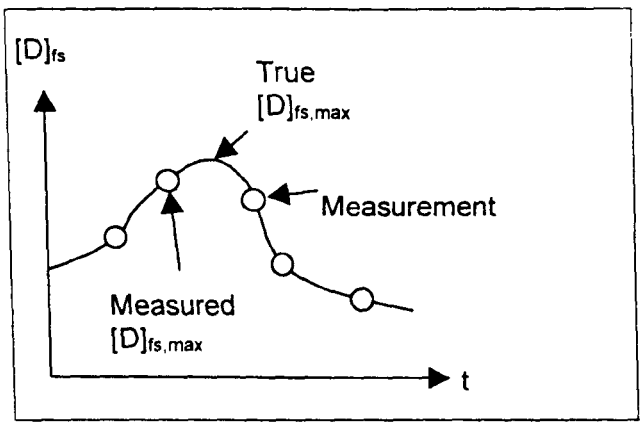

Figure 10.21: Inaccuracies of Interpolation

Fourth, the calculation required an estimate of the salt concentration at 25% exhaustion and its corresponding $[D]_{fs}$-value. As the measurement moment almost never coincided with the moment when 25% exhaustion was reached, the salt concentration, too, had to be determined by interpolation. The value of $v_{sig,surf(c),25}$ was fairly sensitive to this estimate so that a further source of error was introduced.

Finally, and more fundamentally, it is conceivable that the two parameters describe two distinct causes of unlevelness, dyebath inhomogeneities and fibre surface sensitivity to these concentration differences. Probably, $v_{sig(c)}$ is a good measure for the level of dyebath concentration differences in the vessel, i.e. the higher $v_{sig(c)}$ the more pronounced the variation in $[D]_s$. Even if $[D]_{fs}$ is fairly insensitive to changes in $[D]_s$, a high dye uptake rate amplifies any inhomogeneities and thereby nevertheless leads to local differences in the exhaustion speed. As a consequence, both factors, the level of dyebath differences expressed by $v_{sig(c)}$, and the sensitivity of $[D]_{fs}$, expressed by $v_{sig,surf(c)}$, have to be taken into account.

10.5 References

1. Ciba, Customer Information Albegal FFA (1997)
2. Clariant, Technical Information Sandogen EDP liquid (1999)
3. J H Nobbs J H, Data Analysis and Experimental Design, Course Material COLO5090 (1999)

11 Summary and Conclusions

The present work investigated the use of experiments on laboratory and pilot-scale dyeing equipment, in combination with physico-chemical as well as statistical models, for the improvement of the dyeing process of cotton on jet dyeing machines with direct dyes. Considering the objectives of the work outlined in chapter one, the findings may be summarised as follows.

11.1 Scaling of Equipment

Experiments on a pilot-scale jet dyeing machine led to the conclusion that the dye uptake rate on bulk-scale equipment in industry is most likely not affected by the rate of diffusion of the dye in the liquid phase, indicating a sufficiently high rate of dye supply to the fibre surface. The rotating-beaker type laboratory machine was found to be adequate for a kinetic analysis of the dyeing process since boundary layer effects were found not to play any significant role, mirroring the situation on the pilot-scale jet machine. Since recently introduced beaker type machines even allow for the continuous addition of liquids according to pre-defined profiles, it would appear that these machines may be successfully used for the kinetic analysis of processes and recipes, greatly reducing the amount of materials and work required. As low liquor ratios of down to 5:1 can be achieved on modern beaker machines, they are equally well suited for experimental work quantifying equilibrium dye sorption. Regarding the analysis of dye unlevelness, however, this machine type is not suitable because its operating principle is fundamentally different from bulk jet dyeing machines and pilot-scale equipment becomes essential.

An analysis revealed that three parameters appear to be central to the scaling of jet dyeing equipment: the liquor ratio, the number of fabric and dyebath contacts per minute and the dimensionless parameter L, which comprises the fluid velocity v_0 and the flow regime, *l*. The geometrical and hydraulic design of the machine can additionally influence the interaction between substrate and dyeliquor. Its influence is difficult to derive theoretically. A convenient method to take machine design factors into account is to introduce empirical coefficients which modify the "efficiency" of the theoretical contacts, derived from the speed of the fabric rope and the circulation frequency of the dyeliquor. The pilot-scale unit of the present investigation successfully ran at the low liquor ratio used in industry and the fabric speed could be adjusted to give the same circulation frequency as on bulk machines. An identical bath circulation frequency resulted however in a much-reduced fluid velocity-value and a greatly diminished fabric-liquor interchange compared to a bulk machine. It

therefore seemed better to adjust the flow rate on the pilot machine such that the absolute speed difference between the liquid and the fabric in the jet nozzle was approximately equal to the difference on a bulk machine. This setting led to a much shorter dyebath circulation time and consequently process profiles of pilot and bulk machine may not be compared directly on a time-basis but needed to be converted to comparison on a contact-basis. This conversion is particularly relevant for the transfer of experiments analysing dye unlevelness of the processed fabric.

11.2 Development of a Model for the Prediction of Equilibrium Dye Sorption

Two versions of the Gouy-Chapman model and three models derived from the Donnan membrane equilibrium were evaluated in their prediction accuracy for data sets based upon published experiments and on the results of experiments made during this study. The versions varied in that they either neglected or included fibre saturation effects and, in the case of the Donnan model, used different methods to calculate the internal volume. The central evaluation criterion was the variation coefficient of the predicted affinity values, calculated from dyeings at different dye and electrolyte concentrations, varying substrates and pH levels.

The various models showed significant differences in the average performance over all experiments but their differences were even greater in individual aspects. Best overall results were obtained with the Gouy-Chapman model with saturation value, the least accurate results with the variable volume 3-phase Donnan model. Inclusion of saturation effects also considerably improved the prediction of the Donnan model. The Donnan type models better predicted the influence of changes in the degree of ionisation of the hydroxyl and carboxyl groups while the Gouy-Chapman type models gave better results at low electrolyte concentrations.

The better performance at low salt amounts made the Gouy-Chapman model more suitable for the experiments in this study with C.I. Direct Yellow 162, because a wide range of electrolyte concentrations was to be covered. Additionally, the mathematical method employed here determined the initial charge density of the substrate and the area of fibre surface accessible to the dye by regression instead of using literature values, resulting in a smaller prediction error but probably at the cost of physical truthfulness.

The variation coefficient of the affinity values could be further reduced when the fibre saturation value was not constant but was allowed to be a function of the dye amount and the electrolyte concentration, reflecting a well-established observation. The selected functionality used empirical coefficients and led to a saturation value that increased with

the ionic strength of the solution and with the dye amount. The average prediction error of the optimised model for the dye fibre amount was below two per cent and therefore deemed satisfactory.

11.3 Development of a Model for Dynamic Dye Sorption

When it was attempted to fit the progress of dye sorption with time of a series of isothermal all-in dyeings with predictive equations based on solutions of film-diffusion-limited processes, it became clear that the initial dye uptake rate was not determined by film-diffusion but by a faster adsorption step. Consequently, a new dye sorption model was developed that interpreted the exhaustion speed as a two-phase process, combining rapid dye adsorption and desorption at a surface layer phase with slow transfer from the surface into the fibre interior phase by diffusion. Its set of differential equations was solved numerically with a backward difference approximation method. This method became unstable at small values of fractional volume of the fibre surface layer, a problem which could be overcome by using a forward difference approximation method.

Fitting of the experimental results was achieved by empirically adjusting three model parameters, the desorption constant, the diffusion coefficient and the fractional volume of the surface layer. The model predicted the experimental exhaustion values of all the isothermal experiments with an average (absolute) accuracy of +/- 2.3% and a maximum single error of 4.2%. It also accounted well for the effect of changes in the liquor ratio on the dye uptake rate without requiring further adjustment of its coefficients. When tested under conditions resembling those in industry, i.e. with changing salt dosing gradients, results were overall satisfactory but a good fit required, in certain cases, adjustment of one coefficient. Direct measurement of the adsorption constant under varying conditions showed that the values used in the fit of the adsorption-diffusion model agreed only qualitatively with the experimental findings.

The model was also extended to take into account the effects of a boundary layer of liquid at the fibre surface which reduces the dye concentration at the fibre surface and thereby also the exhaustion speed. It was shown that the sorption process is more likely to be influenced by boundary layer effects when high substantivity conditions prevail, when the dyeliquor velocity relative to the fibre surface is low and when the dyeing process is in its early stages (at constant dyeing conditions). It was estimated that the critical fluid velocity, i.e. the velocity below which the influence of the boundary layer would become noticeable, was around $3 m.min^{-1}$ on the pilot-scale machine when an exhaustion speed similar to that occurring in industry was assumed. A comparison of experimental results with model

predictions showed that the boundary layer thickness appeared to increase exponentially with flow rate reduction, contrasting the situation of the boundary layer developing around a plane sheet immersed in a flow parallel to its axis. Due to a number of simplifying model assumptions and uncertainties about several parameter values, particularly concerning the flow regime, caution is recommended in interpreting the quantitative results of the calculations. Nevertheless it appears that although boundary layer effects are not expected to noticeably influence the dye uptake rate on jet dyeing machines under industrial conditions, they could well be responsible for local exhaustion speed differences in the storage chamber, increasing the risk of unlevelness.

Overall, the results reflect the advantages and limitations of models based upon physico-chemical laws rather than merely empirical equations. Even under simplifying assumptions, the model became quite complex, requiring the use of a numerical solver which in turn brought its own problems related to accuracy and stability. The increased initial effort in model development brought the benefit of satisfactory predictions under conditions other than those employed initially for the model development (salt-dosing, change in liquor ratio). This is a substantial benefit. It is equally clear, however, that the true situation during a dyeing process is considerably more complex still, requiring the use of empirical instead of true coefficients and leading to sometimes inaccurate predictions. While the model's performance was altogether satisfactory for the dye under investigation, it remains a task of the future to test it using dye mixtures.

11.4 Development of a Model for Dye Unlevelness

Due to the irregular and changing geometric shape of the fabric rope in the dyeing vessel and the complexity of the flow regime, the development of a three-dimensional model of the dye in fibre distribution was not attempted. Instead, a series of experiments were designed to identify parameters significantly influencing unlevelness. They showed that neither the dye amount nor the two tested non-ionic surfactants nor the holding time had a notable influence on unlevelness. They suggested that there was a linear relationship between the significant exhaustion speed per contact and the resulting unlevelness. It was thus confirmed that the uptake rate on a jet dyeing machine should refer to the dyebath and fabric circulation frequencies, i.e. the number of contacts, rather than time. With a linear exhaustion profile the critical uptake rate per contact was 1.0% when a variation coefficient of 3% of dye on fibre across a fabric sample was deemed to be the upper visual limit of tolerable unlevelness.

It was observed that a degressive profile with a reduction in exhaustion speed towards the end of the dyeing process yielded favourable results compared to a linear exhaustion profile. This demonstrated that the shape of the exhaustion curve could be important, too. Its influence on unlevelness was expressed in the newly introduced variable of the significant fibre surface molality change per contact. Theoretical considerations suggested that the ideal process profile should lead to a constant significant fibre surface molality change and it was shown that the previously developed adsorption-diffusion model could be used to derive the corresponding salt dosing gradient.

A statistical analysis revealed that correlation with unlevelness was improved when only those values of the significant exhaustion speed and the significant surface molality change were taken into account that referred to exhaustion values of more than 25%. It also indicated that the dye addition time, compensated for the dye-amount dependent effect of the First Strike, had a significant influence on unlevelness. These three parameters, when combined in a multiple linear regression, explained nearly 80% of the total variation in unlevelness observed in the experiments. The regression equation permitted the prediction of the degree of unlevelness of any particular process profile.

The pilot-scale dyeings also showed that control of the dye uptake rate by electrolyte dosing led to much lower unlevelness than dye dosing, all other factors being equal, confirming one of the axioms of the controlled-sorption principle. It was clearly demonstrated that it is better to control the substantivity of the dye for the fibre than to control the dye supply to the system. In the case when there is no alternative to starting the process with the entire amount of electrolyte, e.g. because the dyebath had been previously recycled, best results were obtained by dye dosing into a cold dyebath. In this case, rapid dye addition is most likely beneficial because dye supply from the dyebath may be high enough to prevent locations of inadequate dye supply in the machine, even under high substantivity conditions.

The models and methods developed during this work may be used as a set of tools enabling their user to make a dyeing process more efficient and environmentally sound. Viewed from this perspective, the equilibrium sorption model may be used to define the optimum process conditions, such as temperature, salt and dye amounts, required to obtain a desired colour. The statistical model quantifies the critical parameter values which may not be exceeded or under-run during the process in order to obtain a fabric of acceptable unlevelness. One of these parameters, the significant change of the fibre surface molality, requires fairly elaborate models, such as the adsorption-diffusion model developed in this

investigation, for an accurate performance prediction of a certain process profile. The dynamic sorption model additionally helps to derive temperature or salt dosing gradients necessary to obtain a desired exhaustion profile.

For the dye and the dyeing systems examined here, the models performed satisfactorily. For industrial applicability, however, an extension to dye mixtures would be needed since most recipes in bulk production use three dyes, sometimes even more. It would additionally be desirable to develop further the methods in order to make them applicable to reactive, vat and sulphur dyes on cellulosic substrates.